Vibration Analysis of Point and Column Supported Mindlin Plates

by

Mamdouh B. Felemban

A Thesis Presented to the

FACULTY OF THE COLLEGE OF GRADUATE STUDIES

KING FAHD UNIVERSITY OF PETROLEUM & MINERALS

DHAHRAN, SAUDI ARABIA

In Partial Fulfillment of the
Requirements for the Degree of

MASTER OF SCIENCE

In

MECHANICAL ENGIEERING

June, 1989

Order Number 1355743

Vibration analysis of point and column supported mindlin plates

Felemban, Mamdouh B., M.S.

King Fahd University of Petroleum and Minerals (Saudi Arabia), 1989

U·M·I
300 N. Zeeb Rd.
Ann Arbor, MI 48106

VIBRATION ANALYSIS OF POINT AND COLUMN SUPPORTED MINDLIN PLATES

BY

MAMDOUH B. FELEMBAN

A Thesis Presented to the

FACULTY OF THE COLLEGE OF GRADUATE STUDIES

KING FAHD UNIVERSITY OF PETROLEUM & MINERALS

DHAHRAN, SAUDI ARABIA

In Partial Fulfillment of the
Requirements for the Degree of

MASTER OF SCIENCE

In

MECHANICAL ENGINEERING

JUNE, 1989

KING FAHD UNIVERSITY OF PETROLEUM & MINERALS

DHAHRAN 31261 , SAUDI ARABIA

COLLEGE OF GRADUATE STUDIES

This thesis, written by

MAMDOUH B. FELEMBAN

under the direction of his Thesis Advisor and approved by his Thesis committee , has been presented to and accepted by the Dean of the College of Graduate Studies, in partial fulfillment of the requirements for the degree of

MASTER OF SCIENCE IN MECHANICAL ENGINEERING

Thesis Committee

Chairman Dr. Guven Aksu

Member Dr. Abdul Kerim Kar

Member Dr. Mehmet R. Gecit

Dr. Habib Abulhamayel
Department Chairman

Dr. Abdullah S. Al-Zakri
Dean , College of Graduate Studies

Date : June 12, 1989

بسم الله الرحمن الرحيم

الحمد لله رب العالمين والصلاة والسلام
على رسوله الأمين
ان الحمد والشكر والثناء لله تعالى لتوفيقه
لاتمام هذه الرسالة

To

Whom I love

ACKNOWLEDGEMENT

All praises and glory to Almighty Allah without Whose help no work can be accomplished.

Acknowledgement is due King Fahd University of Petroleum and Minerals for its incredible moral and financial support to accomplish this research work.

My deep appreciation and thanks are due to my thesis committee chairman and academic advisor Dr. Guven Aksu. He was generous in time and thoughts. He enlightened my path to the field of vibration. My thanks are due to other committee members, Dr. Abdul Kerim Kar and Dr. Mehmet Gecit, for their constructive criticism. I also extend my thanks to Dr. Yahya Khulief and Dr. Rao Guntur for their review and interest in this work. Sincere thanks are due to Dr. Habib Abulhamayel Chairman of the M.E. Department for his immeasurable cooperation and encouragement..

I thank ME workshop for disposing painful efforts in manufacturing of the " Low Frequency Mounting Table", in particular my thanks are due Mr. Bakr Nooreldin for his coordination in design , Mr. Abdul Baset Shehabel-din for technical drawings , and Mr. Masood A.Khan and Mr. Syed Mumtaz Husain for their collective and individual support in machining the mounting table. Special thanks are due to my colleagues , Mr. S.M. Shaahid and Mr. Abdul Aleem Bangaloor , for their help in typing this manuscript.

My heartfelt thanks and gratefulness go to my parents who had the foresight to provide support and encouragement for my education.

Finally I thank my wife for the time and love she extended and for her indispensable patience through out this research work.

TABLE OF CONTENTS

LIST OF TABLES

LIST OF FIGURES

LIST OF EQUIPMENT

[1] : Exciter Control	type B&K 1047
[2] : Power Amplifier	type B&K 2712
[3] : Vibration Exciter	type B&K 4808
[4] : Accelerometer	type B&K 4343
[5] : Conditioning Amplifier	type B&K 2625
[6] : Two Channel Tracking Filter	type B&K 5716 / WHO255
[7] : Low Frequency Mounting Table	M.E. Workshop (U.P.M.)
[8] : Accelerometer	type B&K 4344
[9] : Charge Amplifier	type B&K 2635
[10] : Phase Meter	type B&K 2971
[11] : Voltmeter	type B&K 2432
[12] : Cross Spectrum Unit	type B&K 5748
[13] : X-Y Recorder	type B&K 2308
[14] : Two Channel Level Recorder	type B&K 2309

NOMENCLATURE

A	: area
A-A	: Antisymmetric-Antisymmetric
[A]	: coefficient matrix
a	: length of a rectangular plate
a	: length of and width of a square plate
b	: width of a rectangular plate
a_{vx} , a_{vy}	: directional cosines
D	: flexural rigidity $\equiv Eh^3/(1-\nu^2)$
D_x	: flexural rigidity in the x-direction
D_y	: flexural rigidity in the y-direction
E	: Young's modulus of elasticity
F	: quadrature function in discrete displacement and rotational components.
f	: radian frequency
f_1 , f_2 , f_3	: strain energy sub-functions
f_4	: kinetic energy sub-functions
G	: shear modulus
H	: linear function of the square of discrete velocities
h	: plate thickness
i , j	: node indicies
k	: shear coefficient $(\pi^2/12)$
M_x, M_y	: bending moment per unit length of sections of a plate perpendicular to x and y axes respectively
M_{xy}	: twisting moment per unit length of sections of a plate perpendicular to x axis

M_v : bending moment per unit length of sections of a plate perpendicular to v axis

M_{vs} : twisting moment per unit length of sections of a plate perpendicular to v axis

M,N : number of rows and columns in the node set , respectively

m : number of rows and columns in the node set of a square plate

$\underline{\pm 90^\circ}$: phase shift of 90 degrees

n_{AA}, n_{SA}, n_{SS} : total number of equations for AA, SA and SS mode , respectively

Q_x , Q_y : shear forces parallel to z-axis per unit length of section of a plate perpendicular to x and y axes , respectively

q_1 , q_2 , q_3 : generalized coordinate

q : external force (or load)

S-A : Symmetric-Antisymmetric

S-S : Symmetric-Symmetric

t : time

T_V : kinetic energy per unit volume

T_A : kinetic energy per unit area

T : total kinetic energy

δT : Virtual kinetic energy

U_V : strain energy per unit volume

U_A : strain energy per unit area

U : total strain energy

δU : Virtual strain energy

U_1 , U_2 , U_3 : sub-strain energies

u : displacement field in x - direction

V : total potential energy

v	: displacement field in y - direction
w	: displacement field in z - direction
u_1, u_2, u_3	: displacement field
v,s	: transformation coordinate
$\overline{w}$	: average displacement components
w	: non-dimensional component
W	: displacement component independant of time
x,y,z	: rectangular coordinate
$[X]$	: eigenvector
L	: lagrangian = U + V
α	: position of the point support
β	: thickness ratio (h/a)
γ	: aspect ratio (a/b)
γ_x , γ_y	: angles of distortion due to shear
$\gamma_{xy} , \gamma_{yz} , \gamma_{zx}$	: unit shearing strains
$\varepsilon_{xx}, \varepsilon_{yy}, \varepsilon_{zz},$	: strain field
$\varepsilon_{xy}, \varepsilon_{yz}, \varepsilon_{zx}$	: strain field
$\varepsilon_x , \varepsilon_y , \varepsilon_z$	: unit elongation in x,y and z directions
$\sigma_x , \sigma_y , \sigma_z$	: normal stresses parallel to X,Y and Z axes respectively
τ	: shear stress
$\tau_{xy} , \tau_{yz} , \tau_{zx}$	: unit elongation in X,Y and Z directions
V	: differential operator $\equiv \partial^2/\partial x^2 + 2\partial^2/\partial x\partial y + \partial^2/\partial y^2$
V^4	: differential operator $\equiv \partial^4/\partial x^4 + 4\partial^4/\partial x^2\partial y^2 + \partial^4/\partial y^4$
ζ , η	: non-dimensional coordinate
$\Delta X , \Delta Y$	: finite differance increments

$\Delta\zeta$, $\Delta\eta$: non-dimensional finite differance increments

Ω : eigen value $\equiv \omega h\sqrt{\rho(1-\nu^2)/E}$

λ : frequency parameter (point support) $\equiv \omega a^2\sqrt{\rho h/D}$

λ_C : frequency parameter (rigid support) $\equiv \omega a^2\sqrt{\rho h/D}$

δ :virtual displacement

ω : natural frequency (rad/sec)

ξ : finite area of rigid support

ν : poisson's ratio

ρ : density

φ_x , φ_y : angles of rotations due to bending in x and y directions respectively

φ_v , φ_s : angles of rotations due to bending in v and s directions respectively

Φ_X , Φ_Y : rotational components independant of time

π : summation of the total strain and potential energies

THESIS ABSTRACT

NAME : MAMDOUH B. FELEMBAN

TITLE : VIBRATION ANALYSIS OF POINT AND COLUMN SUPPORTED MINDLIN PLATES

MAJOR : MECHANICAL ENGINEERING

DATE : 31st MAY , 1989

Free vibration characteristic of an isotropic, homogeneous point supported square plate with no initial deflection and no initial stresses have been critically examined by a method based on the application of variation principle to the energy expressions in conjunction with Finite Difference methods with interlacing grids. Using the symmetry of the geometry of the plate and the symmetry in the distribution of the point supports, only one quarter of the plate was examined. Three mode types were developed to account for the full plate.

The effect of transverse shear deformation and rotary inertia have been considered and the effect of finite area of the point support has also been analyzed. The produced mode shapes and nodal patterns were presented. Experiments were conducted to give an insight to the theoretical predictions. The natural frequencies were obtained from the frequency response of the Real and the Imaginary part. Nyquist (Argand) plots of the corner supported case were also presented.

The convergence of the present method to the theoretical exact value of the frequency parameter were found out to be either from above or below. It has been shown by the theoretical investigation that the effect of transverse shear deformation and rotary inertia were more pronounced in higher modes. It was observed that the fundamental frequency parameter increases as the point support moves towards the center and the maximum occurs at $\alpha = 0.23$ *. The radian natural frequency obtained from the frequency response showed that the theoretical predictions were considerably accurate with maximum discrepancy of 2.48 percentage.*

The result of the studies could be applied in many practical application such as the design of large shakers capable of supplying yaw as well as thrust motion to the test specimens.

MASTER OF SCIENCE DEGREE
KING FAHD UNIVERSITY OF PETROLEUM & MINERALS
Dhahran, Saudi Arabia.

خـــلاصـــة الرسالـــــــة

الاســـــم : ممدوح السيد برليان زبير فلمبـــــان

عنوان الرسالة : تحليل اهتزازات الواح مندلن المثبته بنقطة او عمود
التخصص : هندسة ميكانيكيـــة
تاريخ الشهادة : ٢٦ شوال ١٤٠٩ هـ

لقد استخدمت نظرية تعتمد على تطبيق المبادىء التغيرية على دوال الطاقة بالاتحاد مع أسلوب الفرق المحدد بشبكة متشابكة وذلك لاختبار خواص الاهتزاز الحر للوح مربع مرن وموحد الخواص ومتجانس بدون انحناء او شد اولى . وباستخدام خواص التشابه فى شكل المربع والتوازن فى توزيع نقط التثبيت امكن اختبار ربع اللوح فقط ولذلك طورت ثلاثة اشكال تركيبه حتى تغطى الاشكال التركيبيه للوح الكامل .

لقد أشتمل البحث على دراسة تأثير تضمين التشوه القصى المستعرض والقصور الذاتى الدورانى وكذلك تأثير المساحة المحدده لنقطة التثبيت ايضا تم تقديم الاشكال التركيبيه ورسومات الخطوط العقديه . كذلك اشتملت الدراسه على اجراء تجربة معملية لاعطاء فكره أوضح عن التقديرات النظرية للترددات الطبيعيه . امكن الحصول على الترددات الطبيعيه عن طريق القسم الحقيقى والخيالى لرسومات الذبذبات . كذلك تم تقديم رسومات نايكوست (أرقاند) لهذه الترددات .

لقد أستنتج من هذا البحث ان خاصية الميل للالتقاء بين النظرية الحاليه والقيم الحقيقية النظرية للاهتزازات يمكن ان تكون من أعلى او من أسفل . وأستنتج كذلك خلال الدراسة ان تأثير التشوه القصى المستعرض والقصور الذاتى الدوانى يكون بدرجة كبيره للترددات العالية ، وان التردد الاولى يزيد مع حركة النقطه باتجاه المركز تصل لاعلى قيمة عند ٢٣ر. ووضحت التجربه ان الترددات الطبيعية (راديان) تقارب بدرجة كبيرة التقديرات النظرية بفرق أعلى ٤٨ر٢ ٪ .

ويمكن استخدام نتائج هذا البحث فى عدة تطبيقات عملية مثل تصميم الهزازات الكبيره القادره على تقديم الانعراج بالاضافة الى حركية الدفع للقطع تحت الاختبار .

درجة الماجستير فى العلـــــــوم
جامعة الملك فهد للبترول والمعادن
الظهران ـ المملكه العربيه السعودية
٩ ذو القعـــدة ١٤٠٩ هـ

CHAPTER 1

INTRODUCTION

The problem of conducting free vibration analysis of rectangular plates resting on point supports has received considerable attention during recent years. A through survey of the literature indicates that most of these analyses have been confined to the vibration of square plates with point supports located on the diagonals. A number of papers concerned with the free vibration of square or rectangular plates on four-point supports have already appeared. Theoretical studies based on different methods were applied, namely, Finite Difference method, Rayleigh-Ritz method, Finite Element method , Lagrangian Multiplier method, Finite Element Displacement method, Finite Strip method , Modal Constraint method , Series solution , Superposition method and others . In all of the methods mentioned above, the numerical study was based on thin plate theory where the effect of rotary inertia and transverse shear deformation are neglected .

A limited amount of experimental data has been reported by various researchers. Experimental verification of the results has been reported in some references. Some worked with a plate supported by four bolts which are used as point supports and the plate in turn was mounted on a shaker. The effect of transverse shear deformation and rotary inertia were not investigated since the experiment were conducted on plates with small thickness/dimension ratio (β less than 0.1) .

In the present study , the use of variational principles applied to the energy expressions in conjunction with the finite difference technique with interlacing girds is applied as a method for determination of vibration characteristics , mode shapes and nodal patterns of elastic , isotropic and homogeneous corner and point supported square plates. Expressing the strain and the kinetic energy equations by the finite difference equations with equal intervals , these expressions are obtained in terms of discrete displacement and rotational components. Harmonic motion is assumed to eliminate the time dependence and the energy functional is minimized with respect to discretized components. The natural frequency parameters with mode shapes are determined as the solutions of a linear algebraic eigenvalue problem.

The concept of interlacing grids and nodal sub-domains are applied for the strain energy expression and modified finite difference method is used in the formulation. The strain energy functional is divided into sub-functions. The sub-strain energies are computed as the summation of strain energies summed over the set of non-overlapping sub-domains. Although the total number of nodes remains unchanged , employing interlacing grids technique provides a finite difference formulation with reduced node intervals and results in reduced discretization error.

The use of variational principles in conjunction with finite difference method provides the following advantages :

1. Only first order finite difference approximation is required.
2. First order derivatives provide the interlacing grid technique to be used which results in high degree of accuracy.

3. The stress boundary conditions are satisfied automatically through the minimization process and only geometric boundary conditions are considered.
4. Automatically generated band matrix saves the computation time and computer core storage .

In this study , the dynamic behavior of relatively thick plates (Mindlin) is analyzed including the effect of transverse shear deformation and rotary inertia by applying the finite difference technique. The mode types are divided into three categories namely, Antisymmetric- Antisymmetric, Symmetric-Antisymmetric, and Symmetric-Symmetric , since quarter of the plate is considered. Also the numerical analysis further extended to study the effect of rigid support and the effect of increasing the finite area of the rigid point support .

Experiment was conducted to give insight into the numerical prediction. Three steel plates of different thickness ratios , β , were tested for two different location of the point support namely corner position $\alpha = 0.0$ and point support $\alpha = 0.1$. The frequency response was plotted for the real and imaginary parts. Nyquist plot of the corner supported case is also presented.

A comprehensive survey of literature was conducted and a summary of all related studies is presented in Chapter 2. In Chapter 3, the theory which the numerical results are based on, is explained. The derivation of the energy expressions is presented and the use of the variational principle is explained. Finite difference formulation is presented in short in Chapter 4. Only the interlacing sub-domains are given and for further details references are cited. A description of the experiment, test equipment, instrumentation and test proce-

dure is presented in Chapter 5. The discussion of results, Chapter 6, is divided into four parts. In part one , the convergence study is discussed based on the numerical values obtained for different mesh sizes. Results of corner and point supported case are given in part two. Part three is concerned with the experimental results. Finally , discussion of column supported plate is given in part four. Conclusions and recommendations are presented in Chapter 7. All of the figures related to the convergence study , corner and point supported square plates , and all tables , frequency response , Nyquist plots , mode shapes , nodal patterns and the computer program are given in the appendices.

CHAPTER 2

LITERATURE SURVEY

Considerable interest has been shown in the determination of the vibration characteristics of point-supported plates. Such an investigation finds its application either in the design of large shakers capable of supplying yaw as well as thrust motions to the test specimens, or in the determination of dynamic response of column-supported slabs which experience oscillatory loads from the machinery resting on them.

A large amount of work has been done on the vibration of elastic thin plates of uniform thickness point supported along the diagonals, but none (up to the knowledge of the author) has considered thick plate. Thin plate is considered when the thickness to the plate dimension ratio , β , is less than 0.02 (or 1:50).

The first paper published concerned about the fundamental frequency parameter of uniform isotropic rectangular plate that have free edges and pin-point supports at the four corners was in 1960 [5] by Cox, H. and Boxer, J. They have used Finite Difference expressions, which simplify the treatment of the free boundaries for definite values of Poisson's ratio, in conjunction with extrapolation procedure to obtain the approximate solutions. They had neglected the effect of rotary inertia and transverse shear deformation. They have considered square plate as a special case of rectangular plate. They have presented the first five mode shape of corner supported square plate .

In 1962 [6] Kirk, C. determined the frequency expression and mode shape for a square plate vibrating at the lowest natural frequency by considerations of energy. He stated that the lowest natural frequency of a square plate that is point-supported at the corners may be determined approximately by equating the maximum strain energy of the plate to the maximum kinetic energy. He used the classical theory of plate where the effect rotary inertia and transverse shear deformation were neglected.

In 1965 [7] Reed, R. compared some of the methods in calculating frequencies of corner-supported rectangular plates. He had used two methods namely the Ritz method and the Series solution to the classical differential equation of motion of the plate. The series method showed fast convergence over the Ritz method. He also carried out a short experimental program to see the correlation with the theoretical results. He used a 30-watt sound speaker that excited the plate (β = 1/93) through an attached string. The speaker was driven by variable frequency oscillator and the motion of the plate was measured by a capacitance-type displacement instrument. He visualized the mode shape by sprinkling carborundum chips on the plate during excitation.

In 1966 [8] Tso, W. used Rayleigh-Ritz method with three different assumed deflection to obtain the fundamental frequency. He was the first to study the effect of point location along the diagonals of a square plate to the fundamental frequency. He also conducted an experiment where the plate (β = 0.0035) was supported by four bolts mounted on a shaker, and the fundamental frequency of the plate for various locations of the four support points were determined. To compare his experimental results with the theoretical calculations, the experimental value of the nondimensional frequency parameter for

the corner supported case ($\alpha = 0.0$) was made to coincide with the value given by H. Cox and J. Boxer [5]. Then the experimental results of the other point locations were reduced by the same factor.

In 1969 [10] Johns,D.J. and Nagaraj,V.T. used an alternative finite difference formulation of the governing differential equation of motion and an energy-type analysis involving the assumption of modal forms to determine the fundamental frequency of a square plate symmetrically supported at four points. Because of the symmetry (assumed) of the fundamental mode about the diagonals and about the co-ordinate axes, only a triangular portion of the plate was considered with different mesh sizes.

In 1969 [11] Leissa, A. has presented an extensive review of published literature on vibration of plate up to 1965. Leissa's monograph deals with the classical theory of plates, anisotropy, in-plane force and variable thickness plates. Since the classical thin plate theory assumes that the effects of transverse shear deformation in conjunction with rotary inertia are neglected, the assumption can lead to substantial error for the case of thick plates. The effects of transverse shear deformation and rotary inertia become increasingly important with the increase in plate thickness relative to plate length (β).

In 1971 [12] Dowell, E.H., described a method for the analysis of the free vibration of a linear structure supported in an arbitrary way. It was presented based upon the use of the normal modes of the unsupported or unconstrained structure in Rayleigh-Ritz analysis with the support or constrained conditions enforced by means by Lagrange Multipliers.

In 1971 [13] Mirza, W.H. and Petyt, M. presented some of the results obtained by analyzing the problem of vibration of point-supported plate using finite element technique. Two displacement functions incorporating three degree of freedom per node (viz, w, $\partial w/\partial x$,$\partial w/\partial y$) and four degree of freedom per node (viz, w, $\partial w/\partial x$, $\partial w/\partial y$,$\partial^2 w/\partial x \partial y$), respectively, were used. They have applied this technique for two different mesh size (Quarter of the plate were analyzed) namely 2×2 and 4×4. The first five frequencies of the corner supported square plate were given and also the variation of the fundamental frequency with the point location.

In 1971 [14] Damle, S.K. and Fesser, L. J., used finite element method to find the fundamental frequencies and mode shapes for an elastic thin square plate supported symmetrically at four points on the diagonals of the plate. They have compared their results with Tso, W.K. (1966) [8] which were based on numerical procedures and also experimental results. All the three method (F.E. & Rayleigh Ritz & Experiment seemed to agree with good accuracy up to a value of $\alpha = 0.32$.

In 1972 [15] Petyt, M. and Mirza, W.H., used finite element displacement method of analysis to determine the vibration characteristics of floor slabs resting on four column supports. They have compared their results with other theoretical solutions and also experimental measurements. They also investigated the effect of rigidity and finite area of the column supports. Finally, they have considered the vibration characteristics of various arrangements of slabs on many supports. They were the first to discuss and investigate the effect of joint rigidity. The finite area of the columns, assumed square represented by the four cor-

ner elements.

In 1972 [16] Johns, D.J. and Nataraja, R. presented an alternative analysis of the vibration of a square plate symmetrically supported at four points, and discussion of the corresponding results were given. They have re-examined their previous results. { 1969 [10] Johns, D.J. and Nagaraj, V.T. } and corrected their previous assumption that the fundamental mode shape were symmetric about the diagonals for all diagonal supports points.

In 1973 [17] Venkateswara Rao, G., Raju,I.S. and Amba-Rao,C.L. tried to get a very accurate upper bound for the first few frequencies by using Finite Element Method. They have used double precision arithmetic. For the first three natural frequency of corner supported square plate, Finite Element Method seemed to give upper bound and Finite Difference gave lower bound.

In 1974 [20] Sadasiva Rao, Y.V.K., Venkateswara Rao, G. and Amba Rao, C.L. conducted an experimental study of vibration of a four point supported square plate. An aluminium plate of dimensions 555 by 555 by 1.5 mm (β = 1/370) thick is used to obtain the fundamental frequencies at different locations of the supports along the diagonal. The test setup consisted of a thick horizontal rectangular bottom plate at the corners of which four vertical channels of mild steel of very high stiffness were welded. Two thick steel beams with central longitudinal grooves were welded to each other so as to form a frame of plan form "X". The specimen was supported at four points by means of two screws for each support point. The plate was excited by means of an electromagnetic shaker at the center for all support points except center support where the excitation was in another arbitrary location. They have compared their results

with the Finite Element Method used by Venkatesware Rao, G., Raju, I.S., and Amba - Rao, C.L. (1973) [17] and the experimental values obtained by Tso,W. K. (1966) [8] .

In 1974 [21] Leuner, T.R. performed an experimental and theoretical study to investigate the effect of varying the stiffness of corner elastic point supports on plate vibration. An experiment was conducted in which the bending stiffness of horizontal beams was used to support a square plate at its four corners. He observed that the stiffness of these supports can be varied over such a range that the plate fundamental frequency was lowered up to 40 percentage .

In 1974 [22] Dowell,E.H. commented on the disagreement of the comparison between the results obtained by Venkateswara, G., Raju,I.S. and Amba.Rao, C.L. (1973) [17] and the previous results obtained by Dowell, E.H. (1971) [12] for some certain range at support location. He pointed out that the difference was due to the fact that the lowest frequency mode changes with support positions.

In 1975 [24] Srinivasan, R.S.and Munaswamy,K. were the first to study Finite Strip with a non-uniform support conditions along the edges. They have accomplished the free vibration analysis of skew orthotropic plate with point support by using higher degree skew finite strip. They have derived the expressions of strain energy and kinetic energy by applying small deflection theory. The displacement function for the strip was assumed as a series with polynomials in one direction and beam function in the other direction. Their results can be compared with others for the case of free vibration of square plate symmetrically supported along the diagonals when the skew angle is O degree.

In 1975 [25] Venkateswara, Rao, G., Amba Rao, C.L. and Murthy, T.V.G. commented on the comments given by Dowell, E.H.(1974) [22] where Dowell, E.H. stated that the frequency of point supported square plate with $\alpha = 0.2$ was the fundamental frequency. They have emphasized (at the risk of annoying the reader) that 'fundamental' implies the lowest.

In 1977 [29] Leissa, A.W. summarized all known results for the vibration frequencies, mode shapes and nodal patterns. A thorough search revealed approximately 500 references. In this paper which is part I of a two-part review of literature published over the period 1973-1976 that deals with free, undamped vibrations of plate. This part is limited to problems governed by the classical theory of plates.

In 1978 [32] Leissa,A.W., published part II of his search of sources related to plate vibration. It dealt with complicating effects of free, undamped vibration of plates that appeared from 1973-1975 and in part of 1976. Recent research dealing with the complicating effects of anistropy, inplane forces, variable thickness, surrounding media, large deflections, shear deformation, rotary inertia, and non-homogeneity were summerized. For the case of the vibration of plates including the shear deformation rotary inertia, none of the reviewed paper applied it to point supported rectangular or square plate.

In 1979 [33] Kerstens,J.G.M., described a method for establishing the natural frequencies of a rectangular plate supported at an arbitrary number of points and locations. The method is based on some extensions to the intermediate problem technique of Aronszjan and Weinsten (1941,1961,1972) through the use of finite sets of constraints which is called " Modal Constraint method". The

merit of this method lies in the fact that the eigen values and eigen functions of a completely free vibrating rectangular plate are used as the reference structure and the boundary conditions stemming from the point support are imposed on that reference structure. The modifications associated with the point supports are taken into account by Lagrangian generalized forces of constraint acting on the reference structure. In this paper, Kerstens, tabulated the results for free plate by the mode type, i.e. Antisymmetric- Antisymmetric, Symmetric-Antisymmetric, and Symmetric-Symmetric.

In 1979 [34] Gorman,D.J. developed a Levy type solution for the vibratory response of simply supported rectangular plate subjected to a harmonic force distributed along the diagonal. He extended the solution to determine the free vibration response of the same rectangular plate with inelastic lateral support on the diagonal.

In 1980 [35] Gorman,D.J., introduced a highly accurate mathematical technique for establishing the free vibration eigenvalues and mode shapes of rectangular plate with symmetrically distributed point supports along the edges. The method is based on the principle of superposition. An exact delineation is made between those modes which are fully symmetric, fully antisymmetric or symmetric-antisymmetric with respect to the plate central axes.

In 1981 [38] Gorman, D.J. expanded and continued his previous work (1980) [35] to include the free vibration eigenvalues and mode shapes of rectangular plate with symmetrically distributed point support along the diagonal. The first four frequencies in each mode of fully symmetric, fully antisymmetric and symmetric-antisymmetric were presented. The range of the point support

covers from $\alpha = 0.0$ (corner support) up to $\alpha = 0.4$ with increment of 0.05 .

In 1981 [39] Leissa, A.W. summarized the researches in free, transverse vibrations of plate in the period of 1976-1980. This part covers the classical theory of plates, i.e. homogeneous, isotropic, thin, constant thickness, no inplane initial forces, small transverse displacement, vibrating in a vacuum , etc.

Later in 1981 [40] Leissa,A.W. published the second part of his search of all the researches conducted during 1976-1980 for the plate vibration considering the complicating effects. Complicating effects are those which directly affect the governing differential equation of motion of a plate. Transverse shear deformation and rotary inertia are among those effects. None of the reviewed papers in that research revealed the titled problem (free vibration of corner and point support plate) including the effect of transverse shear deformation and rotary inertia since all the theoretical studies were based on the classical theory of plates.

In 1983 [43] Raju,I.S. and Amba-Rao,C.L. presented the first six symmetric-symmetric, antisymmetric-symmetric and antisymmetric- antisymmetric natural frequencies for a square plate resting on four point supports along the diagonals as obtained by using finite element analysis. They have compared their result with Gorman,D.J. (1981) [38] and explained the discrepancies. Quarter of the plate were analyzed with Poisson's ratio $\nu = 1/3$.

In 1984 [45] Narita, Y. and Leissa, A.W. as a part of their research of vibration of corner supported shallow shells of rectangular plane form , determined the frequency parameter for corner supported flat plate having square planeform with ($\nu = 0.3$). They have used Ritz method, with algebraic

polynomials forming the set of trail functions.

In 1984 [46] Fan, S.C. and Cheung, Y.K. introduced the spline finite strip method and applied it to the study of flexural free vibration response of thin rectangular plates with complex support conditions. The natural frequencies parameter for the square plate with corner supports were given.

In 1984 [48] Narita, Y. used Ritz method, with a trial function expressed in terms of double power series to solve the problem of the free vibrations of point supported rectangular plates. The constraint conditions of the support were taken into account by Lagrange multipliers. The method applied for orthotropic plate and as a special case for isotropic plate (i.e. the flexural rigidity in the X-direction equals the flexural rigidity in the Y-direction ; Dx = Dy).

In 1986 [54] Aksu,G. described a method of determining the dynamic characteristics of a four-point supported square plate with free edge using sweep sine-wave testing. The idea behind this method is to make use of free vibration time-response data such as acceleration to determine the natural frequencies and the associated mode shapes. Detailed experimental results have been obtained for various support locations lying at specified positions along the plate diagonals, to compare with numerical results obtained by others. It was found that experimental results were generally in reasonable agreement with numerical ones. A steel plate of dimensions 250 by 250 by 1.5 mm thick was used ($\beta = 0.006$).

In 1987 [56] Mizusawa, T. used spline element method to deal with the vibration of skew plates resting on point supports. It can be regarded as an alternative form of the displacement formulation of the finite element procedure

in that the minimum total potential energy theorem is used to develop the relationship between the unknown parameters and the applied loading. As a special case of skew plate, (skew angle $\varphi = O^{\circ}$), the results of corner supported square plate can be deduced.

In 1987, Leissa, A.W. presented his third search of all recent studies in the period of 1981-1985 on both classical theory [57] and complicating effect [58] of vibration of plate. As his search was extensive, it is clear up to the knowledge of the author that no study has been done on the vibration of a moderately thick isotropic square plate point supported along the diagonals that included the effect of transverse shear deformation and rotary inertia.

CHAPTER 3

THEORY

Theoretical studies based upon classical theory of plates are limited to those solving the governing differential equation of motion of thin , elastic , homogeneous and isotropic plate is given by the following equation :

$$D\nabla^4 w + \rho h \frac{\partial^2 w}{\partial t^2} = 0 \qquad (3.1)$$

Where ,

D : Flexural rigidity

V : Differential operator

w : Transverse displacement

ρ : Density of plate

h : Plate thickness

To include the effect of transverse shear deformation and rotary inertia , Mindlin plate theory is used. This theory is well explained in Timoshenko [63] . It was established by Mindlin, R.D. [4] who published the first paper about the influence of rotary inertia and shear on flexural motions of isotropic elastic plates.

The derivation of the equation of motion of plate including the transverse shear deformation and rotary inertia will be summarized and presented.

GENERAL ASSUMPTIONS

The present study will be mainly based on the following assumptions:

1. The material of the plate is elastic, homogeneous, and isotropic.
2. The plate is initially flat (i.e. no initial stresses).
3. The deformation is initially straight line normal to the middle surface, and remain straight line but no longer normal to the middle surface. This means that the deformation due to transverse shear will be considered.
4. The deflections are small compared to the plate thickness. i.e high amplitude vibration will not be included.

3.1 STRESS-STRAIN RELATION :

Figure 3.1 shows a cross section element of a uniform plate before and after deflection. Starting in the usual way by proposing displacement field and then deleting stretching effects,

$$u_1 = u(x,y,z,t) = z\Phi_x(x,y,t) = z\Phi_x$$

$$u_2 = v(x,y,z,t) = z\Phi_y(x,y,t) = z\Phi_y$$

$$u_3 = w(x,y,z,t) = \overline{w}(x,y,t) = w \qquad (3.2)$$

where Φ_x and Φ_y are body element rotation angles in x and y directions respectively. They can be expressed as :

$$\Phi_x(x,y,t) = -\left\{\frac{\partial w}{\partial x} + \gamma_x(x,y,t)\right\} \qquad (3.3)$$

$$\Phi_y(x,y,t) = -\left\{\frac{\partial w}{\partial y} + \gamma_y(x,y,t)\right\} \tag{3.4}$$

where γ_x and γ_y are angles of distortion due to shear. The strain field for the assumed displacement follows directly as :

$$\varepsilon_{xx} = z\frac{\partial \varphi_x}{\partial x}$$

$$\varepsilon_{yy} = z\frac{\partial \varphi_y}{\partial y}$$

$$\varepsilon_{zz} = 0$$

$$\varepsilon_{xy} = \frac{1}{2} z \left\{\frac{\partial \varphi_x}{\partial y} + \frac{\partial \varphi_y}{\partial x}\right\}$$

$$\varepsilon_{yz} = \frac{1}{2}\left\{\varphi_y + \frac{\partial w}{\partial y}\right\}$$

$$\varepsilon_{zx} = \frac{1}{2}\left\{\varphi_x + \frac{\partial w}{\partial x}\right\} \tag{3.5}$$

and the unit shearing strains γ_{xy}, γ_{xz}, and γ_{yz}

$$\gamma_{xy} = z\left\{\frac{\partial \varphi_y}{\partial x} + \frac{\partial \varphi_x}{\partial y}\right\}$$

$$\gamma_{yz} = -\gamma_y = \varphi_y + \frac{\partial w}{\partial y}$$

$$\gamma_{zx} = -\gamma_x = \varphi_x + \frac{\partial w}{\partial x} \tag{3.6}$$

Since assumed plane stress distribution employed, i.e the material is elastic and isotropic, the use of the two dimensional Hooke's law is permitted.

$$\sigma_x = E\varepsilon_{xx} + \nu\sigma_y$$

$$\sigma_y = E\varepsilon_{yy} + \nu\sigma_x \qquad (3.7)$$

where E is modulus of elasticity and ν is Poisson's ratio, which relates stress and strain in a plane element. Now using Eq.(3.7) in combination with Eq.(3.5) leads to :

$$\sigma_x = \frac{Ez}{(1-\nu^2)}\left\{\frac{\partial\varphi_x}{\partial x} + \nu\frac{\partial\varphi_y}{\partial y}\right\}$$

$$\sigma_y = \frac{Ez}{(1-\nu^2)}\left\{\frac{\partial\varphi_y}{\partial y} + \nu\frac{\partial\varphi_x}{\partial x}\right\}$$

$$\sigma_z = 0 \qquad (3.8)$$

also the shear stress τ and shear strain γ can be related by Hooke's law

$$\tau = G\gamma \qquad (3.9)$$

The shear stress can be obtained by combination of Eq.(3.9) and Eq.(3.6)

$$\tau_{xy} = Gz\left\{\frac{\partial\varphi_y}{\partial x} + \frac{\partial\varphi_x}{\partial y}\right\}$$

$$\tau_{xz} = G\left\{\varphi_x + \frac{\partial w}{\partial x}\right\}$$

$$\tau_{yz} = G\left\{\varphi_y + \frac{\partial w}{\partial y}\right\} \qquad (3.10)$$

Now the resultant intensity function can be obtained using Eq.(3.8) and Eq.(3.10) in combination with the following equation :

$$M = \int_{-h/2}^{h/2} \tau\, z\, dz \tag{3.11}$$

where h is the plate thickness.

Thus for M_x :

$$M_x = \int_{-h/2}^{h/2} \tau_{xx}\, z\, dz$$

$$= 2 \int_{0}^{h/2} \sigma_x\, z\, dz$$

$$= \frac{2E}{(1-\nu^2)} \int_{0}^{h/2} z^2 \left\{ \frac{\partial \varphi_x}{\partial x} + \nu \frac{\partial \varphi_y}{\partial y} \right\} dz$$

$$= \frac{Eh^3}{12(1-\nu^2)} \left\{ \frac{\partial \varphi_x}{\partial x} + \nu \frac{\partial \varphi_y}{\partial y} \right\}$$

$$= D \left\{ \frac{\partial \varphi_x}{\partial x} + \nu \frac{\partial \varphi_y}{\partial y} \right\} \tag{3.12}$$

where D is the flexural rigidity defined as :

$$D = \frac{Eh^3}{12(1-\nu^2)} \tag{3.13}$$

Following the same procedure ,

$$M_y = \frac{Eh^3}{12(1-\nu^2)}\left\{\frac{\partial \varphi_y}{\partial y} + \nu\frac{\partial \varphi_x}{\partial x}\right\} \tag{3.14}$$

and ,

$$M_{xy} = \frac{Gh^3}{12}\left\{\frac{\partial \varphi_y}{\partial x} + \frac{\partial \varphi_x}{\partial y}\right\} \tag{3.15}$$

where G is the shear modulus and defined as :

$$G = \frac{E}{2(1+\nu)} \tag{3.16}$$

Now we consider the resultant shear force intensity function, for Q_x

$$Q_x = \int_{-h/2}^{h/2} \tau_{xz}\, dz \quad = \tau_{xz}\, h$$

Since there is an error steming from Eq.(3.5) that shear strain ε_{xz} is constant over the thickness of the plate (i.e. $\varepsilon_{xz} \neq \varepsilon_{xz}(z)$), a correction factor should be employed to overcome this error. This factor k is called shear coefficient $\{$ usually taken as $\pi^2/12\}$.

Hence ,

$$Q_x = k\tau_{xz}h \tag{3.17}$$

Now combining Eq.(3.13) and Eq.(3.10) , we have for Q_x :

$$Q_x = khG\left\{\Phi_x + \frac{\partial w}{\partial x}\right\} \tag{3.18}$$

Similarly we get for Q_y:

$$Q_y = khG\left\{\Phi_y + \frac{\partial w}{\partial y}\right\} \tag{3.19}$$

Figure 3.2 represent a three-dimensional element cut out of an isotropic elastic rectangular plate showing the stress distribution. In Figure 3.3 the shear forces are shown for the same element.

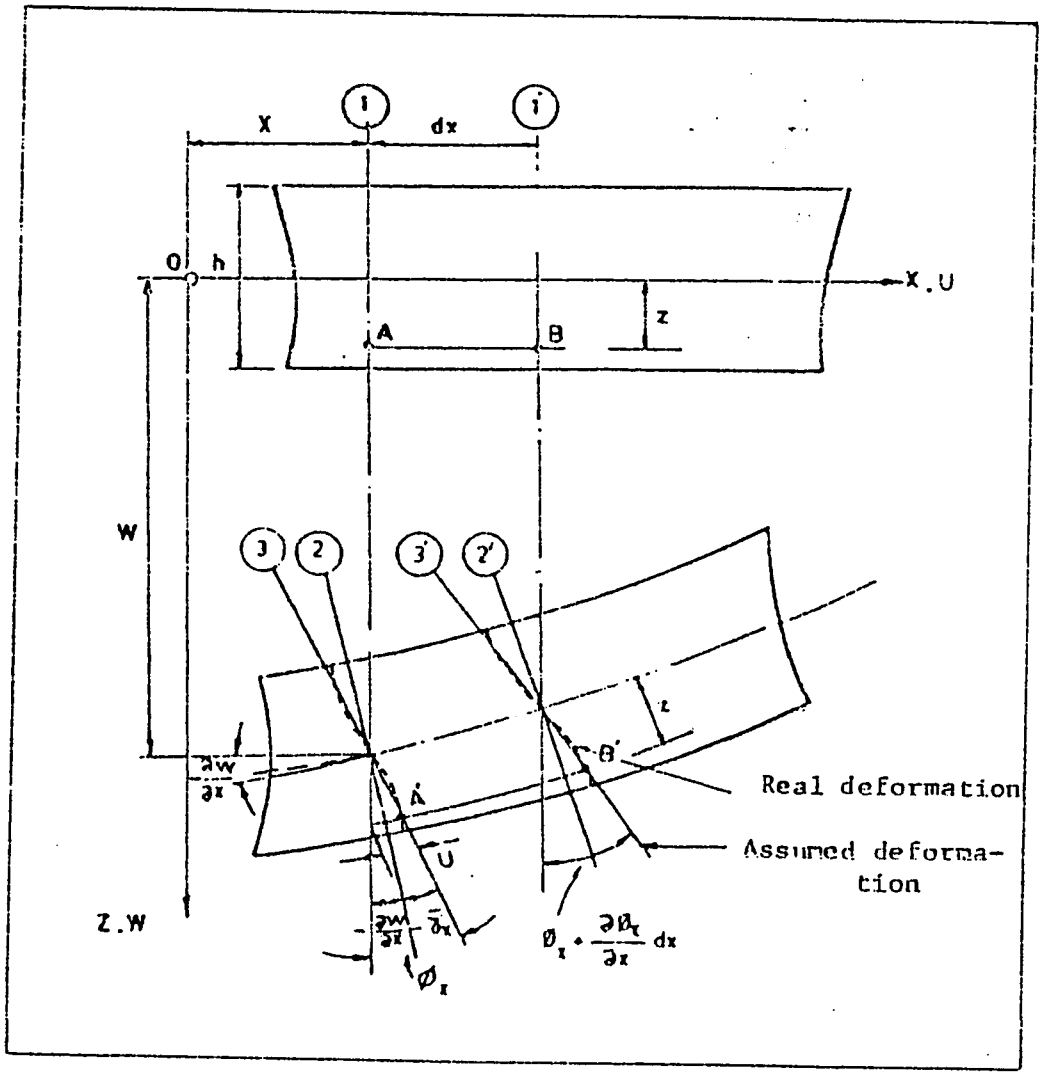

Figure 3.1 : Section before and after deflection

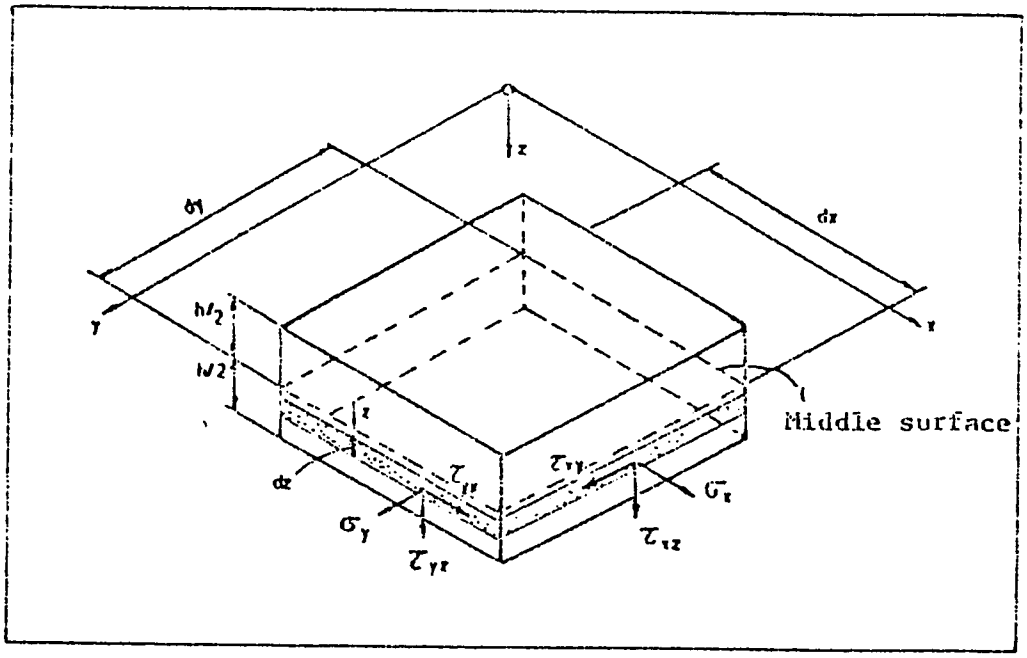

Figure 3.2 : Stresses on a plate element

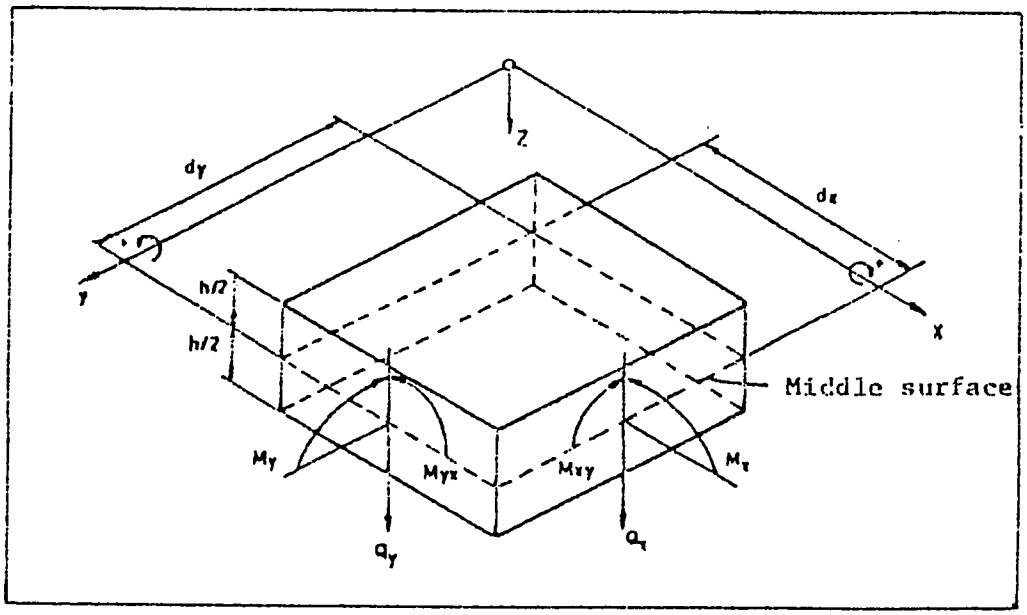

Figure 3.3 : Shear forces and moments

3.2 STRAIN ENERGY :

The strain energy function per unit volume, in the three dimensional theory is given by :

$$U_V = \sigma_x\varepsilon_{xx} + \sigma_y\varepsilon_{yy} + \sigma_z\varepsilon_{zz} + 2\tau_{xy}\varepsilon_{xy} + 2\tau_{yz}\varepsilon_{yz} + 2\tau_{zx}\varepsilon_{zx} \qquad (3.20)$$

Since plane stresses are assumed (i.e dropping σ_z), and employing Hooke's law Eq.(3.7) and Eq.(3.9) for σ_x, σ_y, and τ_{xy}, Eq.(3.20) will be :

$$U_V = \frac{E}{(1-\nu^2)}(\varepsilon_{xx} + \nu\varepsilon_{yy})\varepsilon_{xx} + \frac{E}{(1-\nu^2)}(\varepsilon_{yy} + \nu\varepsilon_{xx})\varepsilon_{yy}$$

$$+ 4G\varepsilon_{xy}^{\ 2} + 2\tau_{xz}\varepsilon_{xz} + 2\tau_{yz}\varepsilon_{yz} \qquad (3.21)$$

Now using Eq.(3.5) to replace the strains in Eq.(3.21) and then integrating over the thickness, the strain energy per unit area will be deduced as follows :

$$U_A = \frac{1}{2}\frac{Eh^3}{12(1-\nu^2)}\left[\left(\frac{\partial\varphi_x}{\partial x}\right)^2 + \left(\frac{\partial\varphi_y}{\partial y}\right)^2 + 2\nu\left(\frac{\partial\varphi_x}{\partial x}\right)\left(\frac{\partial\varphi_y}{\partial y}\right)\right]$$

$$+ \frac{1}{2}\frac{Gh^3}{12}\left(\frac{\partial\varphi_x}{\partial y} + \frac{\partial\varphi_y}{\partial x}\right)^2 + \tau_{xz}\left(\varphi_x + \frac{\partial w}{\partial x}\right) + \tau_{yz}\left(\varphi_y + \frac{\partial w}{\partial y}\right) \qquad (3.22)$$

Now, the total strain energy can be obtained by integrating Eq.(3.22) over the entire region (area) ,

$$U = \frac{1}{2}\iint_R\left\{\frac{Eh^3}{12(1-\nu^2)}\left[\left(\frac{\partial\varphi_x}{\partial x}\right)^2 + \left(\frac{\partial\varphi_y}{\partial y}\right)^2 + 2\nu\left(\frac{\partial\varphi_x}{\partial x}\right)\left(\frac{\partial\varphi_y}{\partial y}\right)\right]\right.$$

$$\left. + \frac{Gh^3}{12}\left(\frac{\partial\varphi_x}{\partial y} + \frac{\partial\varphi_y}{\partial x}\right)^2 + \tau_{xz}\left(\frac{\partial w}{\partial x} + \varphi_x\right) + \tau_{yz}\left(\frac{\partial w}{\partial y} + \varphi_y\right)\right\} dA \qquad (3.23)$$

Now, introducing D and replacing τ_{xz} and τ_{yz} and by using Hooke's Law and Eq.(3.5) , the total strain energy will be :

$$U = \frac{1}{2}\iint_R \Big\{ D\Big[\Big(\frac{\partial \varphi_x}{\partial x}\Big)^2 + \Big(\frac{\partial \varphi_y}{\partial y}\Big)^2 + 2\nu\Big(\frac{\partial \varphi_x}{\partial x}\Big)\Big(\frac{\partial \varphi_y}{\partial y}\Big)\Big]$$

$$+ \frac{Gh^3}{12}\Big(\frac{\partial \varphi_x}{\partial y} + \frac{\partial \varphi_y}{\partial x}\Big)^2$$

$$+ khG\Big[\Big(\frac{\partial w}{\partial x} + \varphi_x\Big)^2 + \Big(\frac{\partial w}{\partial y} + \varphi_y\Big)^2\Big]\Big\}\, dA \qquad (3.24)$$

3.3 KINETIC ENERGY :

The kinetic energy per unit volume, according to the general linear theory is given by the following equation :

$$T_v = \frac{\rho}{2}\Big\{\Big(\frac{\partial u}{\partial t}\Big)^2 + \Big(\frac{\partial v}{\partial t}\Big)^2 + \Big(\frac{\partial w}{\partial t}\Big)^2\Big\} \qquad (3.25)$$

using Eq.(3.2) with the above equation

$$T_v = \frac{\rho}{2}\Big\{z^2\Big(\frac{\partial \varphi_x}{\partial t}\Big)^2 + z^2\Big(\frac{\partial \varphi_y}{\partial t}\Big)^2 + \Big(\frac{\partial w}{\partial t}\Big)^2\Big\} \qquad (3.26)$$

integrating Eq.(3.26) with respect to the plate thickness, it becomes :

$$T_A = \int_{-h/2}^{h/2} \frac{\rho}{2}\Big\{z^2\Big(\frac{\partial \varphi_x}{\partial t}\Big)^2 + z^2\Big(\frac{\partial \varphi_y}{\partial t}\Big)^2 + \Big(\frac{\partial w}{\partial t}\Big)^2\Big\}\, dz$$

$$= \frac{1}{2}\frac{\rho h^3}{12}\Big\{\Big(\frac{\partial \varphi_x}{\partial t}\Big)^2 + \Big(\frac{\partial \varphi_y}{\partial t}\Big)^2\Big\} + \frac{\rho h}{2}\Big(\frac{\partial w}{\partial t}\Big)^2 \Big\} \qquad (3.27)$$

Hence, the total kinetic energy will be obtained by integrating Eq.(3.27) (Kinetic energy per unit length) over the whole region (area).

$$T = 1/2 \int\int \{\frac{\rho h^3}{12}[(\frac{\partial \varphi_x}{\partial t})^2 + (\frac{\partial \varphi_y}{\partial t})^2] + \rho h(\frac{\partial w}{\partial t})^2\} \, dA \qquad (3.28)$$

3.4 EQUATIONS OF MOTION :

Equations of motion can be obtained by applying the principle of virtual work to the equation of the total kinetic energy Eq.(3.23) and the total strain energy Eq.(3.28).

First, for the kinetic energy :

$$\delta T = \frac{1}{2} \int\int_R [\frac{\rho h^3}{12}\{2\frac{\partial \varphi_x}{\partial t}\frac{\partial \delta\varphi_x}{\partial t} + 2\frac{\partial \varphi_y}{\partial t}\frac{\partial \delta\varphi_y}{\partial t}\}$$

$$+ 2\rho h\frac{\partial w}{\partial t}\frac{\partial \delta w}{\partial t}] \, dA \qquad (3.29)$$

Also, for the strain energy:

$$\delta U = \frac{1}{2} \int\int\{D[2\frac{\partial \varphi_x}{\partial x}\frac{\partial \delta\varphi_x}{\partial x} + 2\frac{\partial \varphi_y}{\partial y}\frac{\partial \delta\varphi_y}{\partial y}$$

$$+ 2\nu\frac{\partial \varphi_x}{\partial x}\frac{\partial \delta\varphi_y}{\partial y} + 2\nu\frac{\partial \varphi_y}{\partial y}\frac{\partial \delta\varphi_x}{\partial x}]$$

$$+ 2\frac{Gh^3}{12}[(\frac{\partial \varphi_x}{\partial y} + \frac{\partial \varphi_y}{\partial x})(\frac{\partial \delta\varphi_x}{\partial y} + \frac{\partial \delta\varphi_y}{\partial x})]$$

$$+ khG\Big[2\Big(\frac{\partial w}{\partial x} + \varphi_x\Big)\Big(\frac{\partial \delta w}{\partial x} + \delta\varphi_x\Big)$$

$$+ 2\Big(\frac{\partial w}{\partial y} + \varphi_y\Big)\Big(\frac{\partial \delta w}{\partial y} + \delta\varphi_y\Big)\Big]\Big\}\, dA \qquad (3.30)$$

Now introducing Eq.(3.29) and Eq.(3.30) in the variational principle :

$$\int_{t_1}^{t_2} (\delta T - \delta\pi)\, dt = 0 \qquad (3.31)$$

where π is the summation of the total strain and potential energy (i.e. $\pi = U + V$) and since there is no external load (or force) , (i.e $V = \iint_R wq\, dA = 0$) and hence $\pi = U$, and Eq.(3.31) will be :

$$\int_{t_1}^{t_2}\iint_R \Big\{ \Big[\frac{\rho h^3}{12}\Big\{\frac{\partial \varphi_x}{\partial t}\frac{\partial \delta\varphi_x}{\partial t} + \frac{\partial \varphi_y}{\partial t}\frac{\partial \delta\varphi_y}{\partial t}\Big\} + \rho h\frac{\partial w}{\partial t}\frac{\partial \delta w}{\partial t}\Big]$$

$$- \Big[D\Big\{\frac{\partial \varphi_x}{\partial x}\frac{\partial \delta\varphi_x}{\partial x} + \frac{\partial \varphi_y}{\partial y}\frac{\partial \delta\varphi_y}{\partial y} + \nu\frac{\partial \varphi_x}{\partial x}\frac{\partial \delta\varphi_y}{\partial y} + \nu\frac{\partial \varphi_y}{\partial y}\frac{\partial \delta\varphi_x}{\partial x}\Big\}$$

$$+ \frac{Gh^3}{12}\Big\{\Big(\frac{\partial \varphi_x}{\partial y} + \frac{\partial \varphi_y}{\partial x}\Big)\Big(\frac{\partial \delta\varphi_x}{\partial y} + \frac{\partial \delta\varphi_y}{\partial x}\Big)\Big\}$$

$$+ khG\Big\{\Big(\frac{\partial w}{\partial x} + \varphi_x\Big)\Big(\frac{\partial \delta w}{\partial x} + \delta\varphi_x\Big)$$

$$+ \Big(\frac{\partial w}{\partial y} + \varphi_y\Big)\Big(\frac{\partial \delta w}{\partial y} + \delta\varphi_y\Big)\Big\}\Big]\Big\}\, dA dt = 0 \qquad (3.32)$$

Now, integrating by parts with respect to time for the first three terms keeping in mind that all variations at the limits (i.e at $t = t_1$ and $t = t_2$ are equal

= 0) and for all but the last of the other terms we apply Green's theorem :

$$\iint_R G\frac{\partial H}{\partial x}\,dxdy = -\iint_R H\frac{\partial G}{\partial x}\,dxdy + \oint_\Gamma GHdy$$

and ,

$$\iint_R G\frac{\partial H}{\partial y}\,dxdy = -\iint_R H\frac{\partial G}{\partial x}\,dxdy - \oint_\Gamma GHdx \qquad (3.33)$$

Now, Eq.(3.32) will have the form :

$$\int_{t_1}^{t_2}\iint_R \Big\{ -\Big[\frac{\rho h^3}{12}\frac{\partial^2\varphi_x}{\partial t^2}\delta\varphi_x + \frac{\rho h^3}{12}\frac{\partial^2\varphi_y}{\partial t^2}\delta\varphi_y + \rho h\frac{\partial^2 w}{\partial t^2}\delta w\Big]$$

$$+ D\Big[\frac{\partial^2\varphi_x}{\partial x^2}\delta\varphi_x + \frac{\partial^2\varphi_y}{\partial y^2}\delta\varphi_y + \nu\frac{\partial^2\varphi_x}{\partial x\partial y}\delta\varphi_y + \nu\frac{\partial^2\varphi_y}{\partial x\partial y}\delta\varphi_x\Big]$$

$$+ \frac{Gh^3}{12}\Big[\frac{\partial^2\varphi_x}{\partial y^2}\delta\varphi_x + \frac{\partial^2\varphi_x}{\partial y\partial x}\delta\varphi_y + \frac{\partial^2\varphi_y}{\partial x\partial y}\delta\varphi_x + \frac{\partial^2\varphi_y}{\partial x^2}\delta\varphi_y\Big]$$

$$+ KGh\Big[\frac{\partial^2 w}{\partial x^2}\delta w + \frac{\partial w}{\partial x}\delta\varphi_x - \frac{\partial\varphi_x}{\partial x}\delta w - \varphi_x\delta\varphi_x$$

$$+ \frac{\partial^2 w}{\partial y^2}\delta w + \frac{\partial w}{\partial y}\delta\varphi_y - \frac{\partial\varphi_y}{\partial y}\delta w - \varphi_y\delta\varphi_y\Big]\Big\}\,dAdt$$

$$+ \int_{t_1}^{t_2}\oint_\Gamma \Big\{ -D\Big[\frac{\partial\varphi_x}{\partial x}\delta\varphi_x dy - \frac{\partial\varphi_y}{\partial y}\delta\varphi_y dx - \nu\frac{\partial\varphi_x}{\partial x}dx + \nu\frac{\partial\varphi_x}{\partial y}\delta\varphi_x dy\Big]$$

$$- \frac{Gh^3}{12}\Big[-\frac{\partial\varphi_x}{\partial y}\delta\varphi_x dy + \frac{\partial\varphi_x}{\partial y}\delta\varphi_y dy - \frac{\partial\varphi_y}{\partial x}\delta\varphi_x dx + \frac{\partial\varphi_y}{\partial x}\delta\varphi_y dy\Big]$$

$$- KGh\left[\frac{\partial w}{\partial x}\delta w dy - \varphi_x \delta w dy - \frac{\partial w}{\partial y}\delta w dx + \varphi_y \delta w dx\right]\Big\} dt = 0 \quad (3.34)$$

Collecting terms in the above formulation with respect to variation terms, we have :

$$\int_{t_1}^{t_2}\iint_R \Big\{\Big[- \frac{\rho h^3}{12}\frac{\partial^2 \varphi_x}{\partial t^2} + D\Big(\frac{\partial^2 \varphi_x}{\partial x^2} + \nu\frac{\partial^2 \varphi_y}{\partial x \partial y}\Big) + \frac{Gh^3}{12}\Big(\frac{\partial^2 \varphi_x}{\partial y^2} + \frac{\partial^2 \varphi_y}{\partial x \partial y}\Big)$$

$$+ KGh\Big(\frac{\partial w}{\partial x} - \varphi_x\Big)\Big]\delta\varphi_x$$

$$+ \Big[- \frac{\rho h^3}{12}\frac{\partial^2 \varphi_y}{\partial t^2} + D\Big(\frac{\partial^2 \varphi_y}{\partial x^2} + \nu\frac{\partial^2 \varphi_x}{\partial x \partial y}\Big) + \frac{Gh^3}{12}\Big(\frac{\partial^2 \varphi_y}{\partial x^2} + \frac{\partial^2 \varphi_x}{\partial x \partial y}\Big)$$

$$+ KGh\Big(\frac{\partial w}{\partial y} - \varphi_y\Big)\Big]\delta\varphi_y$$

$$+ \Big[- \rho h\frac{\partial^2 w}{\partial t^2} + KGh\Big(\frac{\partial^2 w}{\partial x^2} - \frac{\partial \varphi_x}{\partial x} + \frac{\partial^2 w}{\partial y^2} - \frac{\partial \varphi_y}{\partial y}\Big)\Big]\delta w\Big\}\, dA\, dt$$

$$+ \int_{t_1}^{t_2}\oint_\Gamma \Big\{\Big[- D\Big(\frac{\partial \varphi_x}{\partial x} + \nu\frac{\partial \varphi_y}{\partial y}\Big)dy + \frac{Gh^3}{12}\Big(\frac{\partial \varphi_x}{\partial y} + \frac{\partial \varphi_y}{\partial x}\Big)\, dx\Big]\delta\varphi_x$$

$$+ \Big[D\Big(\frac{\partial \varphi_y}{\partial y} + \nu\frac{\partial \varphi_x}{\partial x}\Big)dx - \frac{Gh^3}{12}\Big(\frac{\partial \varphi_x}{\partial y} + \frac{\partial \varphi_y}{\partial x}\Big)\, dy\Big]\delta\varphi_y$$

$$- KGh\Big[\frac{\partial w}{\partial x}dy - \varphi_x dy - \frac{\partial w}{\partial y}dx + \varphi_y dx\Big]\delta w\Big\}\, dt = 0 \quad (3.35)$$

In accordance with previous remarks it is clear that each of the coefficients in the integral $\int_{t_1}^{t_2}\iint_R$ for the variations must be zero.

We consider the coefficient for $\delta\varphi_x$ now. We have then:

$$-\frac{\rho h^3}{12}\frac{\partial^2\varphi_x}{\partial t^2} + D\left(\frac{\partial^2\varphi_x}{\partial x^2} + \nu\frac{\partial^2\varphi_y}{\partial x\partial y}\right) + \frac{Gh^3}{12}\left(\frac{\partial^2\varphi_x}{\partial y^2} + \frac{\partial^2\varphi_y}{\partial x\partial y}\right)$$

$$+ KGh\left(\frac{\partial w}{\partial x} - \varphi_x\right) = 0 \qquad (3.36)$$

and similarly for $\delta\varphi_x$ and, δw , we have respectively ,

$$-\frac{\rho h^3}{12}\frac{\partial^2\varphi_y}{\partial t^2} + D\left(\frac{\partial^2\varphi_y}{\partial x^2} + \nu\frac{\partial^2\varphi_x}{\partial x\partial y}\right) + \frac{Gh^3}{12}\left(\frac{\partial^2\varphi_y}{\partial x^2} + \frac{\partial^2\varphi_x}{\partial x\partial y}\right)$$

$$+ KGh\left(\frac{\partial w}{\partial y} - \varphi_y\right) = 0 \qquad (3.37)$$

and

$$-\rho h\frac{\partial^2 w}{\partial t^2} + KGh\left(\frac{\partial^2 w}{\partial x^2} - \frac{\partial\varphi_x}{\partial x} + \frac{\partial^2 w}{\partial y^2} - \frac{\partial\varphi_y}{\partial y}\right) = 0 \qquad (3.38)$$

Eqs. (3.36) , (3.37) and (3.38) are the equations of motion .

Noting that $D = \frac{Eh^3}{12(1-\nu^2)}$ and $G = \frac{E}{2(1+\nu)}$, we may replace the term $\frac{Gh^3}{12}$ by $\frac{D}{2(1-\nu)}$ in the above formulation .

Hence we have the equation of motion in these forms:

$$D\left\{\frac{\partial^2\varphi_x}{\partial x^2} + \frac{1-\nu}{2}\frac{\partial^2\varphi_x}{\partial y^2} + \frac{1+\nu}{2}\frac{\partial^2\varphi_y}{\partial x\partial y}\right\}$$

$$+ KGh\left(\frac{\partial w}{\partial x} - \varphi_x\right) - \frac{\rho h^3}{12}\frac{\partial^2 \varphi_x}{\partial t^2} = 0 \qquad (3.39)$$

$$D\left\{\frac{\partial^2 \varphi_y}{\partial y^2} + \frac{1-\nu}{2}\frac{\partial^2 \varphi_y}{\partial x^2} + \frac{1+\nu}{2}\frac{\partial^2 \varphi_x}{\partial x \partial y}\right\}$$

$$+ KGh\left(\frac{\partial w}{\partial y} - \varphi_y\right) - \frac{\rho h^3}{12}\frac{\partial^2 \varphi_y}{\partial t^2} = 0 \qquad (3.40)$$

$$- KGh\left\{\frac{\partial^2 w}{\partial x^2} + \frac{\partial^2 w}{\partial y^2} - \frac{\partial \varphi_x}{\partial x} - \frac{\partial \varphi_y}{\partial y}\right\} + \rho h\frac{\partial^2 w}{\partial t^2} = 0 \qquad (3.41)$$

Now, the equations of motion are given in Eqs. (3.39) , (3.40) and (3.41) and by eliminating φ_x and φ_y we can have the equation of motion in terms of only the deflection of the middle plane (Dynamic Equilibrium Equation of Motion) :

$$\left\{\nabla^2 - \frac{\rho}{KG}\frac{\partial^2}{\partial t^2}\right\}\left\{D\nabla^2 - \frac{\rho h^3}{12}\frac{\partial^2}{\partial t^2}\right\}w + \rho h\frac{\partial^2 w}{\partial t^2} = 0 \qquad (3.42)$$

If only the rotary inertia is deleted from Equation 3.42 we set $\frac{\rho h^3}{12}\frac{\partial^2 w}{\partial t^2} = 0$

We have :

$$D\left\{\nabla^2 - \frac{\rho}{KG}\frac{\partial^2}{\partial t^2}\right\}\nabla^2 w + \rho h\frac{\partial^2 w}{\partial t^2} = 0 \qquad (3.43)$$

Also, if only the effect of transverse shear deformation is deleted by setting $1/kGh \rightarrow 0$ we have :

$$\left\{D\nabla^2 - \frac{\rho h^3}{12}\frac{\partial^2}{\partial t^2}\right\}\nabla^2 w + \rho h\frac{\partial^2 w}{\partial t^2} = 0 \qquad (3.44)$$

Finally, if both of rotary inertia and transverse shear deformation are to be deleted we can have the classical plate equation (see Equation 3.1)

$$D\,\nabla^4 w + \rho h\frac{\partial^2 w}{\partial t^2} = 0 \qquad (3.45)$$

3.5 BOUNDARY CONDITIONS :

Going back to the line integral in Eq.(3.35) and by arranging the terms we have:

$$\int_{t_1}^{t_2}\oint_{\Gamma}\Big\{ \delta\varphi_x dy\Big[- D\Big(\frac{\partial\varphi_x}{\partial x} + \nu\frac{\partial\varphi_y}{\partial y}\Big)\Big] - \delta\varphi_x dx\Big[- \frac{Gh^3}{12}\Big(\frac{\partial\varphi_x}{\partial y} + \frac{\partial\varphi_y}{\partial x}\Big)\Big]$$

$$+ \delta\varphi_x dy\Big[- \frac{Gh^3}{12}\Big(\frac{\partial\varphi_x}{\partial y} + \frac{\partial\varphi_y}{\partial x}\Big)\Big] - \delta\varphi_y dx\Big[- D\Big(\frac{\partial\varphi_y}{\partial y} + \nu\frac{\partial\varphi_x}{\partial x}\Big)\Big]$$

$$+ \delta w dy\Big[- KGh\Big(\frac{\partial w}{\partial x} - \varphi_x\Big)\Big] - \delta w dx\Big[- KGh\Big(\frac{\partial w}{\partial x} - \varphi_y\Big)\Big] \Big\}\, dt = 0 \qquad (3.46)$$

Now using Eqs. (3.12) , (3.14) , (3.15) , (3.18) and (3.19) we have:

$$\int_{t_1}^{t_2}\oint_{\Gamma}\Big\{M_x\delta\varphi_x dy - M_y\delta\varphi_y dx + M_{yx}\delta\varphi_y dy - M_{xy}\delta\varphi_x dx$$

$$- Q_x\delta w dy + Q_y\delta w dx\Big\}\, dt = 0 \qquad (3.47)$$

Introducing transformation coordinate in accordance with Figure 3.4, we can replace (dx) by $-a_{vy}ds$ and (dy) by $a_{vx}ds$ to get :

$$\int_{t_1}^{t_2}\oint_{\Gamma}\{ - M_x a_{vx}\delta\varphi_x + M_y a_{vy}\delta\varphi_y + M_{xy}a_{vx} + M_{xy}a_{vy}\delta\varphi_x$$

$$- Q_x a_{vx}\delta w - Q_y a_{vy}\delta w\} ds\, dt = 0 \qquad (3.48)$$

Using v and s as coordinates we can state :

$$\varphi_x = a_{vx}\,\varphi_v - a_{vy}\,\varphi_s$$

$$\varphi_y = a_{vy}\,\varphi_v - a_{vx}\,\varphi_s \qquad (3.49)$$

Solving for φ_v and φ_s from Eq.(3.49) , we have :

$$\varphi_v = a_{vx}\,\varphi_x + a_{vy}\,\varphi_y$$

$$\varphi_s = a_{vx}\,\varphi_y - a_{vy}\,\varphi_x \qquad (3.50)$$

Now, substituting in Eq.(3.48) and collecting terms:

$$\int_{t_1}^{t_2}\oint_{\Gamma}\{[\, a^2{}_{vx}M_x + 2a_{vx}a_{vy}M_{xy} + a^2{}_{vy}M_y]\delta\varphi_v$$

$$+ [\, - a_{vx}a_{vy}M_x + a_{vy}a_{vx}M_y + (a^2{}_{vx} - a^2{}_{vy})M_{xy}]\delta\varphi_s$$

$$- [a_{vx}\,Q_x + a_{vy}\,Q_y]\delta w\,\} ds\, dt = 0 \qquad (3.51)$$

Now, using the following suitable moment transformation equation (described in detailes in reference [59]) :

$$M_v = a^2_{vx} M_x + 2a_{vx}a_{vy}M_{xy} + a^2_{vy}M_y$$

$$M_{vs} = a_{vx}a_{vy}(M_y - M_x) + (a^2_{vx} - a^2_{vy})M_{xy}$$

$$Q_v = a_{vx} Q_x + a_{vy} Q_y \qquad (3.52)$$

Hence, Eq.(3.51) will be as follows :

$$\int_{t_1}^{t_2} \oint_{\Gamma} \{M_v \delta\varphi_v + M_{vs}\delta\varphi_s - Q_v \delta w\}\, ds\, dt \qquad (3.53)$$

Now, we can obtain the boundary condition from Eq.(3.53) :

Either $M_v = 0$ OR φ_v is specified (a)

Either $M_{vs} = 0$ OR φ_s is specified (b)

Either $Q_v = 0$ OR w is specified (c) (3.54)

Note that we get three boundary conditions on the edge of the plate as opposed to the two boundary conditions in classical plate theory.

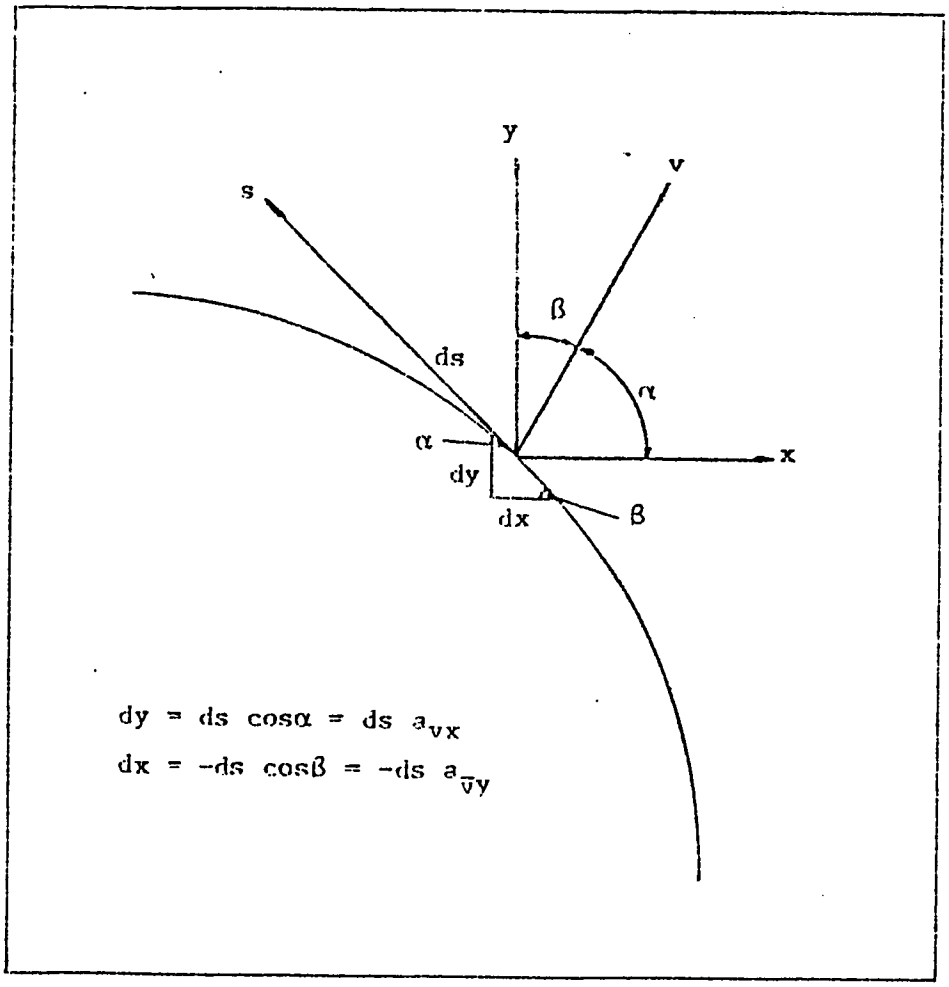

Figure 3.4 : Transformation coordinate

CHAPTER 4

FINITE DIFFERENCE FORMULATION

The strain and kinetic energy equations previously obtained [Eqs.(3.24) and (3.28)] are expressed in dimensionless forms. Then by applying the finite difference method, they are expressed in terms of discrete displacement and rotational components. Harmonic motion is assumed to eliminate time dependence. Euler's necessary condition is applied to minimize the total energy of the system and finally an algebraic eigenvalue problem is obtained.

4.1 DIMENSIONAL ANALYSIS :

Consider a rectangular plate with dimensions shown in Figure 4.1 in which the position coordinates are x,y and z respectively. In accordance with Figure 4.1, the strain and kinetic energy expressions [Eqs.(3.24) and (3.28)] can be expressed as:

$$U = \frac{1}{2}\int_{oo}^{ab}\int \Big\{ D\Big[\Big(\frac{\partial \varphi_x}{\partial x}\Big)^2 + \Big(\frac{\partial \varphi_y}{\partial y}\Big)^2 + 2\nu\Big(\frac{\partial \varphi_x}{\partial x}\Big)\Big(\frac{\partial \varphi_y}{\partial y}\Big)\Big]$$

$$+ \frac{Gh^3}{12}\Big(\frac{\partial \varphi_x}{\partial y} + \frac{\partial \varphi_y}{\partial x}\Big)^2$$

$$+ khG\Big[\Big(\varphi_x + \frac{\partial \overline{w}}{\partial x}\Big)^2 + \Big(\varphi_y + \frac{\partial \overline{w}}{\partial y}\Big)^2\Big]\Big\}\, dy\, dx \qquad (4.1)$$

$$T = \frac{1}{2}\int_{oo}^{ab}\int \left\{\frac{\rho h^3}{12}\left[\left(\frac{\partial \varphi_x}{\partial t}\right)^2 + \left(\frac{\partial \varphi_y}{\partial t}\right)^2\right] + \rho h\left(\frac{\partial \overline{w}}{\partial t}\right)^2\right\} dy\, dx \qquad (4.2)$$

Using the following dimensional parameters in accordance with Figure 4.2 the strain and kinetic energy expressions [Eqs.(4.1) and (4.2)] can be expressed in non-dimensional forms :

$$\zeta = \frac{x}{a} \qquad \partial x = a\partial\zeta$$

$$\eta = \frac{y}{a} \qquad \partial y = a\partial\eta$$

$$w = \frac{\overline{w}}{a} \qquad \partial\overline{w} = a\partial w$$

$$\gamma = \frac{b}{a} \qquad \beta = \frac{h}{a} \qquad (4.3)$$

and ,

$$\Delta x = \frac{a}{M-1} \qquad \Delta\zeta = \frac{1}{M-1}$$

$$\Delta y = \frac{b}{N-1} \qquad \Delta\eta = \frac{1}{N-1} \qquad (4.4)$$

where γ is the aspect ratio , β is the plate thickness/length ratio , and M and N are numbers of nodes per length and width respectively.

Noting that $D = \frac{Eh^3}{12(1-\nu^2)}$, the strain energy will be:

$$U = \frac{1}{2}\int_{o}^{1}\int_{o}^{\gamma}\left\{\frac{Eh^3}{12(1-\nu^2)a^2}\left[\left(\frac{\partial\varphi_\zeta}{\partial\zeta}\right)^2 + \left(\frac{\partial\varphi_\eta}{\partial\eta}\right)^2 + 2\nu\left(\frac{\partial\varphi_\zeta}{\partial\zeta}\right)\left(\frac{\partial\varphi_\eta}{\partial\eta}\right)\right]\right.$$

$$+ \frac{Gh^3}{12a^2}\left(\frac{\partial\varphi_\zeta}{\partial\zeta} + \frac{\partial\varphi_\eta}{\partial\eta}\right)^2$$

$$\left. + khG\left[\left(\varphi_\zeta + \frac{\partial w}{\partial\zeta}\right)^2 + \left(\varphi_\eta + \frac{\partial w}{\partial\eta}\right)^2\right]\right\} a^2\, d\eta\, d\zeta \qquad (4.5)$$

Noting that $G = \frac{E}{2(1+\nu)}$ and $\beta = \frac{h}{a}$ Eq.(4.5) will be

$$U = \frac{1}{2}\frac{Eha^2}{(1-\nu^2)}\int_{o}^{1}\int_{o}^{\gamma}\left\{\frac{\beta^2}{12}\left[\left(\frac{\partial\varphi_\zeta}{\partial\zeta}\right)^2 + \left(\frac{\partial\varphi_\eta}{\partial\eta}\right)^2 + 2\nu\left(\frac{\partial\varphi_\zeta}{\partial\zeta}\right)\left(\frac{\partial\varphi_\eta}{\partial\eta}\right)\right]\right.$$

$$+ \frac{\beta^2}{12}\frac{1-\nu}{2}\left(\frac{\partial\varphi_\zeta}{\partial\zeta} + \frac{\partial\varphi_\eta}{\partial\eta}\right)^2$$

$$\left. + \frac{k(1-\nu)}{2}\left[\left(\varphi_\zeta + \frac{\partial w}{\partial\zeta}\right)^2 + \left(\varphi_\eta + \frac{\partial w}{\partial\eta}\right)^2\right]\right\} a^2\, d\eta\, d\zeta \qquad (4.6)$$

Similarly, for the kinetic energy expression , Eq.(4.2) will be :

$$T = \frac{1}{2}\int_{o}^{1}\int_{o}^{\gamma}\left\{\frac{\rho h^3}{12}\left[\left(\frac{\partial\varphi_\zeta}{\partial\zeta}\right)^2 + \left(\frac{\partial\varphi_\eta}{\partial\eta}\right)^2\right] + \rho ha^2\left(\frac{\partial w}{\partial t}\right)^2\right\} a^2\, d\eta\, d\zeta \qquad (4.7)$$

and by arranging ,

$$T = \frac{1}{2}\rho h^3 a^2\int_{o}^{1}\int_{o}^{\gamma}\left\{\frac{1}{12}\left[\left(\frac{\partial\varphi_\zeta}{\partial\zeta}\right)^2 + \left(\frac{\partial\varphi_\eta}{\partial\eta}\right)^2\right] + \frac{1}{\beta^2}\left(\frac{\partial w}{\partial t}\right)^2\right\} d\eta\, d\zeta \qquad (4.8)$$

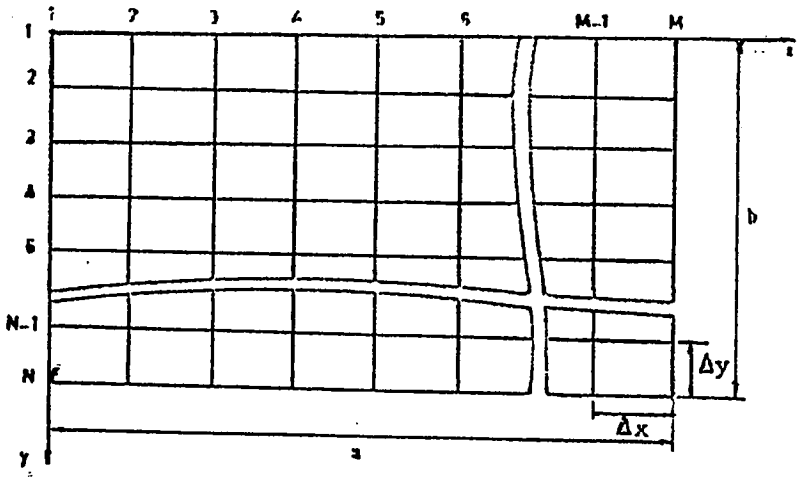

Figure 4.1 : Node set for rectangular plate

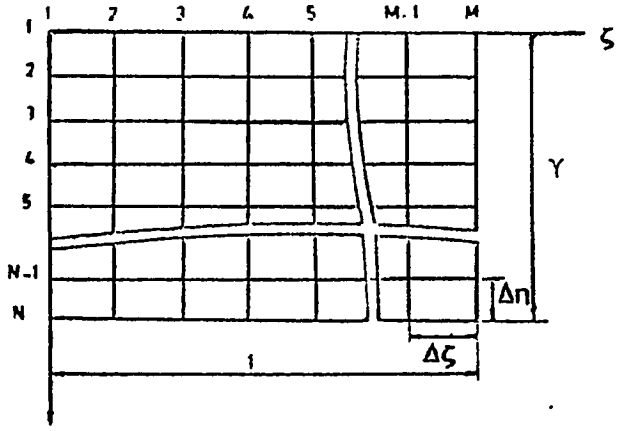

Figure 4.2 : Node set for dimensionless rectangular plate

4.2 EULER'S EQUATION :

The integral in the strain energy expression is replaced by finite approximation summation based on the mesh covering the plate. Subsequently, with the use of standard finite difference formulas, the total strain energy of the plate can be expressed as a quadratic form in discrete displacement and rotational components:

$$F\{\varphi_{\zeta_{i,j}}, \varphi_{\eta_{i,j}}, w_{i,j}\} \approx U \tag{4.9}$$

Similar approximation reduce the kinetic energy to a linear function H of the squares of discrete velocities :

$$H\{(\frac{\partial \varphi_\zeta}{\partial t})^2_{i,j}, (\frac{\partial \varphi_\eta}{\partial t})^2_{i,j}, (\frac{\partial w}{\partial t})^2_{i,j}\} \approx T \tag{4.10}$$

Application of Euler's necessary condition to minimize the total energy of the system gives the relations:

$$\frac{d}{dt}\{\frac{\partial L}{\partial \dot{q}_k}\} - \frac{\partial L}{\partial q_k} = 0 \qquad k = 1,2,3 \tag{4.11}$$

where L is the Lagrangian defined as

$$L = T - U \tag{4.12}$$

Equation (4.11) is known as Lagrange's Equation. The solution of harmonic motion may be assumed in the form of the product :

$$\varphi_\zeta(\zeta,\eta,t) = (A\cos\omega t + B\sin\omega t)\, \Psi_\zeta(\zeta,\eta)$$

$$\varphi_\eta(\zeta,\eta,t) = (A\cos\omega t + B\sin\omega t)\,\Psi_\eta(\zeta,\eta)$$

$$w(\zeta,\eta,t) = (A\cos\omega t + B\sin\omega t)\,w(\zeta,\eta) \qquad (4.13)$$

and the accelerations at the nodes of the mesh are obtained as:

$$\{\ddot{\varphi}_\zeta(\zeta,\eta,t)\}_{i,j} = -\omega^2\{\varphi_\zeta(\zeta,\eta,t)\}_{i,j}(A\cos\omega t + B\sin\omega t)$$

$$\{\ddot{\varphi}_\eta(\zeta,\eta,t)\}_{i,j} = -\omega^2\{\varphi_\eta(\zeta,\eta,t)\}_{i,j}(A\cos\omega t + B\sin\omega t)$$

$$\{\ddot{w}(\zeta,\eta,t)\}_{i,j} = -\omega^2\{w(\zeta,\eta,t)\}_{i,j}(A\cos\omega t + B\sin\omega t) \qquad (4.14)$$

Now applying Eqs.(4.13) and (4.14) to Lagrange's Equation [Eq.(4.11)] , the result will be a matrix eigenvalue problem as follows:

$$[\,A\,]\,\{\,X\,\} = \Omega\,\{\,X\,\} \qquad (4.15)$$

Where Ω is the frequency parameter and can be obtained from Eqs.(4.6) and (4.8) by :

$$\Omega = \omega h\sqrt{\frac{\rho(1-\nu^2)}{E}} \qquad (4.16)$$

A computer program is developed for this analysis. It carries out the substitution of finite difference equation, performs the partial differentiation required by Eq.(4.11) , calculates the natural frequencies and prints out the mode shapes and the nodal patterns.

Note that the formulation was carried for rectangular plate and since this thesis is concerned only about the square plate , the formulation will be the

same but with some minor changes, which are $a = b$, $\Delta x = \Delta y$, $M = N$, $\Delta\zeta = \Delta\eta$, and the aspect ratio $\gamma = 1$, where $\gamma = b/a$.

The total strain energy of the plate is computed as the summation of the strain energies of the nodal sub-domains obtained by using interlacing grids. The integrals in the strain and kinetic energy expressions are replaced by finite approximation summation and applying Euler's necessary condition to minimize the total energy of the system. Finite difference equations are obtained for each of the displacement and rotational components associated with each node.

4.3 CONCEPT OF INTERLACING GRIDS & NODAL SUB-DOMAINS :

For the application of the interlacing grids method, the strain energy function given by Eq.(4.6) is divided into sub functions as follows :

$$U = \frac{1}{2}\frac{Eha^2}{(1-\nu^2)}\int_{oo}^{11}\{f_1 + f_2 + f_3\}\, d\eta\, d\zeta \qquad (4.17)$$

Where ,

$$f_1 = \frac{\beta^2}{12}\left(\frac{\partial\varphi_\zeta}{\partial\zeta}\right)^2 + \frac{k(1-\nu)}{2}\left(\varphi_\zeta + \frac{\partial w}{\partial\zeta}\right)^2 \qquad (4.18)$$

$$f_2 = \frac{\beta^2}{12}\left(\frac{\partial\varphi_\eta}{\partial\eta}\right)^2 + \frac{k(1-\nu)}{2}\left(\varphi_\eta + \frac{\partial w}{\partial\eta}\right)^2 \qquad (4.19)$$

$$f_3 = \frac{\beta^2}{12}\frac{1-\nu}{2}\left(\frac{\partial\varphi_\zeta}{\partial\eta} + \frac{\partial\varphi_\eta}{\partial\zeta}\right)^2 + 2\nu\left(\frac{\partial\varphi_\zeta}{\partial\zeta}\right)\left(\frac{\partial\varphi_\eta}{\partial\eta}\right) \qquad (4.20)$$

The nodal sub-domains used to determine the sub-strain energies for each sub-function f_1, f_2, f_3 are shown in Figures 4.3 , 4.4 and 4.5 . Note that equal intervals are used. The sub-strain energies are computed as the sum of strain energies summed over the set of non-overlapping sub-domains. It is better to mention that employing two sets of interlacing grids provides a finite difference formulation with a reduced mesh size and results in reduced discretization error. The node set associated with kinetic energy function f_4 is shown in Figure 4.6

The total strain energy U can be separated into three sub-strain energies U_1, U_2 and U_3 that associated with f_1, f_2 and f_3 respectively as follows.

$$U_1 = \frac{1}{2}\frac{Eha^2}{(1-\nu^2)}\int_{oo}^{11}\int f_1 \, d\eta \, d\zeta \tag{4.21}$$

$$U_2 = \frac{1}{2}\frac{Eha^2}{(1-\nu^2)}\int_{oo}^{11}\int f_2 \, d\eta \, d\zeta \tag{4.22}$$

$$U_3 = \frac{1}{2}\frac{Eha^2}{(1-\nu^2)}\int_{oo}^{11}\int f_3 \, d\eta \, d\zeta \tag{4.23}$$

By taking small variation in the sub-strain energies , Eqs.(4.21) , (4.22) and (4.23) can be written as:

$$(\Delta U_1)_{i,j+1/2} = \frac{1}{2}\frac{Eha^2}{(1-\nu^2)}\{(f_1)_{i,j+1/2}\Delta\zeta\,\Delta\eta\,\}\Delta\eta\,\Delta\zeta \tag{4.24}$$

$$(\Delta U_2)_{i+1/2,j} = \frac{1}{2}\frac{Eha^2}{(1-\nu^2)}\{(f_2)_{i+1/2,j}\Delta\eta\,\Delta\zeta\,\}\Delta\eta\,\Delta\zeta \tag{4.25}$$

$$(\Delta U_3)_{i+1/2,j+1/2} = \frac{1}{2}\frac{Eha^2}{(1-\nu^2)}\{(f_3)_{i+1/2,j+1/2}\Delta\eta\,\Delta\zeta\}\Delta\eta\,\Delta\zeta \qquad (4.26)$$

Now, the total sub-strain energies can be computed by the summation over the set of non-overlapping sub-domains as follows :

$$(\Delta U_1) \approx \frac{1}{2}\frac{Eha^2}{(1-\nu^2)}\sum_{i=1}^{N}\sum_{j=1}^{M}\{(f_1)_{i,j+1/2}\}(\Delta\eta\,\Delta\zeta)^2 \qquad (4.27)$$

$$(\Delta U_2) \approx \frac{1}{2}\frac{Eha^2}{(1-\nu^2)}\sum_{i=1}^{N}\sum_{j=1}^{M}\{(f_2)_{i+1/2,j}\}(\Delta\eta\,\Delta\zeta)^2 \qquad (4.28)$$

$$(\Delta U_3) \approx \frac{1}{2}\frac{Eha^2}{(1-\nu^2)}\sum_{i=1}^{N}\sum_{j=1}^{M}\{(f_3)_{i+1/2,j+1/2}\}(\Delta\eta\,\Delta\zeta)^2 \qquad (4.29)$$

and, hence the total strain energy will be :

$$U = U_1 + U_2 + U_3 \qquad (4.30)$$

Similarly, by referring to the total kinetic energy Eq.(4.8) , the kinetic energy sub-function can be expressed as:

$$f_4 = \frac{1}{12}\left[\left(\frac{\partial\varphi_\xi}{\partial t}\right)^2 + \left(\frac{\partial\varphi_\eta}{\partial t}\right)^2\right] + \frac{1}{\beta^2}\left(\frac{\partial w}{\partial t}\right)^2 \qquad (4.31)$$

and finally , the total kinetic energy can be presented in the form :

$$T = \frac{1}{2}\rho h^3 a^2 \sum_{i=1}^{N}\sum_{j=1}^{M}\frac{1}{4}\{(f_4)_{i,j} + (f_4)_{i+1,j} + (f_4)_{i,j+1} + (f_4)_{i+1,j+1}\}(\Delta\eta\,\Delta\zeta)^2 \qquad (4.32)$$

Application of the finite difference formulation for the interior node on the

Lagrangian Equation [Eq.(4.11)] and the corresponding formulation is well explained in details in reference [60].

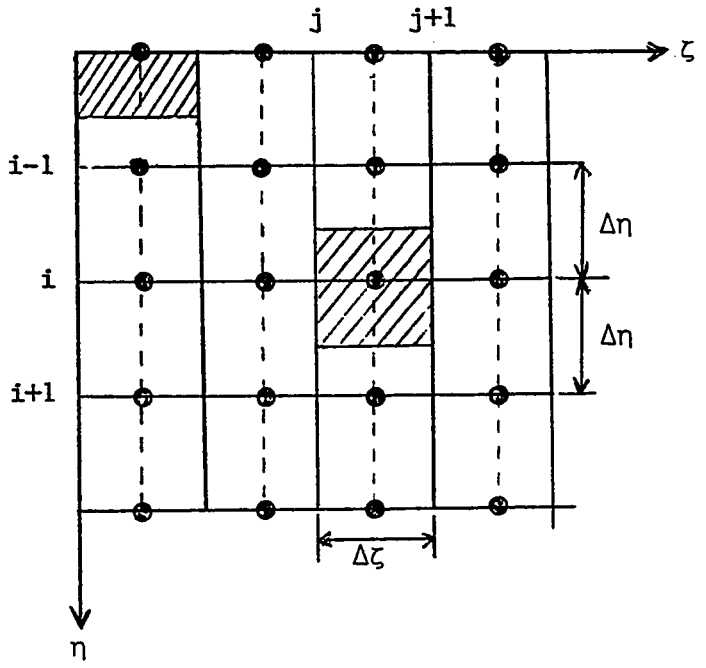

Figure 4.3 : Nodal sub-domain for f_1

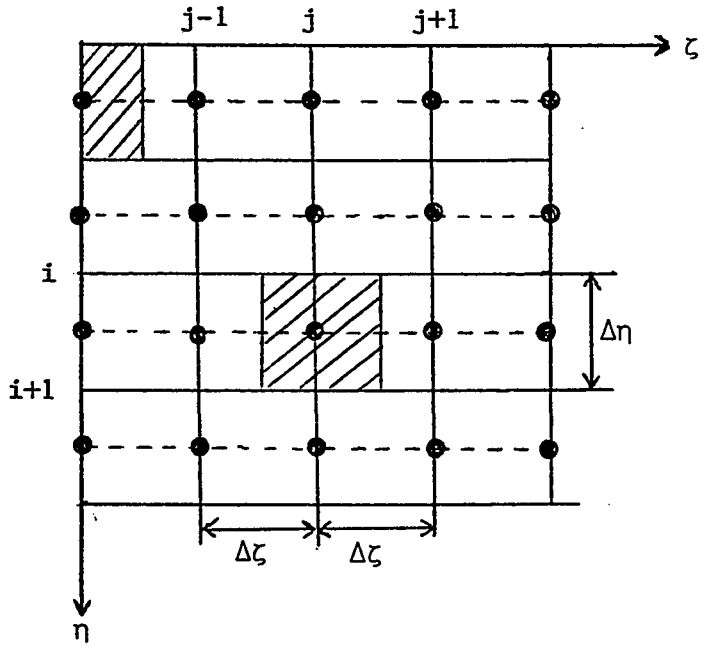

Figure 4.4 : Nodal sub-domain for f_2

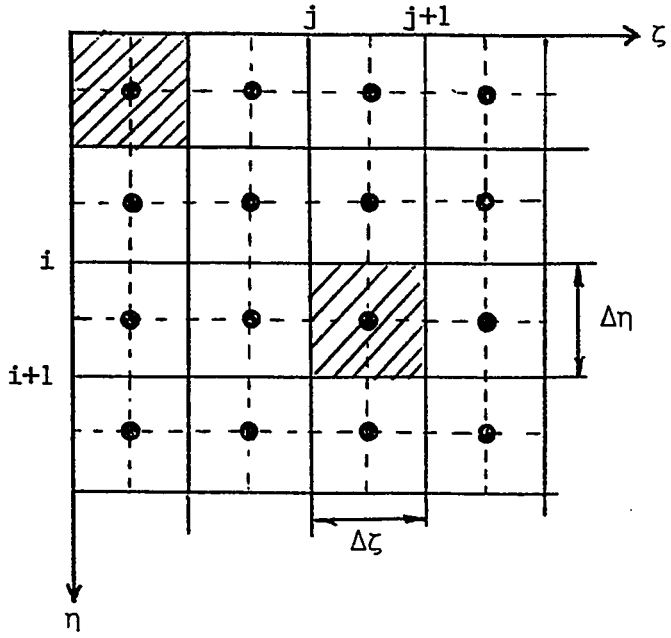

Figure 4.5 : Nodal sub-domain for f_3

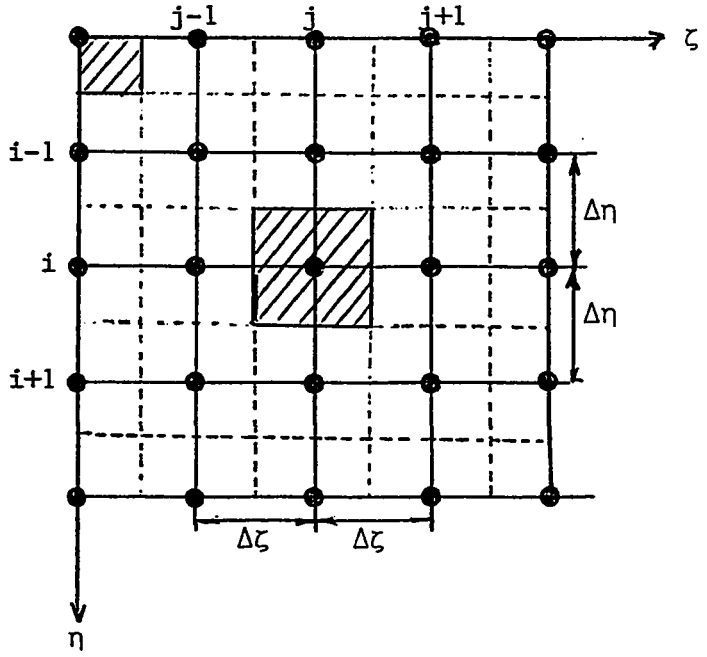

Figure 4.6 : Nodal sub-domain for f_4

CHAPTER 5

EXPERIMENT

The experimental study of structural vibration has always provided a major contribution to our efforts to understand and to control the many vibration phenomena encountered in practice. Since the very early days of awareness of vibrations, experimental observations have been made for the two major objectives of:

a) determining the nature and extent of vibration response levels.

b) verifying theoretical models and predictions.

Today, structural vibration problems present a major hazard and design limitation for a very wide range of engineering products. First, there are a number of structures, from turbine blades to suspension bridges, for which structural integrity is of paramount concern, and for which a thorough and precise knowledge of the dynamic characteristics is essential. Then, there is an even wider set of components or assemblies for which vibration is directly related to performance, either by virtue of causing temporary malfunction during excessive motion or by creating disturbance or discomfort and noise. For all these examples, it is important that the vibration levels encountered in service or operation be anticipated and brought under satisfactory control.

The two vibration measurement objectives indicated above represent two corresponding types of test. The first is one where vibration forces or, more usually, responses are measured during operation of the machine or structure under

study, while the second is a test where the structure component is vibrated with a known excitation , often out of its normal service environment. This second type of test is generally made under much more closely controlled conditions than the former and consequently yields more accurate data acquisition and its subsequent analysis is nowadays called 'Modal Testing'.

5.1 TEST SPECIMEN AND BASE FRAME :

Figure 5.1 shows the square plate of length a symmetrically supported on the diagonals at distance α from the free edges. The case of $\alpha/a = 0$ corresponds to corner supported plate and the one for $\alpha/a = 0.5$ corresponds to a single point support at the center of the plate. In the present study three different steel plates were used with the following dimensions :

Plate 1 : 200 by 200 by 2 mm (i.e. $\beta = 0.01$)

Plate 2 : 200 by 200 by 5 mm (i.e. $\beta = 0.025$)

Plate 3 : 7.5 by 7.5 by 0.375 in (i.e. $\beta = 0.05$)

The material properties of the plates are taken to be :

E : Young's Modulus of Elasticity $= 2.07 \times 10^{11}$ N/m^2

ν : Poisson's Ratio $= 0.3$

ρ : density $= 7.83 \times 10^3$ Kg/m^3

The initial deflection and initial stresses as well as the anisotropy of the material are assumed to be almost negligible.

The details of the test plate and test rig are shown in Figure 5.2. The test rig consists mainly of a vibration isolation table (Low Frequency Mounting

Table) at the sides of which four vertical channels of mild steel of very high stiffness are fixed by means of bolts and nuts. Two thick mild steel beams having T section are welded to each other so as to form a crossed structural frames of form '+'. These two frames are fixed to the vertical channels by means of bolts and nuts. The plate is supported at four points with two screws for each support point at the end of which conical shape is formed in order to give perfect point contact . Two sliding frames for each support point having internal threads to accomplish vertical movement of the screws are free to move horizontally on the flange of the crossed structural frame. These sliding frames are guided in order to support the plate at any desired point. The support structure is shown in Figure 5.3 . The above support structure dimensions (vertical channels , crossed structural frame, sliding frame) limit the dimension of the test plates. The maximum dimension of a square plate that can be tested is 240 mm. Also, the location of the point support is limited to $\alpha = 0.3$. Furthermore modification of the support structure will enable us to perform the test for the entire range of α (from 0 to 0.5) .

The plate is excited via an electromagnetic shaker (Vibration Exciter) which is bolted to the vibration isolation table at the center. By shaking the plate sinusoidally with radian frequency Ω and peak acceleration a (m/s^2) , a uniformly distributed pulsating load is applied to specimen.

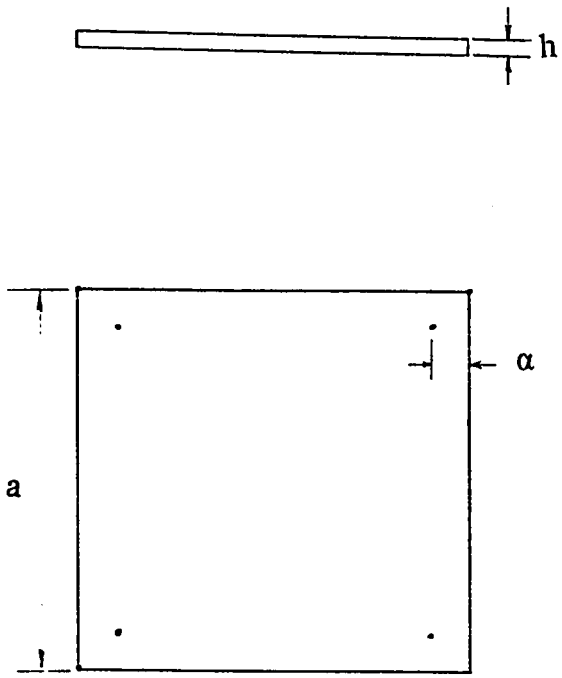

Figure 5.1 : Test specimen

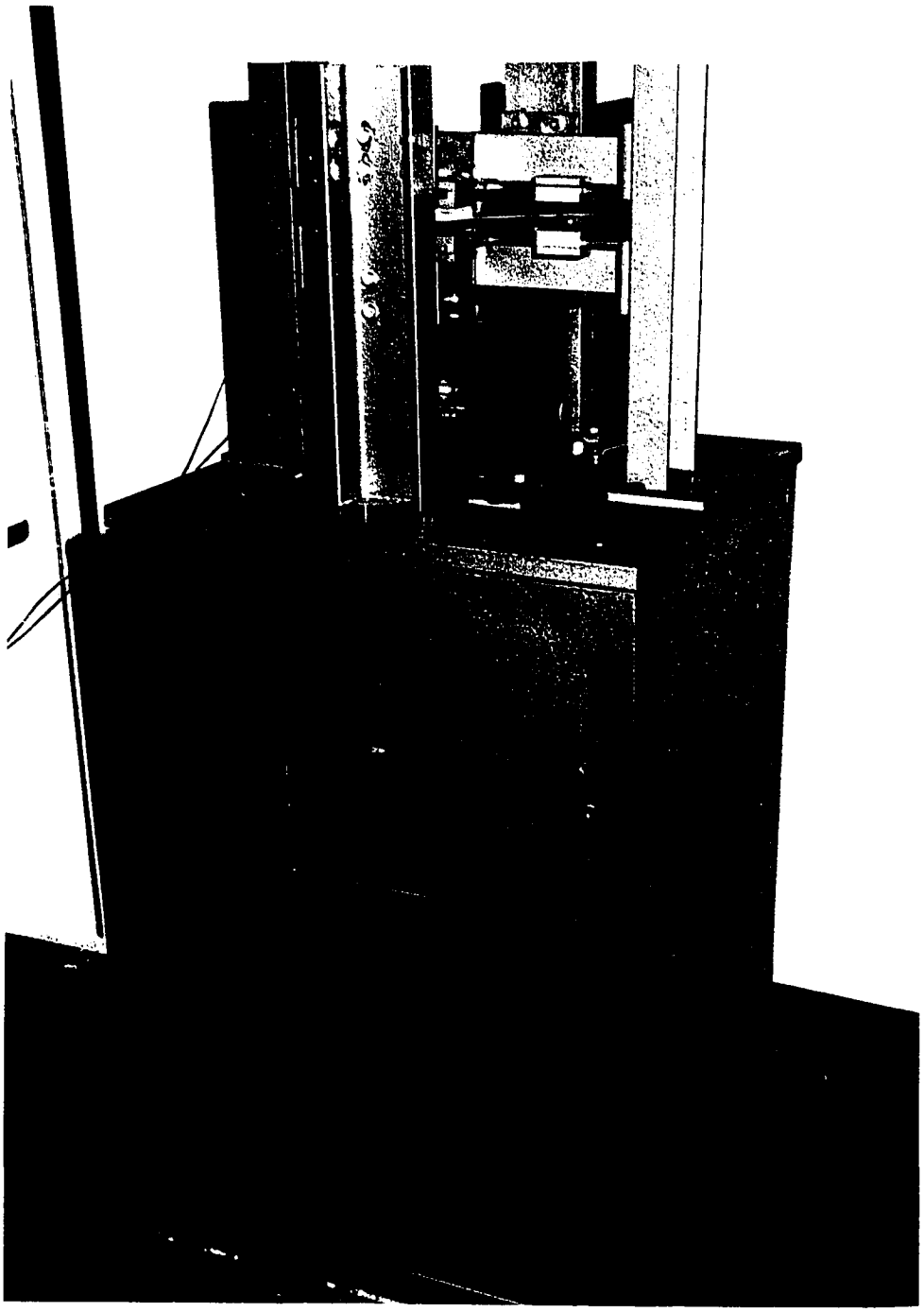

Figure 5.2 : Test plate and test rig

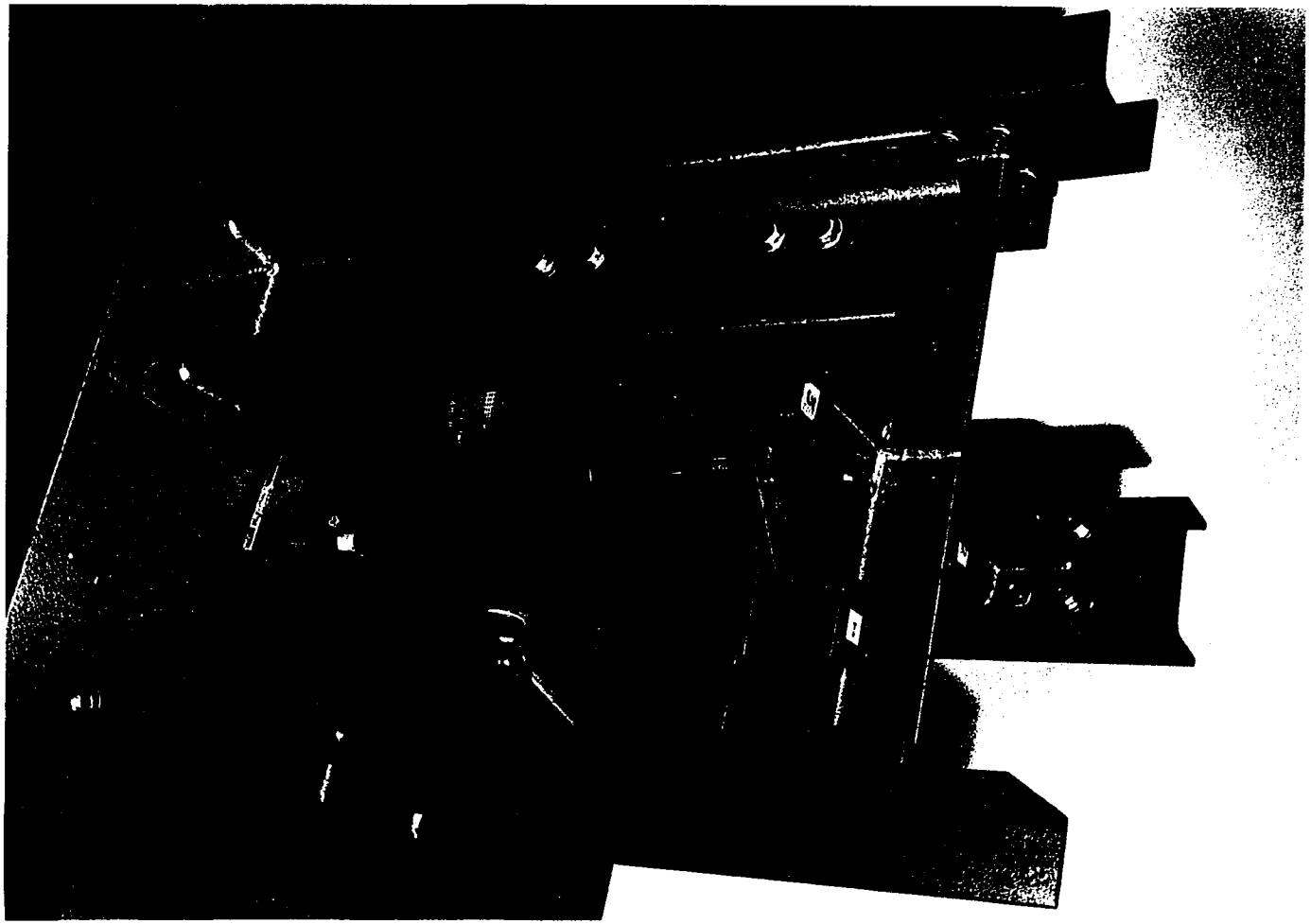

Figure 5.3 : Support structure

5.2 TEST EQUIPMENT AND INSTRUMENTATION :

Although techniques used in the field of vibration testing have become more complicated during the past few years. Vibration testing (Modal Testing) has been performed, the most extensively used technique , however , is still the sweeping sine wave test. The reason for the popularity of this test is that it requires fairly simple and inexpensive electronic equipment , and for laboratory work it is a highly efficient tool for evaluating experimental models for frequency response.

Test will be conducted by exciting the test plate periodically and measuring the absolute acceleration by a piezoelectric accelerometer. The mounting of the test plate, the excitation system and the data recording system arrangements are shown in the block diagram of Figure 5.4 . A piezoelectric accelerometer is used to monitor the acceleration of the exciter head.

Most of the equipment and instruments are Bruel & Kjaer products . For reference , a photograph of the actual experimental lay-out is shown in Figure 5.5 . The apparatus used can be divided into two separate systems namely , the excitation system and the data recording system.

5.2.a Excitation system :

The set-up numbered [1] to [6] in Figure 5.4 is the instrumentation related to the excitation system. In the figure , the Exciter Control type B&K 1047 [1] is used to generate sine signal which covers 5 Hz to 10 kHz in one continuous range. This signal is amplified by using a 180 VA Power Amplifier type B&K 2712 [2] , which has low distortion over wide frequency range. The amplified signal is used to drive the Vibration Exciter type B&K 4808 [3]. The

maximum dynamic force of the Vibration Exciter is about 187 N with assisted air cooling. The Accelerometer type B&K 4343 (charge sensitivity of 1.022 pC/ms^{-2} , voltage sensitivity of 0.922 mV/ms^{-2} and weight 16.3 g) [4] is attached to the Vibration Exciter head. Conditioning Amplifier type B&K 2625 [5] is used in the feed-back through the Two Channel Tracking Filter type B&K 5716 / WHO255 [6] to the Exciter Control [1]. With this arrangement [1] to [6], the compressor or automatic gain section of the Exciter Control regulates the output from the Exciter Control to the Power Amplifier [2] according to the feedback signal from the Vibration Exciter [3] . Thus the vibration is kept constant at the prescribed level.

5.2.b Data recording system :

The measuring response arrangement used in the experiment is shown in the block diagram numbered [8] to [13] . A piezoelectric accelerometer type B&K 4344 (charge sensitivity of 0.310 pC/ms^{-2} , voltage sensitivity of 0.281 mV/ms^{-2} and weight 2.7 g) [8] is used to pick up the response from the vibrating plate [7]. When light structures are tested , such as Plate 1 , light accelerometer should be used to avoid mass loading problem. Because the output signal from the Accelerometer is small , it is entered into a Charge Amplifier type B&K 2635 [9]. The amplified signal is fed to the Two Channel Tracking Filter [6] . The frequency range in the Two Channel Tracking Filter is controlled by the Exciter Control [1] which (as mentioned before) plays as the feedback. Three output signals can be obtained from the Two Channel Tracking Filter [signal A (the excitation), signal B (response) and signal B $\underline{/90^\circ}$] which is used to measure either the phase and the amplitude or the Co-ordinated and the Quadrature components. To measure the phase and the amplitude , the output

signals from the Two Channel Tracking Filter are fed to the Phase Meter type B&K 2971 [10] and the Voltmeter type B&K 2432 [11]. In the second case for measuring the Co-ordinated and the Quadrature components, the three output signals from the Two Channel Tracking Filter are fed to the Cross Spectrum Unit type B&K 5748 [12]. Finally the cross correlated signals are recorded in the X-Y Recorder type B&K 2308 [13] or the Two Channel Level Recorder type B&K 2309 [14].

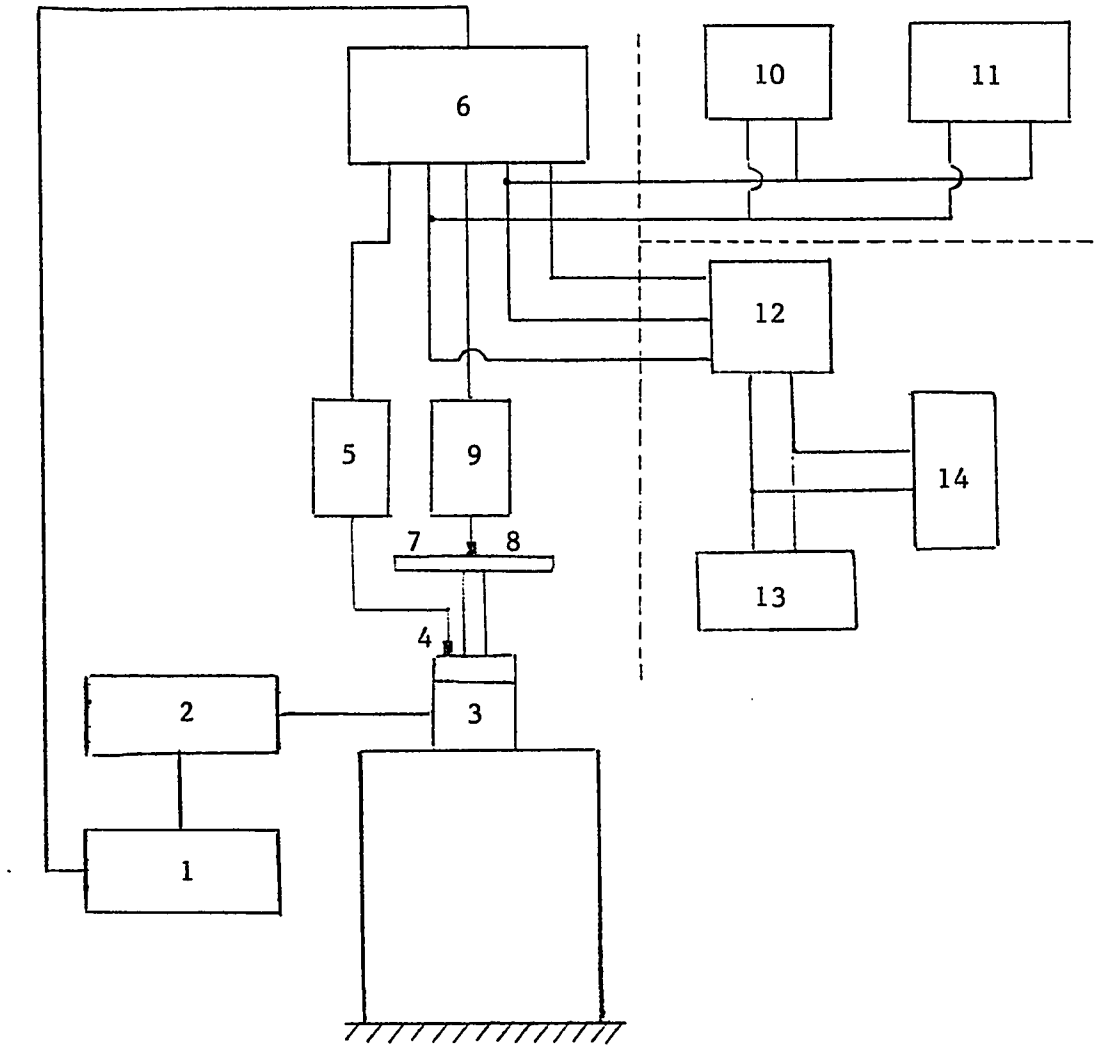

Figure 5.4 : Block diagram of the test arrangement

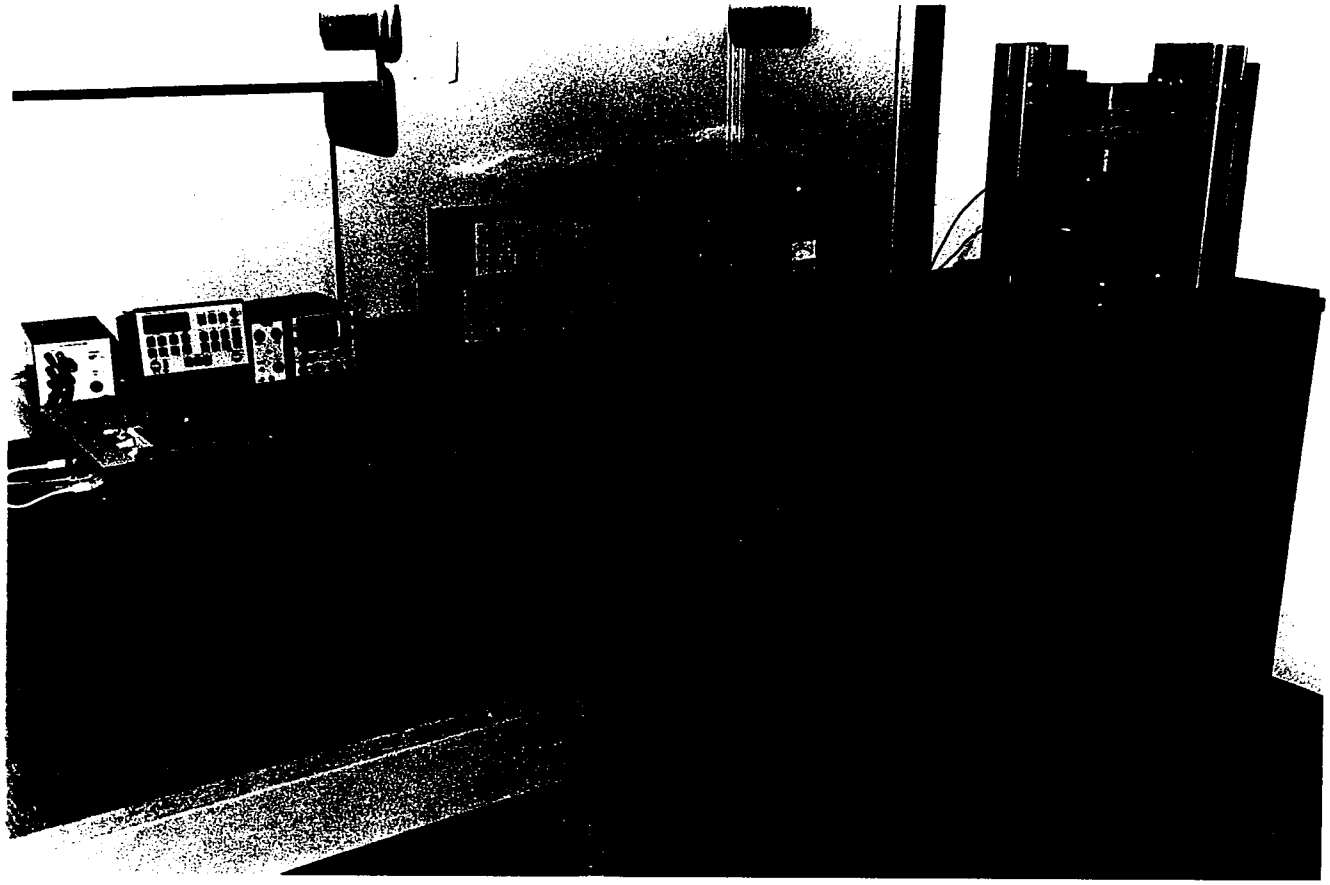

Figure 5.5 : Experiment lay-out

5.3 EXPERIMENTAL PROCEDURE :

The Electromagnetic Vibration Exciter is located at the central position of the test rig where both symmetric and and antisymmetric modes would be excited. The range of frequencies covered in the test was from 85 to 1850 Hz. However, the natural frequencies and the corresponding mode shapes were examined in the frequency band of interest which included the first lowest seven natural frequencies for Plate 1 , the first lowest five natural frequencies for Plate 2 and the first lowest three natural frequencies for Plate 3. The resonance of the test rig and the structure support were observed in the range of frequencies involved in the measurement. However these resonances were notified and examined.

The electromagnetic field created by the Vibration Exciter was sufficient to drive the test plate as a non-contacting exciter. This type of excitation, was used in the vibration measurement for the two examined positions of the point support (i.e. for $\alpha = 0.0$ and for $\alpha = 0.1$).

The mode shape of vibration for a particular natural frequency was obtained by exciting the plate when the Vibration Exciter head was in direct physical contact and the positions of the nodal lines were located by moving the accelerometer with the aid of hand-held probe over a predetermined grid.

The Low Frequency Mounting Table used in this experiment was originally designed by the Research and Development Engineers in ***tecquipment*** Company, Nottingham, ***ENGLAND*** . The cost of this table , which was about 65 Thousands Saudi Riyals (in 1984) , gave us the challenge to manufacture a modified one at the Mechanical Engineering Workshop of King Fahd University of

Petroleum and Minerals. The only part we had to import was the Dunlop Air Spring. The rest of the construction was modified and manufactured at the M.E. Workshop.

We can simply say that the Low Frequency Mounting Table is a heavy box resting on air spring. The object under testing is mounted on that box and by inflating the air spring, the whole box and the object will be isolated from the ground , and as a result the vibration of the surrounding is eliminated.

CHAPTER 6

RESULTS AND DISCUSSION

The examination of the natural frequencies and mode shapes of point supported rectangular plate along the diagonal, can be treated as the free vibration analysis of a completely free rectangular plate except at the given four points distributed symmetrically with respect to the plate central axis. Such a plate is shown in Figure 6.1 .

Because of the symmetry in the distribution of the point supports with respect to the plate central axis as well as the symmetry in the geometry of the plate dimensions, the free vibration modes of this plate will fall into four categories :

1. modes symmetric with respect to both the ζ and η axes (i.e. Symmetric-Symmetric mode : S-S) ,
2. modes antisymmetric with respect to both the ζ and η axes (i.e. Antisymmetric-Antisymmetric mode : A-A) ,
3. modes symmetric with respect to the ζ axis and antisymmetric with respect to the η axis (i.e. Symmetric-Antisymmetric mode: S-A) , and
4. modes antisymmetric with respect to the ζ axis and symmetric with respect to the η axis (i.e. Antisymmetric-Symmetric mode: A-S) .

Also, because of the symmetry of the geometry of the square plate with respect to the plate diagonals, the above for categories can be reduced to only

three modes . The three type of modes are :

1. Antisymmetric - Antisymmetric ,
2. Symmetric - Antisymmetric , and
3. Symmetric - Symmetric.

The Antisymmetric - Symmetric mode will be the same as the Symmetric - Antisymmetric mode with interchanging between the ζ and η axes. Consequently, instead of analyzing the full plate with free edges and point supported at the desired position , one quarter of the plate can be studied in conjunction with imposing the boundary conditions stemming from the symmetry in the distribution of the point supports with respect to the plate central axis as well as the symmetry in the geometry of the plate dimension with respect to the diagonals.

These boundary conditions are summarized as follows (see Figure 6.2)

1. Antisymmetric edge : slope and displacement are zero along the edge.
2. Symmetric edge : normal slope to the edge is zero.

According to the above discussion, the problem was solved three times with A-A , S-A , and S-S boundary conditions on the ζ and η axes. The first lowest six frequencies in each category were obtained.

The results obtained will be divided into four parts. Part one will be concerned about the convergence of the numerical solution used. Four different mesh sizes were used in the analysis of corner supported case (i.e. $\alpha = 0.0$), namely eight by eight, nine by nine, ten by ten and finally eleven by eleven nodes per side.

By studying the effect of increasing the mesh size, in other words, increasing the number of equations in the computation , the convergence was discussed. Since this thesis is concerned about a square plate with equal intervals (see Chapter 4 section 2), the eleven by eleven mesh size was selected over the others to study the vibration of point supported plate because of two reasons :

a) Satisfactory convergence.

b) In order to have the more commonly α values used in literature (i.e α = 0.1, 0.2, 0.3, 0.4 and 0.5) .

The results are given in part two. The mode shapes and the nodal patterns are given in the Appendices. Part three is the discussion of the experimental results. The frequency response and the Nyquist circles are given the Appendices. Part four deals with the effect of rigidity of the point support. The study of increasing the finite area of the support is invcstigated and discussed .

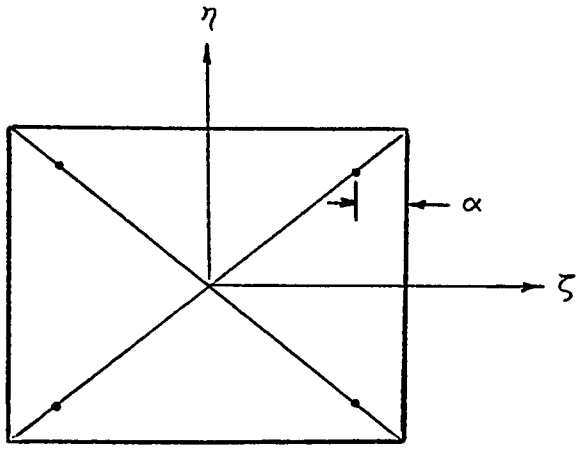

Figure 6.1 : Point supported rectangular plate

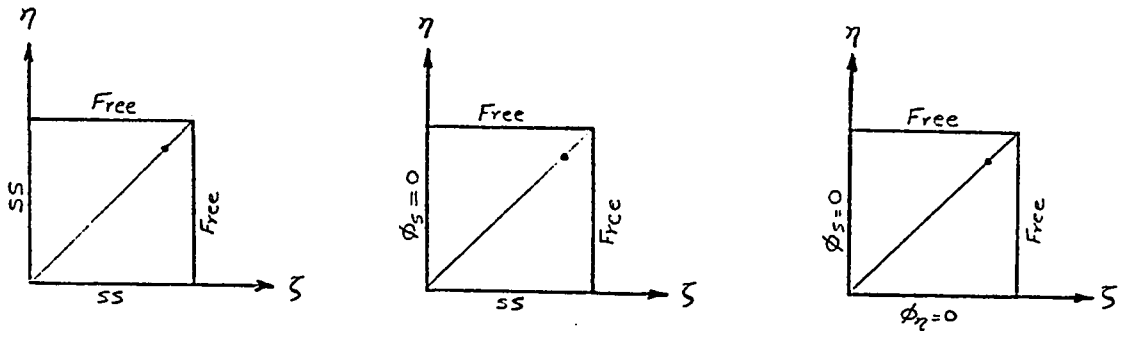

Figure 6.2 : Boundary condition for the square plate

6.1 CONVERGENCE :

All of the results reported here in this study were computed with a value of Poisson's ratio equal to 0.3. Referring to Chapter 4 where the frequency parameter Ω was given by Eq.(4.16) :

$$\Omega = \omega h \sqrt{\frac{\rho(1-\nu^2)}{E}} \tag{4.16}$$

In order to compare this parameter with other studies in literature it was multiplied by a non-dimsional factor $\sqrt{12}/\beta^2$ to have it in the most commonly used form of the frequency parameter :

$$\lambda = \omega a^2 \sqrt{\frac{\rho h}{D}} \tag{6.1}$$

All the results given in the present study are based on the above expression for the frequency parameter λ (non-dimensional).

Four different mesh sizes were examined, namely, eight by eight, nine by nine, ten by ten and eleven by eleven nodes per side. Since we have three variables per node (i.e. displacement w , rotation φ_ξ and rotation φ_η), and equal intervals were used the total equations per mode will be three multiplied by the square of the mesh size. Depending on the mode type (i.e. A-A, S-A, or S-S), the total number of the known variables at the boundaries and at the point support are subtracted from the total number of equations .

Eleven different values of β were computed for each frequency, in each mode type and for the different mesh size. The values of β computed were 0.2,

0.1, 0.05, 0.025, 0.02, 0.0125, 0.01, 0.005, 0.0025, 0.001 and 0.0005.

Referring to Figure 6.2 and the above information, the examined number of equations (i.e. unknown values of w, φ_ξ and φ_η) for the three types of mode can be found as follows:

$$n_{AA} = 3m^2 - (4m-1) - k \qquad (6.2.a)$$

$$n_{SA} = 3m^2 - (3m-1) - k \qquad (6.2.b)$$

$$n_{SS} = 3m^2 - (2m+1) - k \qquad (6.2.c)$$

where m : mesh size

$$k : \text{constant} = \begin{cases} 1 , & \alpha \neq 0.5 \\ 0 , & \alpha = 0.5 \end{cases}$$

Hence, as an example, the total number of equations in S-A mode with nine by nine mesh size is 216 equations.

When the frequency parameter λ is drawn versus the number of equations used in the computation for some selected values of β, the tendency of convergence is obtained. All of the convergence study plots are given in Appendix (A.1) . The selected values of β are 0.2, 0.1, 0.05, 0.01 and 0.0005. In fact , at the early stage of this study , full plate was examined and to investigate the convergence of a mesh size of eighteen by eighteen was reached but the accuracy and the convergence were not satisfactory , and then quarter of the plate were analyzed. Also, the frequency parameter λ is ploted versus the inverse of β in logarithmic scale for the four mesh sizes in order to visualize the variation of λ with the β and how the effect of the transverse shear deformation and rotary

inertia change the computed values of λ. These variation plots are given in Appendix (A.1) .

These figures are arranged by ascending order with respect to the frequency parameter and by the mode type. First, the first lowest six Antisymmetric - Antisymmetric modes are given , followed by the first lowest six Symmetric - Antisymmetric modes and then the first lowest six Symmetric - Symmetric modes. For the sake of clarity, the two types of graphs mentioned previously, are given together in one page. (i.e each page will be for a different frequency parameter).

In Figure A.1.1 the convergence of the first A-A mode is presented for the selected values of β followed by Figure A.1.2 where the variation of the frequency parameter λ of the four mesh sizes computed were presented. As it is clear from Figure A.1.1 , the frequency parameter decreases as the mesh size increases. That means, for this particular frequency parameter, the convergence is from above, and with more refinement of the mesh size (i.e. increasing the mesh size) the exact value can be approached from above. Conversely, Figure A.1.3 shows that the exact value of the frequency parameter λ of the second A-A mode can be approached from below. The reason of this contrast is due to the following remark :

" It should be remembered that energy methods always overestimate the fundamental frequency , so with more refined analysis the exact value can be approached from above. Conversely the Finite Difference method appears to underestimate the natural frequency and with increasing refinement in the analysis the exact value can be approached from below [10] " , and as mentioned in the Introduction, that this study will be based on the variational principle

applied to the energy expression in conjunction with Finite Difference technique, the exact value can be approached either from above (as in A-A 1) or from below (as in A-A 2). It should be noted that , in Figure A.1.4 , the comparison of the variation of the frequency parameter with β is only for the upper mesh size (i.e. eleven by eleven) and the lower mesh size (i.e. eight by eight). This is intended only for the sake of clarity, since the in-between mesh sizes are always limited between the upper and lower mesh sizes. For the second and third modes (S-A and S-S modes), also the four mesh sizes are given for only the lowest frequency parameter in each type.

6.2 CORNER AND POINT SUPPORTED SQUARE PLATE :

When the solution of the algebraic equations is obtained by the developed program, a subroutine was written in order to arrange the computed values of w , φ_ξ and φ_η. These values are arranged in such a way that the mode shape can be graphed in three dimensional figures. The mode shapes of the first lowest six frequencies for the six selected values of α (i.e α = 0.0 , 0.1 , 0.2 , 0.3 , 0.4 , and 0.5) are given in Appendix (A.a). Also the nodal patterns for the first lowest six frequency parameters in each mode type are given for two different values of β namely β = 0.2 and β = 0.0005 in Appendix (A.b).

This section will be divided into two parts, namely corner and point supported square plate. In part one , the numerical values of the frequency parameter are tabulated in Table A.3.1 to Table A.3.12 . Each mesh size is computed for the three types of modes. In the present study the Poisson's ratio ν is taken to be 0.3 . At the end of each table the values of the frequency parameter

computed by Gorman [38] and Amba-Rao [43] are entered. It should be mentioned that Gorman [38] used a value of Poisson's ratio of 0.333 while Amba-Rao [43] used a value of 1/3.

6.2.a Corner supported square plate :

The computed values of the frequency parameter λ for each of the three types of modes for the different mesh size are first tabulated and second, the variation of λ with β are graphed and third the correction in λ are plotted. In all the tables (Table A.3.1 to Table A.3.12) excellent agreement is observed between the present results and those of Gorman [38] and Amba-Rao [43] . The comparison is made for the value of $\beta = 0.0005$ which means the frequency parameter of thin plate, since both of Gorman and Amba-Rao applied their numerical solution to the classical governing differential equation of motion of the plate [see Eqs.(3.1) & (3.45)]. In Figure A.2.1 the variation of λ with β for the first six A-A modes with mesh size of eight by eight is given. In this figure we can observe that higher modes are more affected by increasing the thickness ratio β. To have more insight of this effect, the correction in the frequency parameter is graphed versus β. Figure A.2.2 shows this effect. The frequency parameter at the lowest value of β (i.e $\lambda(\beta = 0.0005)$) is considered to be the thin plate solution including the effect of transverse shear deformation and rotary inertia, and then the ratio of the frequency parameter for the other values of β to that frequency parameter is graphed (i.e. $\lambda(\beta)/\lambda(\beta = 0.0005)$ v.s β). The following observations of Tables A.3.1 to A.3.12 and Figures A.2.1 to A.2.24 can be summarized :

1) Higher modes show slow convergence to thin plate solution. This also

means that the effect of transverse shear deformation and rotary inertia is more pronounced in higher modes with the increasing thickness ratio β.

2) Correction in the frequency parameter increases with higher modes.

3) The S-S modes show faster convergence to thin plate solution either than S-A or A-A modes.

4) The second and fifth S-S modes , as well as the second and fifth A-A modes that characterized by nodal lines along the diagonals [see the Nodal Patterns in Appendix (A.b)] show low correction factors.

5) The first S-A mode will have the line of antisymmetry (when full plate is plotted) along the center line. In all the studies reviewed (Chapter 2) where full plate is analyzed this mode is sometimes have the line of antisymmetry along one of the diagonals. This can explained by the type of solution used. When full plate is considered, the second shape of nodal lines is obtained, while the former shape is obtained when only quarter of the plate is examined. That is due to antisymmetry boundary condition imposed on one of the edges.

6) The correction in λ for $\beta = 0.01$ is very small for almost all the mode types and all the frequencies with maximum value of 5.0 percentage . Hence, the approximation of $\beta = 0.01$ to be thin plate is more accurate than 0.02 .

6.2.b Point supported square plate :

The eleven by eleven mesh size was selected over the other three mesh sizes in order to have appropriate values of α. Again in this section, the computed values of λ are tabulated for each mode type for the five locations of

α i.e α = 0.1 , 0.2 , 0.3 , 0.4 and 0.5) in Tables A.3.13 to A.3.27 and also the values obtained by Gorman [38] and Amba-Rao [43] are tabulated for comparison. The following observations can be made :

1) Repeated modes are obtained for various location of the point support These modes are characterized by nodal lines along the diagonals and can be found also for the vibration of completely free plates.
2) Most of the modes change slightly their nodal patterns. To visualize these changes the nodal patterns for each mode is given for two values of β namely β = 0.0005 , which represent thin plate , and β = 0.2000 , which represent Mindlin plate (thick plate) .
3) Most of the nodal pattern at β = 0.2 appear to be similar for those associated with β = 0.0005 and exactly the same for repeated modes.
4) Some modes interchange their order. An example is A-A 4 for point supported plate with α = 0.3 (Table A.3.19)
5) In the A-A case , (Tables A.3.13 , A.3.16 , A.3.19 , A.3.22 , and A.3.25) , show certain discrepancies between the present results and those of Gorman [38] For α = 0.2 , 0.3 , and 0.4 the present solution gave a lower frequency for the first mode than that reported in [38]. In fact , examination of the associated tables (A.3.16, A.3.19 and A.3.22) suggests that in [38] the first frequency may have been missed for α = 0.2, 0.3, and 0.4. If one assumes that this is true , excellent agreement will be observed for α = 0.2, 0.3, and 0.4 between the first, second, third and fourth, fifth modes of the present solution, respectively. Hence, in the tables mentioned , the values obtained by [38] will be arranged according to the above observation for the matter of easy

comparison.

6) For the A-A case, excellent agreement is observed when comparing the present method and that of Amba-Rao [43].

7) For the S-A case , (Tables A.3.14 , A.3.17 , A.3.20 , A.3.23 , and A.3.26), excellent agreement is found between the present solution and that of Gorman [38] and Amba-Rao [43] for all modes and for all values of α.

8) For the S-S case , (Tables A.3.15 , A.3.18 , A.3.21 , A.3.24 and A.3.27), excellent agreement is noted with the exception of the case of $\alpha = 0.3$. First mode given by [38] and [43] is one of the repeated modes which has two nodal line along the diagonals, while the first mode computed in the present study is not. The nodal pattern for the fundamental frequency in the present method is characterized by a circle passing through the point supports as it is seen in Appendix (A.b). And for the sake of easy comparison the result obtained in this study for the frequency parameter in the case of $\alpha = 0.3$ is tabulated in the 2nd column in Table A.3.21 .

It should be kept in mind that the above comparison is performed for $\beta = 0.0005$

6.2.c Fundamental frequency :

The fundamental frequency which implies the lowest was found to be always from the S-S mode. It is plotted versus the location of the point support α for some selected values of β (see Figure 6.3). Not only the fundamental frequencies are symmetric about the center lines, but also they are symmetric, about the diagonals except for $\alpha = 0.2$. Johns, D. and Nagran, V. [10]

assumed that the fundamental frequencies where symmetric about the central axes and also symmetric about the diagonals. As a result , they have analyzed only one eight of the square plate.

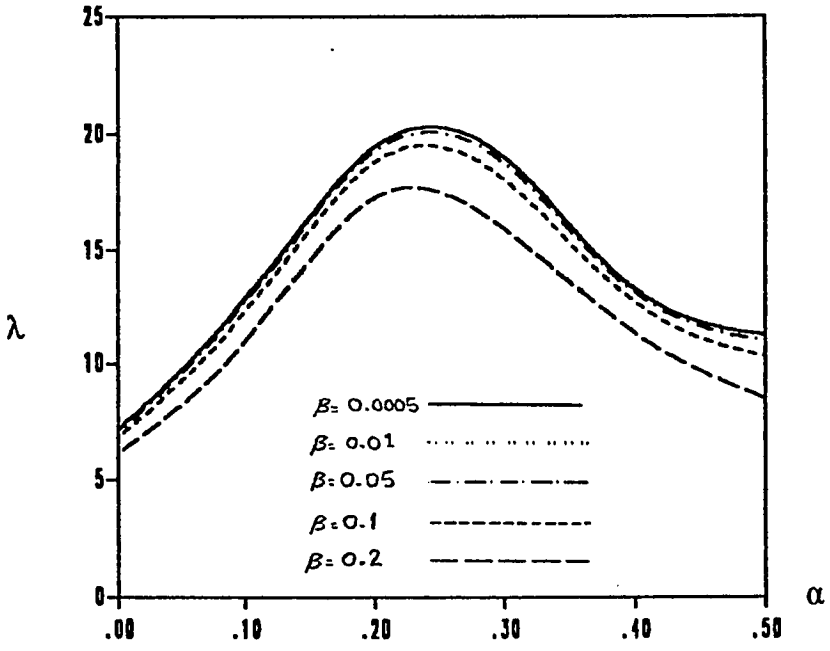

Figure 6.3 : Fundemental frequency

6.3 EXPERIMENT :

One of the major requirements of the subject of modal testing is a thorough integration of three components :

1) the theoretical basis of vibration ,

2) accurate measurement of vibration and

3) realistic and detailed data analysis.

There has been in the past a tendency to regard these as three different specialist areas, with individual experts in each. However , the subject of Modal Testing now demands a high level of understanding and competence in all and cannot reach its full potential without the proper and judicious mixture of the necessary three components.

Before discussing the experimental results, a brief discussion of the theoretical basis of vibration will be introduced. A detailed and thorough account can be found in literature (see reference [62]).

It is very important that a clear distinction is made between the free vibration and the forced vibration analyses. For a single degree of freedom (i.e. only one parameter is needed to define the motion), a free vibration analysis yields its natural frequency and damping factor while a particular type of forced response analysis, assuming a harmonic excitation, leads to the definition of the Frequency Response Function (FRF) such as mobility, the ratio of velocity response to force input. These two types of results are referred to as "modal properties" and "frequency response characteristics" respectively. It is appropriate to consider the form which a plot of a FRF takes.

Three alternative ways to plotting this information are a) Linear, b) Logarithmic, and c) Nyquist plot. Although very few practical structures could realistically be modelled by a single degree of freedom (SDOF) system, the properties of such a system are very important because those for a more complex multi-degree of freedom (MDOF) system can always be represented as the linear superposition of a number of SDOF characteristics.

So far we have defined the mobility frequency response function as the ratio of velocity response to force input. Another FRF is receptance which is the ratio between a harmonic displacement response and the harmonic force. Inertance or sometimes called acceleranace is another FRF defined as the ratio of the acceleration response and the input force.

There is an overriding complication to plotting FRF data which derives from the fact that they are complex and thus there are three quantities ; frequency plus two parts of the complex function, and these cannot be fully displayed on a standard x-y graph. Because of this, any such single plot can only show two of the three quantities and so there are different possibilities available.

The three most common forms of presentation are:

a) The Bode type of plot consisting of two graphs of Modulus (FRF) versus Frequency and Phase versus Frequency.

b) Two plots consisting of Real part (of FRF) versus Frequency, and Imaginary part versus Frequency.

c) Nyquist plot which is a single graph of Real part of (of FRF) versus Imaginary Part, and this does not explicitly contain frequency information.

In the present study, the experimental results are presented in the last two types with some modification. This modification can be explained in the following paragraph.

The Cross Spectrum Unit type B&K 5748 enables the Two-Channel Tracking Filter type B&K 5716/WHO255 to be used for cross-correlation measurement, which can be useful for identifying the origins of unwanted noises and vibration. It takes three input signals from the Two Channel Tracking Filter [X , Y and $Y\underline{\lfloor 90^\circ}$] derived from transducers (or accclerometers) cited at two positions fo which the cross correlation is to be measured. It generates four positive direct voltages proportional to the functions g(X), g(Y), C(XY), and Q(XY) defined as follows:

$$g(X) = \frac{1}{2T}\int_{-T/2}^{T/2} X^2\,dt \ ,$$

$$g(Y) = \frac{1}{2T}\int_{-T/2}^{T/2} Y^2\,dt \ ,$$

$$C(XY) = \frac{1}{10T}\int_{-T/2}^{T/2} X\,Y\,dt \ ,$$

$$Q(XY) = \frac{1}{10T}\int_{-T/2}^{T/2} X\,Y\underline{90^\circ}\,dt \ ,$$

and if these output voltages are used to deflect the pen of the Two Channel Level Recorder type B&K 2309 or the X-Y Recorder type B&K 2308 which is synchronized with the sweep of the Two Channel Tracking Filter , C(XY) and Q(XY) will give the Co-ordinated and the Quadrature cross spectra respectively, and g(X) and g(Y) will give the frequency spectra of A and B signals (the two

transducers signals) respectively at the inputs to the Two Channel Tracking Filter (X corresponds to A , Y to B , and Y$\lfloor\underline{90°}$ to B$\lfloor\underline{90°}$ on the Two Channel Tracking Filter). The averaging time T for all four outputs may be selected on a switch giving a choice of 0.1, 0.3, and 1.0 second. The averaging characterized by the integration functions is performed with exponential weighting. Because of the lack of the Remote Control instrument which should be used to synchronize the Two Channel Level Recorder or X-Y Recorder with the Two Channel Tracking Filter, the excitation signal (from the Accelerometer block [4] in Figure 5.4) is used as the input signal A. Signal A is now the point Inertance (since the response and the excitation coordinate are the same , if they are different , it will be called Transfer Inertance). By this modification the presentation of the FRF as Real part versus Frequency and Imaginary part versus Frequency will not be as the theoretical plots. The theoretical presentation of Real part versus Frequency, Imaginary part versus Frequency and Nyquist plots for the FRF are given in Figure 6.4 for a Damped SDOF system. The difference between the plots in this study and the theoretical plots will be clear as we proceed in the discussion.

The experiment was conducted on three different steel plates with the dimensions given in Chapter 5 - section 1. In accordance with Eq.(6.1) the computed nondimensional values of the frequency parameter λ for the three β ratios are dimensionalized by the following expression (to obtain the frequency in Hz):

$$f = \frac{h}{a^2}\left\{\frac{1}{2\pi}\sqrt{\frac{E}{12(1-\nu^2)\rho}}\right\}\lambda \qquad \text{(Hz)} \qquad (6.3)$$

where ,

h : plate thickness (m).

a : plate dimension (m).

E : Young's of Elasticity $= 2.07 \times 10^{11}$ (N/m^2)

v: poissons's Ratio $= 0.3$

ρ : Density 7.83×10^3 (Kg/m^3)

and hence,for

Plate 1 , $f = 12.38178\ \lambda$ (Hz)

Plate 2 , $f = 30.95445\ \lambda$ (Hz)

Plate 3 , $f = 64.99622\ \lambda$ (Hz) (6.4)

Two positions of the point support were examined - corner supported ($\alpha = 0.0$) and point supported ($\alpha = 0.1$). The experimental results of these two cases are given in Tables A.3.28 to A.3.33 . The Co-ordinated and the Quadrature components are presented in Figures A.4.1 to A.4.15 . The Nyquist plots are presented for only the first case (corner supported, $\alpha = 0.0$). in Figure A.5.1 to Figure A.5.14 .

A view over the above tables will lead to the following observations:

1) Two experimental modes are obtained for each symmetric-Antisymmetric theoretical mode. In theory, the S-A mode will be the same as A-S (as discussed earlier in the introduction of this chapter) and this means that two modes are expected to be excited at the same frequency. In practice , two different frequencies are expected to occur at or close to the predicted frequency . At one of these two frequencies, the maximum discrepancy in frequency spectra is observed, for example in Table A.3.29 the maximum discrepancy is observed for the S-A mode

(2.33 %) and (− 2.20 %) for the second mode S-A 1 .

2) Symmetric-Symmetric modes show low discrepancy and this is due to the position selected for the response accelerometer. This position was selected by examining the nodal patterns for the frequencies under observation.

3) In plate 1, most of the discrepancies are positive which means that the theoretical values of λ are higher. As β increase the theoretical values are observed to be lower such as in Plate 3.

The values of the frequency in Tables A.3.28 to A.3.33 are obtained by observing the peaks in the frequency response. When the frequency response is plotted for the Co-ordinated and the Quadrature Components , as an overall , the peaks are approximated and by close sweep rate , a more accurate reading can be obtained from the Exciter Control.

Refering to Figures A.4.1 to A.4.15 , the following observation can be deduced:

1) The difference between these figures and the theoretical representation of the Real part versus Frequency and the Imaginary part versus Frequency plots for a FRF is quite clear. The Co-ordinated and the Quadrature components given in these figures are interchanging with each other for different modes. This is due to modification of the experiment lay-out. However, since only the frequencies are demanded by this method, it gives quite reasonable agreement with the predicted theoretical values.

2) Test rig vibration exists in the frequency band of interest. This vibration

was reduced by low power excitation.

3) Mode couplings are observed to occur close to the predicted frequencies of the S-A modes. When slow sweep rate is selected more clear picture can be obtained.

From Nyquist plots being shown in Figures A.5.1 to A.5.14 , one can deduce the following :

1) Natural frequencies can also be determined by observing the frequencies when the pen of the X-Y Recorder pass by the tangent of the circle. Slow sweep rate of the frequency leads to better chance to observe the natural frequency.

2) A very interesting observation is the mode coupling. Figure A.5.2 shows the mode coupling of the second mode (SA1). The frequency noted at the interconnection between the two circles of the Nyquist plot gives a more close value to the predicted one. As an example, the predicted value of the second mode ($\alpha = 0.0$, $\beta = 0.01$) is 194.97 Hz and the frequency at the interconnection of the two circles showed to be 195 Hz.

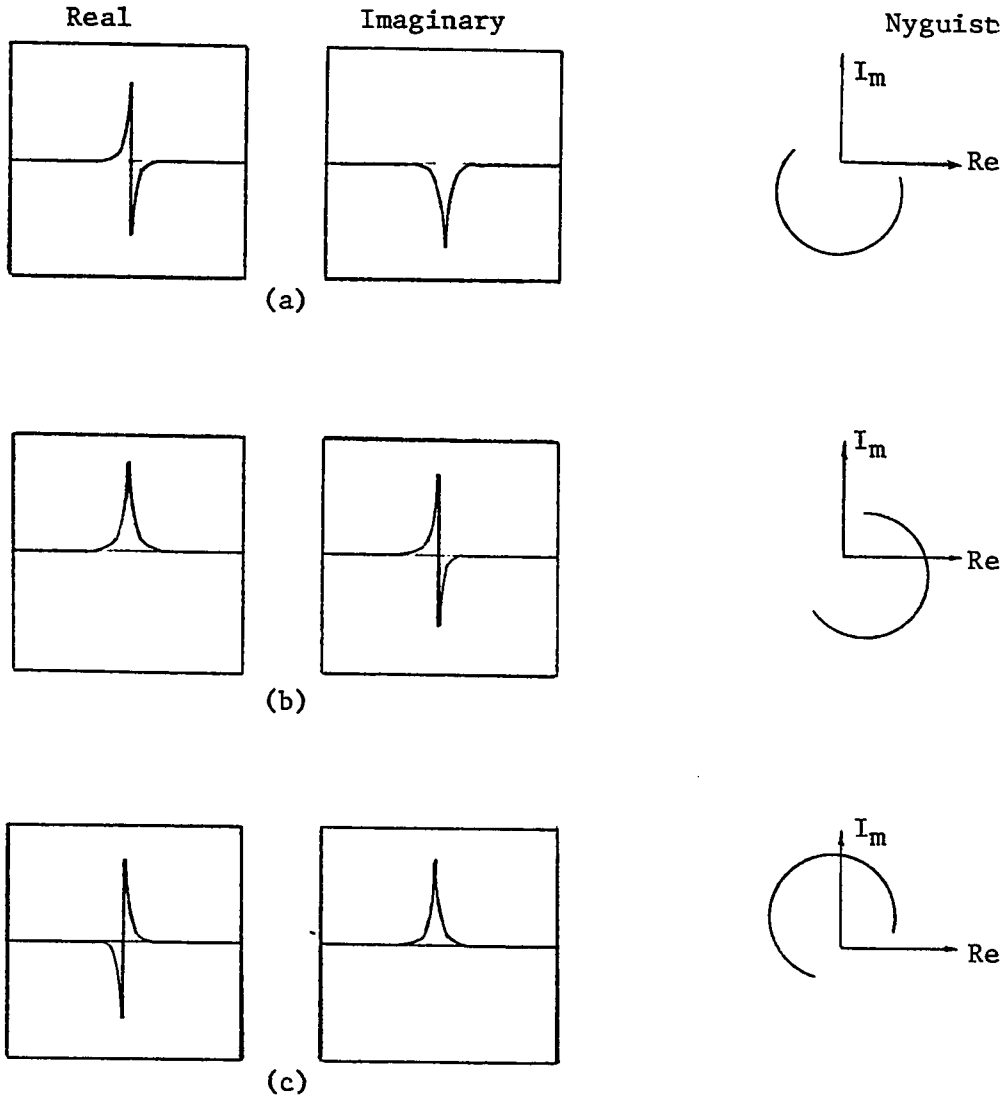

Figure 6.4 : Plots of FRF of a SDOF system

(a) Receptance
(b) Mobility
(c) Inertance

6.4 COLUMN SUPPORTED PLATE :

Column-supported floor slabs are a common feature in contemporary building construction. The columns are generally located in a regular pattern so as to facilitate the partitioning of the floor area for various purposes. The dynamic response of such a configuration is of interest when the slabs experience out - of -plane oscillatory loads from machinery resting upon them. The simplest representation of a column - supported floor slab is a point - supported plate. In this this section an investigation into the effect of the rigidity of the column support is presented. The term Point - Support is used to denote a constraint of zero deflection which suggests a simply supported boundary condition. The term "Rigid - Support" is used to constraints of zero deflection and rotation which suggests a clamped supported boundary condition.

Only the first lowest four frequency parameters are investigated. By modification of the developed program , the numerical values of these frequencies are obtained. The only paper found in literature was written in 1972 by Petyt, M. and Mirza, W.H. [12]. They used Finite Element Displacement method of analysis to determine the vibration characteristic of floor slabs resting on four column supports. No numerical values for the frequency parameters were given in this paper, instead a graphical presentation of the ratio of frequency with hinged joint versus the finite area of the column support ξ (see Figure 6.4). The finite area of the column supported plate ξ investigated ranged from zero (correspond to rigid point support) to 0.15 with increment of 0.05. Following the same monograph of Chapter 6-section 2, the computed values of this study will be presented. The variation of λ_c with the inverse of β is plotted and the correction in

λ_c for each case of ξ (i.e. for ξ = 0.0 , 0.05 , 0.10 and 0.15). These plots being shown in Figures A.6.1 to A.6.8 . It can be observed that as the finite area of column support increases the frequency parameter λ_c tends to slow in convergence to thin column support frequency (i.e. $\lambda_c(\beta = 0.0005)$) and hence the correction in λ_c tends to increase. To have clear insight of the effect of rigidity , the ratio of the frequency parameter with rigid point (or column) support to the frequency parameter of corner supported plate is plotted versus the finite area of the column support ξ . (i.e $\lambda_c/\lambda(\alpha = 0)$. These plots are given in Figures A.6.9 to A.6.19 , and one con observe the following :

1) The effect of rigid support is more pronounced in thin plate with small β ratios. Changing the point support to column support will allow the transverse shear deformation term to increase. The content of this should be more pronounced with large values of β, but since only the ratio of λ_c/λ is plotted, the percentage increment in thick plate is smaller than the content in thin plate. This is more clear if the variation plots are reviewed.

2) Even for the rigid point support, there is a large increase in the fundamental frequency when w , $\partial w/\partial x$, and $\partial w/\partial y$ are constraints at the joints.

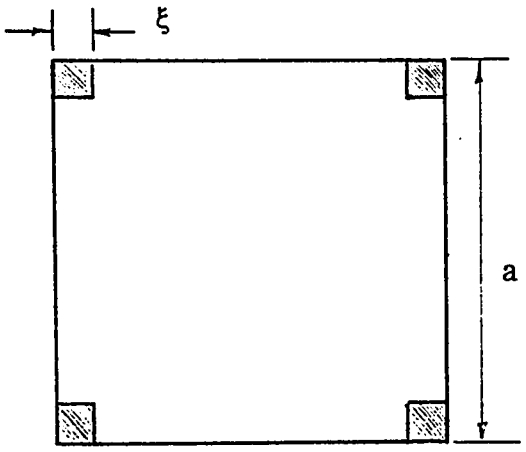

Figure 6.5 : Column supported plate

CHAPTER 7

CONCLUSION

Concerning the present method used in this study, the following conclusions are deduced:

1) Although the number of equations used in the present Finite Difference formulation is small, the accuracy maintained is quite good in the comparison of the existing results. The use of interlacing grids in addition to analyzing only one quarter of the plate are the two factors behind this comparatively small number of equations. Solving quarter of the plate with interlacing grids of eight by eight mesh size is like solving full plate with ordinary grids of thirty by thirty mesh size .

2) The effect of transverse shear deformation and rotary inertia are found to be more pronounced in higher modes. This is clear from the correction plots given in the Appendices.

3) The effect of transverse shear deformation and rotary inertia are not included in all (up to the knowledge of the author) the papers found in literature for point supported plate along the diagonals, and only the classical theory of plates were analyzed for this problem. The comparison of the present method is compared with existing studies for the case of small thickness ratio β.

4) Plates with $\beta = 0.01$ have small discrepancy with $\beta = 0.0005$, which can

be considered as thin plate solution. In the correction plots of λ for the three mode types , A-A , S-A and S-S , and for all point position , it can be verified that this β ratio has good approximation for thin plate case.

5) Even for the rigid point support, there is a large increase in the fundamental frequency when w , $\partial w/\partial x$, and $\partial w/\partial y$ are constraints at the joints.

6) With the available equipment in the Dynamic Labs, the performed experiment shows very reasonable agreement with predicted theoretical values of the frequency parameter. Slow sweep rate over the natural frequency gives very dependable readings. The use of the Real part and the Imaginary Part (or the Co-ordinate and the Quadrature) signals enable us to spot the natural frequency very precisely.

7) Hand pressure at the point support is sufficient to hold the plate and insure a zero deflection of the plate. Increasing the pressure of the point support yields higher frequencies than expected. This is due to effect of rigidity which moves the point support to rigid support. This effect is more pronounced in the case of a thin plate. It was found out in the experiment that hand pressure will be enough for thin plate , since it permits the transverse shear to occur rather than increasing this term more significantly. Contrarily, it was found out for a large value of β , the hand pressure is not enough as it yields lower frequencies than those theoretically predicted . Increasing the pressure of the point will permit the transverse deformation to occur and the fre-

quency obtained will be more accurate and close to theoretical predictions .

8) Even if the increment in increase of the natural frequency for a rigid square plate is more pronounced in small values of β, the study of the correction shows that the effect of the rigidity of the point support is more pronounced in large values of β. This contrast is solved by reminding the reader that the Effect of Rigidity plots are given in terms of the ratio between the frequency parameter with column support and the frequency parameter of corner support (i.e. $\lambda_c/\lambda(\alpha=0.0)$).

9) Nyquist plot , where the Real Part and the Imaginary Part of the Frequency Response Function are graphed verses each other as in polar plots , yields a one plot and does not explicitly contain the radian frequency . To calculate the loss factor (or structural damping) from this type of plot needs repeated run over the natural frequency in the range of interest . First when the Nyquist circle is ploted , the X-Y Recorder B&K type 2309 is set on the ***servo on*** position and then another run is performed and the point under question is notified.

10) Wide range of frequency could be obtained and investigated if the proper logarithmic paper for the X-Y Recorder is available .

11) Some of the modes interchange their order or their shapes (Nodal Pattern) depending on thickness variations . The nodal lines (characterized by zero deflection) of mode shapes which correspond to Mindlin plate tend to change to the nodal lines of mode shapes correspond to

thin plate in the direction of decreasing β .

REFERENCES

1. Waller, Many D. *" Vibration of Free Square Plates : Part I: Normal Vibrating Modes "*. **Proceedings of the London Physical Societies** . 51, (1939), pp. 835-843.
2. Young, Dana *" Vibration of Rectangular Plates By the Ritz Method "*. **Journal of Applied Mechanics** . 17(4), (1950),pp 448-453 .
3. Salvadori, M.G. *" Numerical Computation On Buckling Loads By Finite Difference "* . **Transaction of ASCE** . 116, Paper 2441, (1951), pp 590-636.
4. Mindlin ,R.D. *" Influence of Rotary Inertia and Flexural Motion of Isotropic Elastic Plate "* . **Journal of Applied Mechanics** . 18,(1951), pp 31-38.
5. Cox, H.L. and Boxe, J. *" Vibration of Rectangular Plates Point-Supported at the Corners "*. **The Aeronautical Quarterly** . 11(1), (1960), PP 41-50 .
6. Kirk, C.L. *" A Note on the Lowest Natural Frequency of a Square Plate Point-Supported at the Corners "*. **Journa of Royal Aeronautical Society** . 66(4), (1962), PP 240-241.
7. Reed, R.E. *" Comparison of Methods in Calculating Frequency of Corner Supported Rectangular Plate "*. **NASA TN D-3030** . (Sep 1965).
8. Tso, W.K. *" On the Fundamental Frequency of a Four Point-Supported Square Elastic Plate "*. **AIAA Journal** . 4(4), (1966), pp. 733-735.
9. Mason, V. *" Rectangular Finite Element for Analysis of Plate Vibrations "*. **Journal of Sound and Vibration** . 7(3), (1968), pp 437-448.
10. Johns, D.J. and Nagaraj, V.T. *" On the Fundamental Frequency of a Square Plate Symmetrically Supported at Four Points "*. **Journal of Sound and Vibration** . 10(3), (1969), pp 404-410.
11. Leissa, A.W. *" Vibration of Plates "*. **NASA SP-160** . (1969).

12. Dowel, E.H. *" Free Vibration of a Linear Structure with Arbitrary Support Conditions "*. **Journal of Applied Mechanics** . 38(3), (1971), pp 595-600.

13. Mirza, W.H. and Petyt, M. *" On the Vibration of Point Supported Plates "*. **Journal of Sound and Vibration** . 15(1), (1971), pp 143-145.

14. Damle, S. and Feeser, L. *" Vibration of Four Point Supported Plates By Finite Element Method "*. **Journal of the Aeronautical Society of India** . 24(3),(1972), pp 375-377.

15. Petyt, M. and Mirza, W.H. *" Vibration of Column Supported Floor Slabs "*. **Journal of Sound and Vibration** . 21(3), (1972), pp 355-364.

16. Johns, D.J. and Nataraja, R. *" Vibration of Square Plate Symmetrically Supported at Four Points "*. **Journal of Sound and Vibration** . 25(1), (1972), pp 75-82.

17. Venkateswara Rao, V.G., Raju, I.S. and Amba Rao, C.L. *" Vibration of Point Supporeted Plates "*. **Journal of Sound and Vibration** . 29(3), (1973), pp 387-391.

18. Dowell, E.H. *" Theoretical Vibration and Flutter Studies of Point Supported Plates "*. **Journal of Spacecraft and Rockets** . 10(6), (June 1973), pp 389-395.

19. Venkateswara Rao, V.G., Raju, I.S. and Murthy, T.V. *" Vibration of Rectangular Plates with Mixed Boundary Conditions "*. **Journal of Sound and Vibration** . 31(2), (1973), pp 257-260.

20. Venkateswara Rao, V.G., Sadasiva Rao, Y. and Amba Rao, C.L. *" Experimental Study of Vibrations of a Four Point Supported Square Plate "*. **Journal of Sound and Vibration** . 32(2), (1974), pp 286-288.

21. Leuner, T.R. *" An Experimental-Theoretical Study of Free Vibrations of Plates on Elastic Point-Supports "*. **Journal of Sound and Vibration** . 32(4), (1974), pp 481-490.

22. Dowell, E.H. *" Vibration of Point - Supported Plates "*. **Journal of Sound and**

Vibration . 32(4), (1974), 524.

23. Venkateswara Rao, V.G. *" Fundamental Frequency of a Square Panel with Multiple Point Supports on the Edges "*. **Journal of Sound and Vibration** . 38(2), (1975), 271.

24. Srinivasan, R.S. and Munaswamy, K. *" Frequency Analysis of Skew Orthotropic Point Supported Plates "*. **Journal of Sound and Vibration** . 39(2), (1975), pp 207-216.

25. Venkateswara Rao, V.G., Amba Rao, C.L. and Murthy, T. *" On the Fundamental Frequency of Point Supported Plates "*. **Journal of Sound and Vibration** . 40(4), (1975), pp 561-562.

26. Aksu, G. and Ali, R. *" Determination of Dynamic Characteristics of Rectangular Plate with Cutouts Using Finite Difference Formulation "*. **Journal of Sound and Vibration** . 44(1), (1976), pp 147-158.

27. Gorman, D.J. *" Free Vibration Analysis of Cantilever Plates By the Method of Superposition "*. **Journal of Sound and Vibration** . 49(4), (1976), pp 453-467.

28. Stanisic, M.M. *" Dynamics Response of a Diagonal Line Loaded Rectangular Plate "*. **AIAA Journal** . 15(12), (Dec.1977), pp 1804-1807.

29. Leissa, A.W. *" Research in Plate Vibrations 1973-1976 Classical Theory "*. **Shock Vibration Digest** . 9(10), (1977), pp. 13-24.

30. Gorman, D.J. *" Free Vibration Analysis of the Completely Free Rectangular Plate By the Method of Superposition "*. **Journal of Sound and Vibration** . 57(3), (1978), pp 437-477.

31. Gorman, D.J. *" Free Vibration Analysis of Rectangular Plates with Inelastic Lateral Support on the Diagonals "*. **Journal of the Acoustical Society of America** . 64(3), (1978), pp 823-826.

32. Leissa, A.W. *" Recent Research in Plate Vibrations 1973-1976 Complicating*

Effects ". **Shock Vibration Digest** . 10(12), (1978), pp 21-35.

33. Kerstens, J.G.M. " ***Vibration of a Rectangular Plate Supported at an Arbitrary Number of Points*** ". **Journal of Sound and Vibration** . 65(4), (1979), pp 493-504.

34. Gorman, D.J. " ***Solution of the Levy Type For the Free Vibration Analysis of Diagonally Supported Rectangular Plates*** ". **Journal of Sound and Vibration** . 66(2), (1979), pp 239-246.

35. Gorman, D.J. " ***Free Vibration Analysis of Rectangular Plates with Symmetrically Distributed Point Support Along the Edges*** ". **Journal of Sound and Vibration** . 73(4), (1980), pp 563-574.

36. Aksu, G. " ***A Finite Difference Method for the Free Vibration of Orthrotropic Plates Allowing for Transverse Shear Deformation and Rotary Inertia*** ". **International Conference on Numerical Methods for Coupled Problems.** Swansea, U.K., (1981).

37. Laura, P.A.A. and Gutierrez, R.H. " ***Transverse Vibrations of Thin, Elastic Plates with Concentrated Masses and Internal Elastic Supports*** ". **Journal of Sound and Vibration** . 75(1), (1981), pp 135-143.

38. Gorman, D.J. " ***An Analytical Solution for the Free Vibration Analysis of Rectangular Plates Resting on Symmetrically Distributed Point Supports*** ". **Journal of Sound and Vibration** . 79(4), (1981), pp 561-574.

39. Leissa, A.W. " ***Plate Vibration Research 1976 - 1980 Classical Theory*** ". **Shock Vibration Digest** . 13(9), (1981), pp 11-22.

40. Leissa, A.W. " ***Plate Vibration Research 1976 - 1980 Complicating Effects*** ". **Shock Vibration Digest** . 13(10), (1981), pp 19-36.

41. Ganesan, N. and Dhotarad, M.S. " ***Vibration Analysis of Mindlin Plates*** ". **Journal of Sound and Vibration** . 87(4), (1983), pp 643-645.

42. Kertsten, J.G.M. and Laura, P.A.A. " ***Vibrations of Rectangular Plates with***

Point Supports Comparison of Results ". **Journal of Sound and Vibration** . 89(2), (1983), pp 291-293.

43. Raju, I.S. and Amba Rao, C.L. " *Free Vibration of a Square Plate Symmetrically Supported at Four Points on the Diagonals* ". **Journal of Sound and Vibration** . 90(2), (1983), pp 291-297.

44. Aksu, G. " *Free Vibration Analysis at Rectangular Plates with Cutouts Allowing for Transverse Shear Deformation and Rotary Inertia* ". **Journal of Earthquake Engineering and Structural Dynamics** . Vol. (12), (1984), pp 709-714.

45. Narita, Y. and Leissa, A.W. " *Vibration of Corner Point Supported Shallow Shells of Rectangular Planform* ". **Earthquake Engineering and Structural Dynamics** . 12(5), (Sep/Oct. 1984), pp. 651-661.

46. Fan, S.C. and Cheung, Y. " *Flexural Free Vibrations of Rectangular Plates with Complex Support Conditions* ". **Journal of Sound and Vibration** . 93(1), (1984), pp 81-94.

47. Gorman, D.J. " *An Exact Analytical Approach to the Free Vibration Analysis of Rectangular Plates with Mixed Boundary Conditions* ". **Journal of Sound and Vibration** . 93(2), (1984), pp 235-247.

48. Narita, Y. " *Note on Vibration of Point Supported Rectangular Plates* ". **Journal of Sound and Vibration** . 93(4), (1984), pp 593-597.

49. Utjes, J.C. and Laura, P.A.A. " *Vibrations of Thin Elastic Plates with Point Supports - A Comparative Study* ". **Applied Accoustics** . 19(1), (1984), pp 17-24.

50. Laura, P.A.A, Utjex, J.C. and Sarmiannteg, G.S. " *Comments on Flexural Free Vibrations of Rectangular Plates with Complex Support Conditions* ". **Journal of Sound and Vibration** . 97(1), (1984), pp 176-178.

51. Laura, P.A.A. and Cortinez, V.H. " *Fundamental Frequency of Point Supported Square Plates Carrying Concentrated Masses* ". **Journal of Sound and Vibration** .

100(3), (1984), pp 456-458.

52. Ganesan, N. and Nagraja Rao, S. *" Vibration Analysis of Moderately Thick Skew Plates By a Variational Approach "*. **Journal of Sound and Vibration** . 101(1), (1985), pp 117-119.

53. Yamada, G., Irie, T. and Takahashi, T. *" Determination of the Steady State Response of a Visco Elastically Point Supported Rectangular Plate "*. **Journal of Sound and Vibration.** 102(2), (1985), pp 285-295.

54. Aksu, G. *" Free Vibration Analysis of Point Supported Plates By Vibration Testing Technique "*. **Mechanism and Machine Theory** . 21(2), (1986), pp 153-166.

55. Sadasiva Rao, Y. and Singh, G. *" Vibration of Corner Supported Thick Composite Plates "*. **Journal of Sound and Vibration** . 111(3), (1986), pp 510-514.

56. Mizusawa, T. and Kajita, T. *" Vibration of Skew Plates Resting on Point Supports "*. **Journal of Sound and Vibration** . 115(2), (1987), pp 243-251.

57. Leissa, A.W. *" Recent Research in Plate Vibrations 1981-1985, Part I: Classical Theory "*. **Shock and Vibration Digest** . 19(2), (Feb. 1987), pp 11-18.

58. Leissa, A.W. *" Recent Research in Plate Vibration 1981-1985, Part II: Complicating Effects "*. **Shock and VIbration Digest** . 19(3), (1987), pp 10-24.

59. Dym and Shames. *Solid Mechanics: A Variational Approach* . **Mc-Graw Hill** , (1973).

60. Al-Kaabi, Saif A. *Free Vibration Analysis of Mindlin Plates with Variable Thickness* . **M.Sc. Thesis.** U.P.M. (University of Petroleum and Minerals) Dhahran (May 1985).

61. *Mechanical Vibration and Shock Measurements* . **Bruel & Kjaer.** 2nd Edition (1980).

62. Ewins, D.J. *Model Testing: Theory and Practice* . **Research Studies Press** . Letchworth, Hertfordshire, England (1984).

63. Timoshenko, S and Young, D.H. *Vibration Problems in Engineering* . **Van Nostrand Reinhold Company.** New York.3rd Edition.(1955).

64. Gorman, D.J. *Free Vibration Analysis of Rectangular Plates* . **Elsevier** . New York (1982).

APPENDICES

APPENDIX A.1

CONVERGENCE

Legend used in the Convergence Plots :

$\beta = 0.0005$ ——————

$\beta = 0.0100$ .. ..

$\beta = 0.0500$.-.-.-.-.-.-.-

$\beta = 0.1000$ ----------

$\beta = 0.2000$ ----------

Legend used in the Variation Plots :

8 x 8 Mesh Size .. ..

9 x 9 Mesh Size ----------

10x10 Mesh Size .-.-.-.-.-.-.-.-.-.-

11x11 Mesh Size ——————

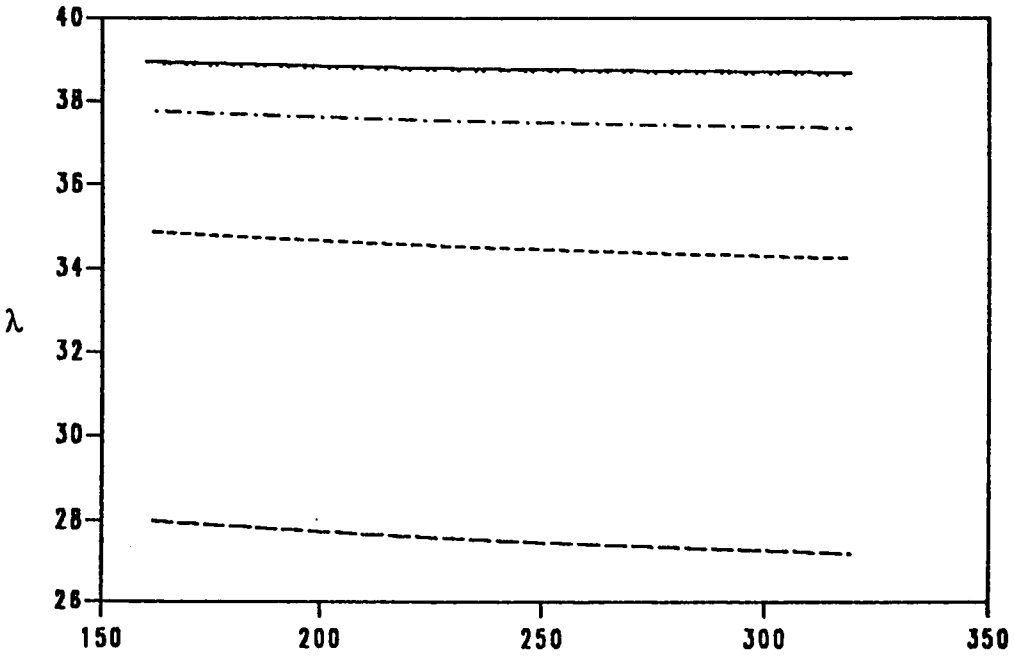

Figure A.1.1 : Convergence of the 1st A-A Mode.
Corner Supported : $\alpha = 0.0$

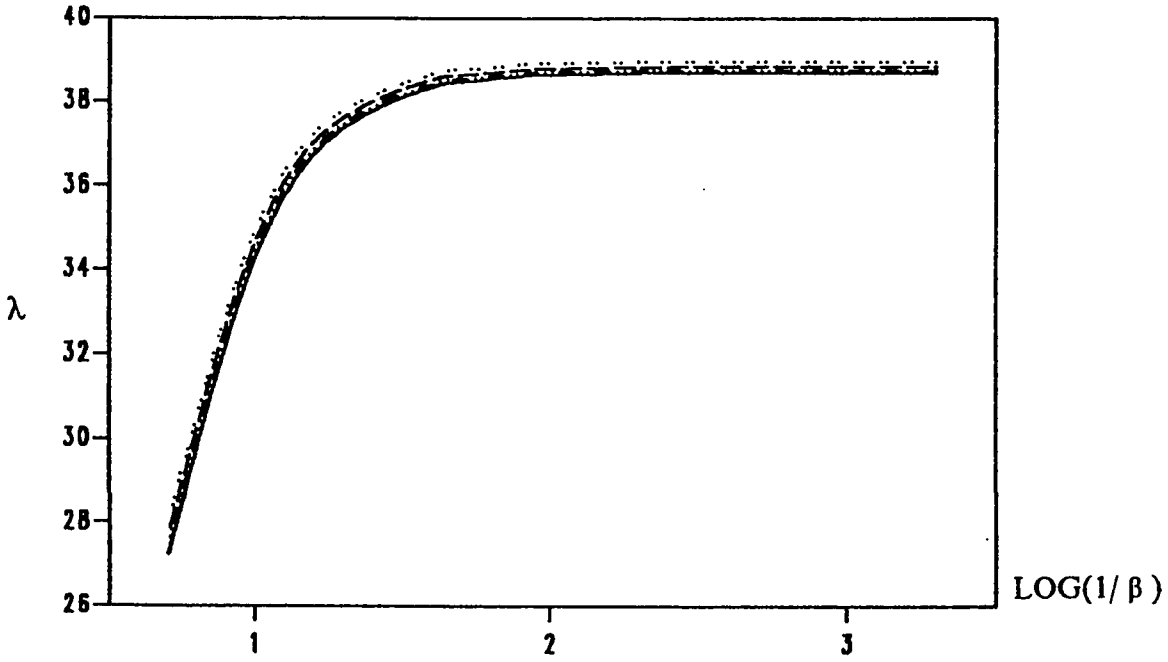

Figure A.1.2 : Comparison of λ for the 1st A-A Mode.
Corner Supported : $\alpha = 0.0$

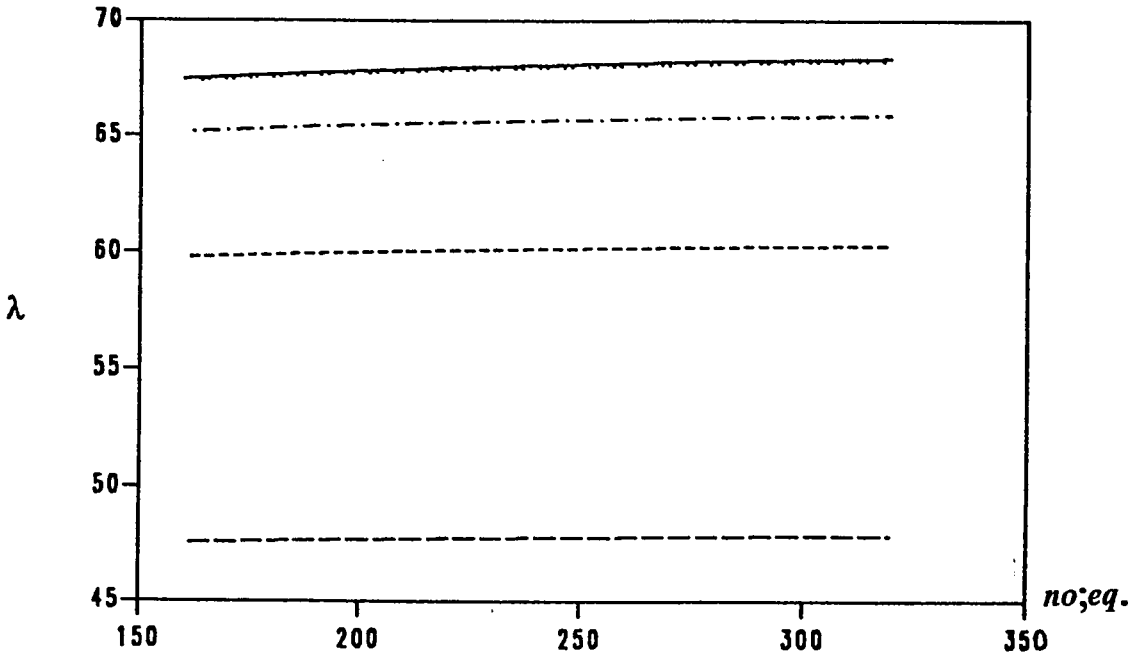

Figure A.1.3 : Convergence of the 2nd A-A Mode.
Corner Supported : $\alpha = 0.0$

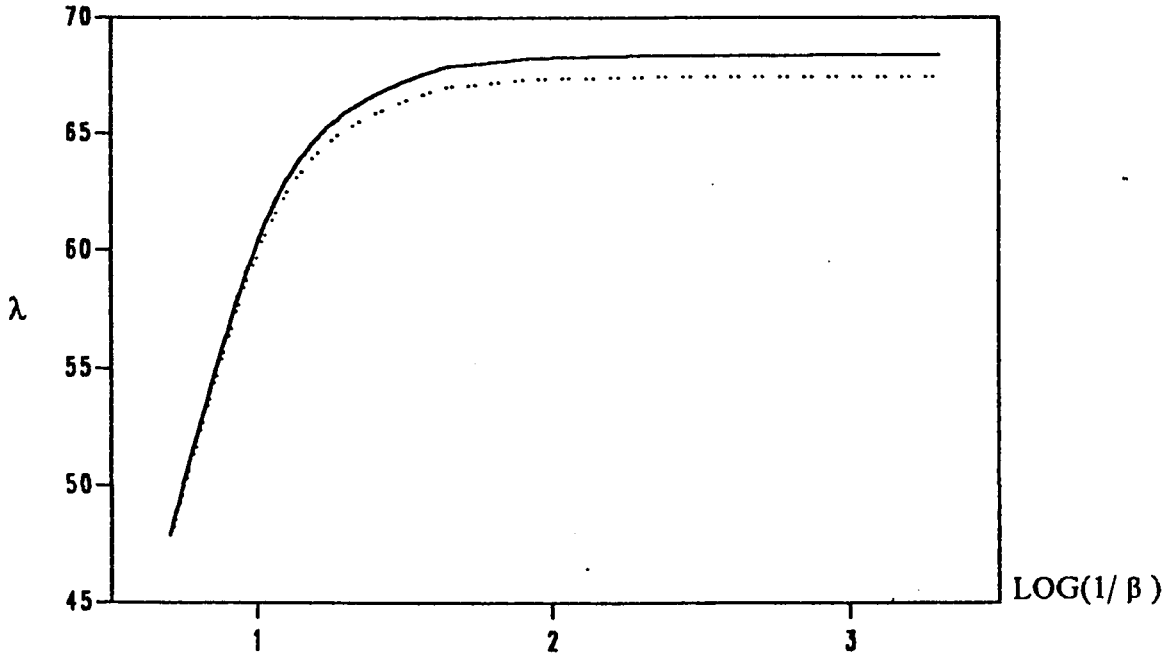

Figure A.1.4 : Comparison of λ for the 2nd A-A Mode.
Corner Supported : $\alpha = 0.0$

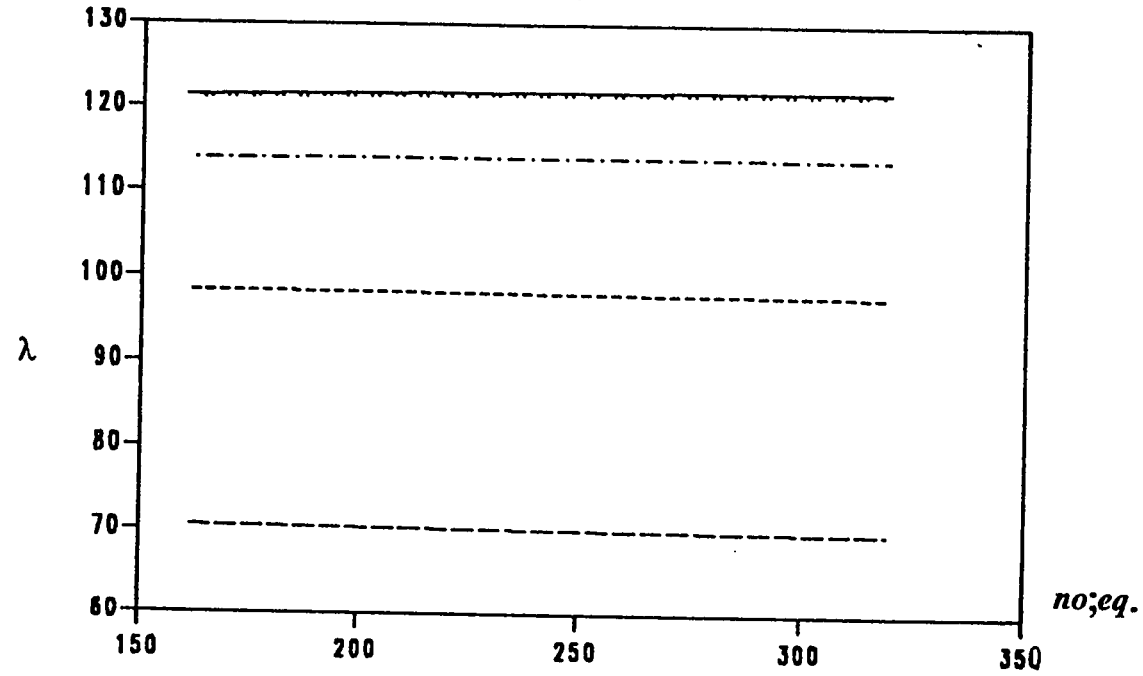

Figure A.1.5 : Convergence of the 3rd A-A Mode.
Corner Supported : $\alpha = 0.0$

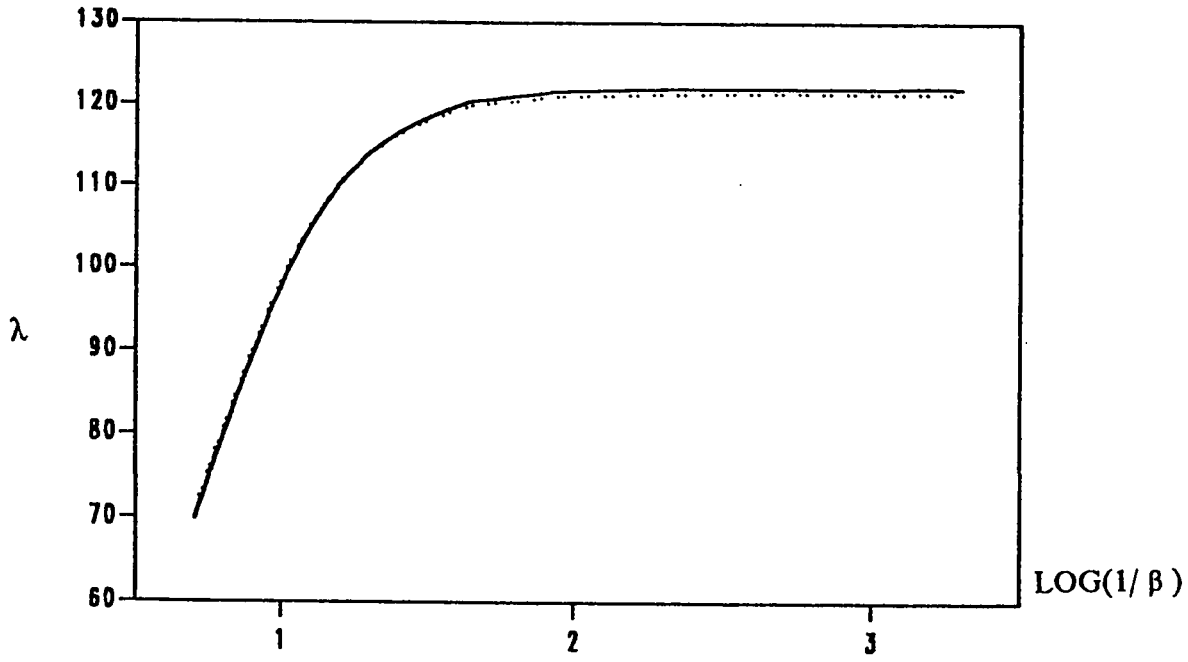

Figure A.1.6 : Comparison of λ for the 3rd A-A Mode.
Corner Supported : $\alpha = 0.0$

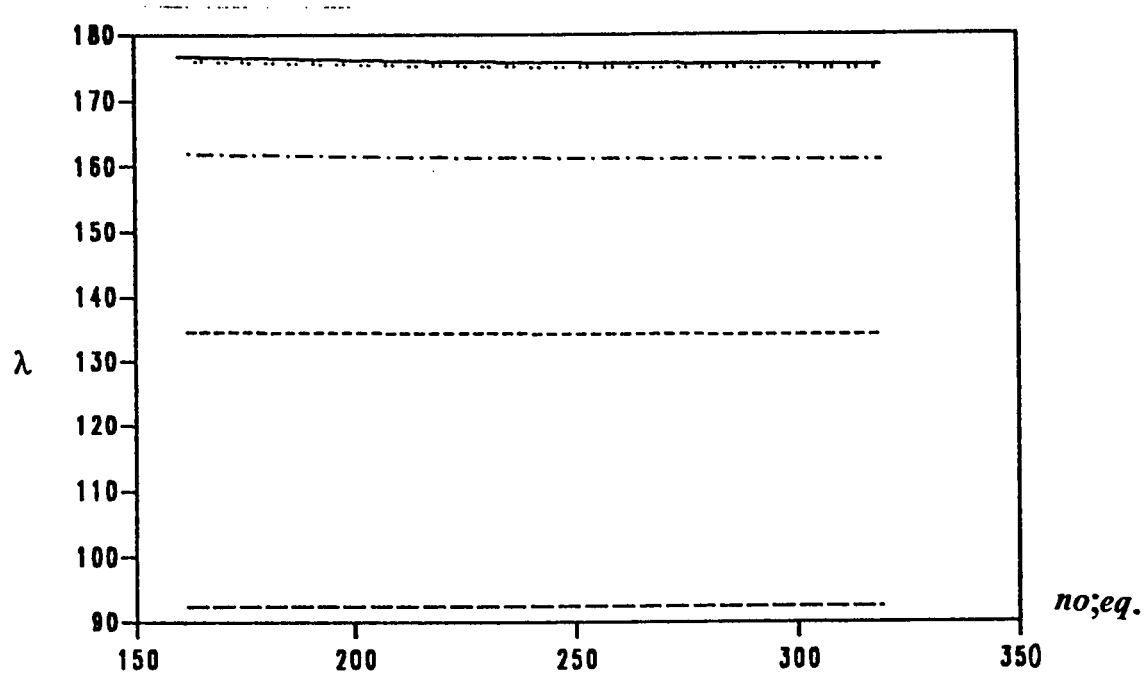

Figure A.1.7 : Convergence of the 4th A-A Mode.
Corner Supported : $\alpha = 0.0$

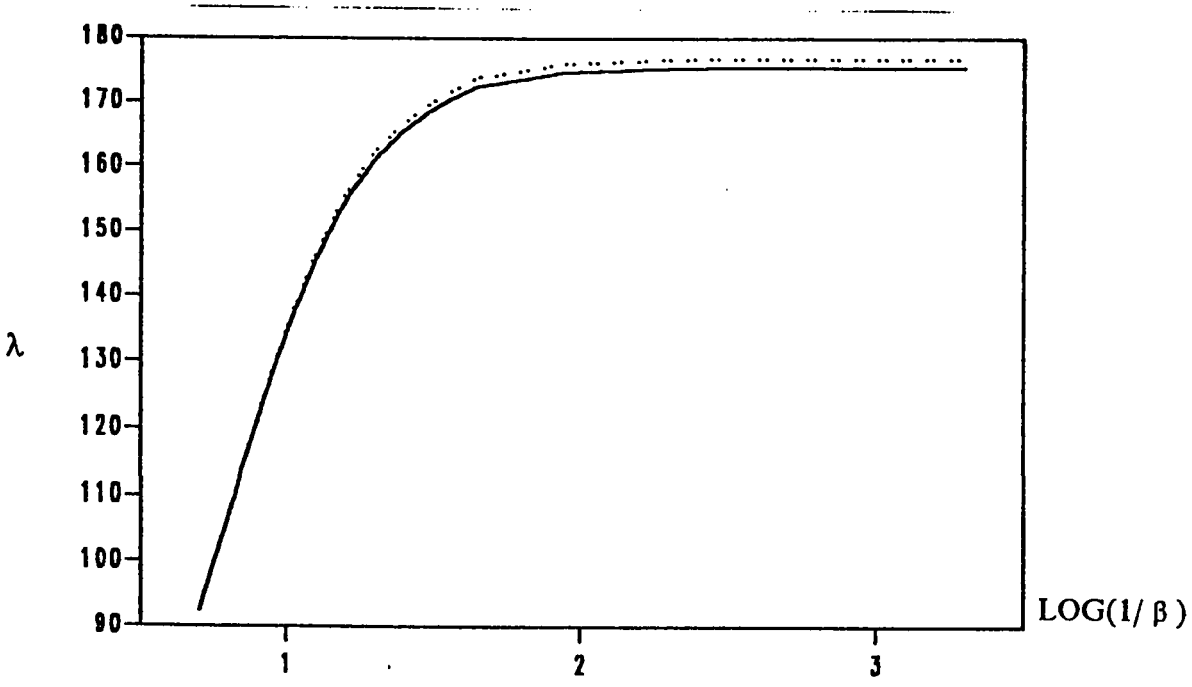

Figure A.1.8 : Comparison of λ for the 4th A-A Mode.
Corner Supported : $\alpha = 0.0$

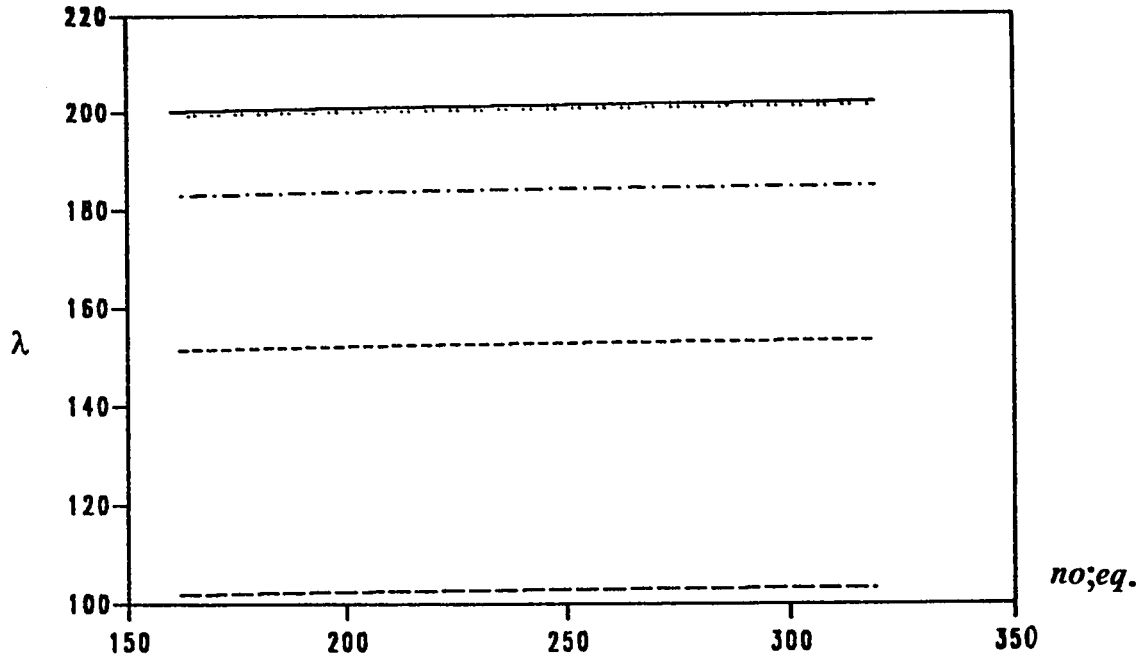

Figure A.1.9 : Convergence of the 5th A-A Mode.
Corner Supported : α = 0.0

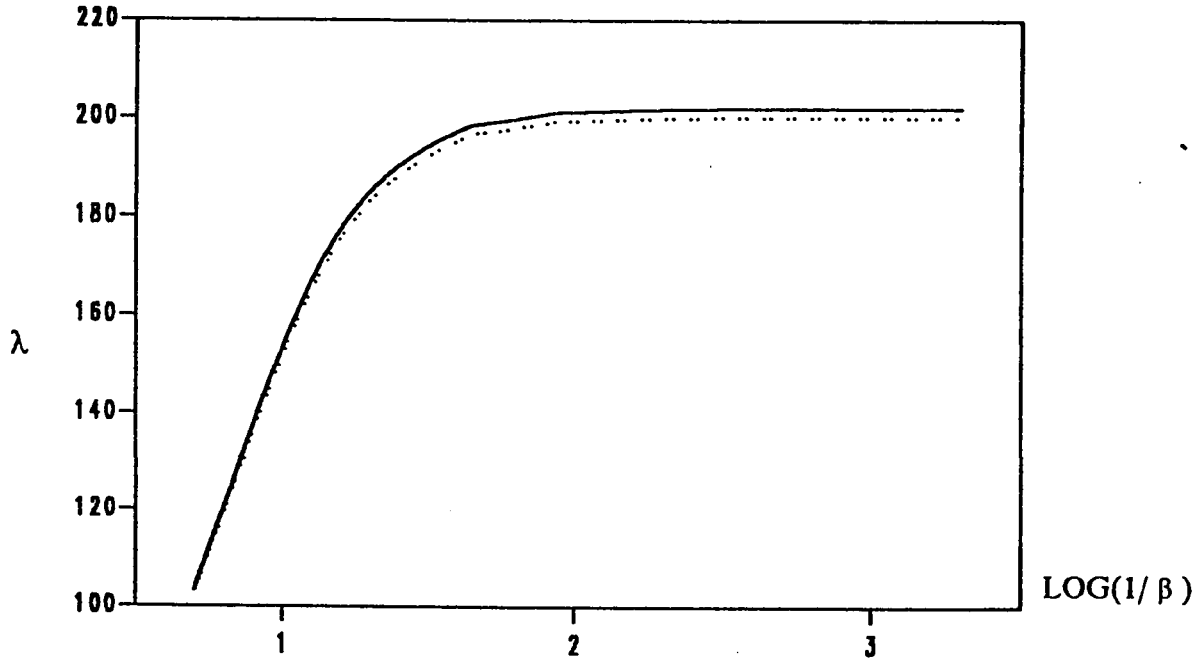

Figure A.1.10 : Comparison of λ for the 5th A-A Mode.
Corner Supported : α = 0.0

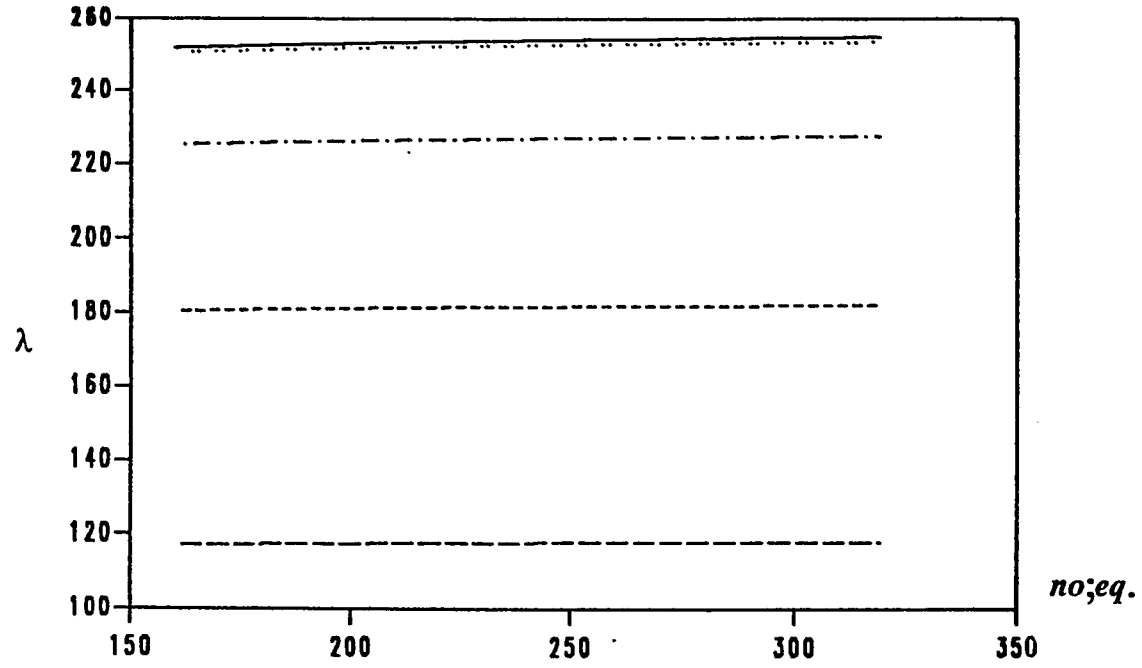

Figure A.1.11 : Convergence of the 6th A-A Mode.
Corner Supported : $\alpha = 0.0$

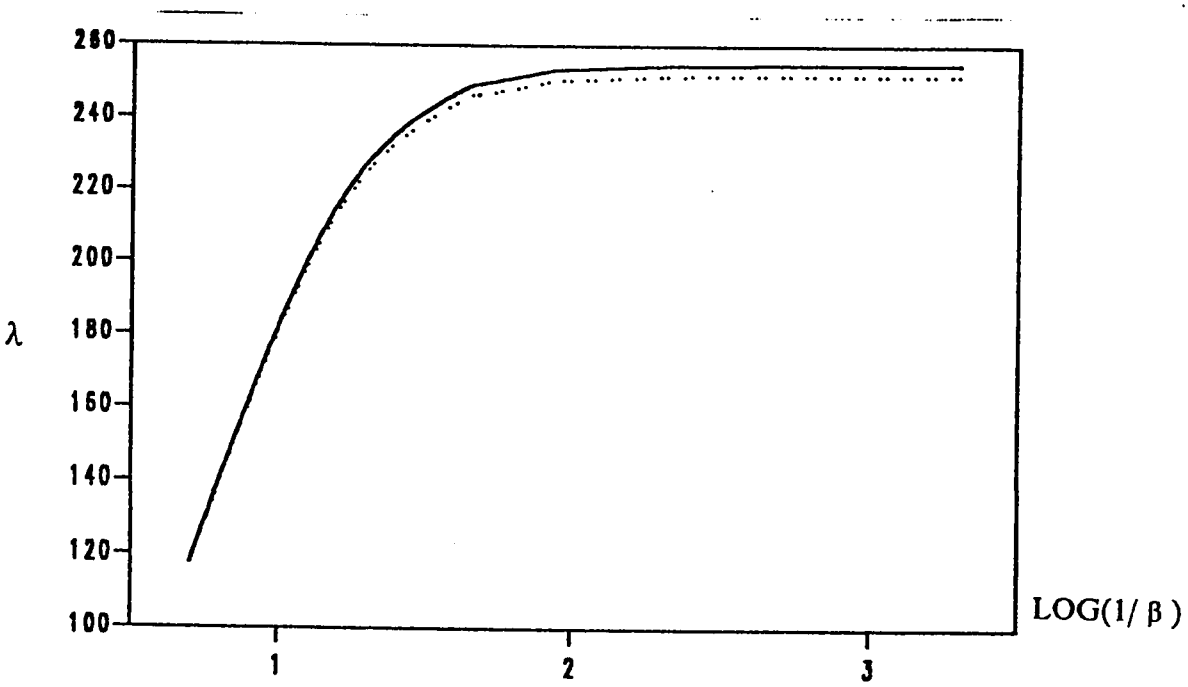

Figure A.1.12 : Comparison of λ for the 6th A-A Mode.
Corner Supported : $\alpha = 0.0$

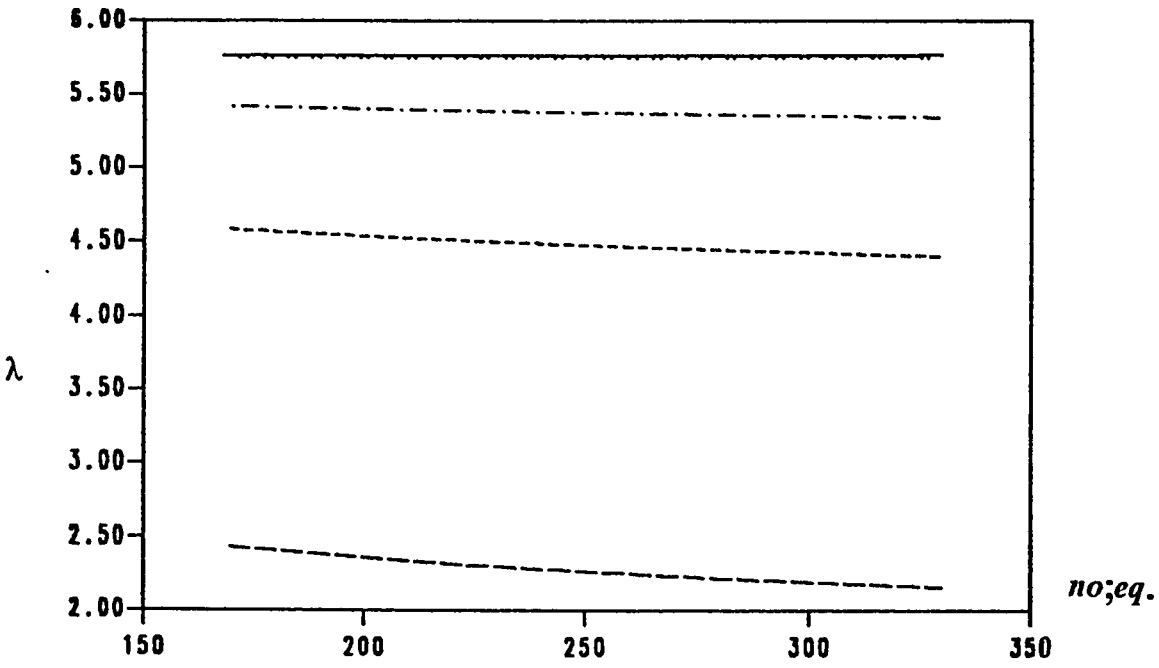

Figure A.1.13 : Convergence of the 1st S-A Mode.
Corner Supported : $\alpha = 0.0$

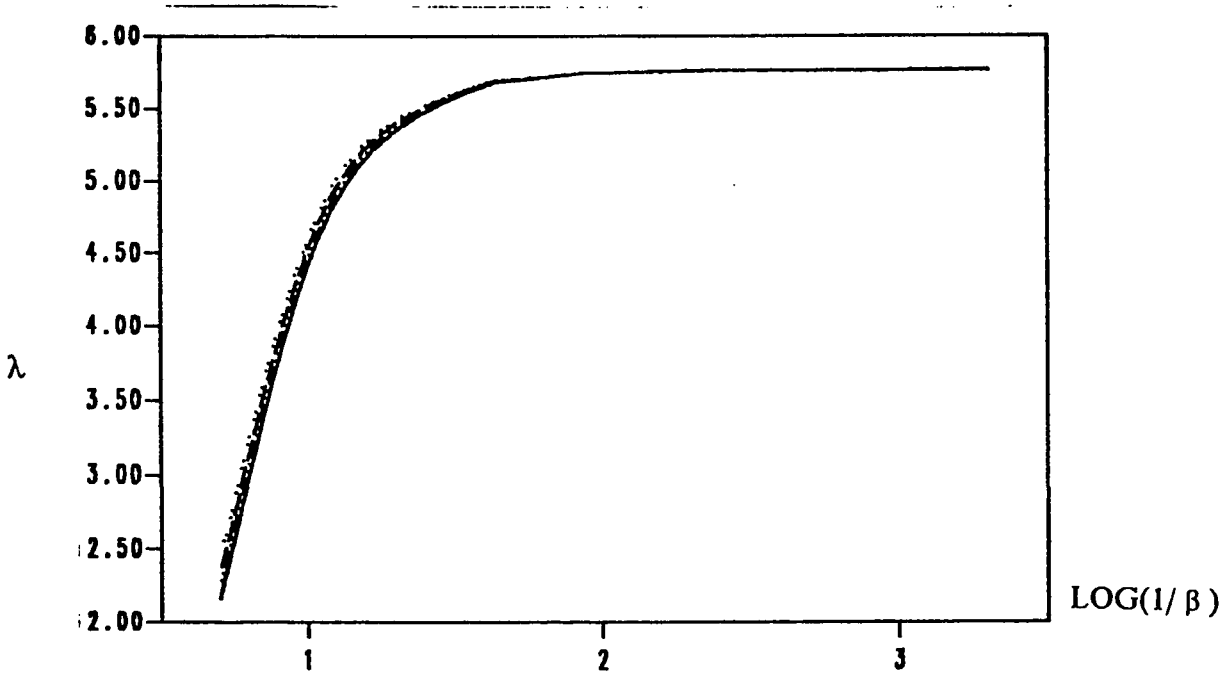

Figure A.1.14 : Comparison of λ for the 1st S-A Mode.
Corner Supported : $\alpha = 0.0$

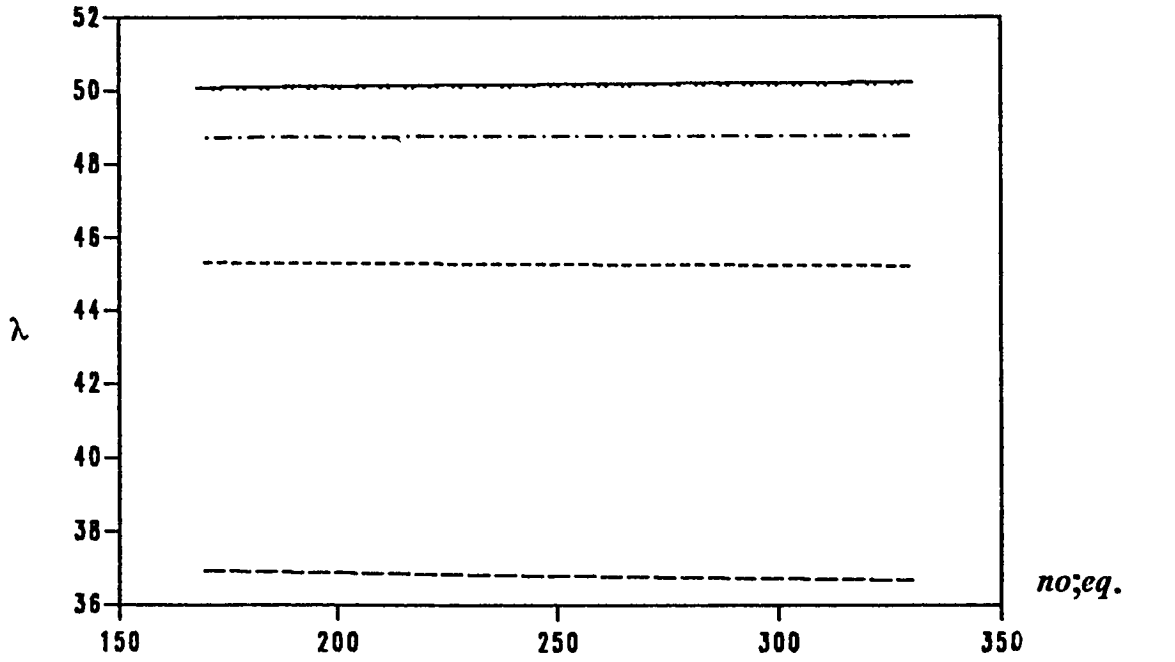

Figure A.1.15 : Convergence of the 2nd S-A Mode.
Corner Supported : $\alpha = 0.0$

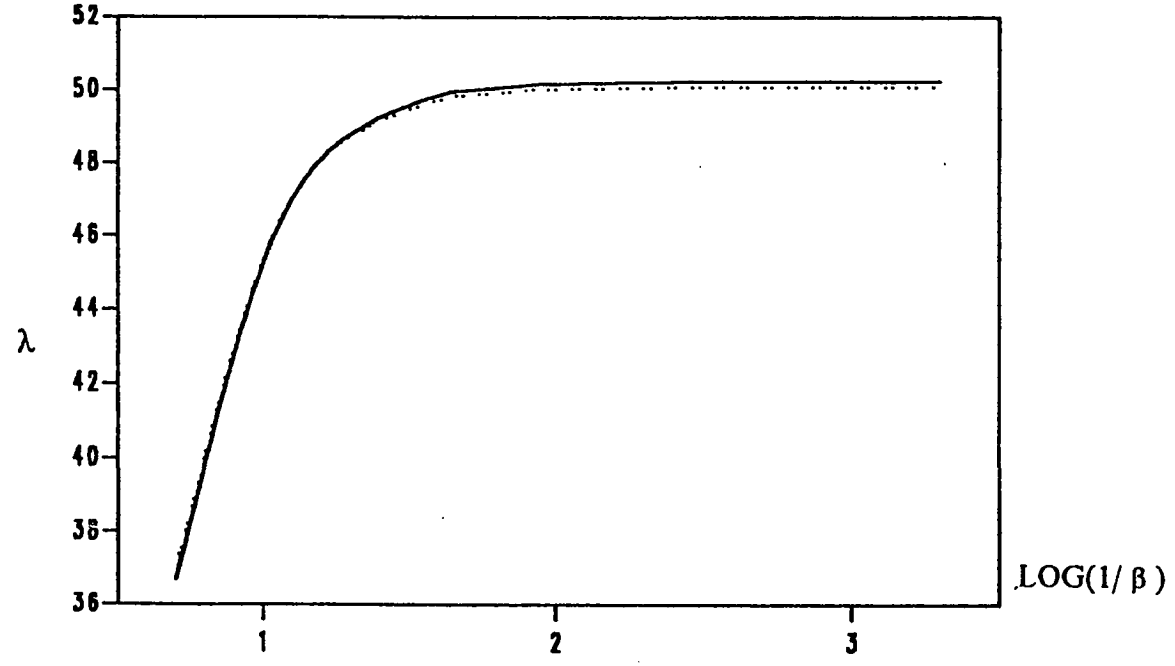

Figure A.1.16 : Comparison of λ for the 2nd S-A Mode.
Corner Supported : $\alpha = 0.0$

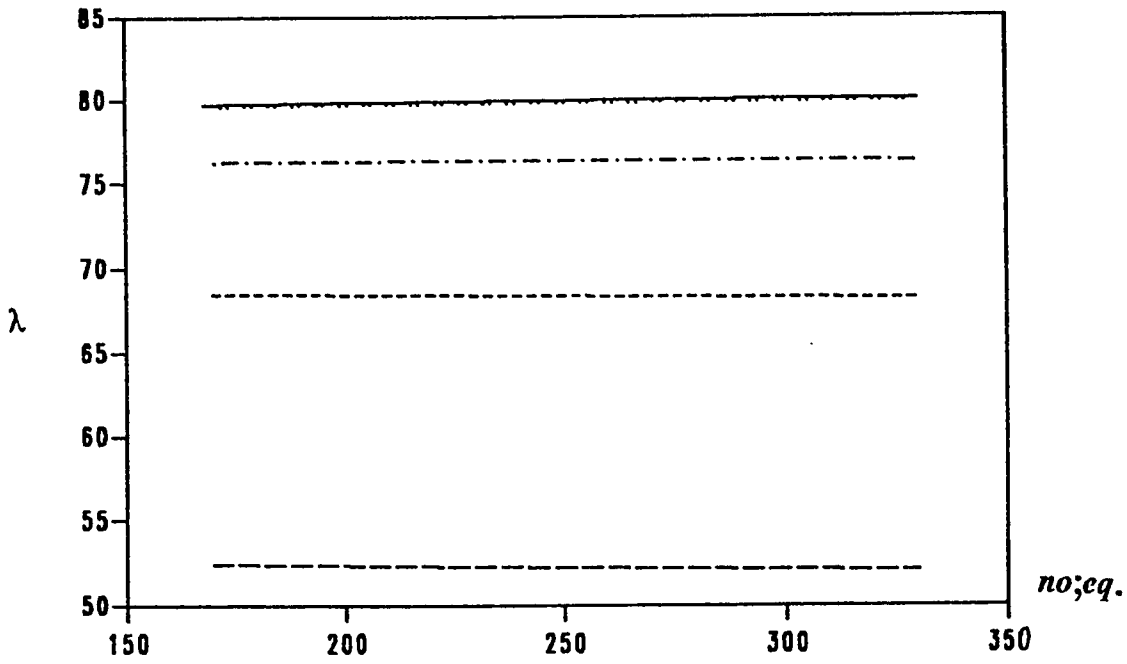

Figure A.1.17 : Convergence of the 3rd S-Λ Mode.
Corner Supported : α = 0.0

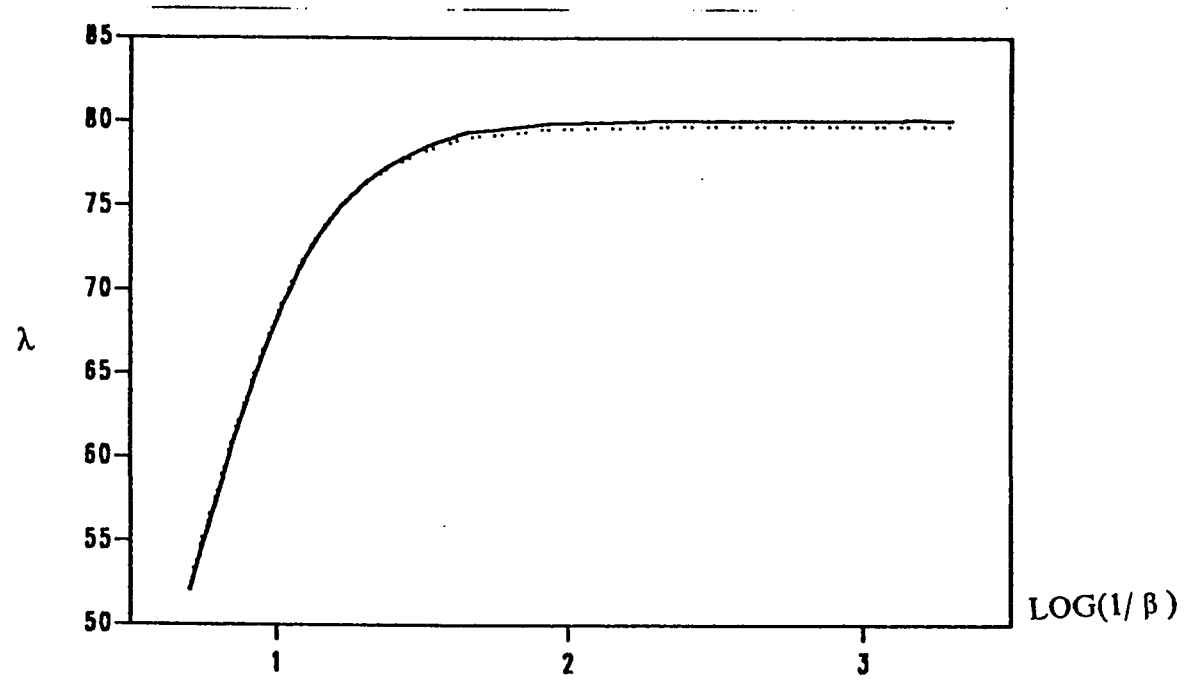

Figure A.1.18 : Comparison of λ for the 3rd S-A Mode.
Corner Supported : α = 0.0

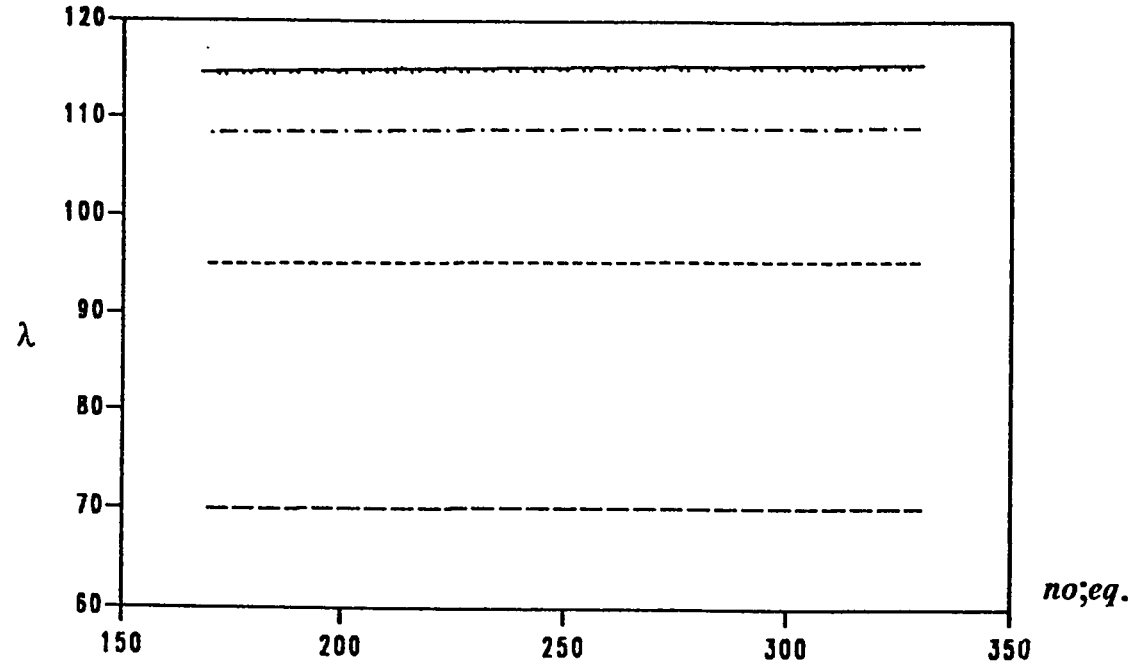

Figure A.1.19 : Convergence of the 4th S-A Mode.
Corner Supported : $\alpha = 0.0$

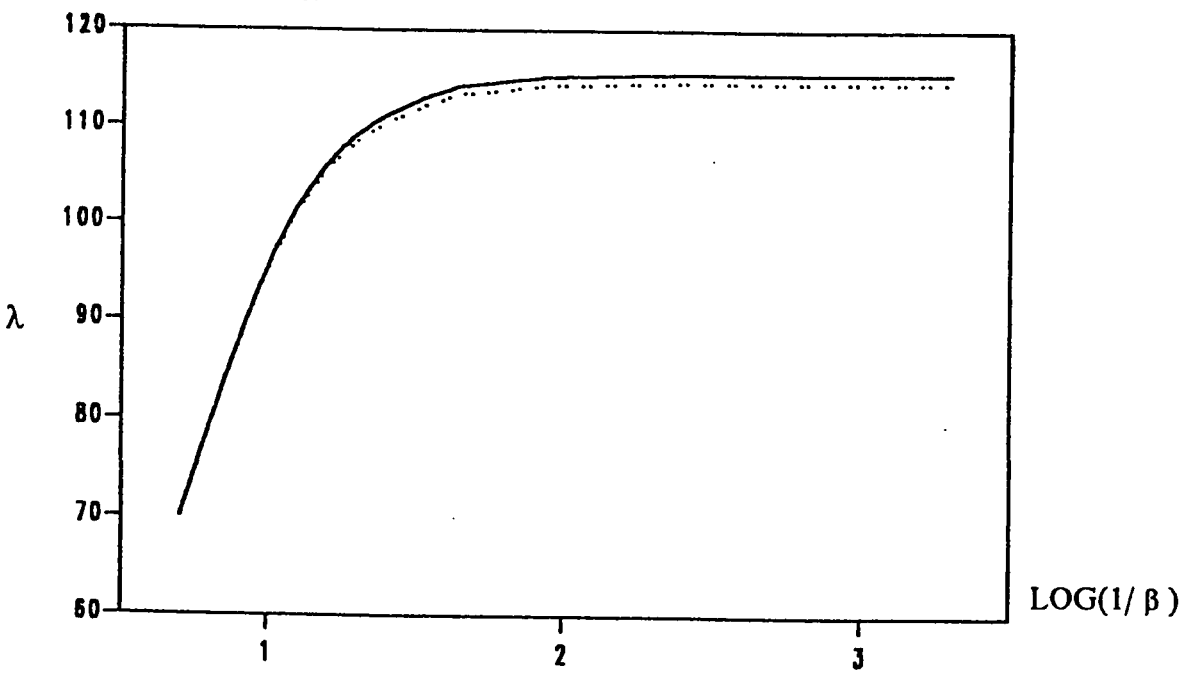

Figure A.1.20 : Comparison of λ for the 4th S-A Mode.
Corner Supported : $\alpha = 0.0$

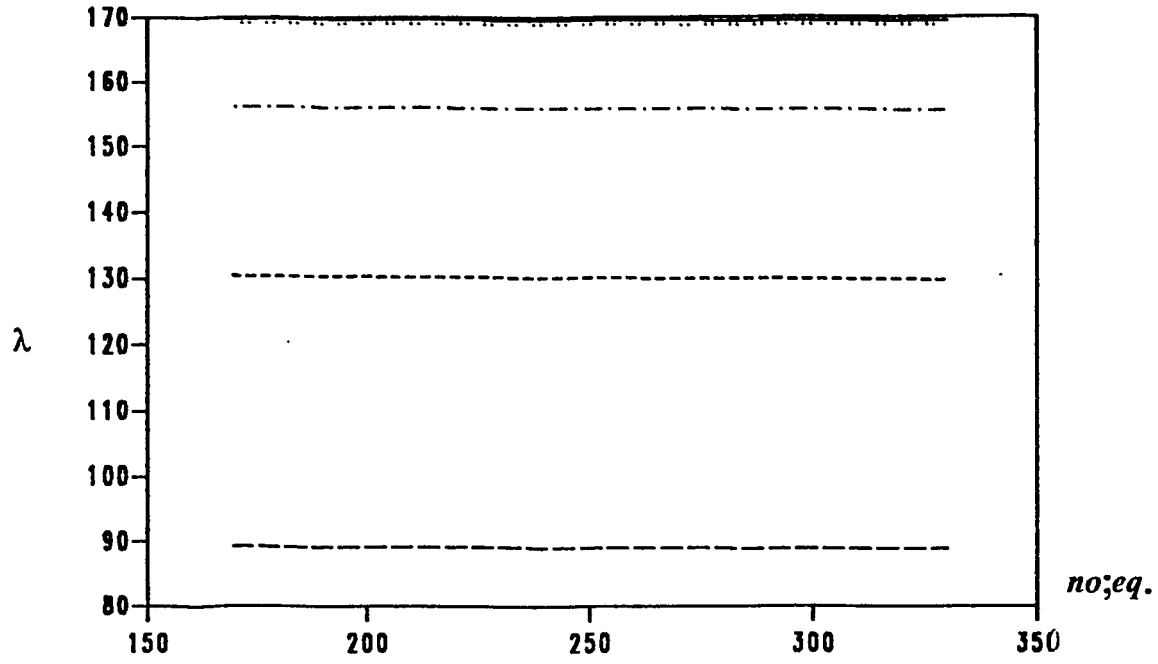

Figure A.1.21 : Convergence of the 5th S-A Mode.
Corner Supported : $\alpha = 0.0$

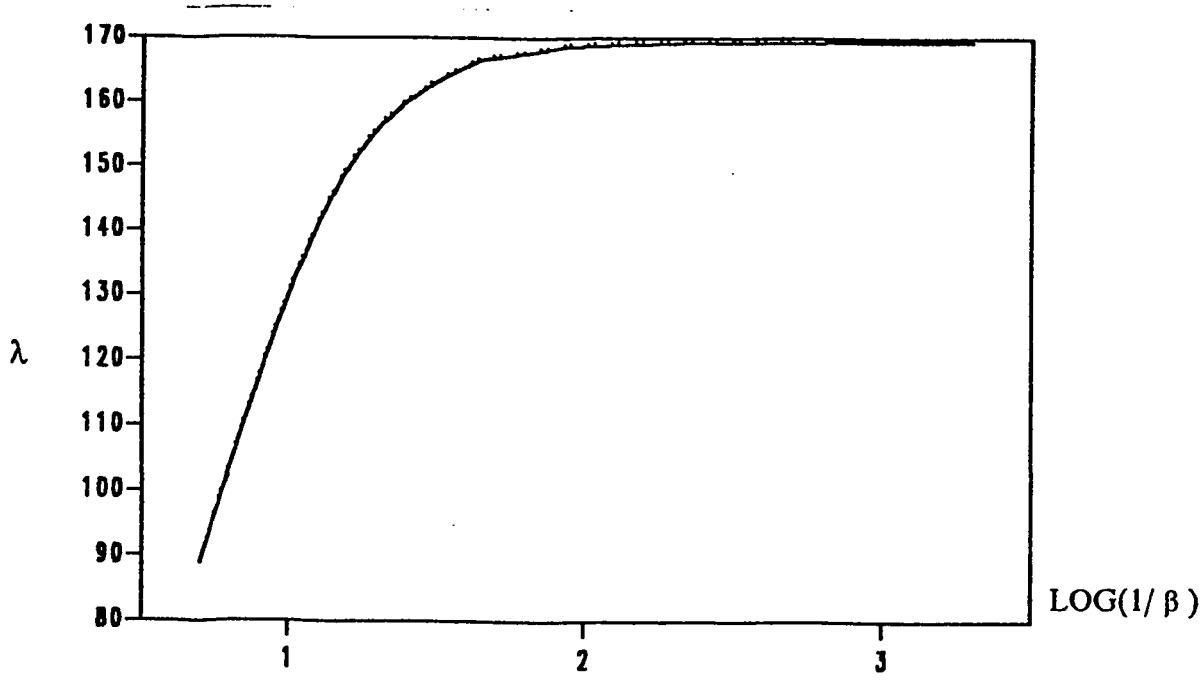

Figure A.1.22 : Comparison of λ for the 5th S-A Mode.
Corner Supported : $\alpha = 0.0$

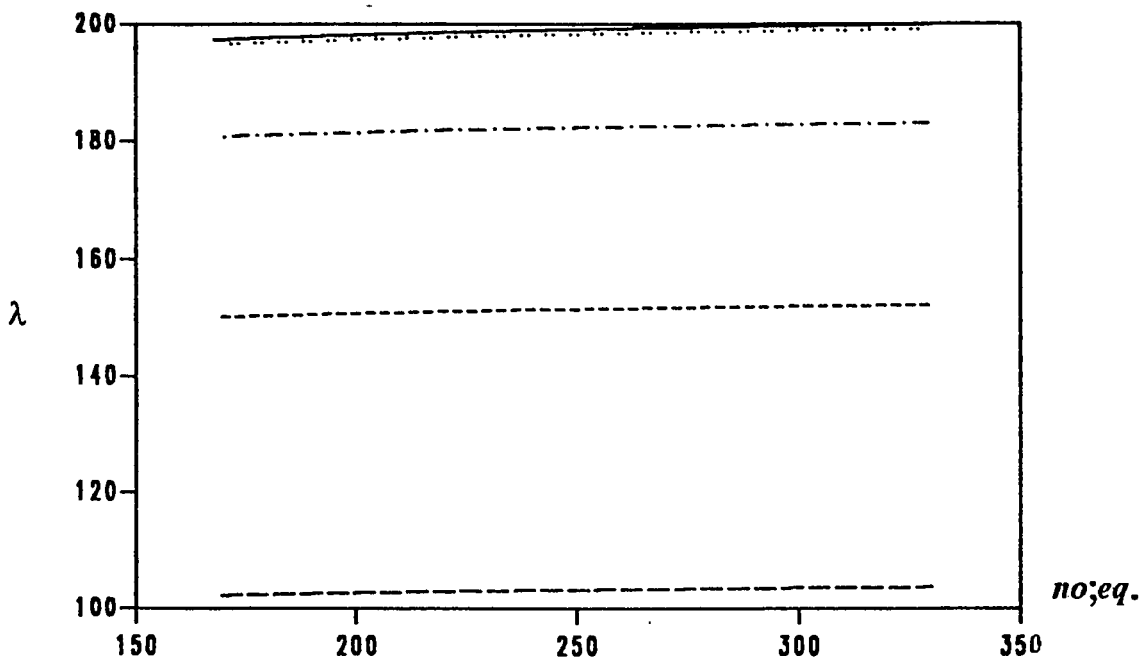

Figure A.1.23 : Convergence of the 6th S-A Mode.
Corner Supported : $\alpha = 0.0$

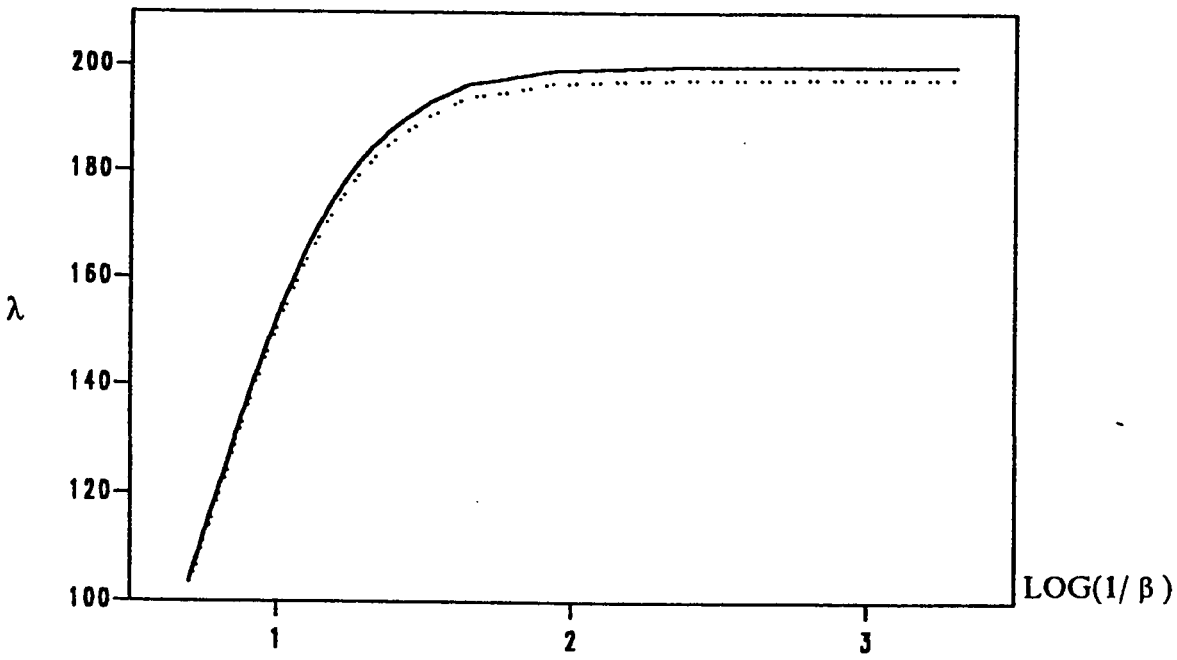

Figure A.1.24 : Comparison of λ for the 6th S-A Mode.
Corner Supported : $\alpha = 0.0$

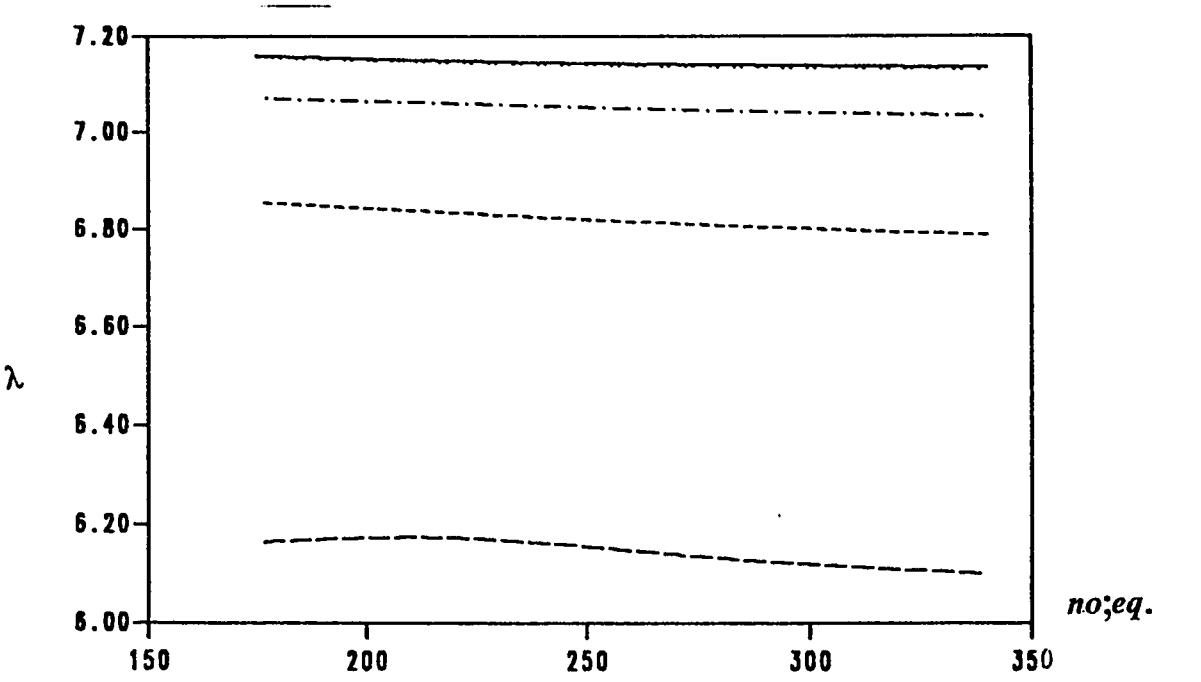

Figure A.1.25 : Convergence of the 1st S-S Mode.
Corner Supported : α = 0.0

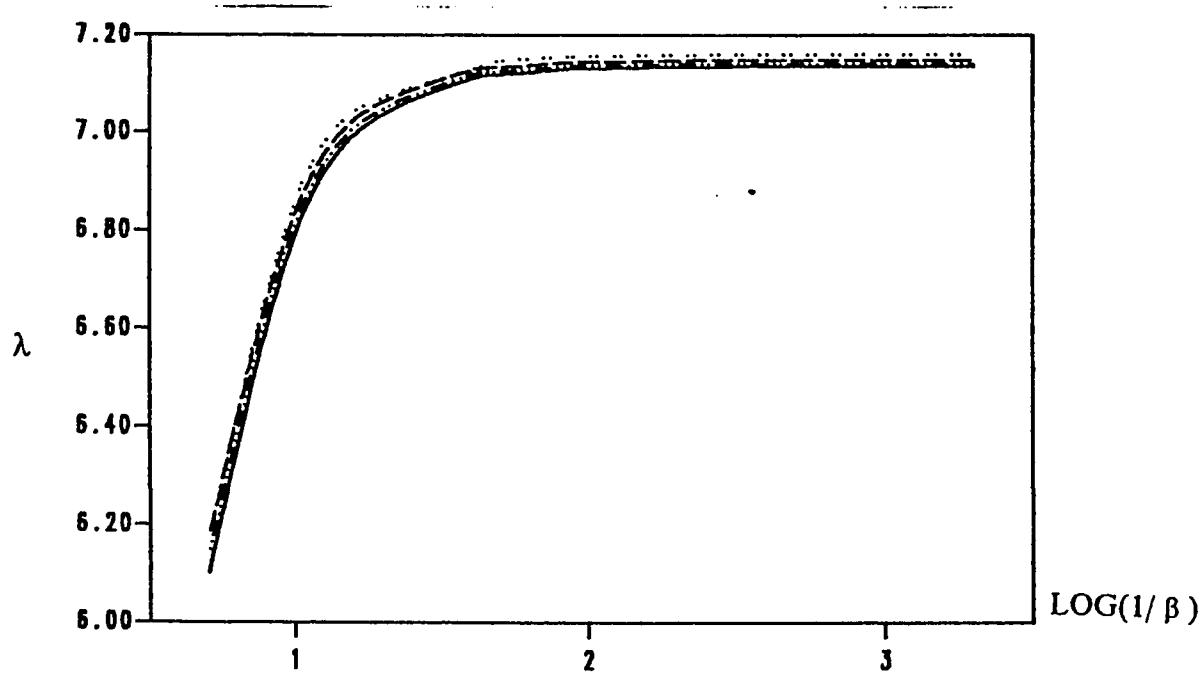

Figure A.1.26 : Comparison of λ for the 1st S-S Mode.
Corner Supported : α = 0.0

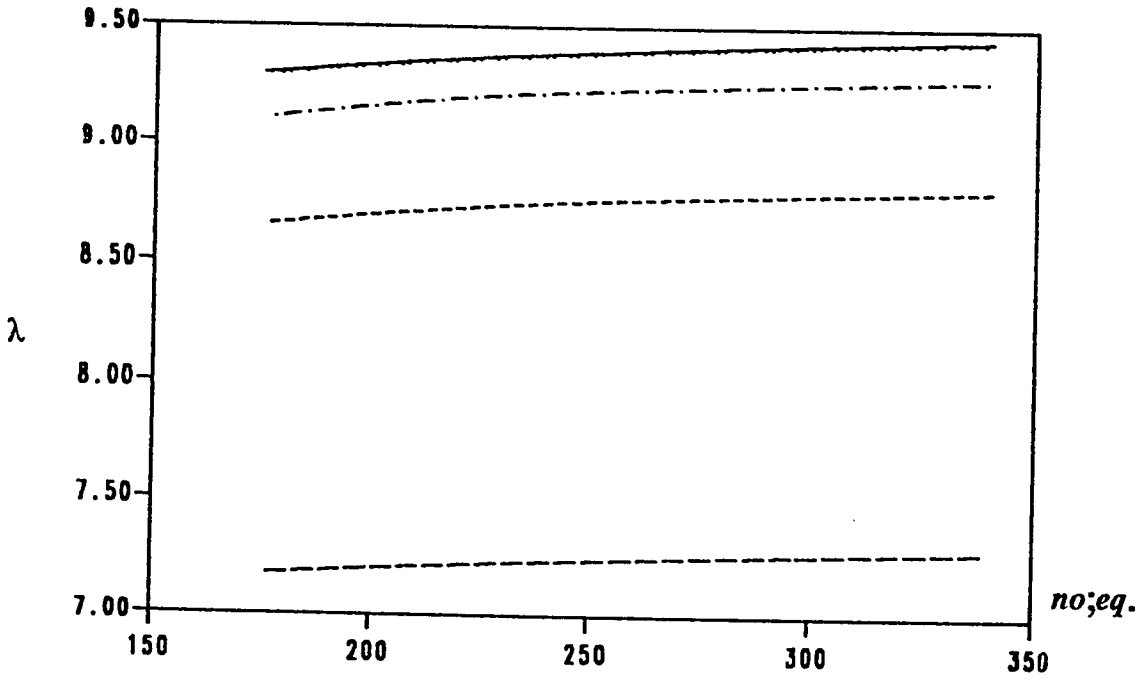

Figure A.1.27 : Convergence of the 2nd S-S Mode.
Corner Supported : $\alpha = 0.0$

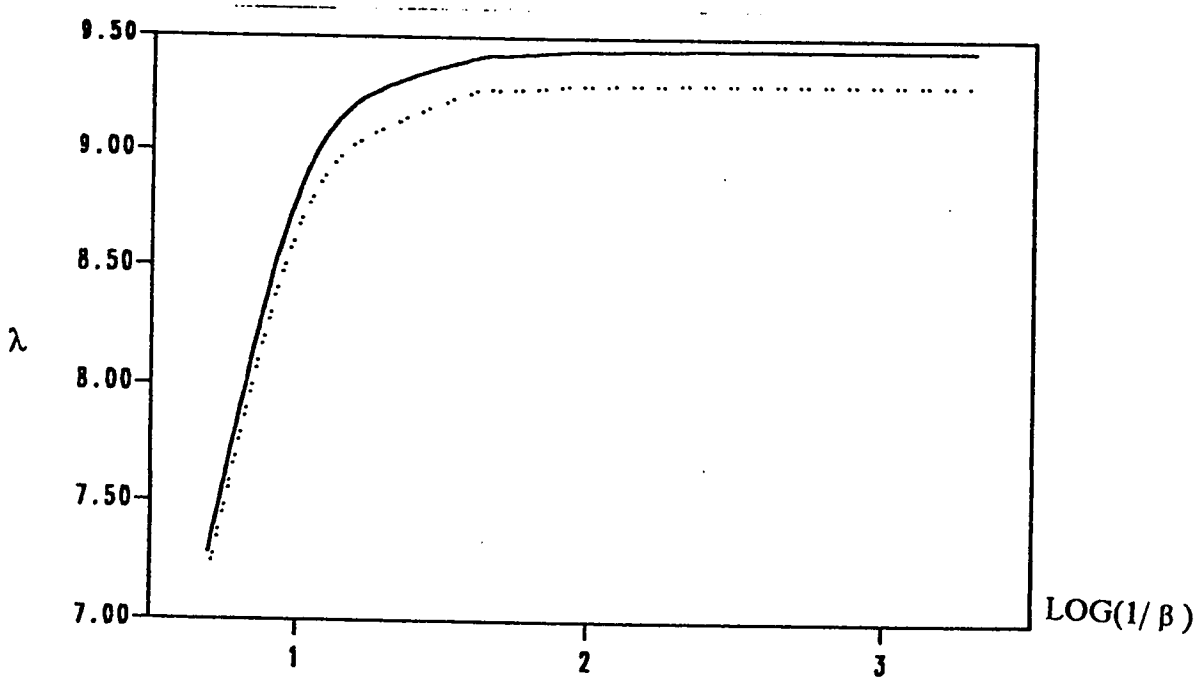

Figure A.1.28 : Comparison of λ for the 2nd S-S Mode.
Corner Supported : $\alpha = 0.0$

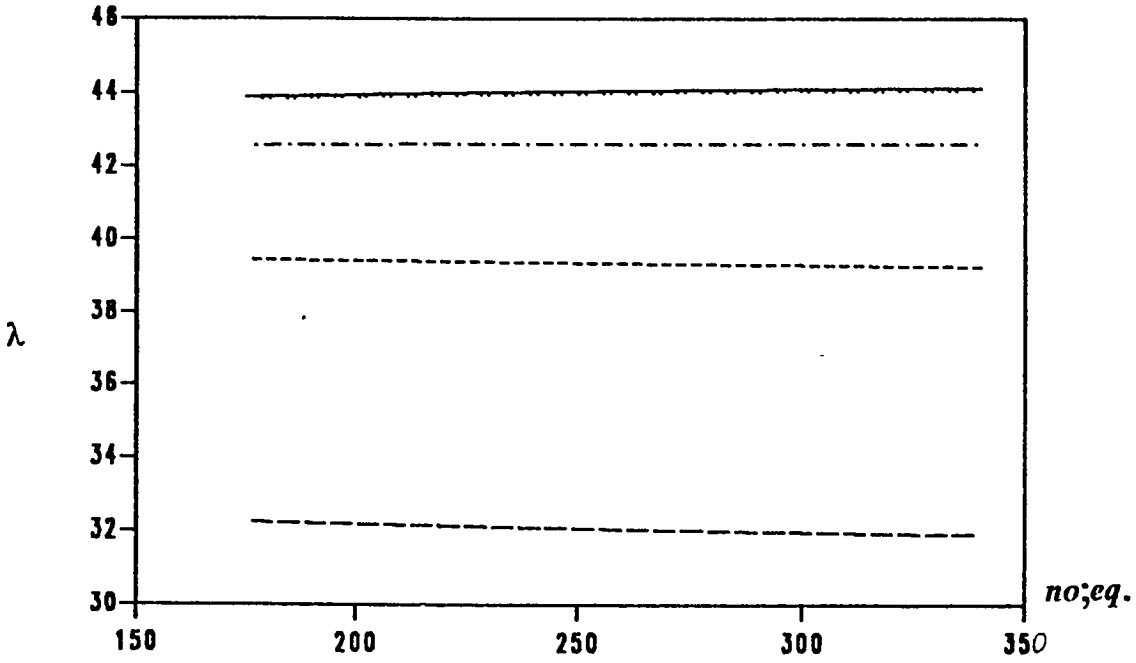

Figure A.1.29 : Convergence of the 3rd S-S Mode.
Corner Supported : $\alpha = 0.0$

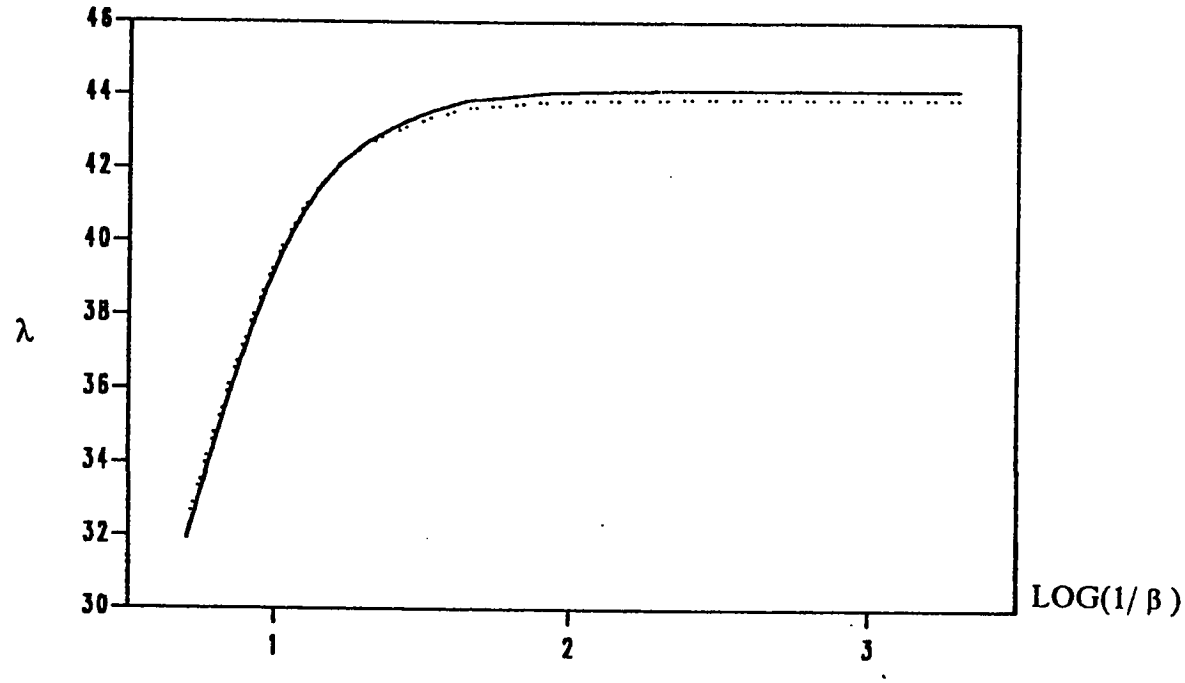

Figure A.1.30 : Comparison of λ for the 3rd S-S Mode.
Corner Supported : $\alpha = 0.0$

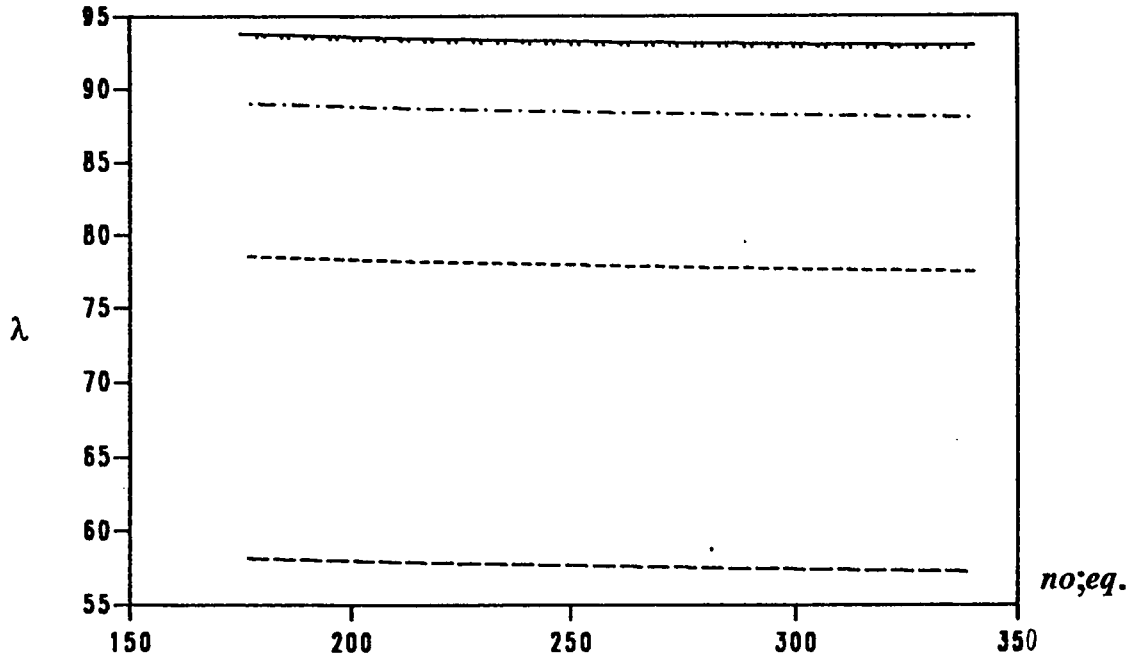

Figure A.1.31 : Convergence of the 4th S-S Mode.
Corner Supported : $\alpha = 0.0$

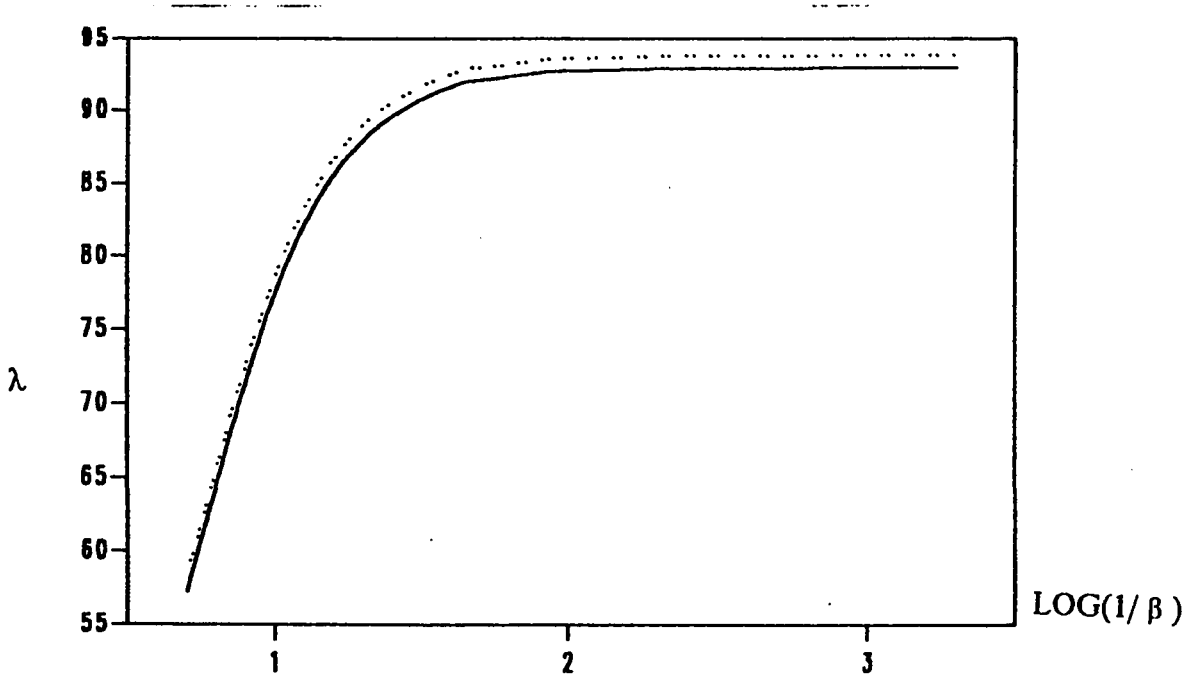

Figure A.1.32 : Comparison of λ for the 4th S-S Mode.
Corner Supported : $\alpha = 0.0$

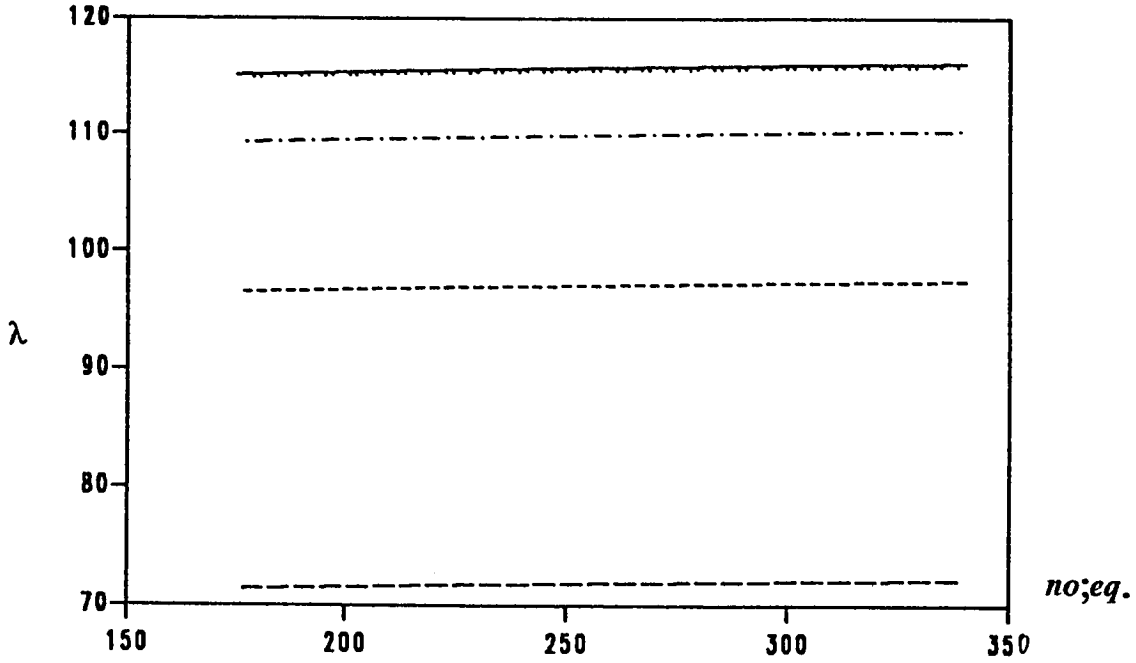

Figure A.1.33 : Convergence of the 5th S-S Mode.
Corner Supported : $\alpha = 0.0$

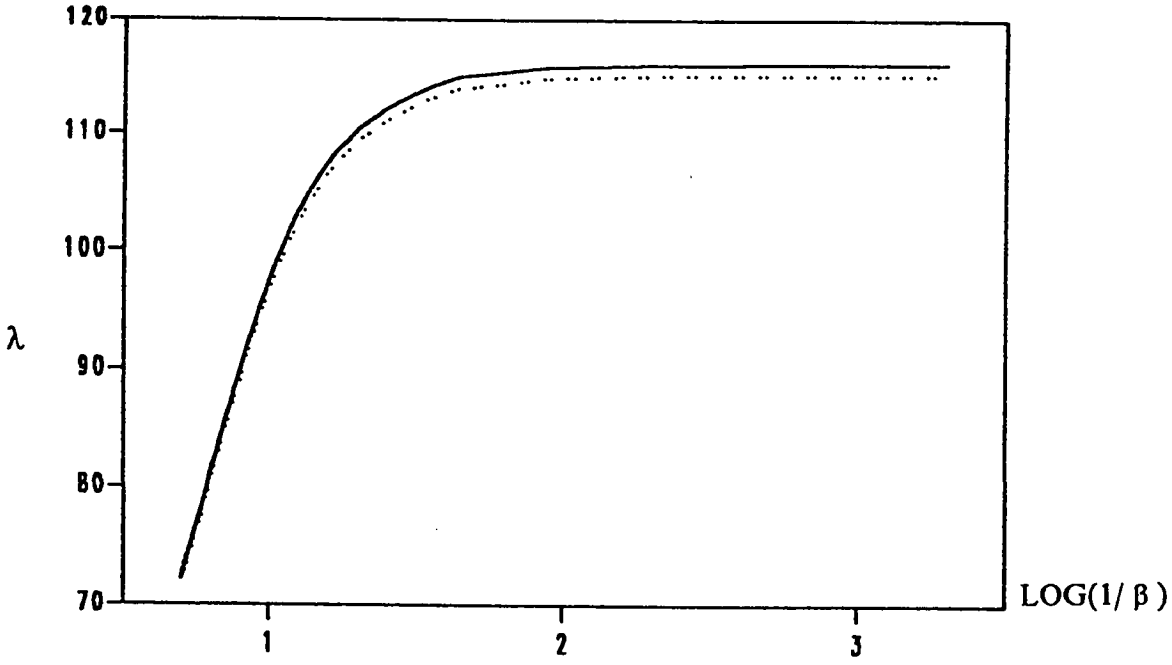

Figure A.1.34 : Comparison of λ for the 5th S-S Mode.
Corner Supported : $\alpha = 0.0$

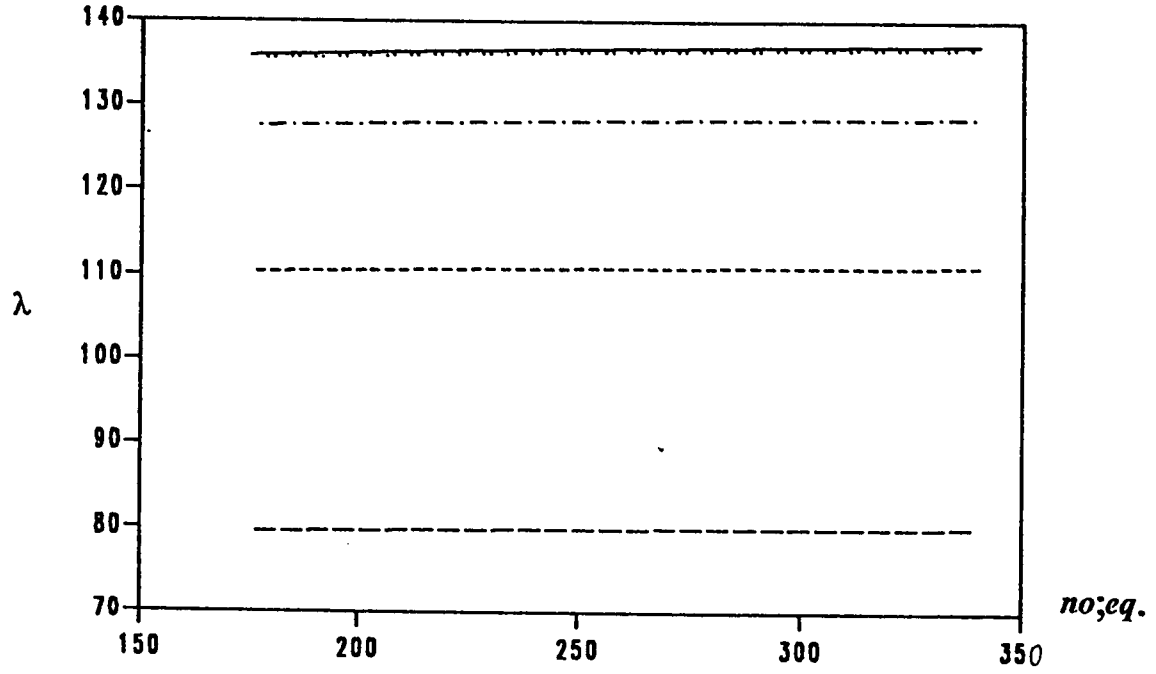

Figure A.1.35 : Convergence of the 6th S-S Mode.
Corner Supported : $\alpha = 0.0$

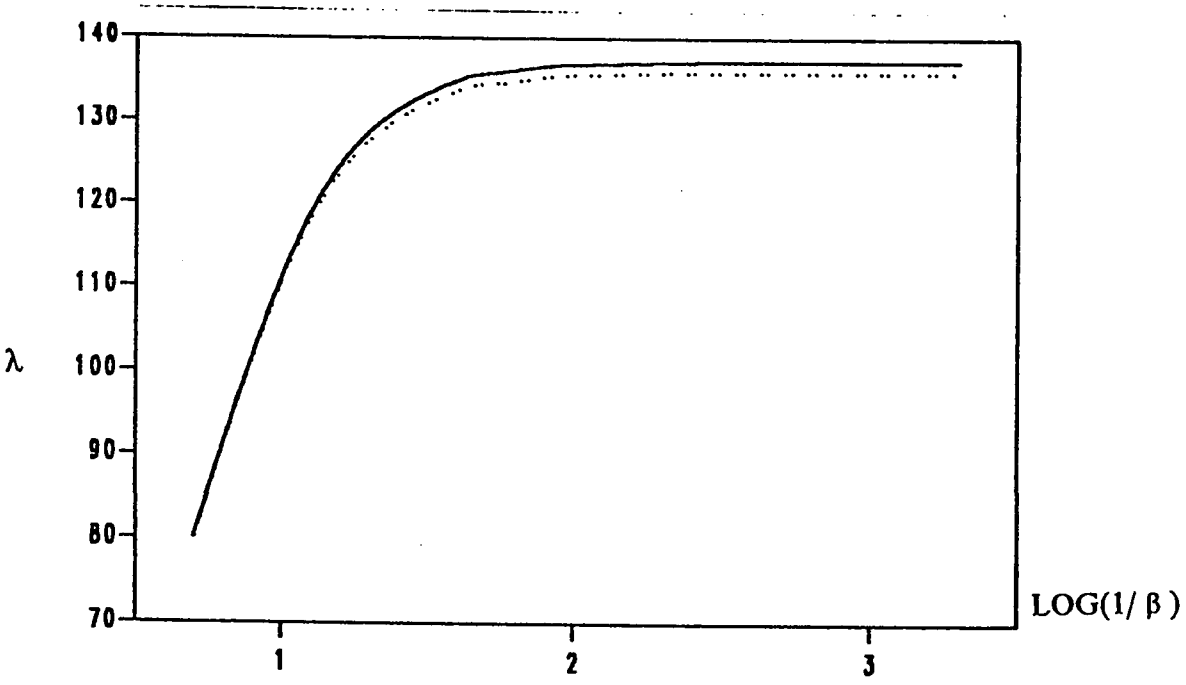

Figure A.1.36 : Comparison of λ for the 6th S-S Mode.
Corner Supported : $\alpha = 0.0$

APPENDIX A.2

CORNER & POINT SUPPORTED PLATES

Legend used in the Variation Plots :

Mode 1 : ——————

Mode 2 : — — — — — —

Mode 3 : —.—.—.—.—.

Mode 4 : - - - - - - - - - - - -

Mode 5 : —..—..—..—..—

Mode 6 : .. ..

Legend used in the Correction Plots :

Mode 1 : ——————

Mode 2 : — — — — — —

Mode 3 : —.—.—.—.—.

Mode 4 : - - - - - - - - - - - -

Mode 5 : —..—..—..—..—

Mode 6 : ——————

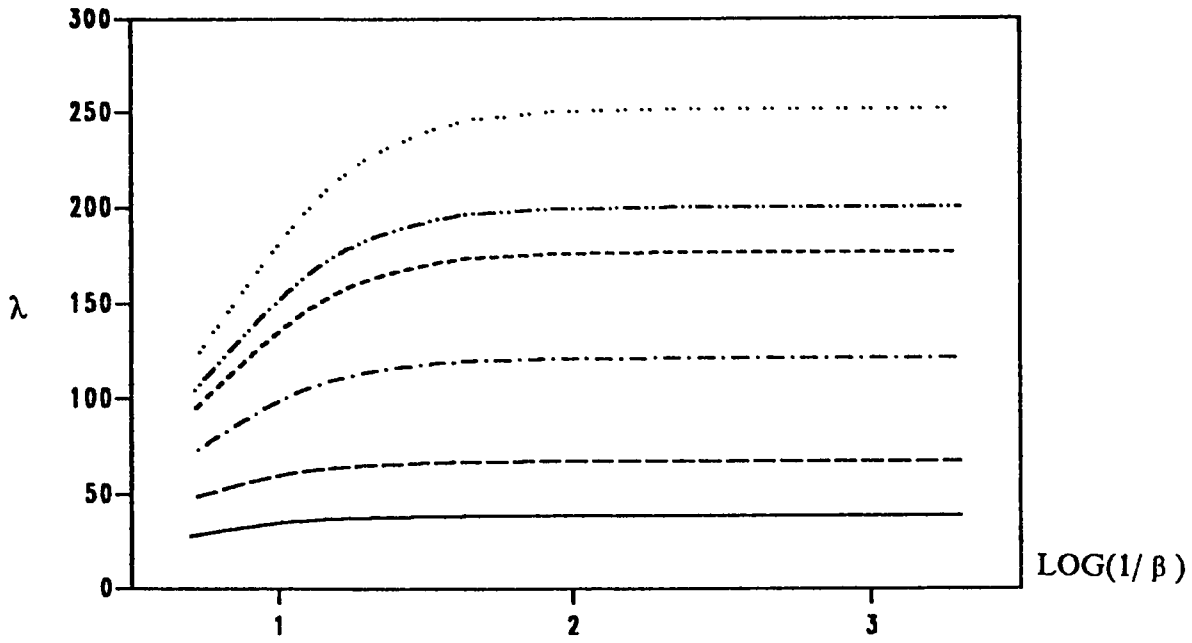

Figure A.2.1 : Variation of λ with β for the First Six A-A Modes.
Corner Supported : α = 0.0 , Mesh Size 8 x 8.

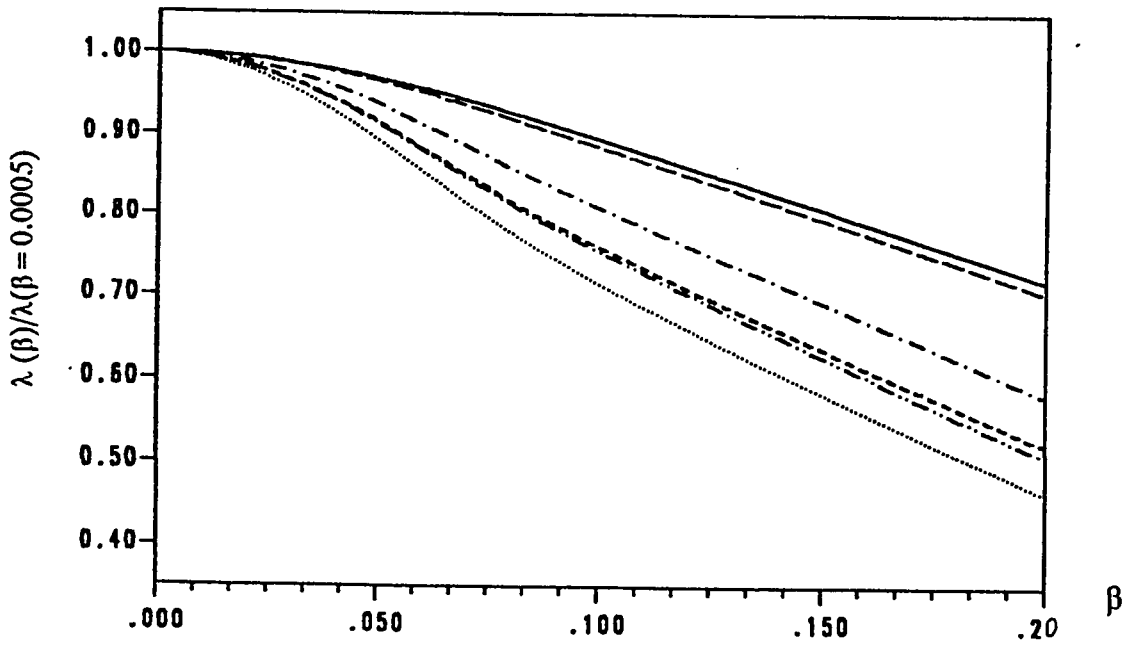

Figure A.2.2 : Correction in λ for the First Six A-A Modes.
Corner Supported : α = 0.0 , Mesh Size 8 x 8.

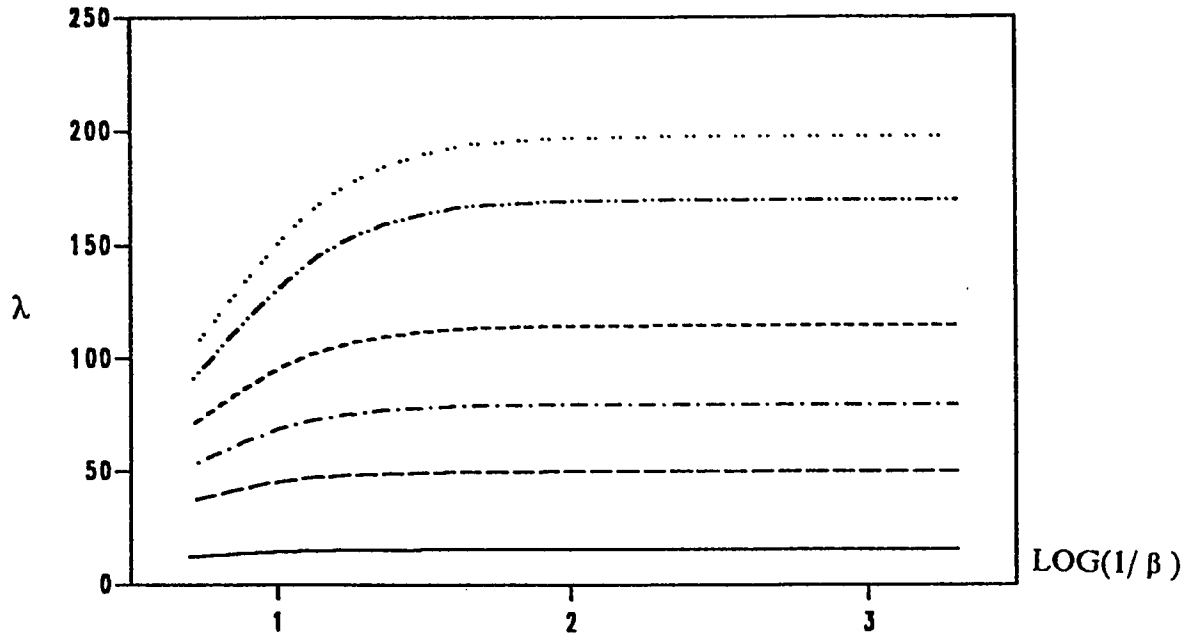

Figure A.2.3 : Variation of λ with β for the First Six S-A Modes.
Corner Supported : α = 0.0 , Mesh Size 8 x 8.

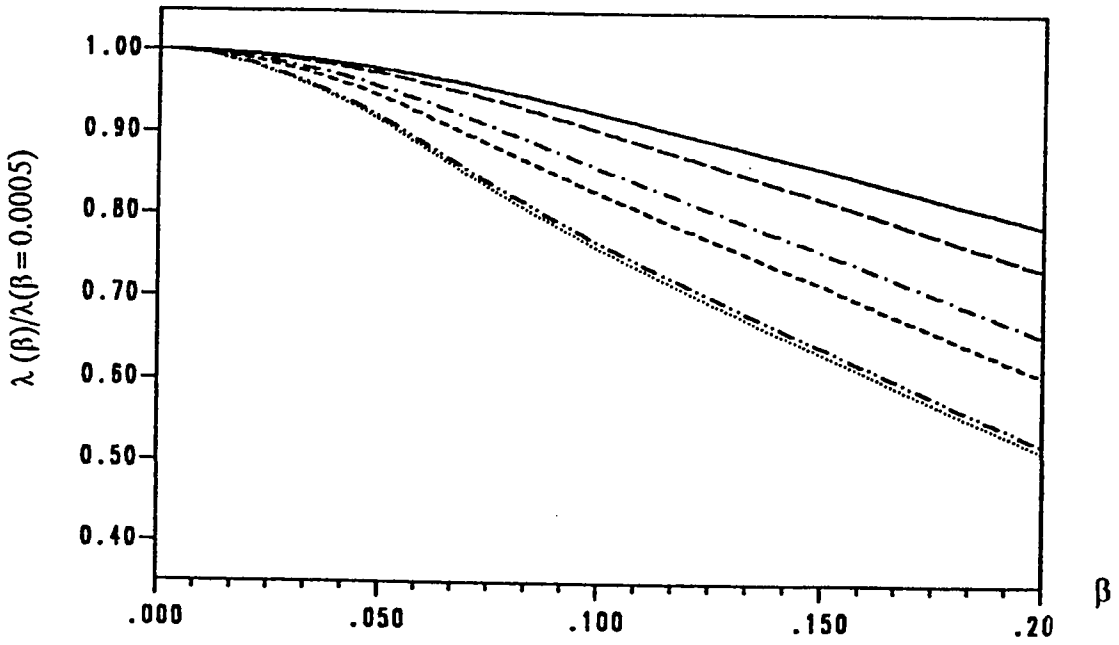

Figure A.2.4 : Correction in λ for the First Six S-A Modes.
Corner Supported : α = 0.0 , Mesh Size 8 x 8.

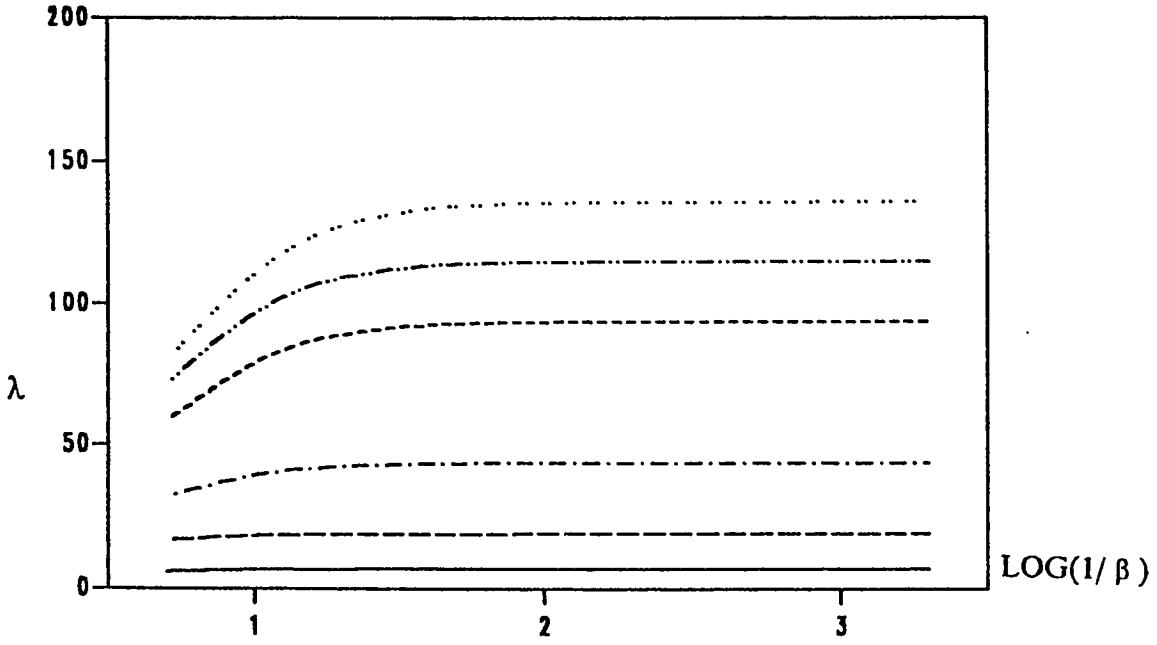

Figure A.2.5 : Variation of λ with β for the First Six S-S Modes.
Corner Supported : α = 0.0 , Mesh Size 8 x 8.

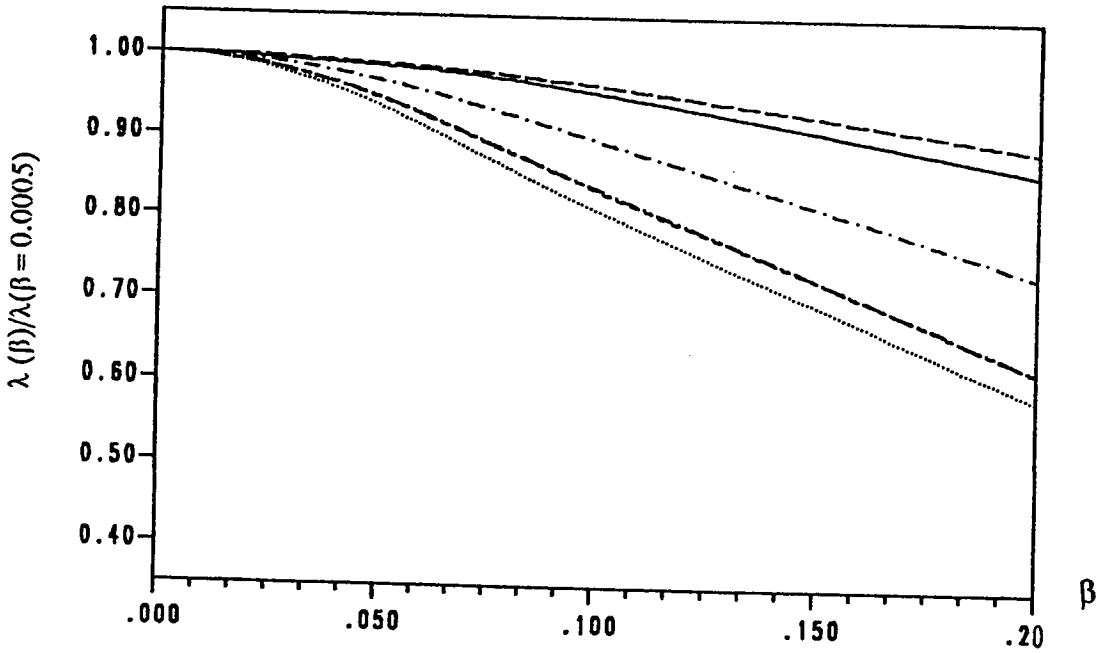

Figure A.2.6 : Correction in λ for the First Six S-S Modes.
Corner Supported : α = 0.0 , Mesh Size 8 x 8.

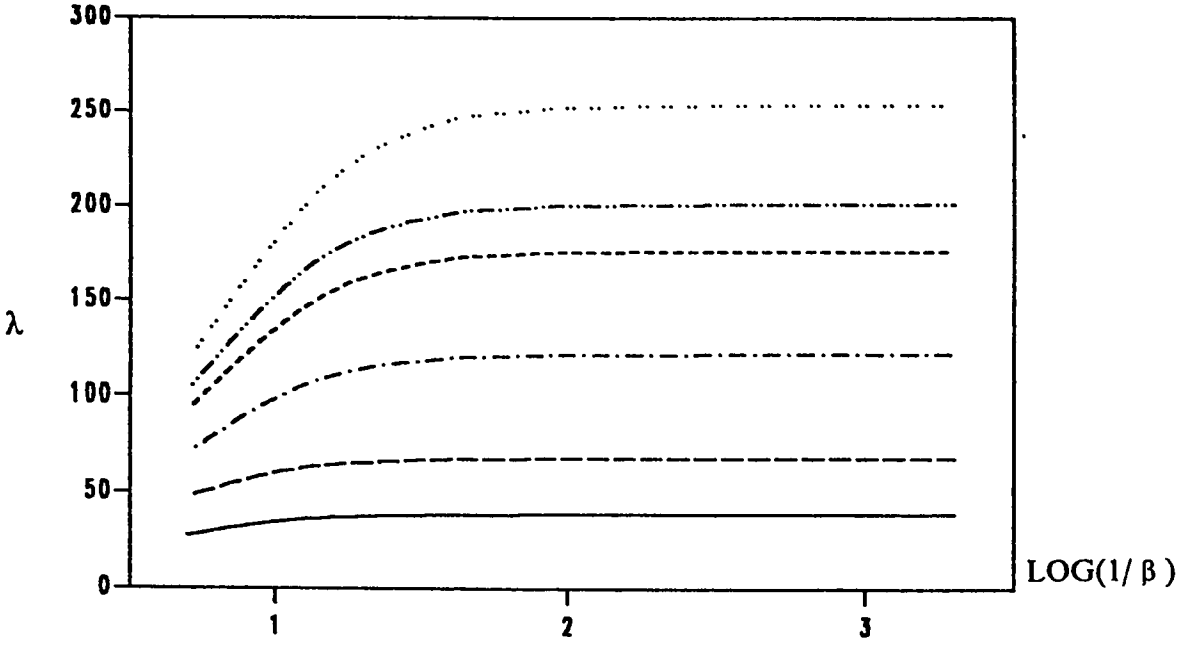

Figure A.2.7 : Variation of λ with β for the First Six A-A Modes.
Corner Supported : α = 0.0 , Mesh Size 9 x 9.

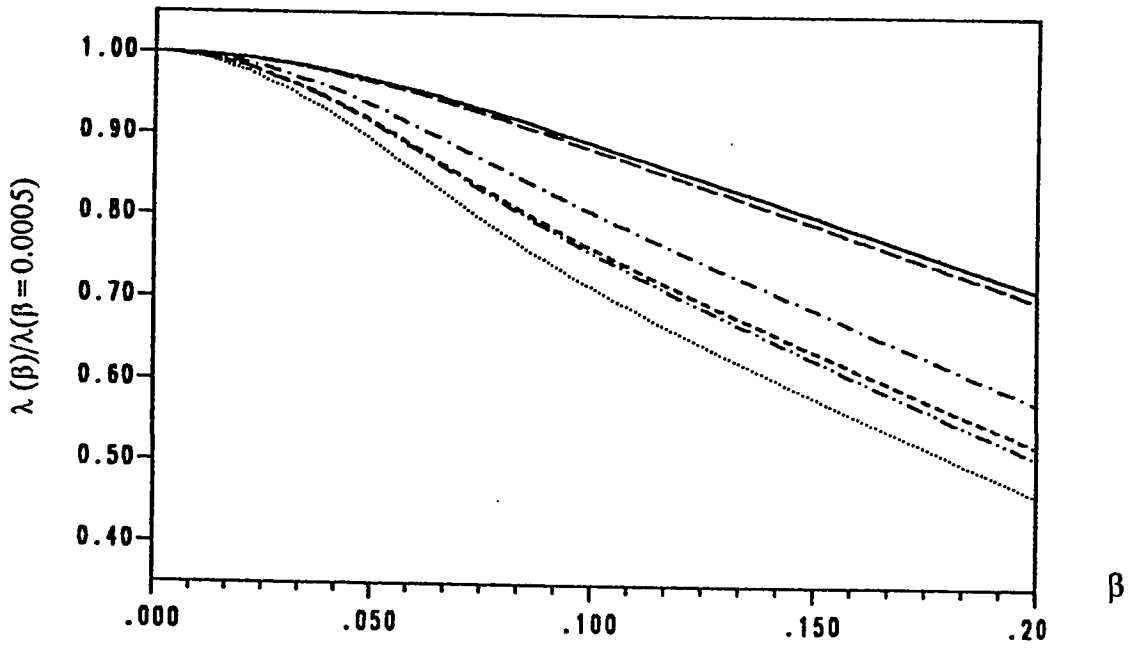

Figure A.2.8 : Correction in λ for the First Six A-A Modes.
Corner Supported : α = 0.0 , Mesh Size 9 x 9.

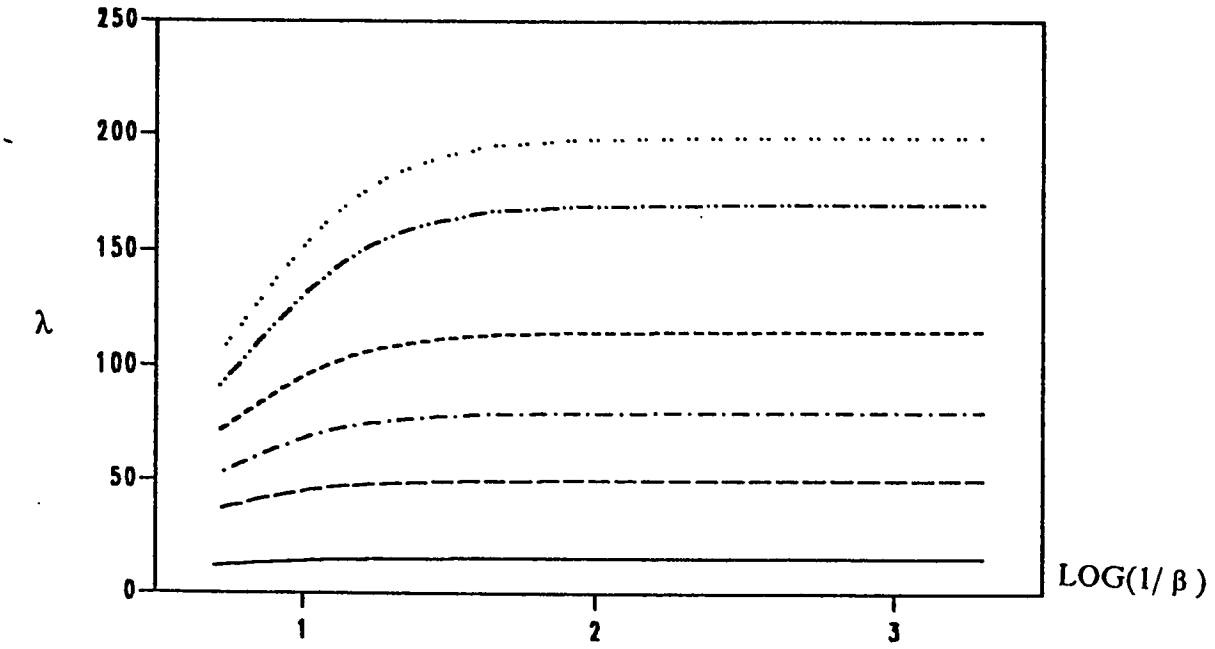

Figure A.2.9 : Variation of λ with β for the First Six S-A Modes.
Corner Supported : α = 0.0 , Mesh Size 9 x 9.

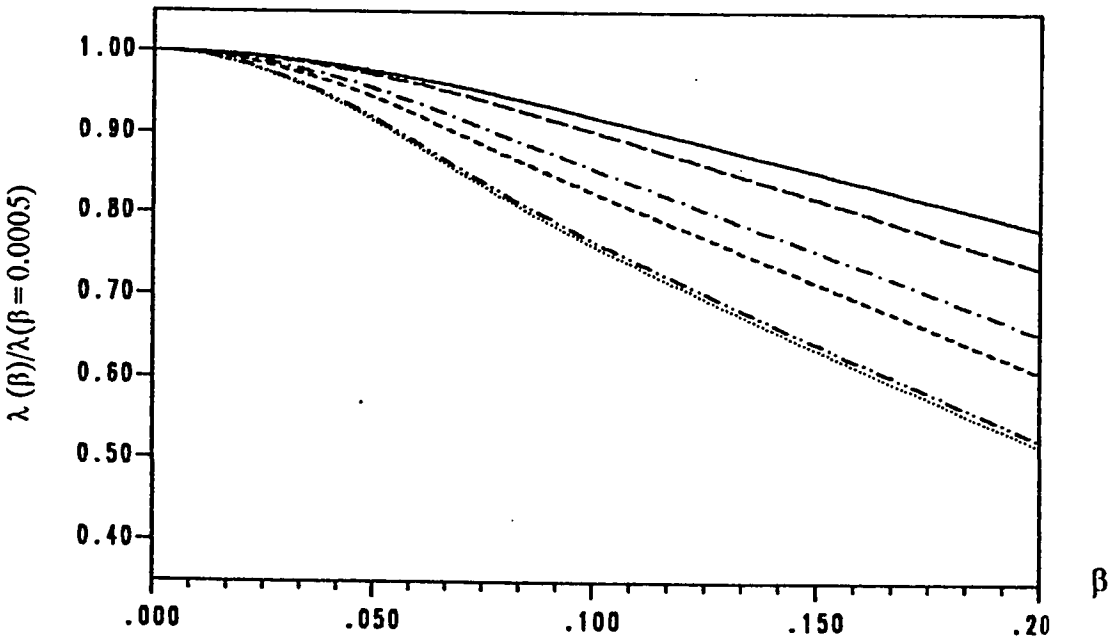

Figure A.2.10 : Correction in λ for the First Six S-A Modes.
Corner Supported : α = 0.0 , Mesh Size 9 x 9.

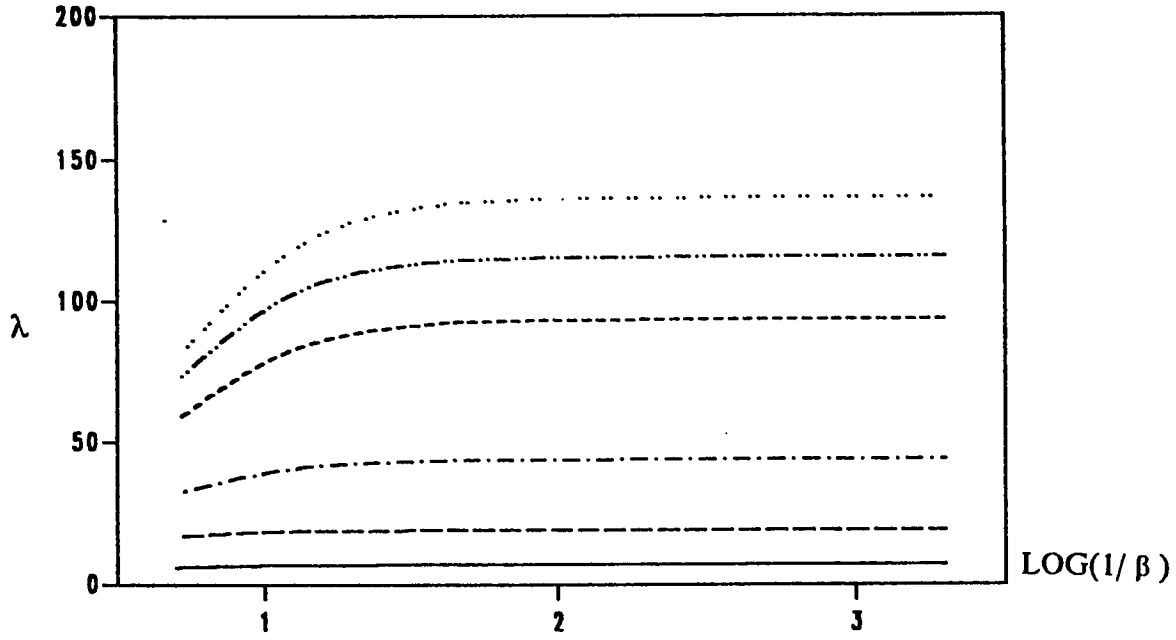

Figure A.2.11 : Variation of λ with β for the First Six S-S Modes.
Corner Supported : α = 0.0 , Mesh Size 9 x 9.

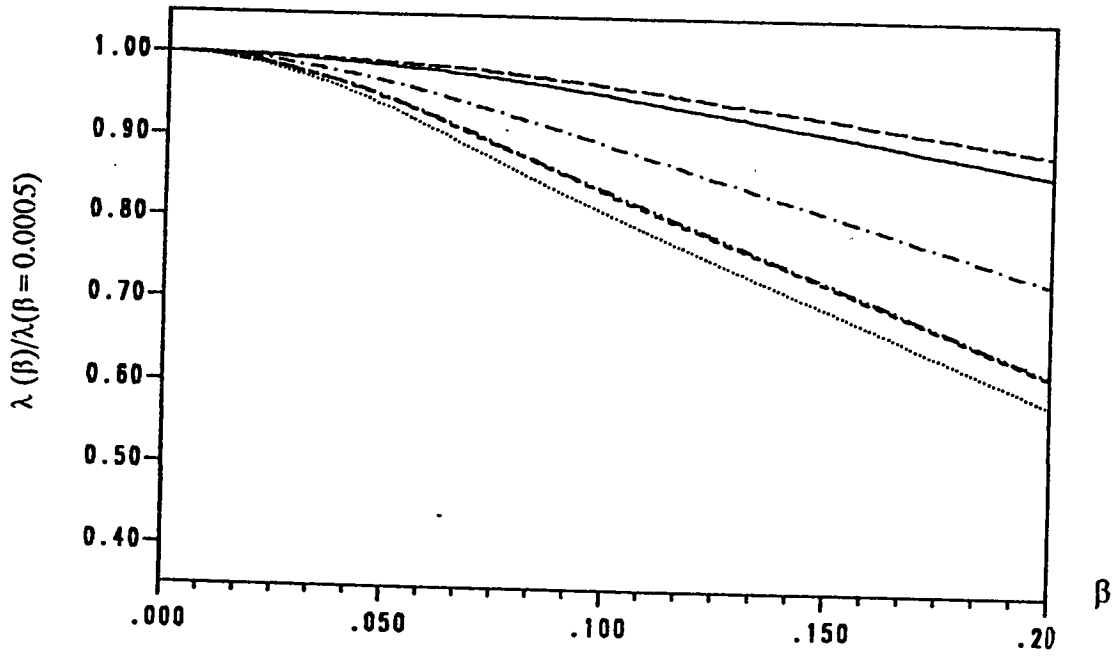

Figure A.2.12 : Correction in λ for the First Six S-S Modes.
Corner Supported : α = 0.0 , Mesh Size 9 x 9.

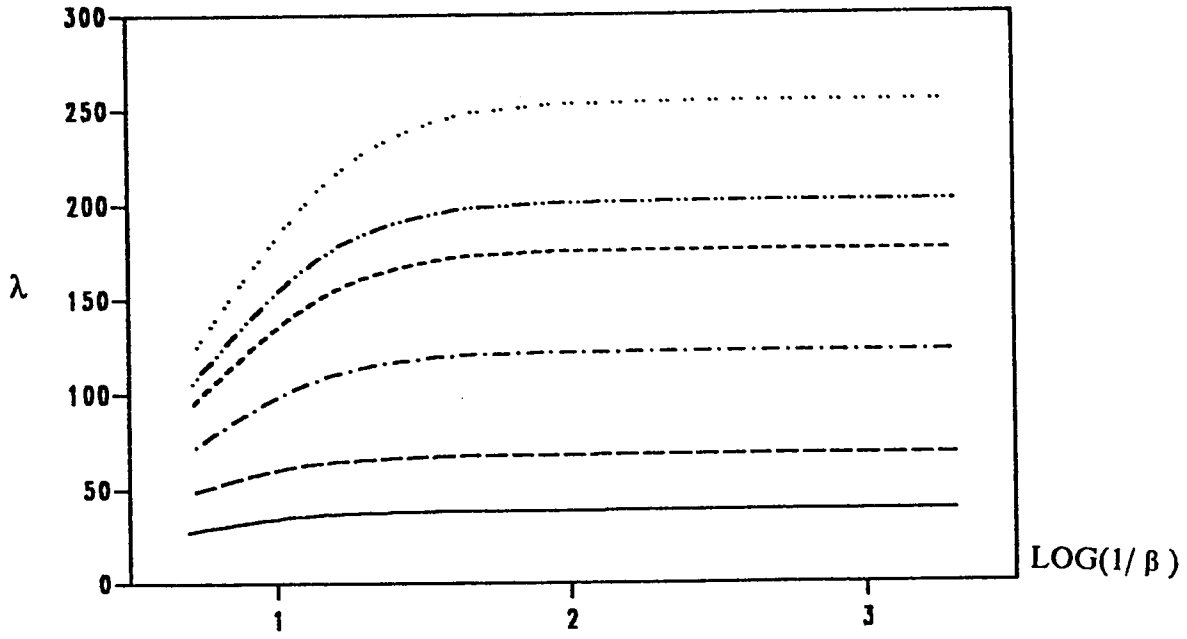

Figure A.2.13 : Variation of λ with β for the First Six A-A Modes.
Corner Supported : α = 0.0 , Mesh Size 10 x 10.

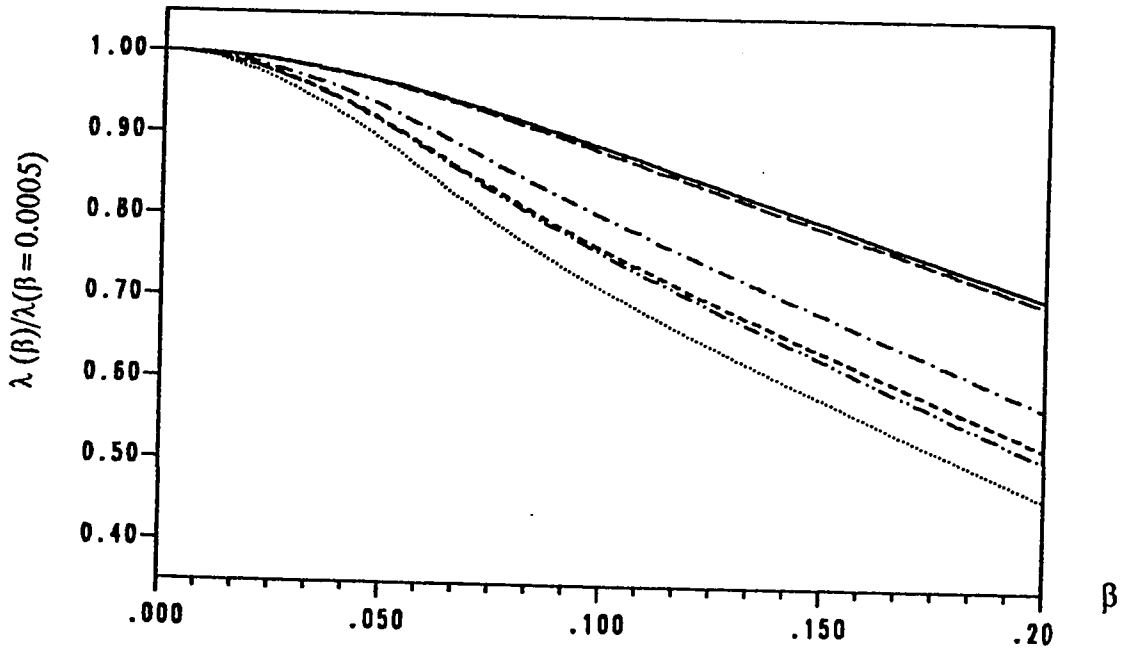

Figure A.2.14 : Correction in λ for the First Six A-A Modes.
Corner Supported : α = 0.0 , Mesh Size 10 x 10.

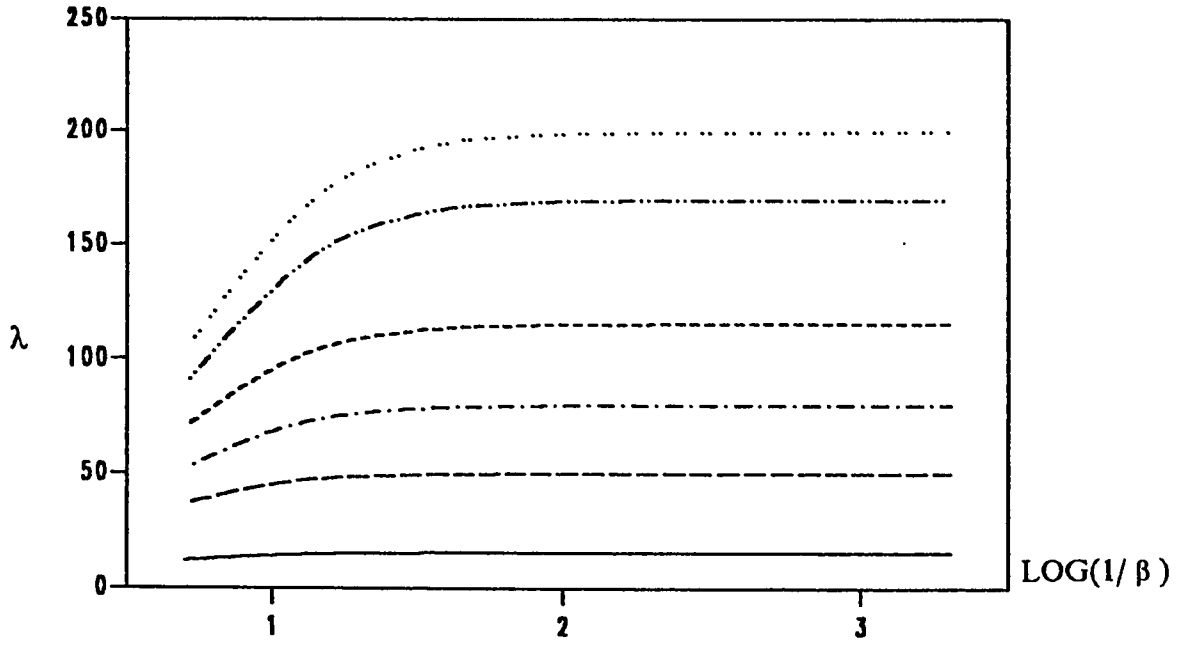

Figure A.2.15 : Variation of λ with β for the First Six S-A Modes.
Corner Supported : α = 0.0 , Mesh Size 10 x 10.

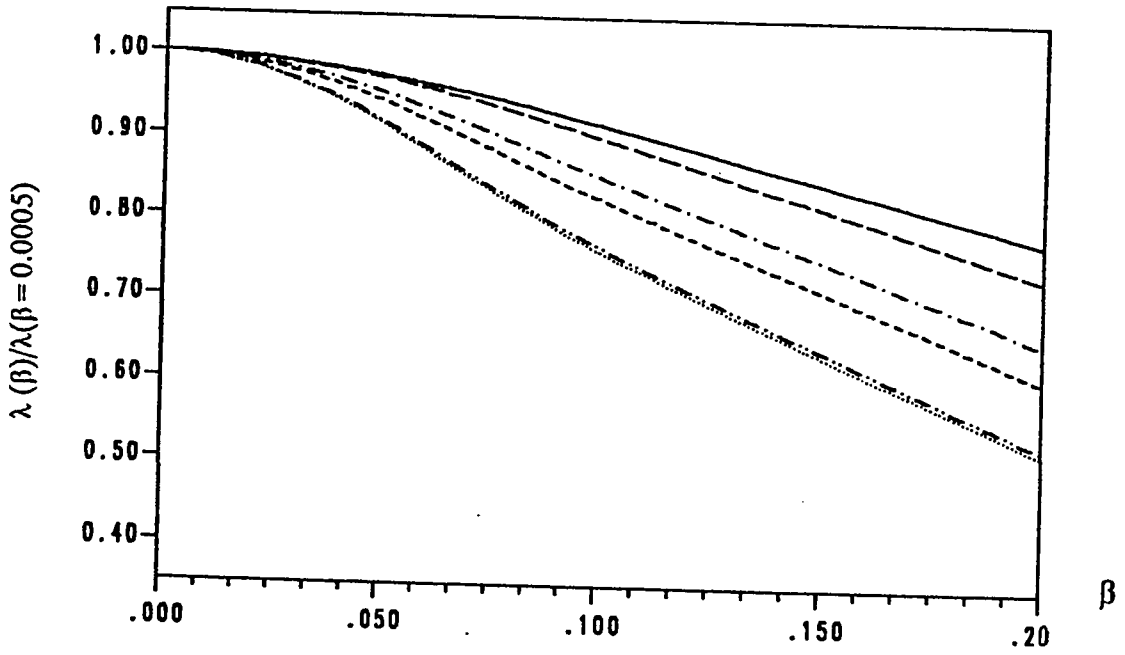

Figure A.2.16 : Correction in λ for the First Six S-A Modes.
Corner Supported : α = 0.0 , Mesh Size 10 x 10.

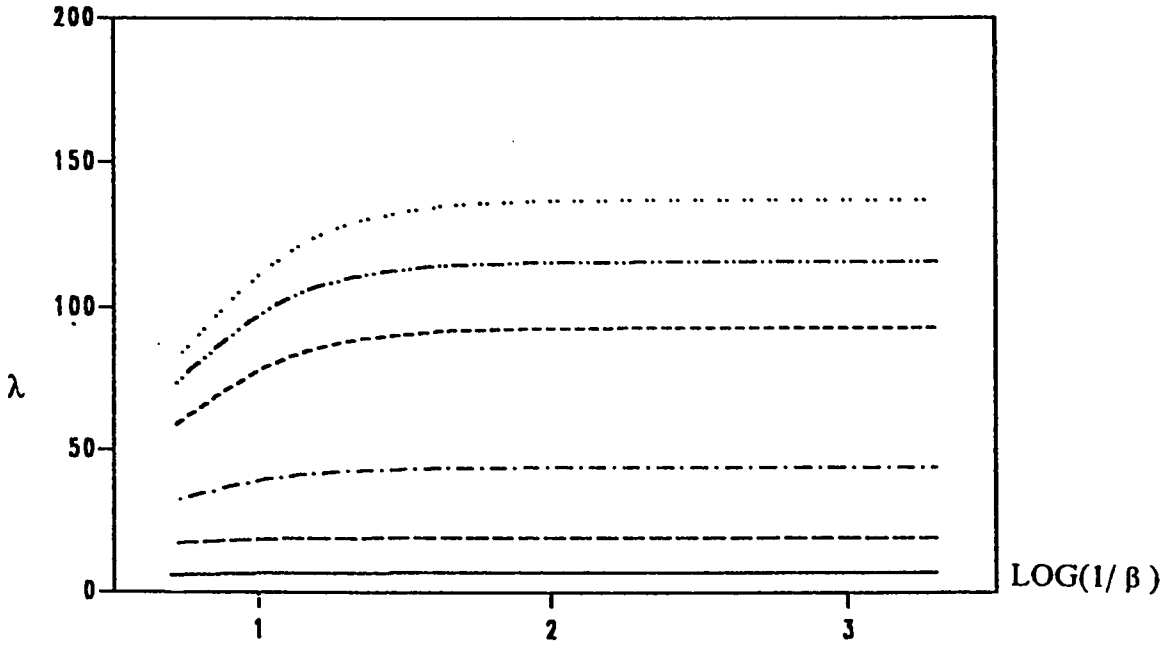

Figure A.2.17 : Variation of λ with β for the First Six S-S Modes.
Corner Supported : α = 0.0 , Mesh Size 10 x 10.

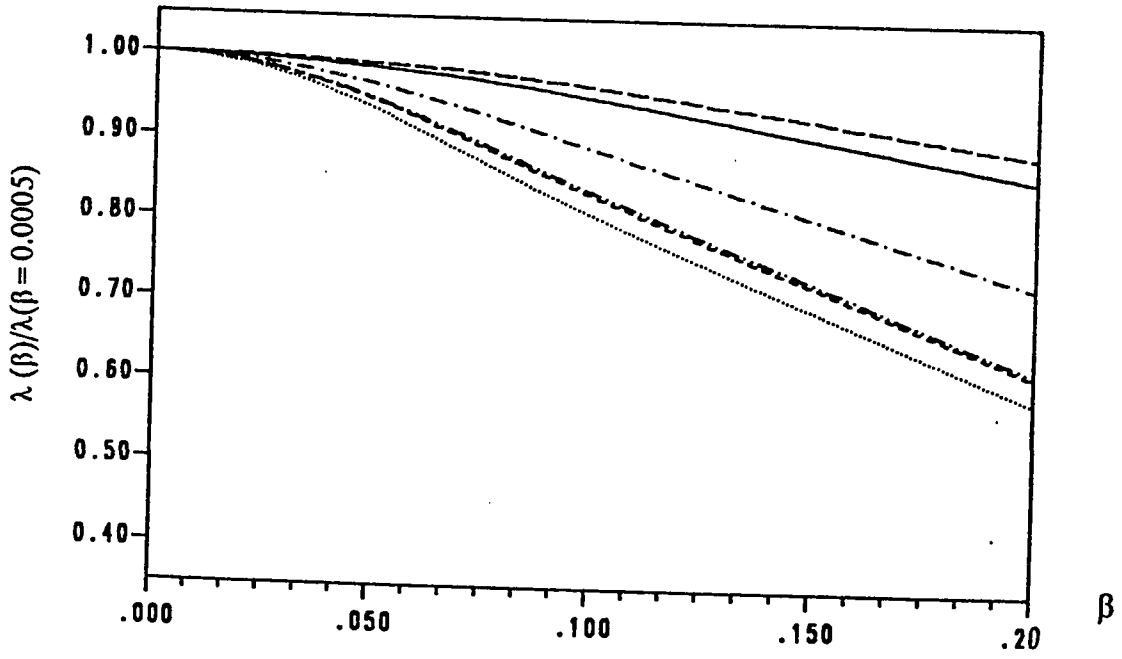

Figure A.2.18 : Correction in λ for the First Six S-S Modes.
Corner Supported : α = 0.0 , Mesh Size 10 x 10.

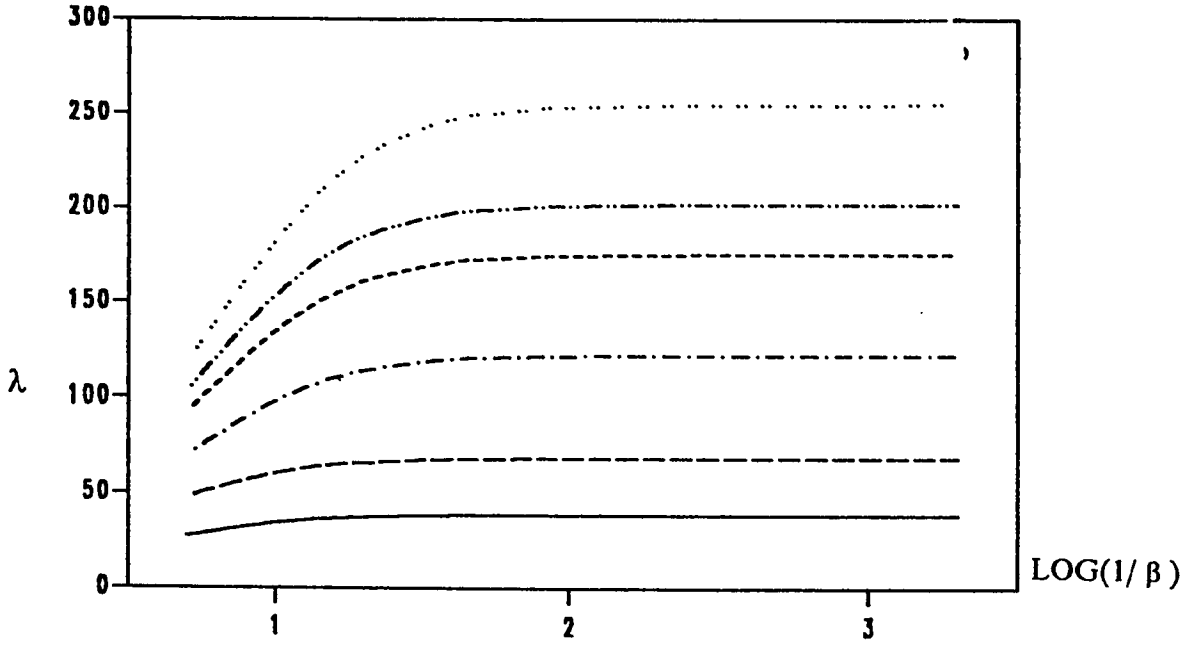

Figure A.2.19 : Variation of λ with β for the First Six A-A Modes.
Corner Supported : α = 0.0 , Mesh Size 11 x 11.

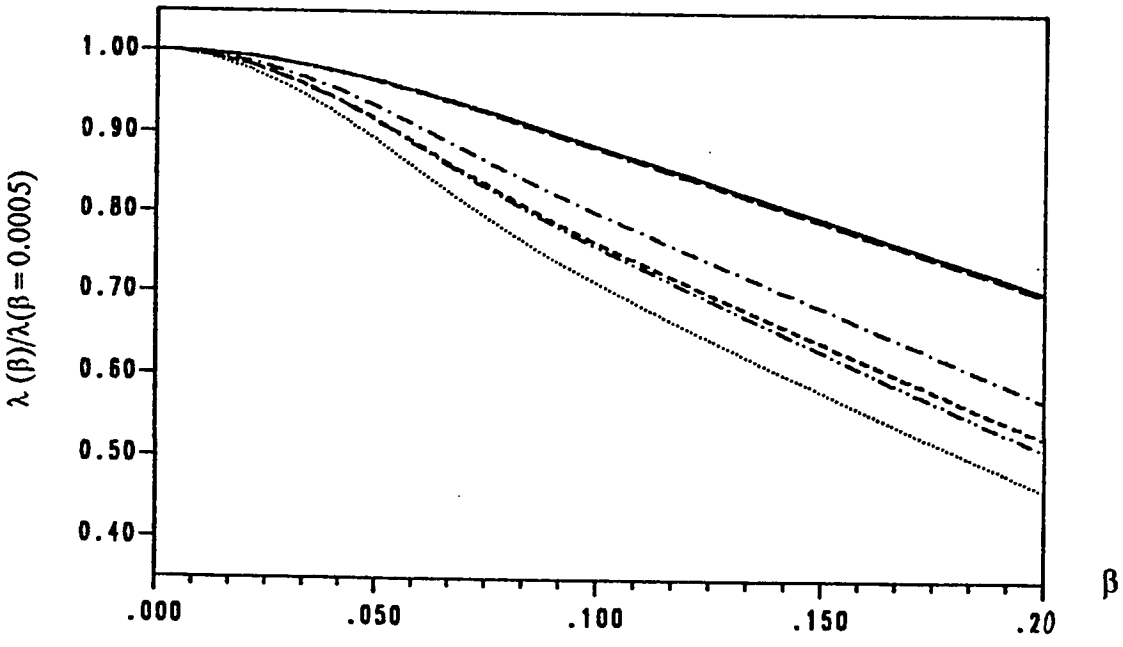

Figure A.2.20 : Correction in λ for the First Six A-A Modes.
Corner Supported : α = 0.0 , Mesh Size 11 x 11.

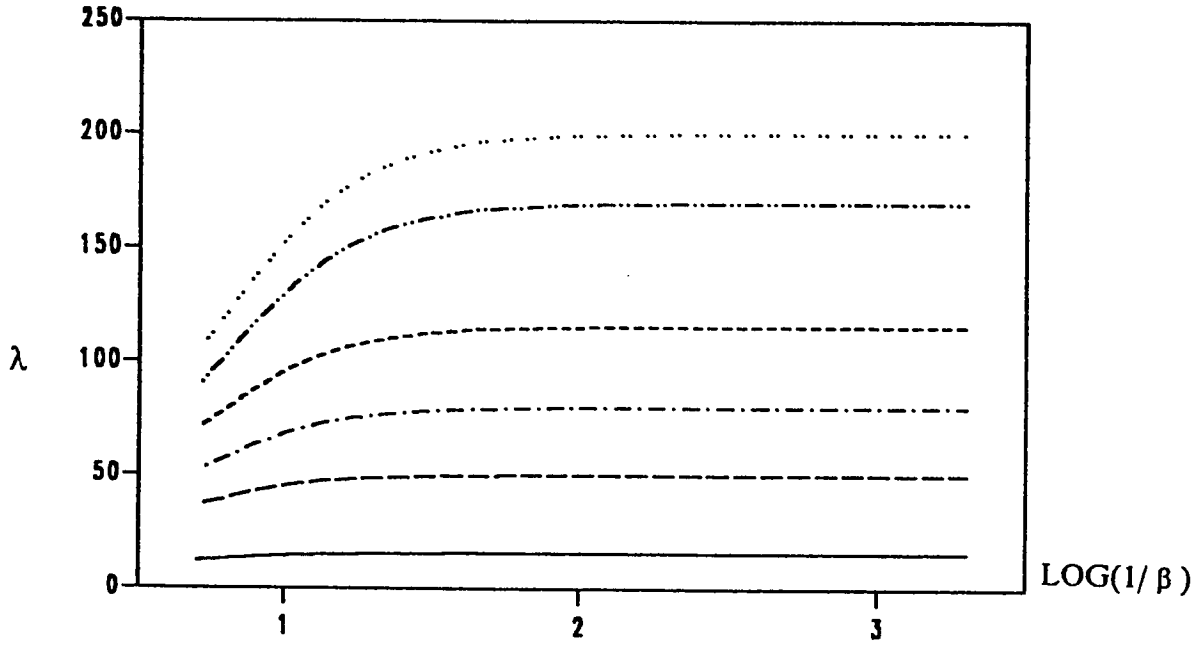

Figure A.2.21 : Variation of λ with β for the First Six S-A Modes.
Corner Supported : α = 0.0 , Mesh Size 11 x 11.

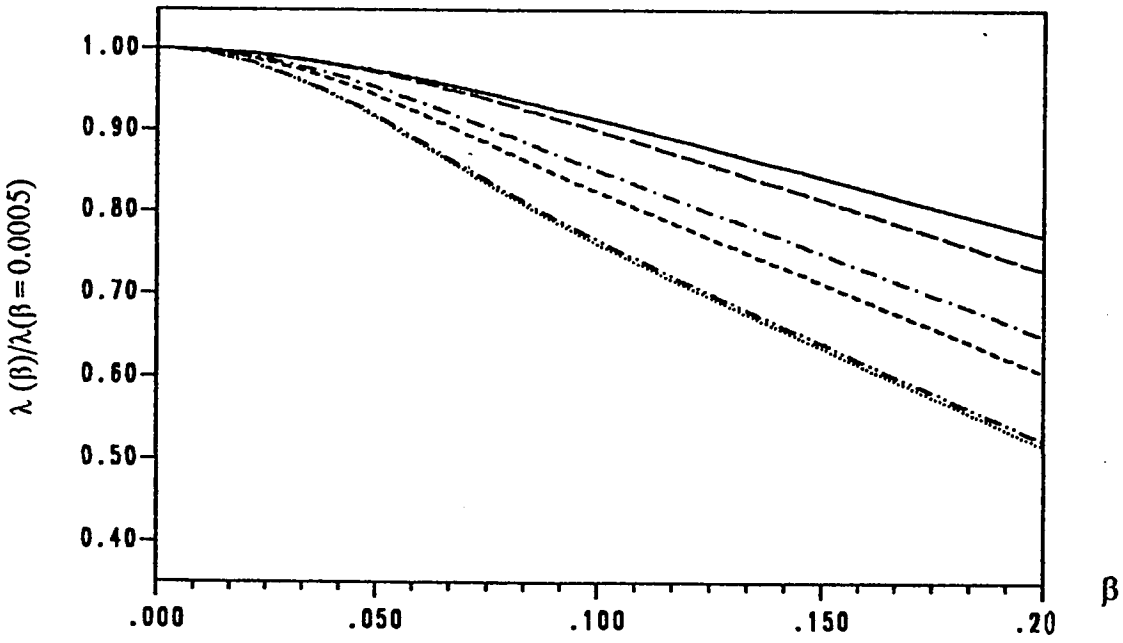

Figure A.2.22 : Correction in λ for the First Six S-A Modes.
Corner Supported : α = 0.0 , Mesh Size 11 x 11.

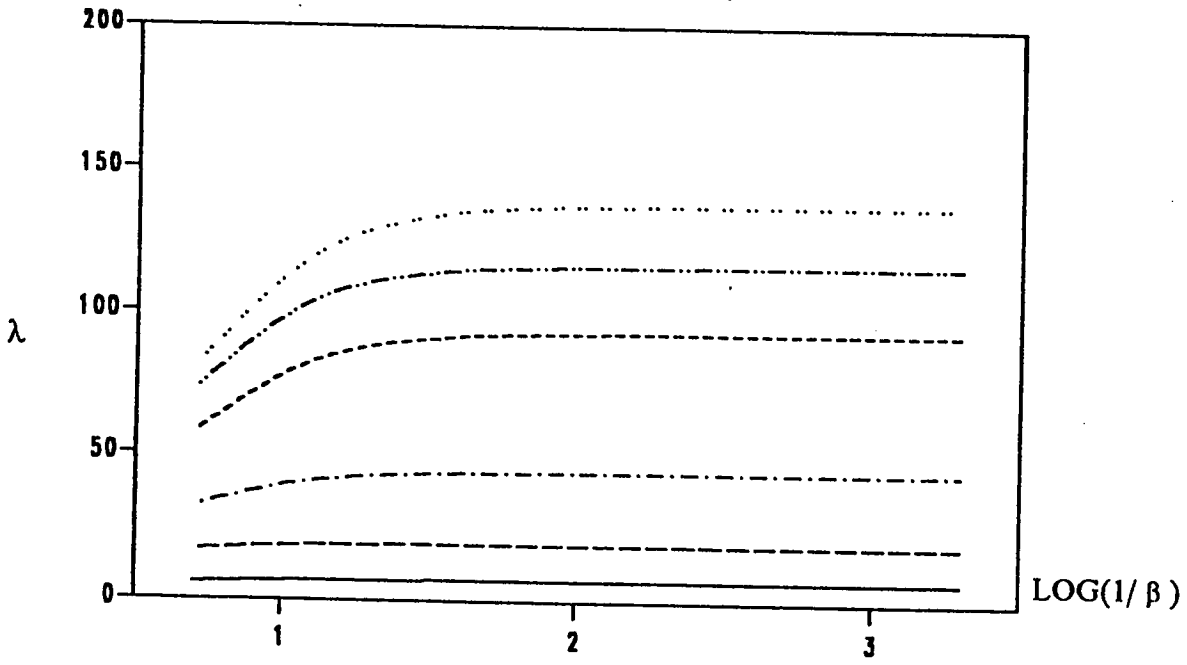

Figure A.2.23 : Variation of λ with β for the First Six S-S Modes.
Corner Supported : α = 0.0 , Mesh Size 11 x 11.

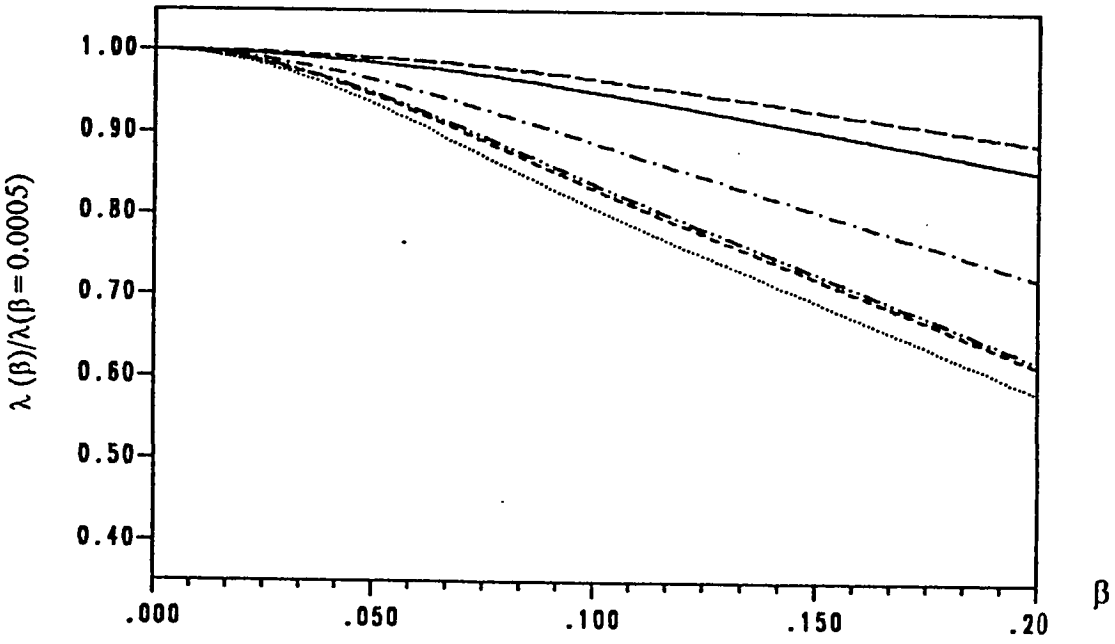

Figure A.2.24 : Correction in λ for the First Six S-S Modes.
Corner Supported : α = 0.0 , Mesh Size 11 x 11.

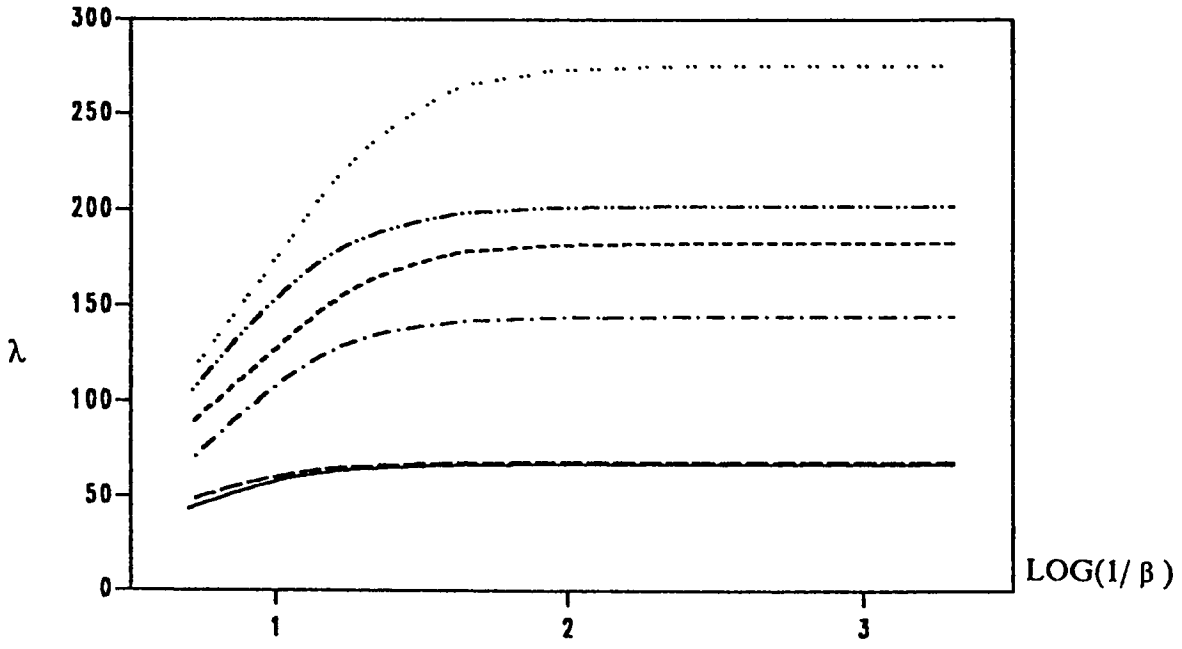

Figure A.2.25 : Variation of λ with β for the First Six A-A Modes.
Corner Supported : α = 0.1 , Mesh Size 11 x 11.

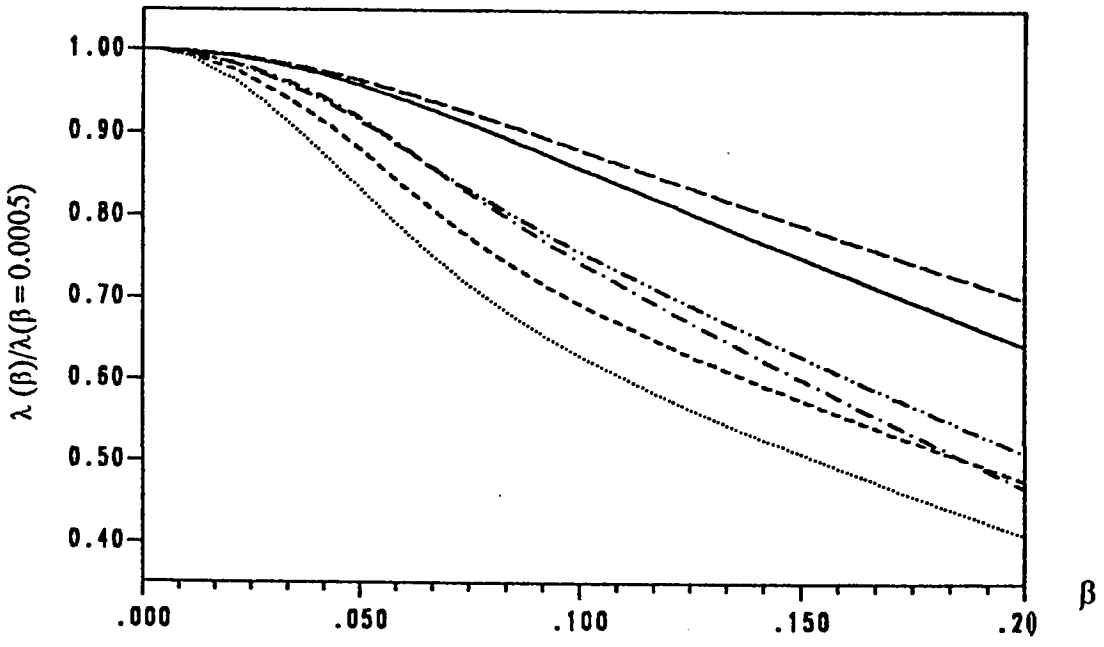

Figure A.2.26 : Correction in λ for the First Six A-A Modes.
Corner Supported : α = 0.1 , Mesh Size 11 x 11.

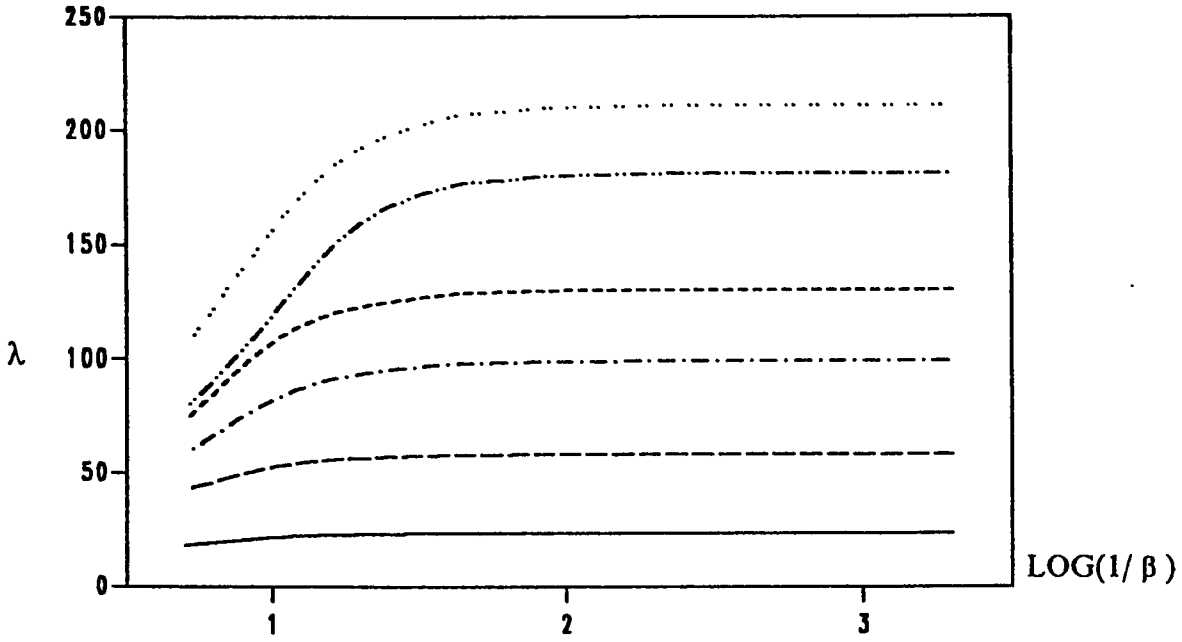

Figure A.2.27 : Variation of λ with β for the First Six S-A Modes.
Corner Supported : α = 0.1 , Mesh Size 11 x 11.

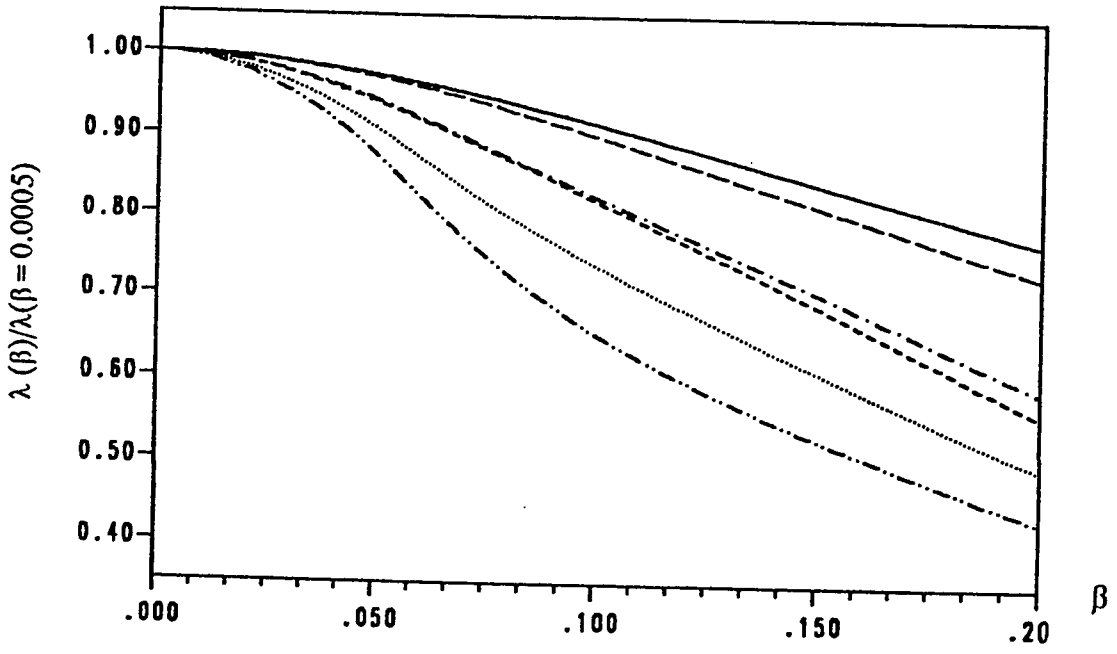

Figure A.2.28 : Correction in λ for the First Six S-A Modes.
Corner Supported : α = 0.1 , Mesh Size 11 x 11.

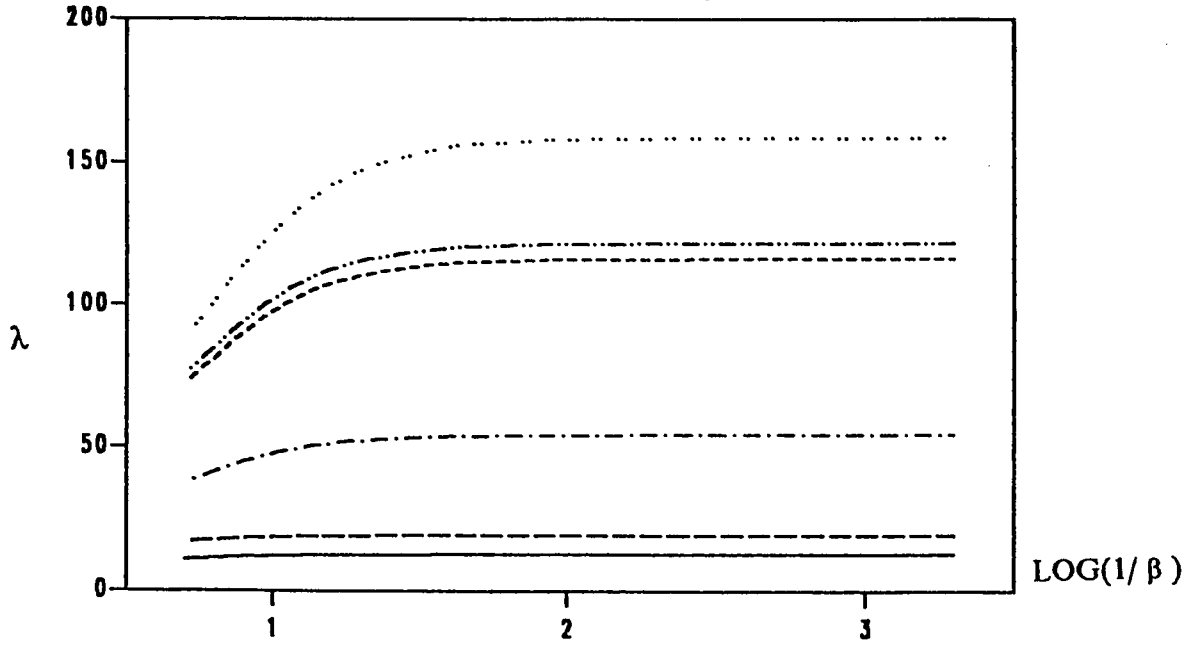

Figure A.2.29 : Variation of λ with β for the First Six S-S Modes.
Corner Supported : α = 0.1 , Mesh Size 11 x 11.

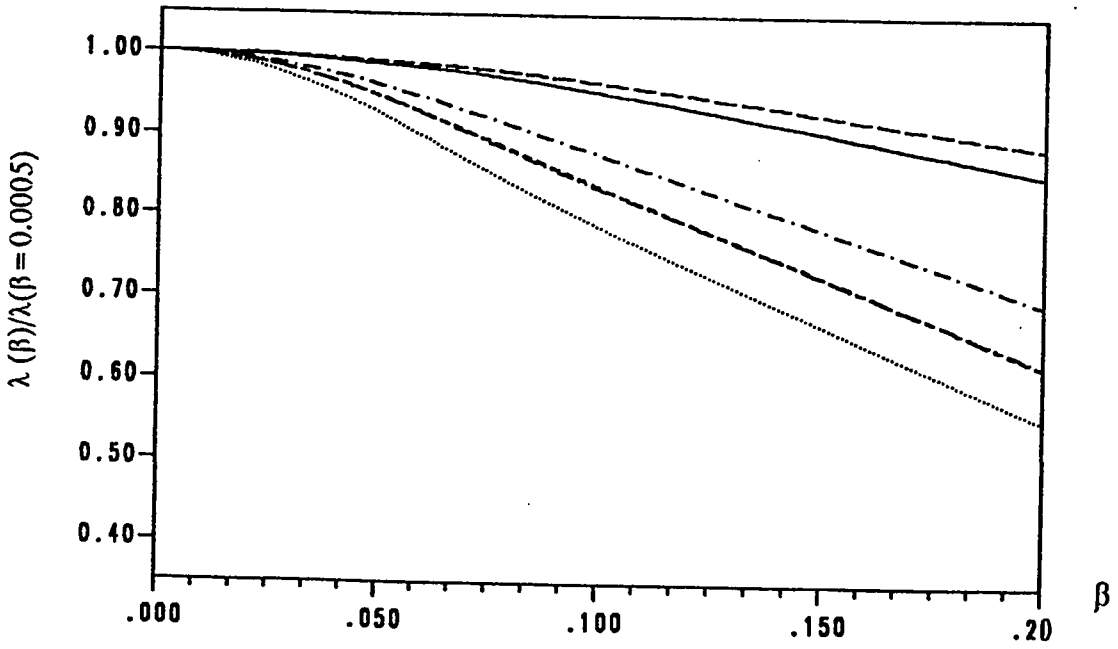

Figure A.2.30 : Correction in λ for the First Six S-S Modes.
Corner Supported : α = 0.1 , Mesh Size 11 x 11.

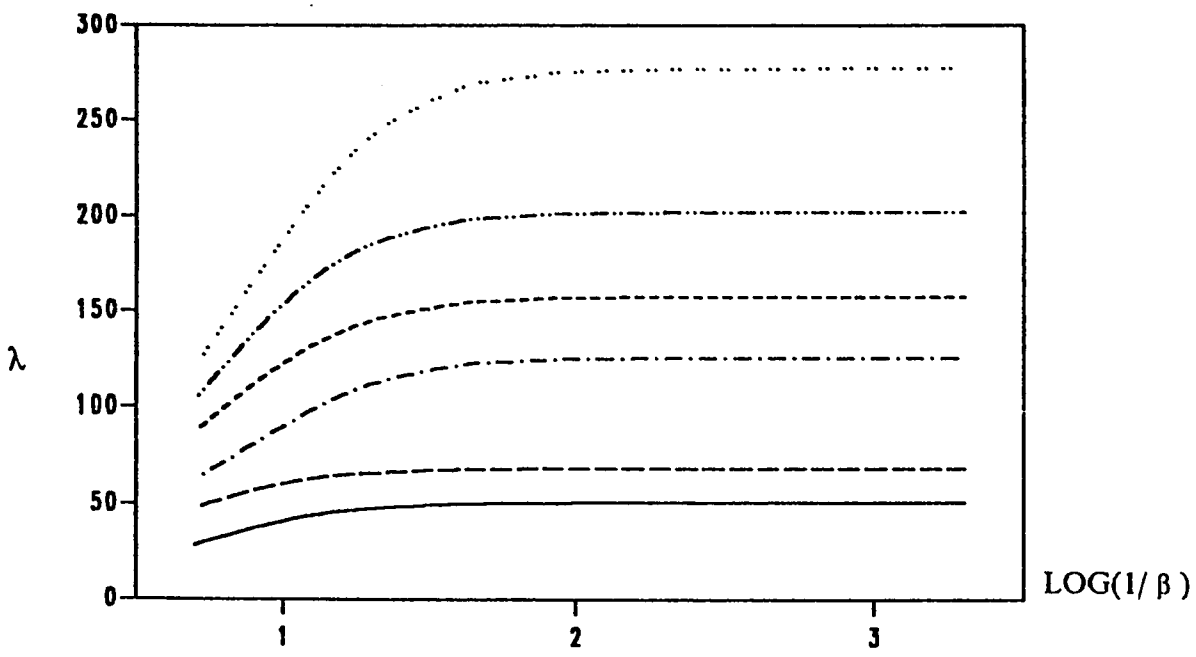

Figure A.2.31 : Variation of λ with β for the First Six A-A Modes.
Corner Supported : α = 0.2 , Mesh Size 11 x 11.

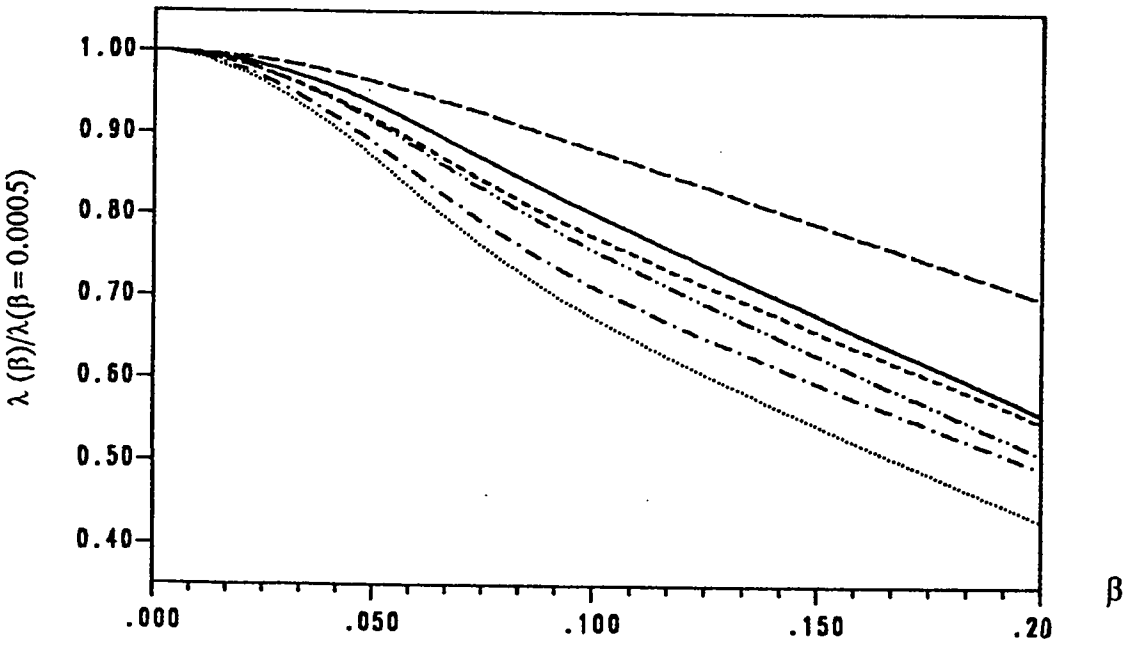

Figure A.2.32 : Correction in λ for the First Six A-A Modes.
Corner Supported : α = 0.2 , Mesh Size 11 x 11.

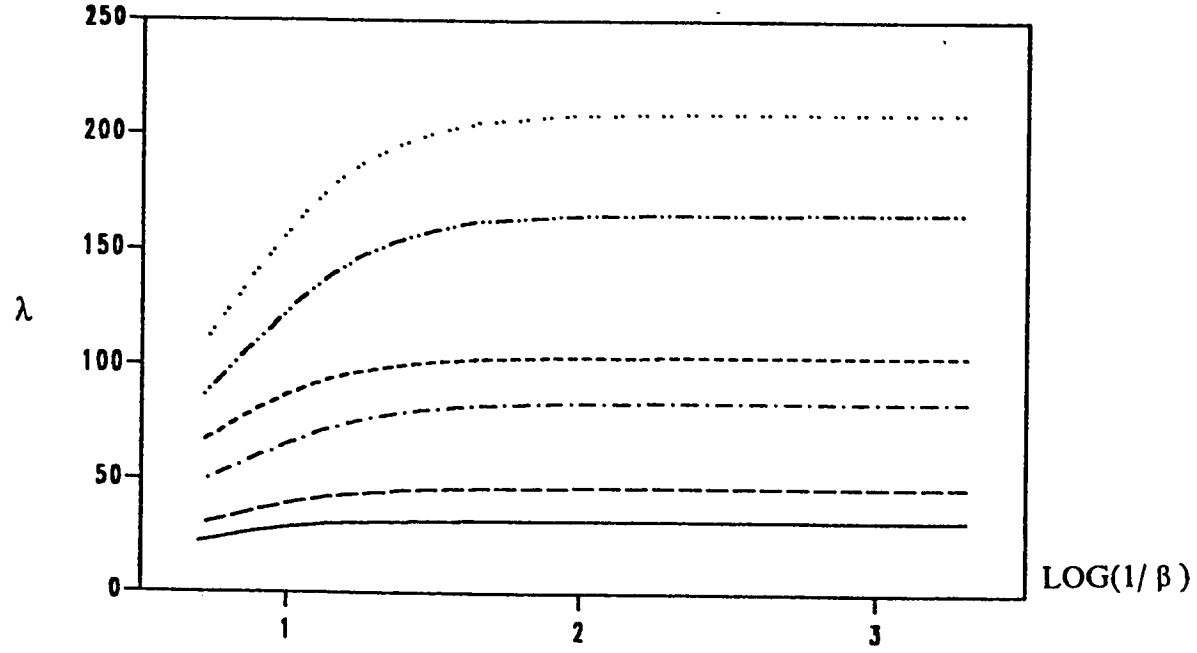

Figure A.2.33 : Variation of λ with β for the First Six S-A Modes.
Corner Supported : α = 0.2 , Mesh Size 11 x 11.

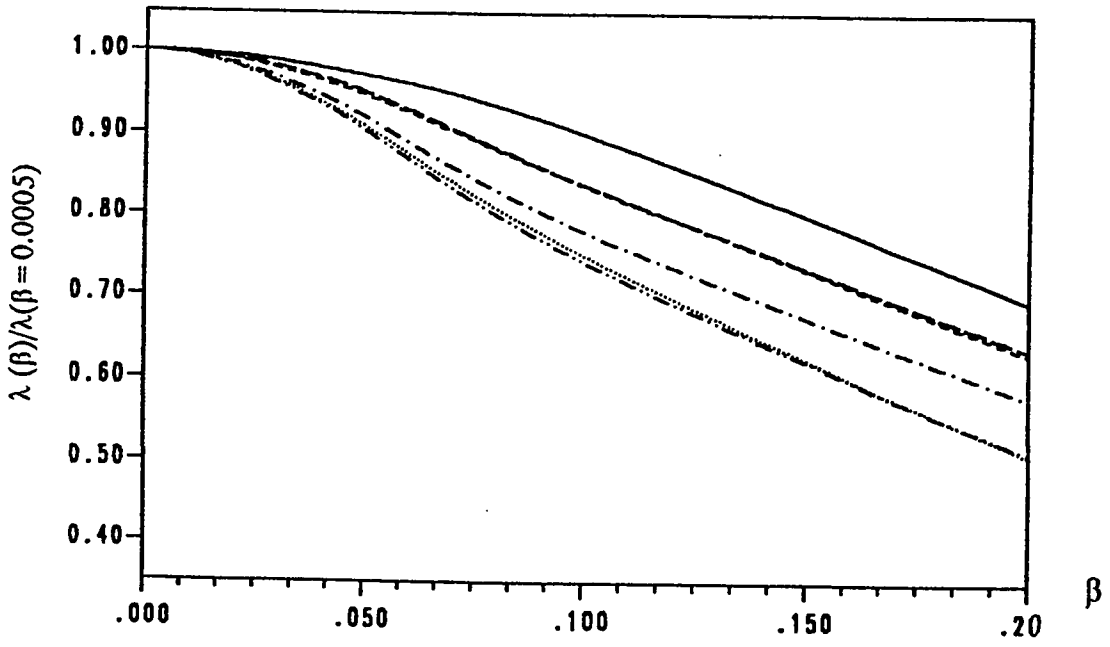

Figure A.2.34 : Correction in λ for the First Six S-A Modes.
Corner Supported : α = 0.2 , Mesh Size 11 x 11.

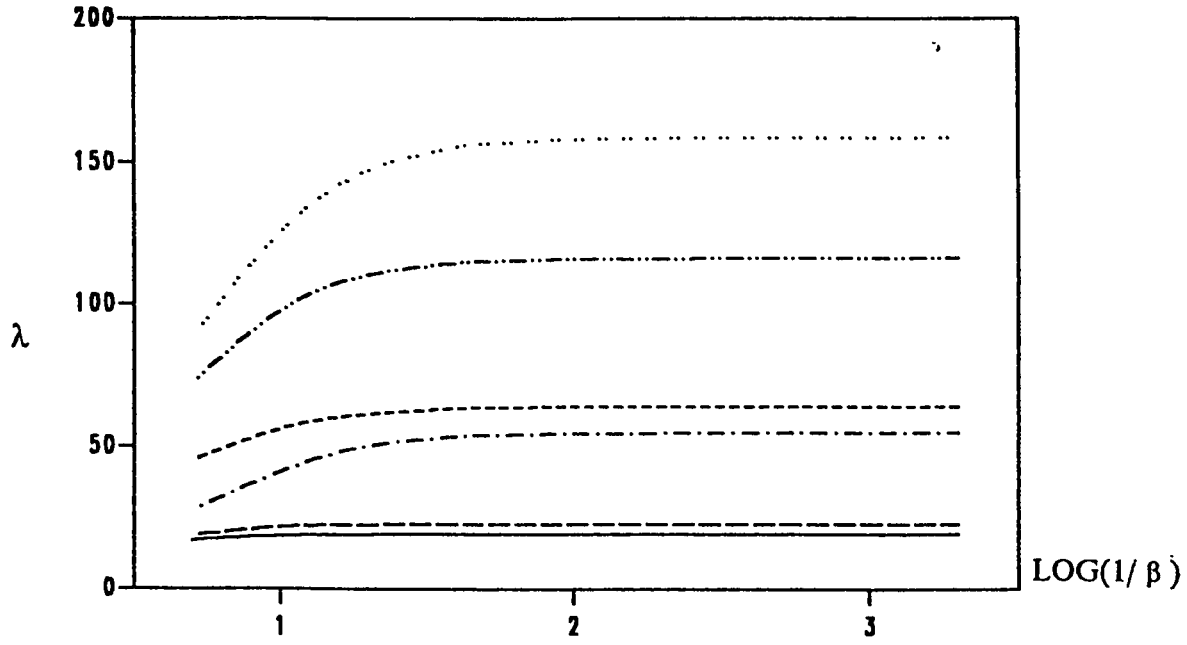

Figure A.2.35 : Variation of λ with β for the First Six S-S Modes.
Corner Supported : α = 0.2 , Mesh Size 11 x 11.

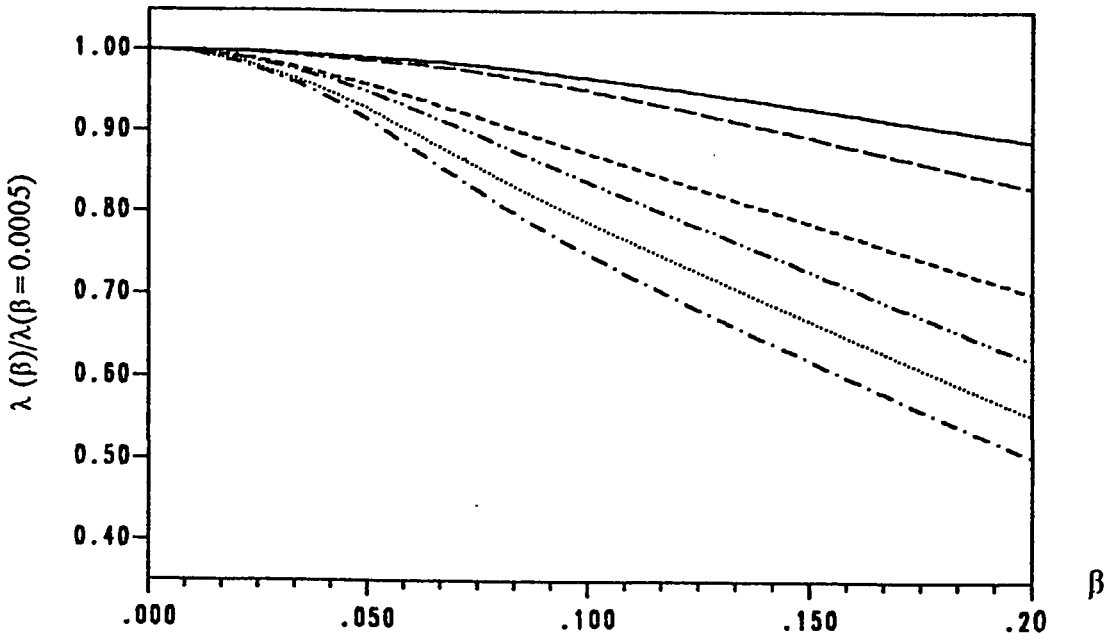

Figure A.2.36 : Correction in λ for the First Six S-S Modes.
Corner Supported : α = 0.2 , Mesh Size 11 x 11.

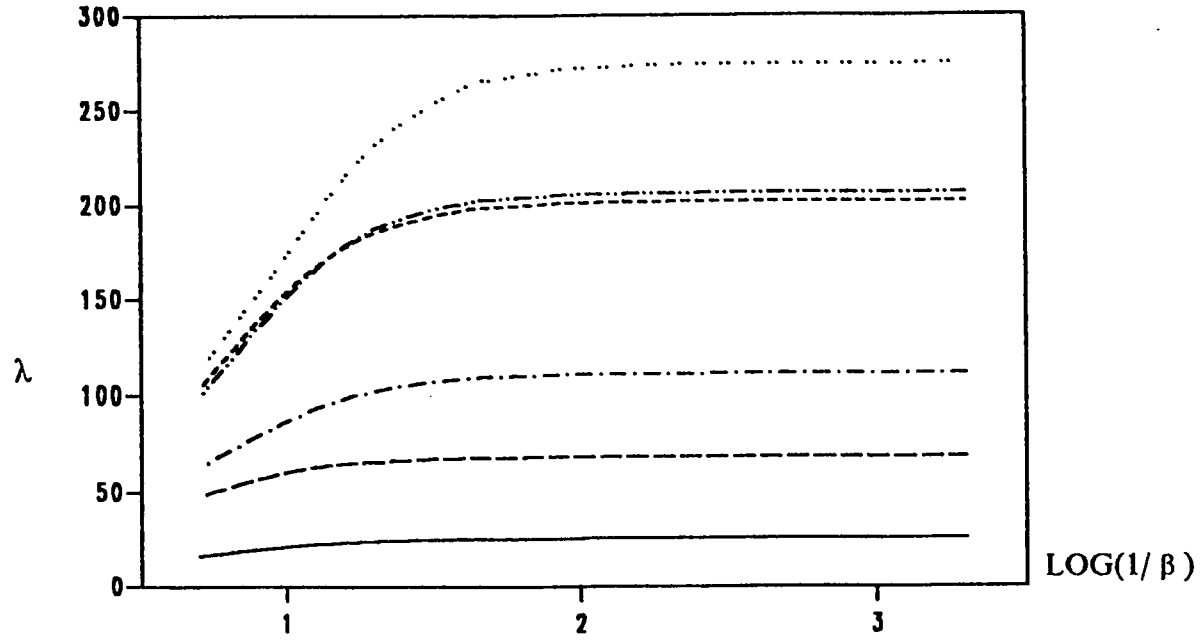

Figure A.2.37 : Variation of λ with β for the First Six A-A Modes.
Corner Supported : α = 0.3 , Mesh Size 11 x 11.

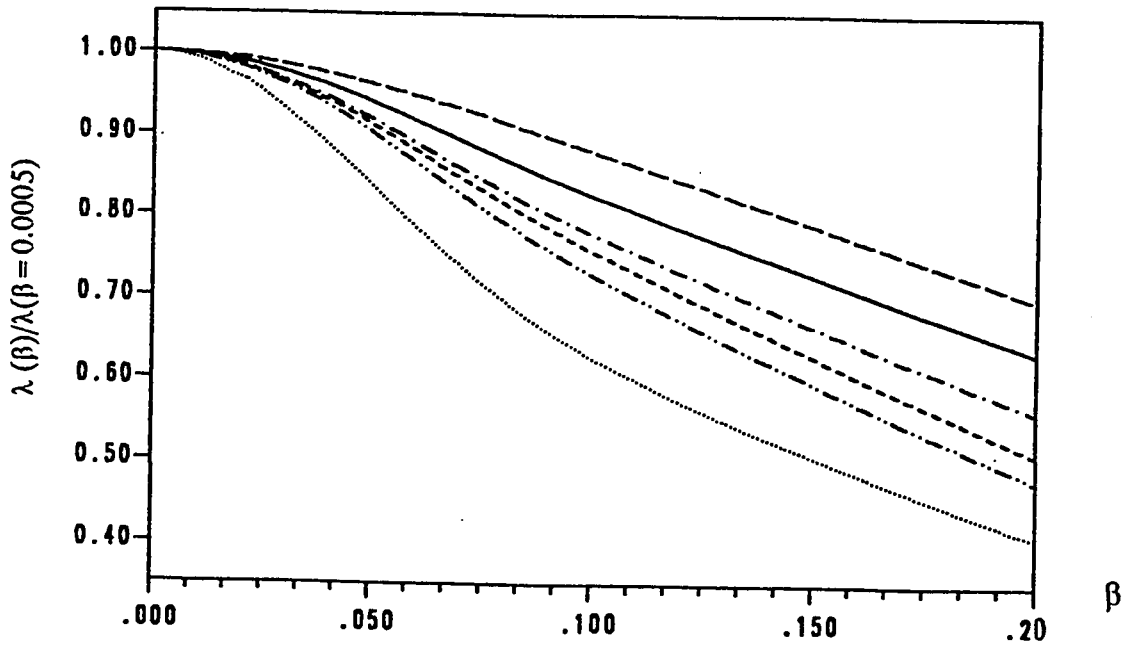

Figure A.2.38 : Correction in λ for the First Six A-A Modes.
Corner Supported : α = 0.3 , Mesh Size 11 x 11.

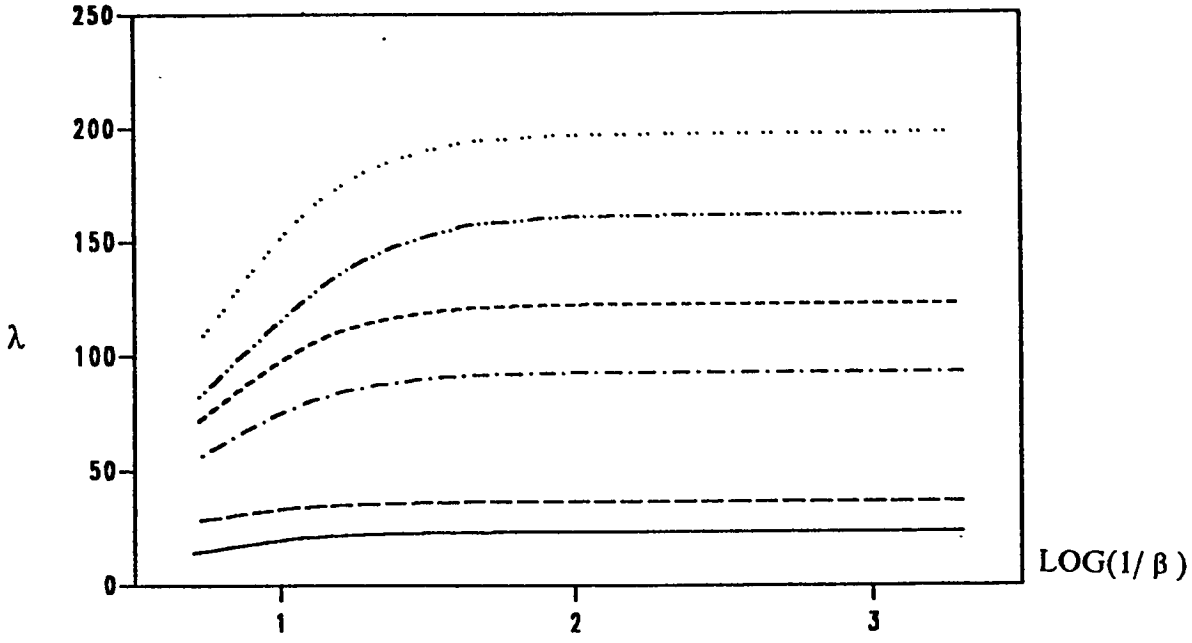

Figure A.2.39 : Variation of λ with β for the First Six S-A Modes.
Corner Supported : α = 0.3 , Mesh Size 11 x 11.

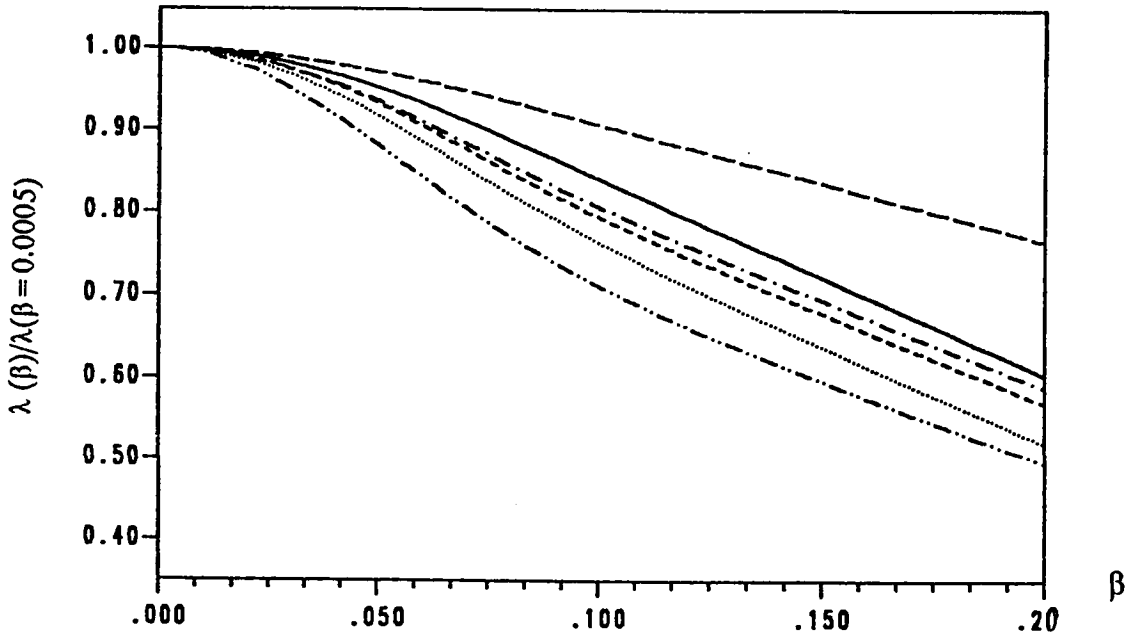

Figure A.2.40 : Correction in λ for the First Six S-A Modes.
Corner Supported : α = 0.3 , Mesh Size 11 x 11.

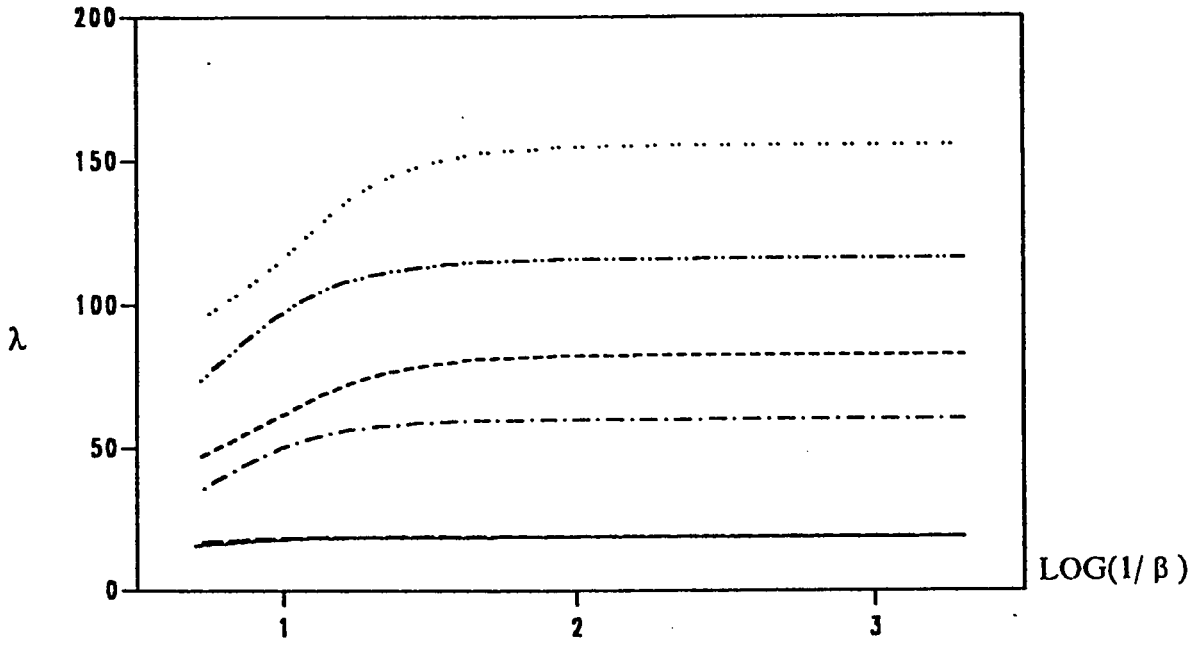

Figure A.2.41 : Variation of λ with β for the First Six S-S Modes.
Corner Supported : α = 0.3 , Mesh Size 11 x 11.

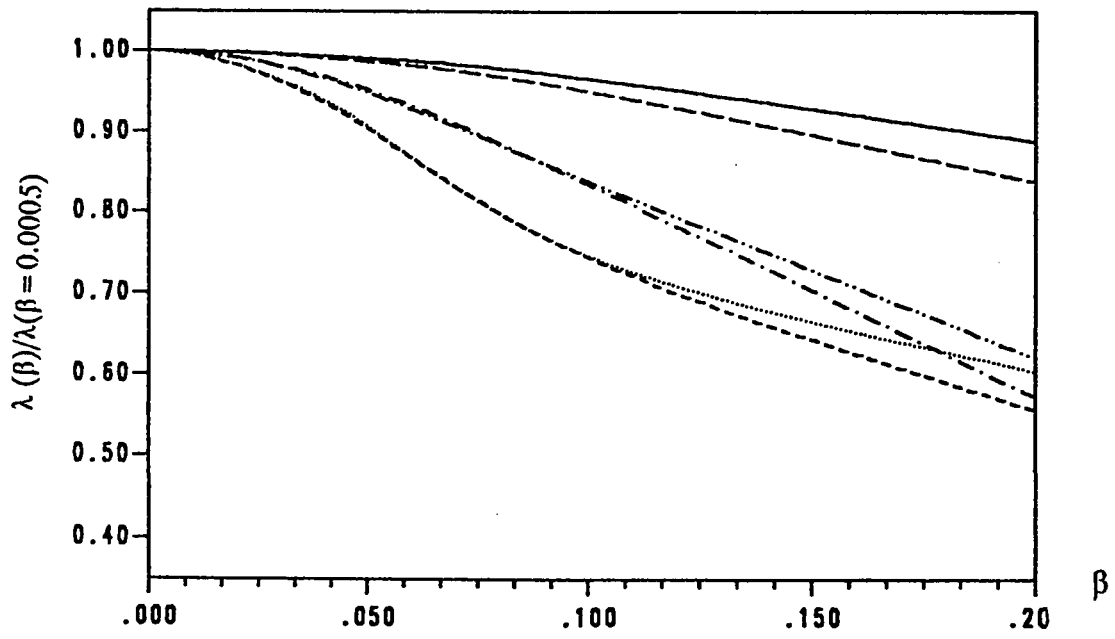

Figure A.2.42 : Correction in λ for the First Six S-S Modes.
Corner Supported : α = 0.3 , Mesh Size 11 x 11.

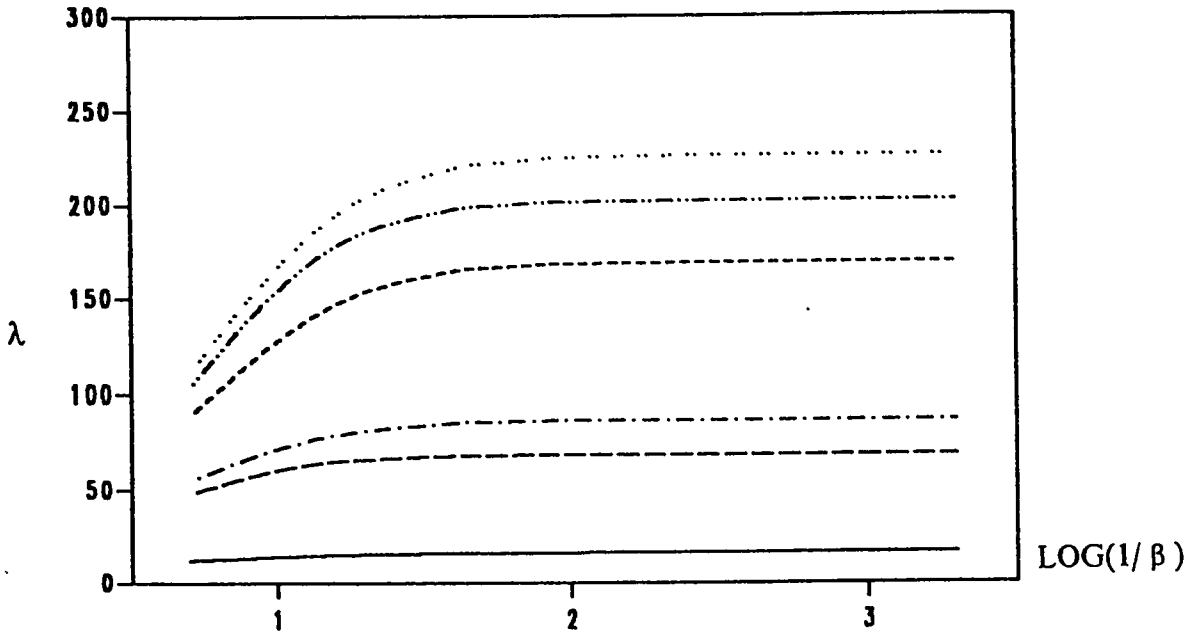

Figure A.2.43 : Variation of λ with β for the First Six A-A Modes.
Corner Supported : α = 0.4 , Mesh Size 11 x 11.

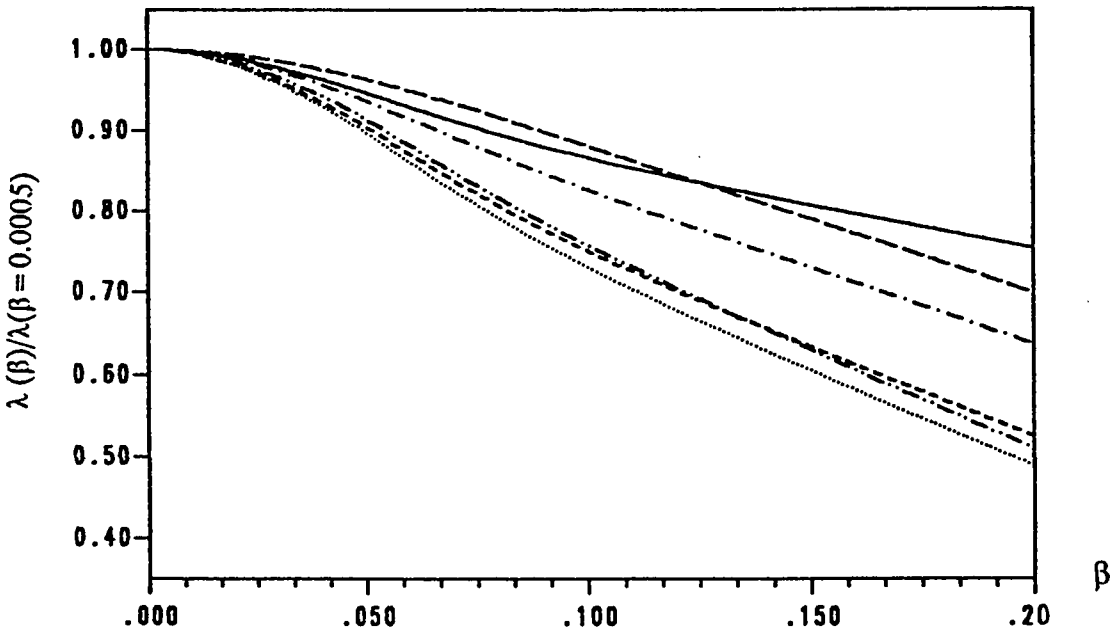

Figure A.2.44 : Correction in λ for the First Six A-A Modes.
Corner Supported : α = 0.4 , Mesh Size 11 x 11.

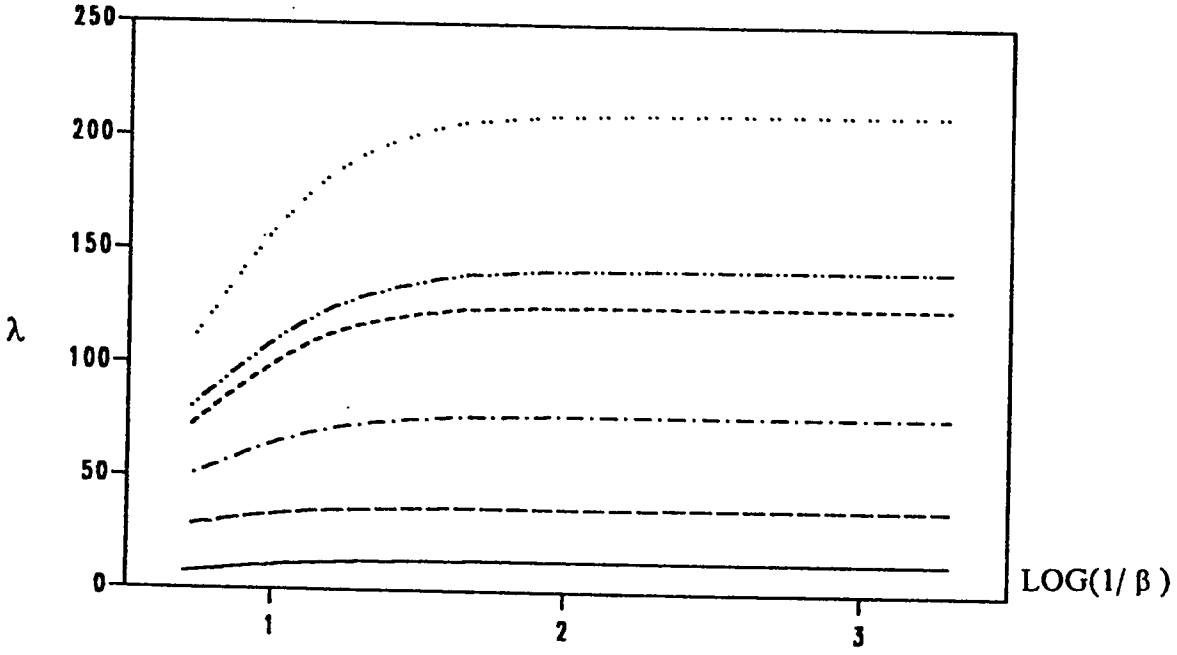

Figure A.2.45 : Variation of λ with β for the First Six S-A Modes.
Corner Supported : α = 0.4 , Mesh Size 11 x 11.

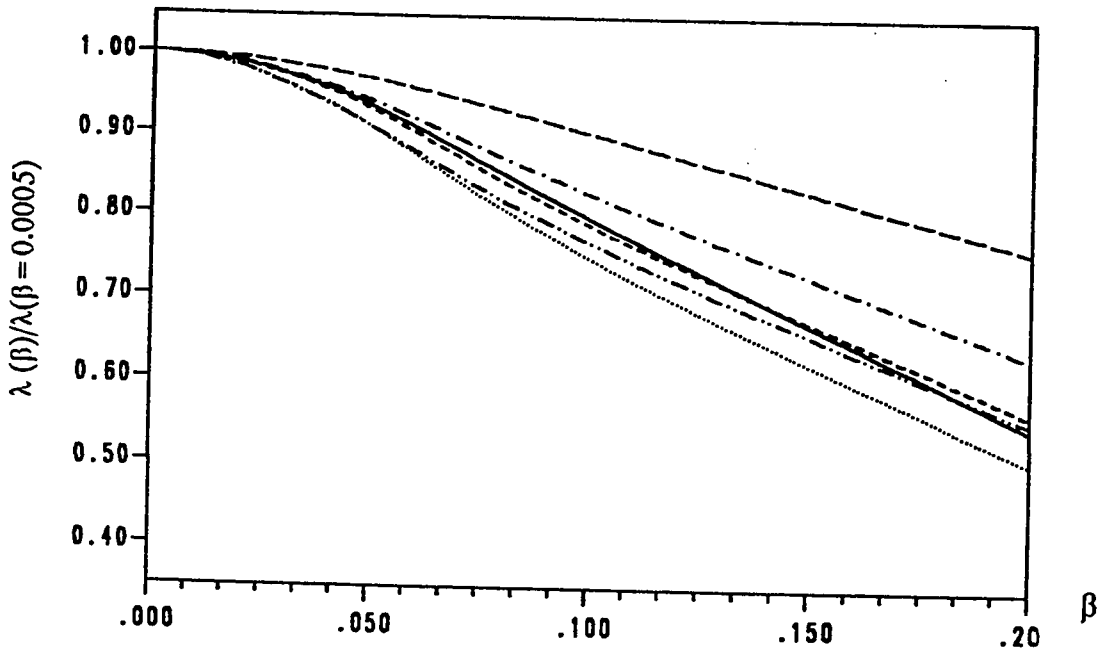

Figure A.2.46 : Correction in λ for the First Six S-A Modes.
Corner Supported : α = 0.4 , Mesh Size 11 x 11.

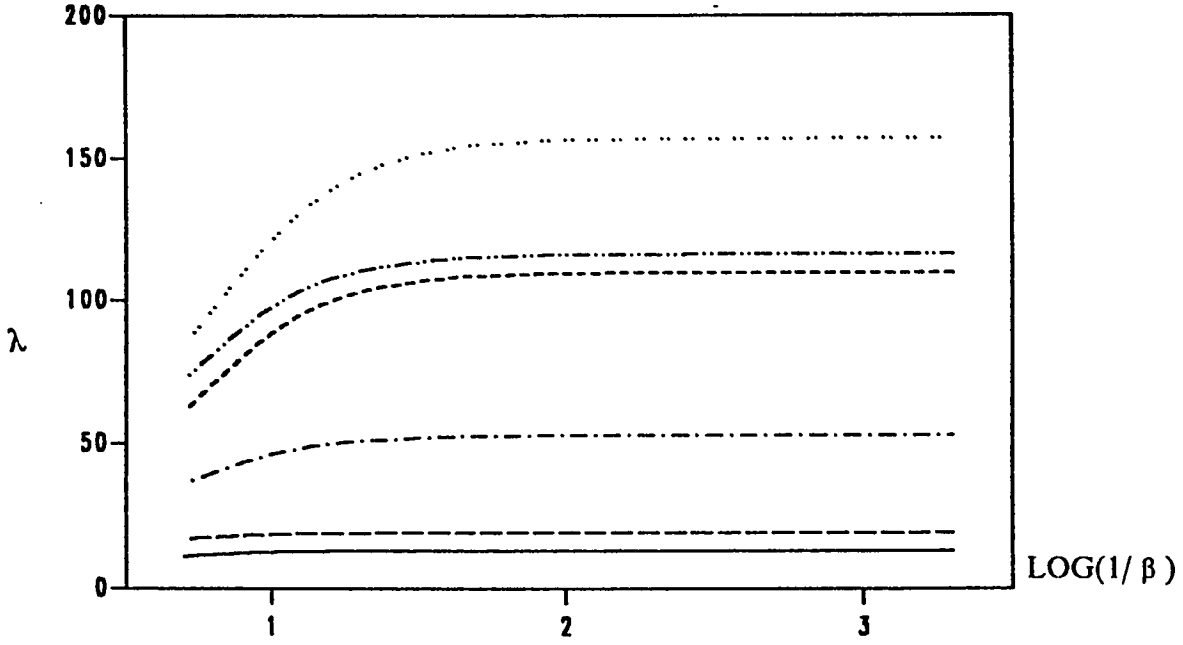

Figure A.2.47 : Variation of λ with β for the First Six S-S Modes.
Corner Supported : α = 0.4 , Mesh Size 11 x 11.

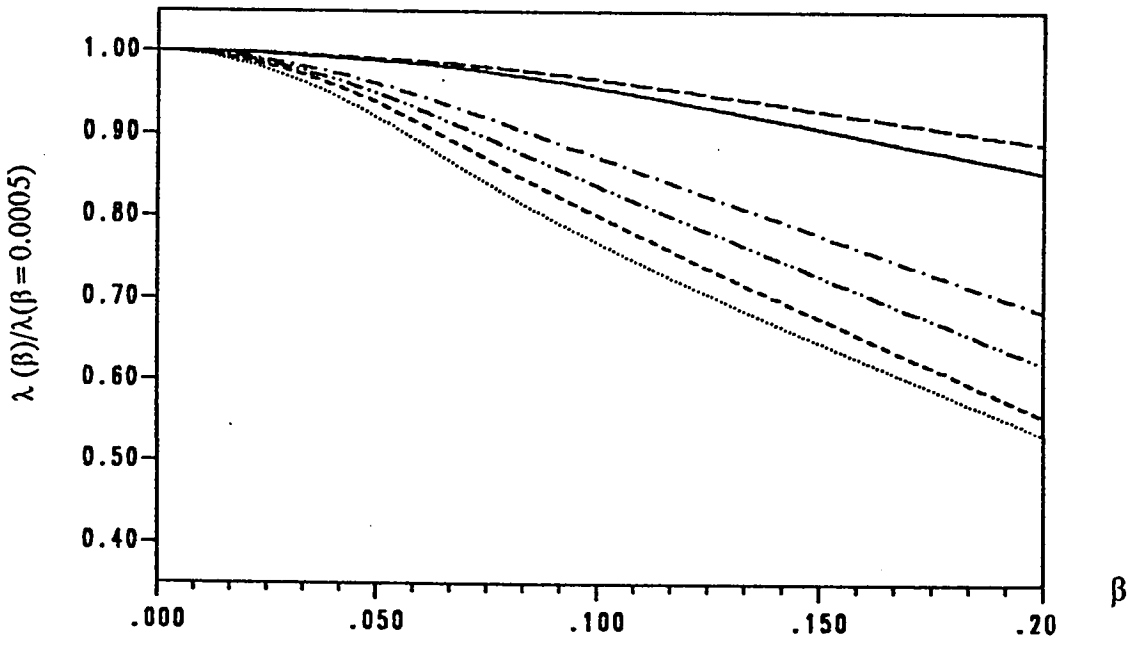

Figure A.2.48 : Correction in λ for the First Six S-S Modes.
Corner Supported : α = 0.4 , Mesh Size 11 x 11.

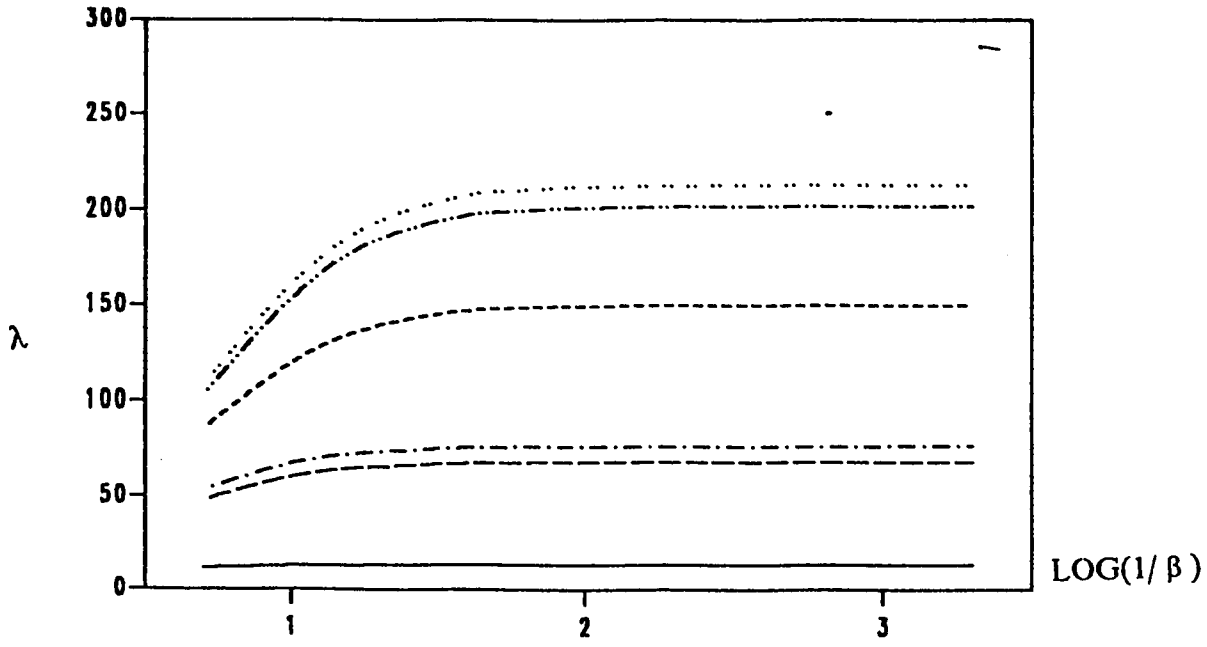

Figure A.2.49 : Variation of λ with β for the First Six A-A Modes.
Corner Supported : α = 0.5 , Mesh Size 11 x 11.

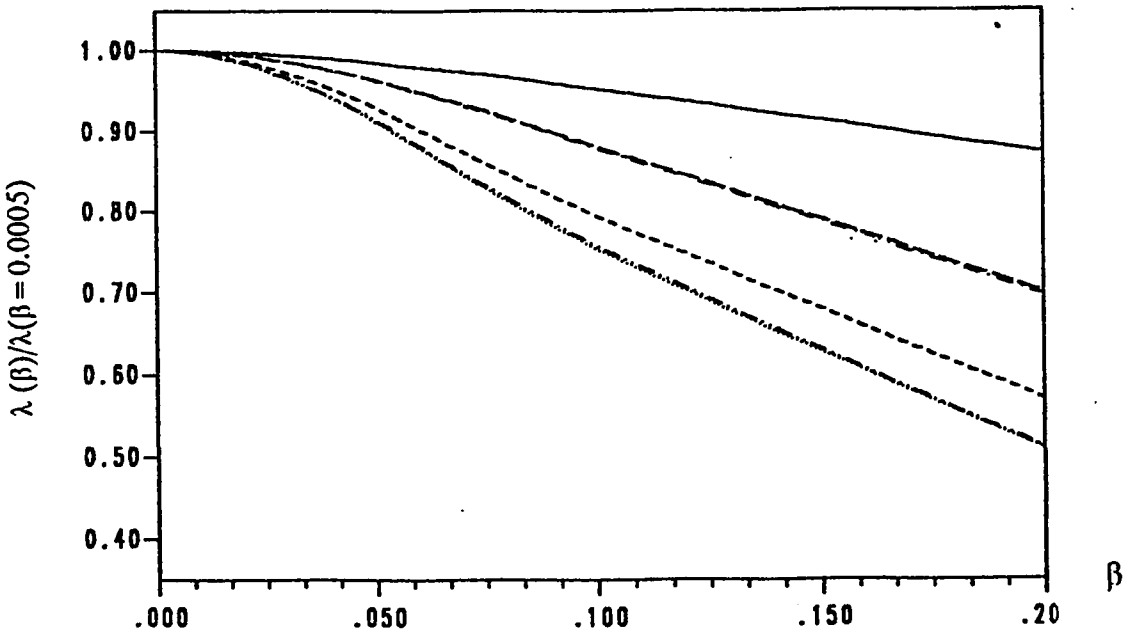

Figure A.2.50 : Correction in λ for the First Six A-A Modes.
Corner Supported : α = 0.5 , Mesh Size 11 x 11.

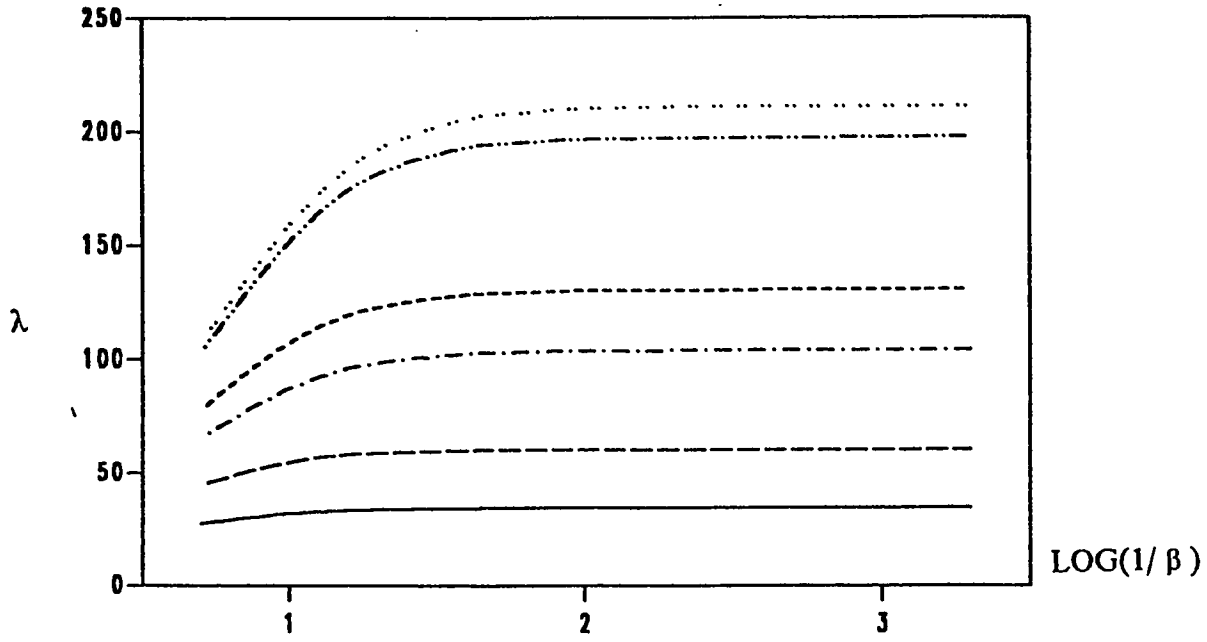

Figure A.2.51 : Variation of λ with β for the First Six S-A Modes.
Corner Supported : α = 0.5 , Mesh Size 11 x 11.

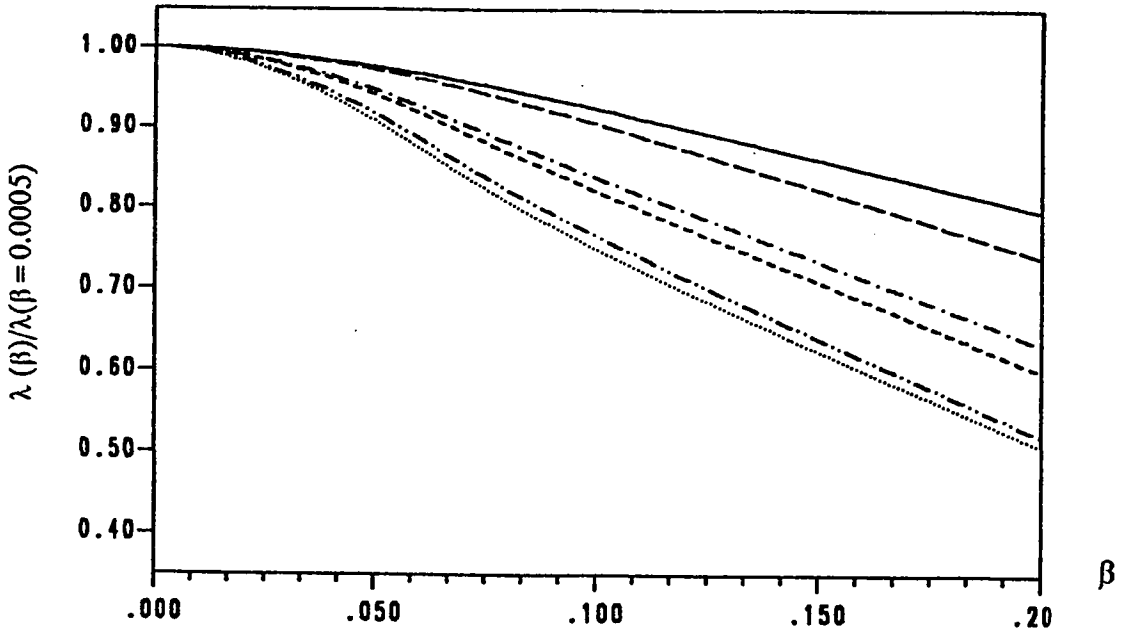

Figure A.2.52 : Correction in λ for the First Six S-A Modes.
Corner Supported : α = 0.5 , Mesh Size 11 x 11.

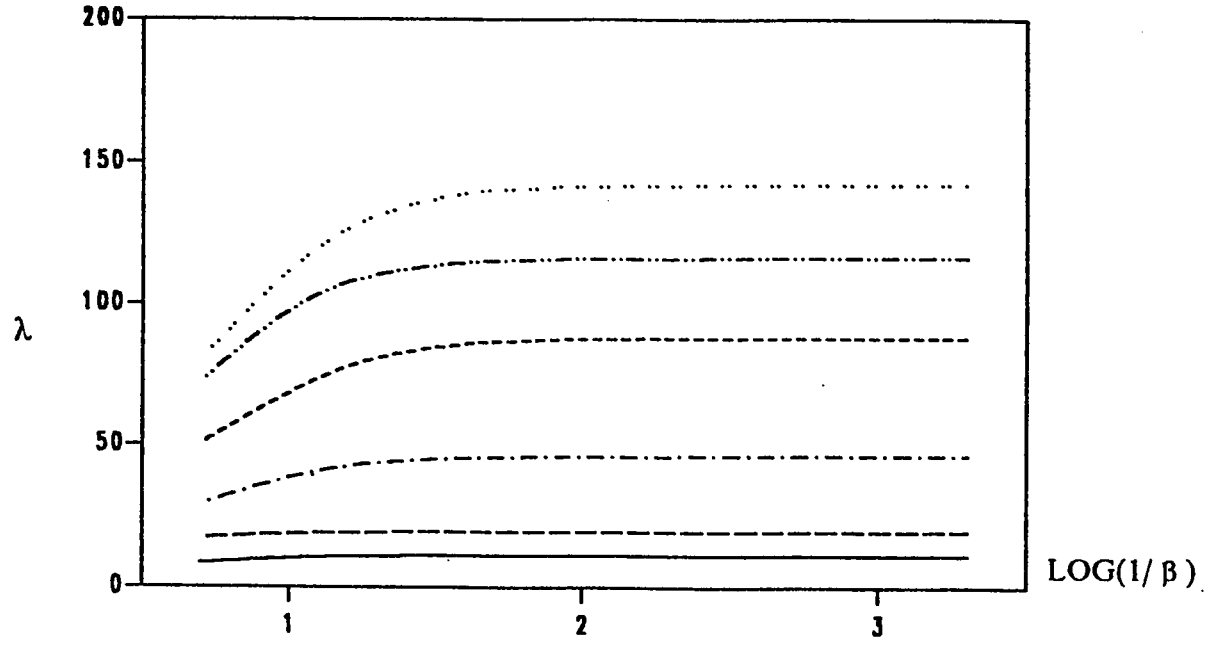

Figure A.2.53 : Variation of λ with β for the First Six S-S Modes.
Corner Supported : α = 0.5 , Mesh Size 11 x 11.

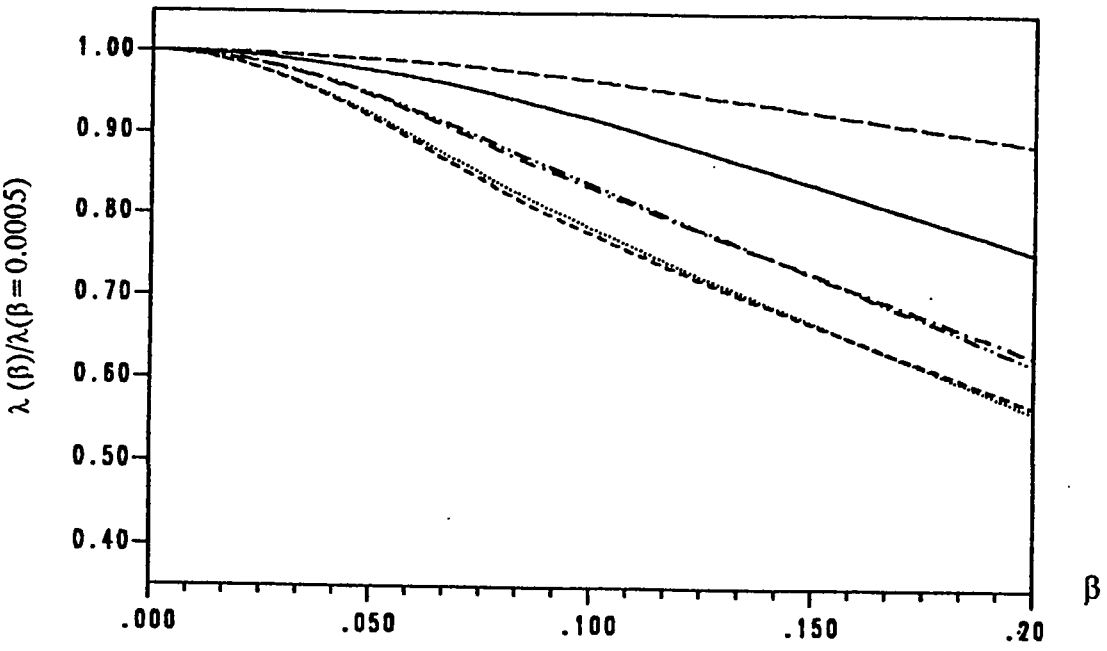

Figure A.2.54 : Correction in λ for the First Six S-S Modes.
Corner Supported : α = 0.5 , Mesh Size 11 x 11.

APPENDIX A.3

TABLES

TABLE A.3.1

The Frequency Parameter λ for the First Six A-A Modes.

$\alpha = 0.0$, Mesh Size = 8×8

β	Mode #1	Mode #2	Mode #3	Mode #4	Mode #5	Mode #6
0.2000	28.0187	47.5595	70.5953	92.4330	101.382	117.088
0.1000	34.8893	59.7856	98.4055	134.652	151.418	180.434
0.0500	37.7751	65.1714	113.879	161.999	182.946	225.166
0.0250	38.6527	66.8541	119.348	172.652	195.310	244.151
0.0200	38.7636	67.0686	120.073	174.111	197.009	246.843
0.0125	38.8854	67.3042	120.875	175.743	198.914	249.887
0.0100	38.9137	67.3591	121.063	176.128	199.363	250.609
0.0050	38.9516	67.4326	121.316	176.646	199.968	251.583
0.0025	38.9611	67.4510	121.379	176.776	200.120	251.829
0.0010	38.9637	67.4561	121.379	176.812	200.163	251.899
0.0005	38.9641	67.4569	121.399	176.818	200.169	251.908
{ 43 }	38.176	68.118	121.810	173.110	202.550	256.770
{ 38 }	38.360	68.120	121.280	173.560	_____	_____

TABLE A.3.2

The Frequency Parameter λ for the First Six S-A Modes.

$\alpha = 0.0$, Mesh Size = 8×8

β	Mode #1	Mode #2	Mode #3	Mode #4	Mode #5	Mode #6
0.2000	12.4406	36.9327	52.2410	69.8917	89.2516	102.216
0.1000	14.5853	45.3140	68.4786	95.0133	130.404	150.214
0.0500	15.4191	48.7162	76.2454	108.357	156.156	180.761
0.0250	15.6709	49.7279	78.7815	112.939	165.988	192.700
0.0200	15.7028	49.8548	79.1088	113.539	167.324	194.388
0.0125	15.7378	49.9938	79.4696	114.204	168.817	196.174
0.0100	15.7459	50.0261	79.5538	114.359	169.169	196.606
0.0050	15.7568	50.0693	79.6667	114.568	169.641	197.189
0.0025	15.7596	50.0801	79.6950	114.620	169.760	197.336
0.0010	15.7604	50.0831	79.7029	114.635	169.794	197.335
0.0005	15.7604	50.0835	79.7040	114.637	169.799	197.383
{ 43 }	15.540	49.824	80.030	115.120	168.020	201.610
{ 38 }	15.564	50.000	80.200	115.080	_____	_____

TABLE A.3.3

The Frequency Parameter λ for the First Six S-S Modes.

$\alpha = 0.0$, Mesh Size = 8×8

β	Mode #1	Mode #2	Mode #3	Mode #4	Mode #5	Mode #6
0.2000	6.2195	17.1699	32.2698	58.1986	71.3979	79.6170
0.1000	6.8621	18.6698	39.4491	78.5455	96.4788	110.379
0.0500	7.0778	19.1325	42.5633	89.0322	109.231	127.535
0.0250	7.1389	19.2556	43.5343	92.5369	113.500	133.615
0.0200	7.1464	19.2706	43.6581	92.9919	114.055	134.420
0.0125	7.1547	19.2869	43.7942	93.4942	114.667	135.314
0.0100	7.1567	19.2907	43.8259	93.6115	114.810	135.523
0.0050	7.1592	19.2957	43.8684	93.7687	115.002	135.804
0.0025	7.1599	19.2969	43.8790	93.8082	115.050	135.875
0.0010	7.1600	19.2973	43.8820	93.8193	115.063	135.895
0.0005	7.1601	19.2973	43.8824	93.8209	115.065	135.898
{ 43 }	7.1020	19.2200	44.0400	91.4600	116.420	138.180
{ 38 }	7.1800	19.2240	44.2800	91.8000	_____	_____

TABLE A.3.4

The Frequency Parameter λ for the First Six A-A Modes.

$\alpha = 0.0$, Mesh Size = 9×9

β	Mode #1	Mode #2	Mode #3	Mode #4	Mode #5	Mode #6
0.2000	27.7131	47.7092	70.3321	92.5082	102.590	117.558
0.1000	34.6324	60.0321	98.2635	134.448	152.279	181.275
0.0500	37.5944	65.5138	113.989	161.482	183.764	226.307
0.0250	38.5109	67.2471	119.610	171.989	196.081	245.462
0.0200	38.6272	67.4691	120.357	173.427	197.772	248.181
0.0125	38.7559	67.7134	121.188	175.036	199.668	251.256
0.0100	38.7858	67.7704	121.383	175.416	200.115	251.985
0.0050	38.8258	67.8466	121.644	175.926	200.717	252.970
0.0025	38.8358	67.8658	121.719	176.055	200.868	253.219
0.0010	38.8386	67.8712	121.728	176.091	200.911	253.289
0.0005	38.8390	67.8719	121.731	176.096	200.917	253.299
{ 43 }	38.176	68.118	121.810	173.110	202.550	256.770
{ 38 }	38.360	68.120	121.280	173.560	_____	_____

TABLE A.3.5

The Frequency Parameter λ for the First Six S-A Modes.

$\alpha = 0.0$, Mesh Size = 9×9

β	Mode #1	Mode #2	Mode #3	Mode #4	Mode #5	Mode #6
0.2000	12.3312	36.8506	52.3043	70.0260	89.1654	102.892
0.1000	14.5164	45.2937	68.4142	95.2235	130.218	151.156
0.0500	15.3919	48.7504	76.3053	108.668	155.942	181.809
0.0250	15.6646	49.7862	78.9154	113.313	165.786	193.794
0.0200	15.6996	49.9166	79.2541	113.923	167.126	195.440
0.0125	15.7381	50.0595	79.6281	114.599	168.623	197.283
0.0100	15.7471	50.0927	79.7155	114.757	168.975	197.718
0.0050	15.7591	50.1371	79.8326	114.970	169.450	198.303
0.0025	15.7621	50.1483	79.8620	115.023	169.569	198.451
0.0010	15.7630	50.1514	79.8702	115.038	169.602	198.492
0.0005	15.7631	50.1518	79.8714	115.040	169.607	198.498
{ 43 }	15.540	49.824	80.030	115.120	168.020	201.610
{ 38 }	15.564	50.000	80.200	115.080	_____	_____

TABLE A.3.6

The Frequency Parameter λ for the First Six S-S Modes.

$\alpha = 0.0$, Mesh Size = 9×9

β	Mode #1	Mode #2	Mode #3	Mode #4	Mode #5	Mode #6
0.2000	6.17227	17.2216	32.1390	57.8531	71.7417	79.8589
0.1000	6.83248	18.7328	39.3892	78.1044	96.8963	110.727
0.0500	7.05961	19.1997	42.6036	88.5931	109.666	128.011
0.0250	7.12541	19.3240	43.6288	92.1157	113.938	134.170
0.0200	7.13367	19.3392	43.7607	92.5741	114.493	134.987
0.0125	7.14272	19.3557	43.9061	93.0803	115.107	135.895
0.0100	7.14482	19.3595	43.9401	93.1986	115.250	136.108
0.0050	7.14763	19.3646	43.9855	93.3573	115.442	136.394
0.0025	7.14834	19.3658	43.9970	93.3971	115.490	135.466
0.0010	7.14854	19.3662	44.0002	93.4082	115.503	136.486
0.0005	7.14856	19.3663	44.0006	93.4098	115.505	136.489
{ 43 }	7.10200	19.2200	44.0400	91.4600	116.420	138.180
{ 38 }	7.18000	19.2240	44.2800	91.8000	_____	_____

TABLE A.3.7

The Frequency Parameter λ for the First Six A-A Modes.

$\alpha = 0.0$, Mesh Size = 10×10

β	Mode #1	Mode #2	Mode #3	Mode #4	Mode #5	Mode #6
0.2000	27.4582	47.8074	70.0613	92.5048	103.046	117.801
0.1000	34.4218	60.1893	98.0578	134.259	152.875	181.732
0.0500	37.4534	65.7395	113.981	161.134	184.356	226.998
0.0250	38.4082	67.5149	119.737	171.587	196.669	246.319
0.0200	38.5308	67.7437	120.507	173.018	198.360	249.067
0.0125	38.6657	67.9959	121.364	174.621	200.255	252.176
0.0100	38.6973	68.0548	121.565	174.999	200.702	252.914
0.0050	38.7395	68.1337	121.835	175.508	201.304	253.911
0.0025	38.7501	68.1534	121.903	175.636	201.456	254.162
0.0010	38.7531	68.1590	121.922	175.672	201.498	254.233
0.0005	38.7535	68.1598	121.925	175.677	201.504	254.243
{ 43 }	38.176	68.118	121.810	173.110	202.550	256.770
{ 38 }	38.360	68.120	121.280	173.560	_____	_____

TABLE A.3.8

The Frequency Parameter λ for the First Six S-A Modes.

$\alpha = 0.0$, Mesh Size = 10×10

β	Mode #1	Mode #2	Mode #3	Mode #4	Mode #5	Mode #6
0.2000	12.2394	36.7666	52.1832	70.0921	89.0258	103.346
0.1000	14.4558	45.2601	68.3225	95.3371	129.992	151.790
0.0500	15.3656	48.7647	76.3148	108.866	155.728	182.536
0.0250	15.6575	49.8234	78.9930	113.571	165.611	194.577
0.0200	15.6955	49.9572	79.3428	114.191	166.959	196.233
0.0125	15.7347	50.1040	79.7296	114.879	168.466	198.088
0.0100	15.7472	50.1381	79.8201	115.040	168.821	199.526
0.0050	15.7604	50.1838	79.9414	115.256	169.298	199.116
0.0025	15.7637	50.1953	79.9719	115.311	169.419	199.264
0.0010	15.7646	50.1985	79.9804	115.326	169.452	199.306
0.0005	15.7648	50.1989	79.9817	115.328	169.457	199.312
{ 43 }	15.540	49.824	80.030	115.120	168.020	201.610
{ 38 }	15.564	50.000	80.200	115.080	———	———

TABLE A.3.9

The Frequency Parameter λ for the First Six S-S Modes.

$\alpha = 0.0$, Mesh Size = 10×10

β	Mode #1	Mode #2	Mode #3	Mode #4	Mode #5	Mode #6
0.2000	6.13355	17.2571	32.0174	57.5487	71.9779	80.0016
0.1000	6.80833	18.7762	39.3164	77.7429	97.1868	110.929
0.0500	7.04530	19.2461	42.6113	88.2665	109.973	128.313
0.0250	7.11559	19.3713	43.6856	91.8233	114.252	134.544
0.0200	7.12451	19.3866	43.8253	92.2875	114.808	135.374
0.0125	7.13431	19.4032	43.9797	92.8007	115.422	136.296
0.0100	7.13660	19.4070	44.0158	92.9207	115.566	136.513
0.0050	7.13966	19.4122	44.0642	93.0816	115.758	136.804
0.0025	7.14042	19.4135	44.0764	93.1220	115.806	135.877
0.0010	7.14064	19.4138	44.0798	93.1333	115.820	136.897
0.0005	7.14067	19.4139	44.0803	93.1349	115.822	136.900
{ 43 }	7.10200	19.2200	44.0400	91.4600	116.420	138.180
{ 38 }	7.18000	19.2240	44.2800	91.8000	_____	_____

TABLE A.3.10

The Frequency Parameter λ for the First Six A-A Modes.

$\alpha = 0.0$, Mesh Size = 11×11

β	Mode #1	Mode #2	Mode #3	Mode #4	Mode #5	Mode #6
0.2000	27.2412	47.8750	69.8000	92.4605	103.367	117.917
0.1000	34.2445	60.2934	97.8308	134.078	153.299	181.968
0.0500	37.3384	65.8926	113.915	160.871	184.792	227.413
0.0250	38.3298	67.7040	119.795	171.317	197.114	246.889
0.0200	38.4582	67.9389	120.585	172.750	198.807	249.666
0.0125	38.6000	68.1983	121.467	174.356	200.706	252.810
0.0100	38.6331	68.2590	121.674	174.734	201.154	253.556
0.0050	38.6776	68.3403	121.953	175.244	201.757	254.565
0.0025	38.6888	68.3607	122.023	175.373	201.909	254.820
0.0010	38.6919	68.3664	122.042	175.409	201.951	254.891
0.0005	38.6923	68.3673	122.045	175.414	201.957	254.902
{ 43 }	38.176	68.118	121.810	173.110	202.550	256.770
{ 38 }	38.360	68.120	121.280	173.560	_____	_____

TABLE A.3.11

The Frequency Parameter λ for the First Six S-A Modes.

$\alpha = 0.0$, Mesh Size = 11×11

β	Mode #1	Mode #2	Mode #3	Mode #4	Mode #5	Mode #6
0.2000	12.1611	36.6851	52.0658	70.1199	88.8653	103.664
0.1000	14.4026	45.2208	68.2210	95.3938	129.755	152.230
0.0500	15.3405	48.7672	76.2967	108.992	155.523	183.047
0.0250	15.6501	49.8475	79.0377	113.752	165.462	195.145
0.0200	15.6909	49.9846	79.3980	114.382	166.821	196.811
0.0125	15.7362	50.1352	79.7974	115.082	168.341	198.679
0.0100	15.7469	50.1702	79.8910	115.246	168.699	199.120
0.0050	15.7612	50.2172	80.0165	115.466	169.182	199.714
0.0025	15.7648	50.2289	80.0481	115.521	169.303	199.864
0.0010	15.7658	50.2322	80.0569	115.537	169.337	199.906
0.0005	15.7659	50.2327	80.0582	115.539	169.342	199.912
{ 43 }	15.540	49.824	80.030	115.120	168.020	201.610
{ 38 }	15.564	50.000	80.200	115.080	_____	_____

TABLE A.3.12

The Frequency Parameter λ for the First Six S-S Modes.

$\alpha = 0.0$, Mesh Size = 11×11

β	Mode #1	Mode #2	Mode #3	Mode #4	Mode #5	Mode #6
0.2000	6.10102	17.2825	31.9064	57.2792	72.1468	80.0847
0.1000	6.78818	18.8074	39.2409	77.4366	97.3956	111.046
0.0500	7.03357	19.2794	42.6007	88.0091	110.197	128.508
0.0250	7.10805	19.4054	43.7196	91.6081	114.482	134.805
0.0200	7.11761	19.4207	43.8668	92.0795	115.040	135.646
0.0125	7.12816	19.4374	44.0299	92.6013	115.655	136.582
0.0100	7.13062	19.4413	44.0682	92.7234	115.799	136.802
0.0050	7.13392	19.4464	44.1195	92.8872	115.991	137.098
0.0025	7.13475	19.4477	44.1325	92.9283	116.040	137.172
0.0010	7.13498	19.4481	44.1361	92.9398	116.053	137.193
0.0005	7.13502	19.4481	44.1366	92.9415	116.055	137.196
{ 43 }	7.10200	19.2200	44.0400	91.4600	116.420	138.180
{ 38 }	7.18000	19.2240	44.2800	91.8000	_____	_____

TABLE A.3.13

The Frequency Parameter λ for the First Six A-A Modes.

$\alpha = 0.1$, Mesh Size = 11×11

β	Mode #1	Mode #2	Mode #3	Mode #4	Mode #5	Mode #6
0.2000	43.1737	47.8750	67.8300	87.4709	103.367	113.347
0.1000	57.7173	60.2934	107.811	126.985	153.299	174.056
0.0500	64.2950	65.8926	132.668	161.057	184.792	230.181
0.0250	66.3705	67.7040	141.188	176.500	197.114	261.765
0.0200	66.6366	67.9389	142.318	178.661	198.807	266.577
0.0125	66.9299	68.1983	143.574	181.093	200.706	272.057
0.0100	66.9984	68.2590	143.869	181.668	201.154	273.361
0.0050	67.0902	68.3403	144.266	182.444	201.757	275.123
0.0025	67.1132	68.3607	144.366	182.640	201.909	275.567
0.0010	67.1196	68.3664	144.394	182.695	201.951	275.692
0.0005	67.1206	68.3673	144.398	182.703	201.957	275.710
{ 43 }	66.549	68.118	145.490	188.290	202.550	272.850
{ 38 }	66.520	68.120	145.440	187.920	_____	_____

TABLE A.3.14

The Frequency Parameter λ for the First Six S-A Modes.

$\alpha = 0.1$, Mesh Size = 11×11

β	Mode #1	Mode #2	Mode #3	Mode #4	Mode #5	Mode #6
0.2000	18.2427	42.4990	58.3883	72.9902	78.2841	104.563
0.1000	21.7260	52.5957	81.8501	106.912	118.716	155.872
0.0500	23.1158	56.6901	93.5688	122.616	158.806	191.712
0.0250	23.5520	57.9083	97.5704	128.085	174.984	205.359
0.0200	23.6084	58.0614	98.0982	128.807	177.130	207.263
0.0125	23.6708	58.2290	98.6838	129.608	179.507	209.407
0.0100	23.6854	58.2679	98.8211	129.796	180.064	209.914
0.0050	23.7050	58.3201	99.0055	130.048	180.813	210.598
0.0025	23.7099	58.3331	99.0518	130.111	181.001	210.771
0.0010	23.7113	58.3368	99.0648	130.129	181.054	210.819
0.0005	23.7115	58.3373	99.0667	130.131	181.061	210.826
{ 43 }	23.387	58.300	99.149	130.48	184.57	213.17
{ 38 }	23.388	58.320	99.160	130.480	_____	_____

TABLE A.3.15

The Frequency Parameter λ for the First Six S-S Modes.

$\alpha = 0.1$, Mesh Size = 11×11

β	Mode #1	Mode #2	Mode #3	Mode #4	Mode #5	Mode #6
0.2000	10.9651	17.2825	37.7493	72.1468	75.6563	88.0578
0.1000	12.2456	18.8074	47.6405	97.3956	101.755	125.138
0.0500	12.6639	19.2794	52.1891	110.197	115.310	147.044
0.0250	12.7800	19.4054	53.6769	114.482	119.870	155.274
0.0200	12.7945	19.4207	53.8708	115.040	120.464	156.391
0.0125	12.8102	19.4374	54.0853	115.655	121.120	157.640
0.0100	12.8139	19.4413	54.1356	115.799	121.273	157.934
0.0050	12.8188	19.4464	54.2030	115.991	121.479	158.329
0.0025	12.8200	19.4477	54.2199	116.040	121.530	158.429
0.0010	12.8204	19.4481	54.2247	116.053	121.545	158.456
0.0005	12.8204	19.4481	54.2254	116.055	121.547	158.460
{ 43 }	12.810	19.220	54.009	116.42	122.49	159.88
{ 38 }	12.808	19.224	54.000	116.44	_____	_____

TABLE A.3.16

The Frequency Parameter λ for the First Six A-A Modes.

$\alpha = 0.2$, Mesh Size = 11×11

β	Mode #1	Mode #2	Mode #3	Mode #4	Mode #5	Mode #6
0.2000	28.4514	47.8750	62.1564	86.8188	103.367	119.802
0.1000	40.7855	60.2934	89.5992	122.166	153.299	187.424
0.0500	47.5976	65.8926	111.591	144.662	184.792	241.483
0.0250	49.9130	67.7040	121.398	153.757	197.114	266.508
0.0200	50.2165	67.9389	122.797	155.035	198.807	270.157
0.0125	50.5532	68.1983	124.383	156.480	200.706	274.316
0.0100	50.6322	68.2590	124.760	156.823	201.154	275.308
0.0050	50.7385	68.3403	125.270	157.286	201.757	276.652
0.0025	50.7653	68.3607	125.399	157.403	201.909	276.992
0.0010	50.7728	68.3664	125.435	157.436	201.951	277.087
0.0005	50.7738	68.3673	125.441	157.440	201.957	277.101
{ 43 }	51.087	68.118	122.840	157.650	202.550	278.800
{ 38 }	?	68.120	122.600	157.560	202.560	_____

TABLE A.3.17

The Frequency Parameter λ for the First Six S-A Modes.

$\alpha = 0.2$, Mesh Size = 11×11

β	Mode #1	Mode #2	Mode #3	Mode #4	Mode #5	Mode #6
0.2000	22.3857	29.9447	48.8827	65.8342	85.0162	106.657
0.1000	28.9864	39.4028	65.8317	87.2828	123.322	157.279
0.0500	31.2560	44.6418	77.5420	98.5577	149.969	190.394
0.0250	31.9211	46.3089	82.3035	102.500	161.127	203.757
0.0200	32.0056	46.5214	82.9627	103.023	162.696	205.620
0.0125	32.0987	46.7554	83.7040	103.604	164.465	207.716
0.0100	32.1204	46.8101	83.8795	103.741	164.884	208.213
0.0050	32.1496	46.8834	84.1166	103.924	165.451	208.881
0.0025	32.1569	46.9012	84.1764	103.970	165.594	209.050
0.0010	32.1589	46.9070	84.1933	103.983	165.634	209.097
0.0005	32.1592	46.9078	84.1957	103.985	165.640	209.104
{ 43 }	31.771	47.380	83.455	104.19	164.24	211.34
{ 38 }	31.772	47.360	83.360	104.20	_____	_____

TABLE A.3.18

The Frequency Parameter λ for the First Six S-S Modes.

$\alpha = 0.2$, Mesh Size = 11×11

β	Mode #1	Mode #2	Mode #3	Mode #4	Mode #5	Mode #6
0.2000	17.2825	19.1069	27.6741	45.0566	72.1468	88.0378
0.1000	18.8074	21.8581	41.1220	56.0497	97.3956	125.138
0.0500	19.2794	22.6750	50.1776	61.4353	110.197	147.044
0.0250	19.4054	22.8924	53.5373	63.3542	114.482	155.274
0.0200	19.4207	22.9190	53.9858	63.6149	115.040	156.391
0.0125	19.4374	22.9479	54.4854	63.9070	115.655	157.640
0.0100	19.4413	22.9546	54.6030	63.9763	115.799	157.934
0.0050	19.4464	22.9635	54.7614	64.0690	115.991	158.329
0.0025	19.4477	22.9658	54.8014	64.0925	116.040	158.429
0.0010	19.4481	22.9664	54.8126	64.0990	116.053	158.456
0.0005	19.4481	22.9665	54.8142	64.1000	116.055	158.460
{ 43 }	19.220	23.121	54.566	63.878	116.42	159.88
{ 38 }	19.224	23.120	54.480	63.880	_____	_____

TABLE A.3.19

The Frequency Parameter λ for the First Six A-A Modes.

$\alpha = 0.3$, Mesh Size = 11×11

β	Mode #1	Mode #2	Mode #3	Mode #4	Mode #5	Mode #6
0.2000	16.2661	47.8750	62.6953	103.367	98.9485	112.413
0.1000	21.1739	60.2934	86.6496	153.299	150.729	172.626
0.0500	24.1124	65.8926	102.350	184.792	186.889	230.716
0.0250	25.1801	67.7040	108.617	197.114	200.972	261.562
0.0200	25.3233	67.9389	109.485	198.807	202.901	266.045
0.0125	25.4831	68.1983	110.462	200.706	205.062	271.111
0.0100	25.5207	68.2590	110.693	201.154	205.572	272.313
0.0050	25.5715	68.3403	111.005	201.757	206.259	273.936
0.0025	25.5843	68.3607	111.084	201.909	206.432	274.345
0.0010	25.5878	68.3664	111.106	201.951	206.480	274.460
0.0005	25.5884	68.3673	111.109	201.957	206.487	274.477
{ 43 }	25.396	68.118	110.730	202.550	208.240	275.820
{ 38 }	?	68.120	110.640	202.560	208.160	_____

TABLE A.3.20

The Frequency Parameter λ for the First Six S-A Modes.

$\alpha = 0.3$, Mesh Size = 11×11

β	Mode #1	Mode #2	Mode #3	Mode #4	Mode #5	Mode #6
0.2000	14.2693	28.1696	54.7232	70.0376	80.3505	103.009
0.1000	19.8433	33.3699	75.0096	97.6916	115.238	151.176
0.0500	22.4598	35.7125	86.9254	114.485	142.683	181.284
0.0250	23.2820	36.4785	91.2058	120.441	155.945	192.952
0.0200	23.3874	36.5783	91.7767	121.226	157.902	194.551
0.0125	23.5037	36.6887	92.4123	122.097	160.138	196.342
0.0100	23.5309	36.7145	92.5617	122.301	160.673	196.765
0.0050	23.5674	36.7492	92.7628	122.575	161.399	197.333
0.0025	23.5766	36.7579	92.8134	122.644	161.583	197.476
0.0010	23.5792	36.7604	92.8276	122.663	161.635	197.516
0.0005	23.5796	36.7607	92.8296	122.666	161.642	197.522
{ 43 }	23.600	36.355	92.353	122.85	161.59	198.05
{ 38 }	23.580	36.356	92.320	122.800	_____	_____

TABLE A.3.21

The Frequency Parameter λ for the First Six S-S Modes.

$\alpha = 0.3$, Mesh Size = 11×11

β	Mode #1	Mode #2	Mode #3	Mode #4	Mode #5	Mode #6
0.2000	17.2825	15.9645	34.4919	46.1610	72.1468	94.0485
0.1000	18.8074	18.1165	50.2542	61.6785	97.3956	116.103
0.0500	19.2794	18.7941	57.3155	74.9041	110.197	141.069
0.0250	19.4054	18.9762	59.4010	80.5270	114.482	151.378
0.0200	19.4207	18.9985	59.6672	81.3026	115.040	152.794
0.0125	19.4374	19.0229	59.9607	82.1732	115.655	154.379
0.0100	19.4413	19.0285	60.0293	82.3792	115.799	154.753
0.0050	19.4464	19.0361	60.1213	82.6574	115.991	155.991
0.0025	19.4477	19.0380	60.1444	82.7277	116.040	155.384
0.0010	19.4481	19.0385	60.1509	82.7474	116.053	155.420
0.0005	19.4481	19.0386	60.1518	82.7503	116.055	155.425
{ 43 }	19.220	19.268	59.560	81.319	116.42	155.80
{ 38 }	19.224	19.264	59.560	_____	116.44	_____

TABLE A.3.22

The Frequency Parameter λ for the First Six A-A Modes.

$\alpha = 0.4$, Mesh Size = 11×11

β	Mode #1	Mode #2	Mode #3	Mode #4	Mode #5	Mode #6
0.2000	12.2247	47.8750	55.0733	88.9107	103.367	110.981
0.1000	14.0509	60.2934	71.4694	126.864	153.299	165.582
0.0500	15.3466	65.8926	80.9138	152.770	184.792	203.219
0.0250	15.9434	67.7040	84.7431	163.978	197.114	219.427
0.0200	16.0311	67.9389	85.2882	165.598	198.807	221.766
0.0125	16.1314	68.1983	85.9069	167.442	200.706	224.428
0.0100	16.1554	68.2590	86.0542	167.882	201.154	225.063
0.0050	16.1880	68.3403	86.2537	168.478	201.757	225.923
0.0025	16.1963	68.3607	86.3041	168.628	201.909	226.141
0.0010	16.1986	68.3664	86.3183	168.671	201.951	226.202
0.0005	16.1989	68.3673	86.3203	168.677	201.957	226.210
{ 43 }	15.900	68.118	86.368	169.80	202.550	226.65
{ 38 }	?	68.120	86.320	169.68	202.560	_____

TABLE A.3.23

The Frequency Parameter λ for the First Six S-A Modes.

$\alpha = 0.4$, Mesh Size = 11×11

β	Mode #1	Mode #2	Mode #3	Mode #4	Mode #5	Mode #6
0.2000	7.46426	28.3407	49.7330	71.2487	79.0115	106.723
0.1000	10.8925	33.6496	65.1897	99.8814	109.614	158.185
0.0500	12.7610	36.1072	74.0620	117.617	129.620	191.727
0.0250	13.3975	36.9311	77.3584	123.900	138.619	205.300
0.0200	13.4813	37.0394	77.8046	124.722	139.934	207.193
0.0125	13.5738	37.1596	78.3035	125.632	141.436	209.323
0.0100	13.5956	37.1878	78.4212	125.845	141.795	209.827
0.0050	13.6250	37.2257	78.5799	126.131	142.282	210.507
0.0025	13.6324	37.2353	78.6199	126.202	142.405	210.678
0.0010	13.6345	37.2379	78.6311	126.222	142.440	210.726
0.0005	13.6348	37.2383	78.6327	126.225	142.445	210.733
{ 43 }	13.551	36.811	78.469	126.80	142.30	213.11
{ 38 }	13.536	36.812	78.440	126.76	_____	_____

TABLE A.3.24

The Frequency Parameter λ for the First Six S-S Modes.

$\alpha = 0.4$, Mesh Size = 11×11

β	Mode #1	Mode #2	Mode #3	Mode #4	Mode #5	Mode #6
0.2000	11.3311	17.2825	36.2970	61.1461	72.1468	83.8570
0.1000	12.6816	18.8074	46.2384	88.1406	97.3956	120.841
0.0500	13.1059	19.2794	50.8538	102.919	110.197	144.478
0.0250	13.2196	19.4054	52.3678	107.887	114.482	153.432
0.0200	13.2335	19.4207	52.5654	108.534	115.040	154.648
0.0125	13.2487	19.4374	52.7844	109.250	115.655	156.008
0.0100	13.2522	19.4413	52.8357	109.417	115.799	156.328
0.0050	13.2569	19.4464	52.9046	109.642	115.991	156.759
0.0025	13.2581	19.4477	52.9219	109.699	116.040	156.868
0.0010	13.2584	19.4481	52.9267	109.715	116.053	156.898
0.0005	13.2585	19.4481	52.9274	109.717	116.055	156.902
{ 43 }	13.373	19.220	52.551	110.51	116.42	157.62
{ 38 }	13.372	19.224	52.560	110.48	116.44	———

TABLE A.3.25

The Frequency Parameter λ for the First Six A-A Modes.

$\alpha = 0.5$, Mesh Size = 11×11

β	Mode #1	Mode #2	Mode #3	Mode #4	Mode #5	Mode #6
0.2000	11.7287	47.8750	53.3660	85.7703	103.367	108.651
0.1000	12.7915	60.2934	67.4088	119.508	153.299	160.757
0.0500	13.2257	65.8926	73.8022	139.651	184.792	194.352
0.0250	13.3707	67.7040	75.8491	147.228	197.114	207.643
0.0200	13.3899	67.9389	76.1128	148.257	198.807	209.477
0.0125	13.4113	68.1983	76.4034	149.408	200.706	211.534
0.0100	13.4163	68.2590	76.4713	149.678	201.154	212.020
0.0050	13.4231	68.3403	76.5622	150.043	201.757	212.674
0.0025	13.4248	68.3607	76.5850	150.135	201.909	212.839
0.0010	13.4253	68.3664	76.5914	150.160	201.951	212.885
0.0005	13.4253	68.3673	76.5923	150.164	201.957	212.892
{ 43 }	13.165	68.118	76.969	151.21	202.550	213.67
{ 38 }	13.168	68.120	76.960	151.24	202.560	213.64

TABLE A.3.26

The Frequency Parameter λ for the First Six S-A Modes.

$\alpha = 0.5$, Mesh Size = 11×11

β	Mode #1	Mode #2	Mode #3	Mode #4	Mode #5	Mode #6
0.2000	27.5109	44.8538	65.8303	78.1484	102.975	107.499
0.1000	31.9425	54.9298	87.2821	107.076	151.139	158.186
0.0500	33.7547	58.9895	98.5576	122.668	181.136	191.780
0.0250	34.3320	60.1931	102.500	128.121	192.691	205.421
0.0200	34.4070	60.3440	103.023	128.842	194.268	207.326
0.0125	34.4899	60.5092	103.604	129.641	196.032	209.472
0.0100	34.5093	60.5475	103.740	129.828	196.448	209.979
0.0050	34.5354	60.5989	103.923	130.079	197.007	210.664
0.0025	34.5419	60.6117	103.969	130.143	197.148	210.837
0.0010	34.5437	60.6153	103.982	130.160	197.187	210.885
0.0005	34.5440	60.6158	103.984	130.163	197.193	210.892
{ 43 }	34.227	60.931	104.19	130.73	197.77	213.63
{ 38 }	_____	_____	_____	_____	_____	_____

TABLE A.3.27

The Frequency Parameter λ for the First Six S-S Modes.

$\alpha = 0.5$, Mesh Size = 11×11

β	Mode #1	Mode #2	Mode #3	Mode #4	Mode #5	Mode #6
0.2000	8.50482	17.2825	29.0163	50.1203	72.1468	80.0289
0.1000	10.3337	18.8074	38.3816	68.3648	97.3956	111.523
0.0500	10.9933	19.2794	43.5555	80.8759	110.197	131.171
0.0250	11.1783	19.4054	45.3246	85.8608	114.482	138.901
0.0200	11.2013	19.4207	45.5571	86.5450	115.040	139.968
0.0125	11.2264	19.4374	45.8150	87.3124	115.655	141.166
0.0100	11.2323	19.4413	45.8756	87.4937	115.799	141.450
0.0050	11.2401	19.4464	45.9571	87.7385	115.991	141.832
0.0025	11.2421	19.4477	45.9776	87.8003	116.040	141.929
0.0010	11.2426	19.4481	45.9834	87.8176	116.053	141.956
0.0005	11.2427	19.4481	45.9842	87.8201	116.055	141.959
{ 43 }	11.297	19.220	45.666	87.478	116.42	142.19
{ 38 }	_____	19.224	_____	_____	116.44	_____

TABLE (A.3.28)

Experimental Results, $\beta = 0.01$ $\alpha = 0.0$

#	MODE	THEORY	EXP.	% DISCREPANCY
1st	SS 1	87.289	88.7	+0.46
2nd	SA 1	194.974	192.5	-1.27
"	AS 1	194.974	197.1	+1.09
3rd	SS 2	240.717	241.3	+0.24
4th	AA 1	478.347	475.6	-0.57
5th	SS 3	545.640	554.6	+1.64
6th	SA 2	621.196	620.9	-0.05
"	AS 2	621.196	630.5	+1.50
7th	AA 2	845.167	860.5	+1.80

TABLE (A.3.29)

Experimental Results, $\beta = 0.01$ $\alpha = 0.1$

#	MODE	THEORY	EXP.	% DISCREPANCY
1st	SS 1	158.66	160.2	+0.97
2nd	SS 2	240.72	241.5	+0.32
3rd	SA 1	293.27	290.5	-0.94
"	AS 1	293.27	300.1	+2.33
4th	SS 3	670.29	675.3	+0.75
5th	SA 2	721.46	705.6	-2.20
"	AS 2	721.46	732.3	+1.50
6th	AA 1	829.56	840.1	+1.27
7th	AA 2	845.17	857.2	+1.42

TABLE (A.3.30)

Experimental Results, $\beta = 0.025$ $\alpha = 0.0$

#	MODE	THEORY	EXP.	% DISCREPANCY
1st	SS 1	220.03	216.5	-1.60
2nd	SA 1	484.44	486.0	+0.32
3rd	SS 2	600.68	609.3	+1.44
4th	AA 1	186.48	1190.6	+0.35
5th	SS 3	1353.31	1319.9	-2.47

TABLE (A.3.31)

Experimental Results, $\beta = 0.025$ $\alpha = 0.1$

#	MODE	THEORY	EXP.	% DISCREPANCY
1st	SS 1	395.60	385.2	-2.48
2nd	SS 2	600.68	610.5	+1.63
3rd	SA 1	729.04	724.5	-0.62
"	AS 1	729.04	739.2	+1.39
4th	SS 3	1661.53	1635.5	-1.57
5th	SA 2	1792.52	1813.2	+1.15

TABLE (A.3.32)

Experimental Results, $\beta = 0.05$ $\alpha = 0.0$

#	MODE	THEORY	EXP.	% DISCREPANCY
1st	SS 1	457.15	447.5	-2.11
2nd	SA 1	997.07	972.3	-2.48
"	AS 1	997.07	1012.5	+1.55
3rd	AA 1	1253.09	1231.2	-1.75

TABLE (A.3.33)

Experimental Results, $\beta = 0.05$ $\alpha = 0.1$

#	MODE	THEORY	EXP.	% DISCREPANCY
1st	SS 1	823.10	820.9	-0.27
2nd	SS 2	1253.09	1230.5	-1.80
3rd	SA 1	1502.44	1480.0	-1.49
"	AS 1	1502.44	1490.0	-0.83

TABLE A.3.34

The Frequency Parameter λ_c for the First Four Modes.

$\xi = 0.00$

β	Mode #1	Mode #2	Mode #3	Mode #4
0.2000	7.74033	13.7059	18.8075	28.3854
0.1000	9.11584	17.3516	21.5179	38.4201
0.0500	9.60023	19.0849	23.2737	43.5676
0.0250	9.73695	19.7367	24.2593	45.2731
0.0200	9.75395	19.8313	24.4312	45.4942
0.0125	9.77255	19.9409	24.6434	45.7384
0.0100	9.77687	19.9675	24.6975	45.7954
0.0050	9.78264	20.0041	24.7737	45.8719
0.0025	9.78409	20.0135	24.7937	45.8911
0.0010	9.78450	20.0161	24.7994	45.8965
0.0005	9.78455	20.0165	24.8002	45.8972

TABLE A.3.35

The Frequency Parameter λ_c for the First Four Modes.
$\xi = 0.05$

β	Mode #1	Mode #2	Mode #3	Mode #4
0.2000	11.2841	18.8408	22.4591	37.7752
0.1000	13.4253	23.9331	27.3876	51.7686
0.0500	14.5991	26.5255	30.1413	59.6252
0.0250	15.3226	27.6687	31.2171	63.0569
0.0200	15.4651	27.8596	31.3710	63.6266
0.0125	15.6493	28.0951	31.5507	64.3275
0.0100	15.6976	28.1554	31.5956	64.5056
0.0050	15.7662	28.2405	31.6600	64.7550
0.0025	15.7842	28.2630	31.6778	64.8198
0.0010	15.7893	28.2694	31.6830	64.8381
0.0005	15.7900	28.2703	31.6838	64.8407

TABLE A.3.36

The Frequency Parameter λ_c for the First Four Modes.

$\xi = 0.10$

β	Mode #1	Mode #2	Mode #3	Mode #4
0.2000	14.9734	23.8567	26.8215	46.8794
0.1000	18.3410	30.9465	34.0218	66.2904
0.0500	20.2747	34.4960	37.7568	77.9649
0.0250	21.2316	35.8467	39.1123	82.7667
0.0200	21.3951	36.0476	39.3026	83.4953
0.0125	21.6037	36.2883	39.5214	84.3738
0.0100	21.6597	36.3494	39.5744	84.5980
0.0050	21.7422	36.4363	39.6471	84.9182
0.0025	21.7648	36.4593	39.6658	85.0034
0.0010	21.7713	36.4659	39.6710	85.0277
0.0005	21.7722	36.4668	39.6718	85.0312

TABLE A.3.37

The Frequency Parameter λ_c for the First Four Modes.

$\xi = 0.15$

β	Mode #1	Mode #2	Mode #3	Mode #4
0.2000	19.5483	29.8829	32.4588	57.8018
0.1000	24.7939	39.9307	42.7696	84.9415
0.0500	27.8081	45.0460	48.1201	102.755
0.0250	29.1429	46.8906	50.0000	110.239
0.0200	29.3619	47.1562	50.2541	111.377
0.0125	29.6448	47.4760	50.5396	112.768
0.0100	29.7238	47.5595	50.6073	113.134
0.0050	29.8475	47.6841	50.6998	113.682
0.0025	29.8841	47.7195	50.7241	113.837
0.0010	29.8950	47.7300	50.7313	113.882
0.0005	29.8966	47.7315	50.7324	113.888

APPENDIX A.4

FREQUENCY RESPONSE

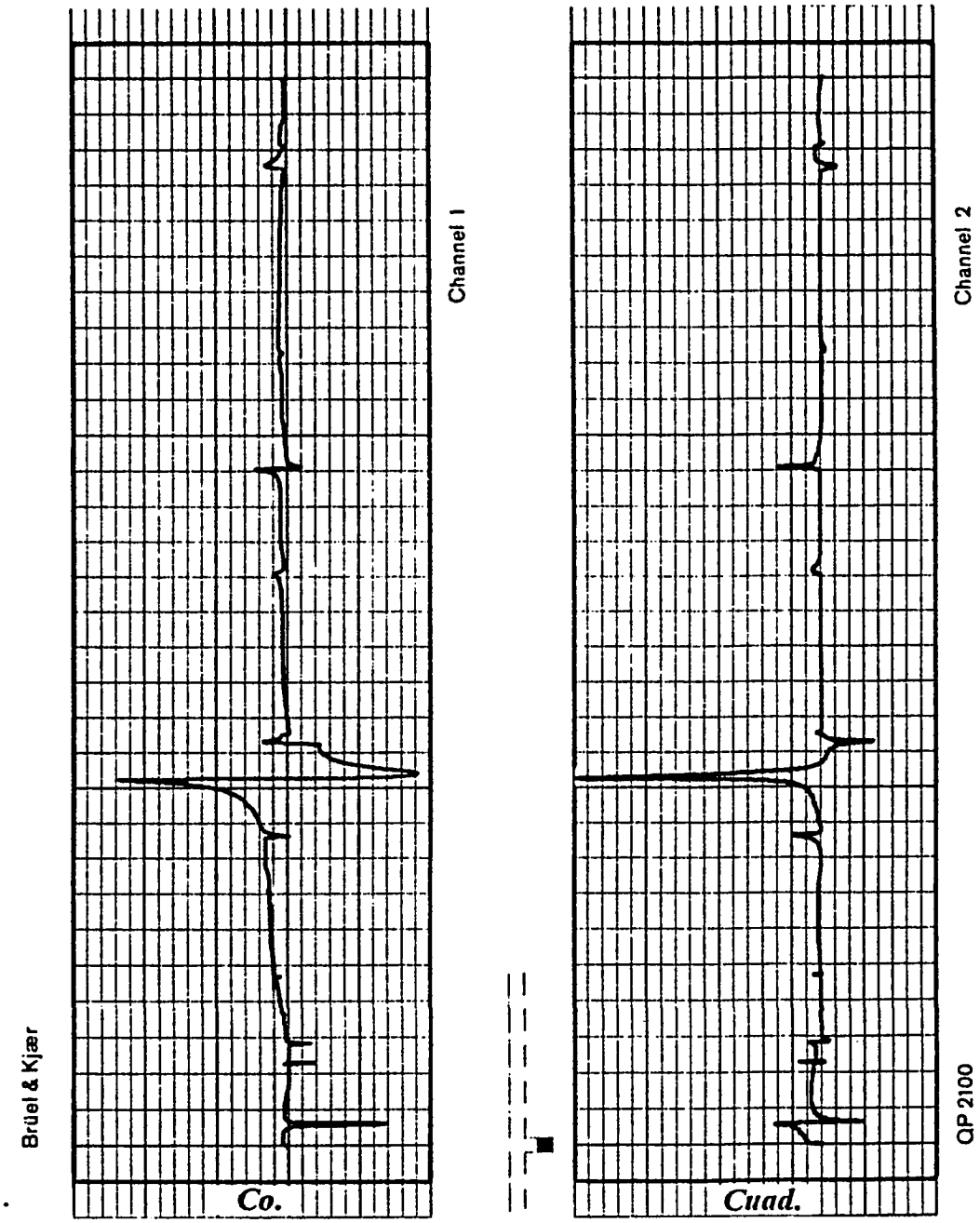

Figure A.4.1 Overall frequency response.
$\alpha = 0.0$, $\beta = 0.01$

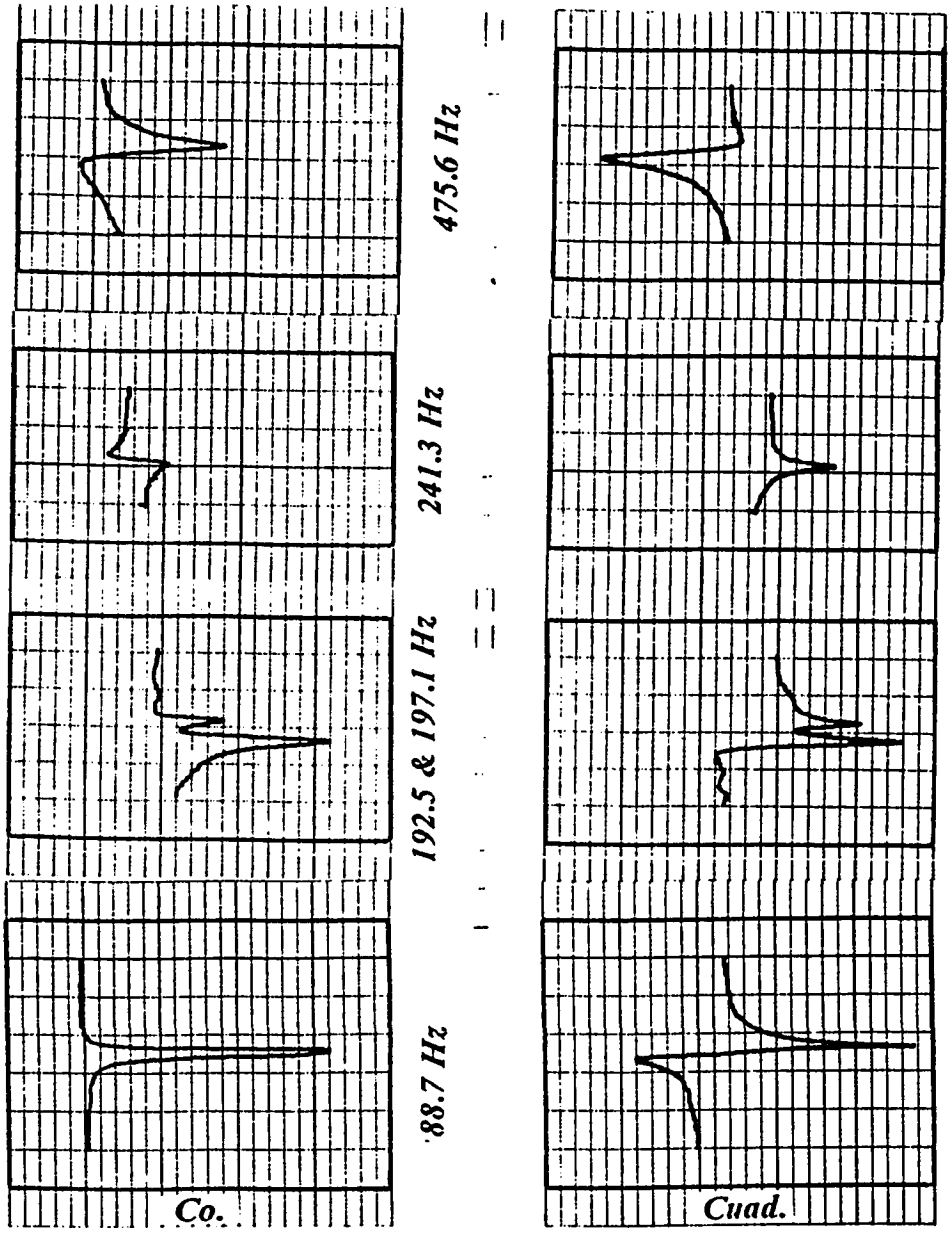

Figure A.4.2 Slow sweep of the 1st , 2nd , 3rd and 4th modes.
$\alpha = 0.0$, $\beta = 0.01$

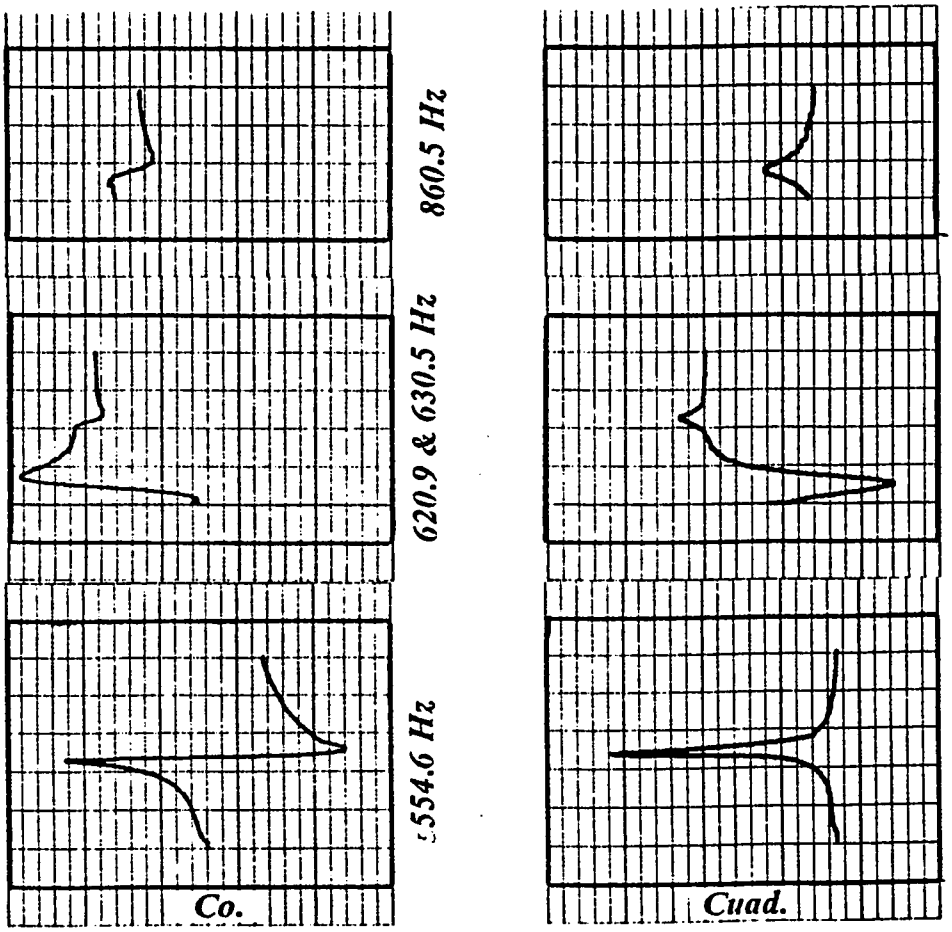

Figure A.4.3 Slow sweep of the 5th , 6th and 7th modes.
$\alpha = 0.0$, $\beta = 0.01$

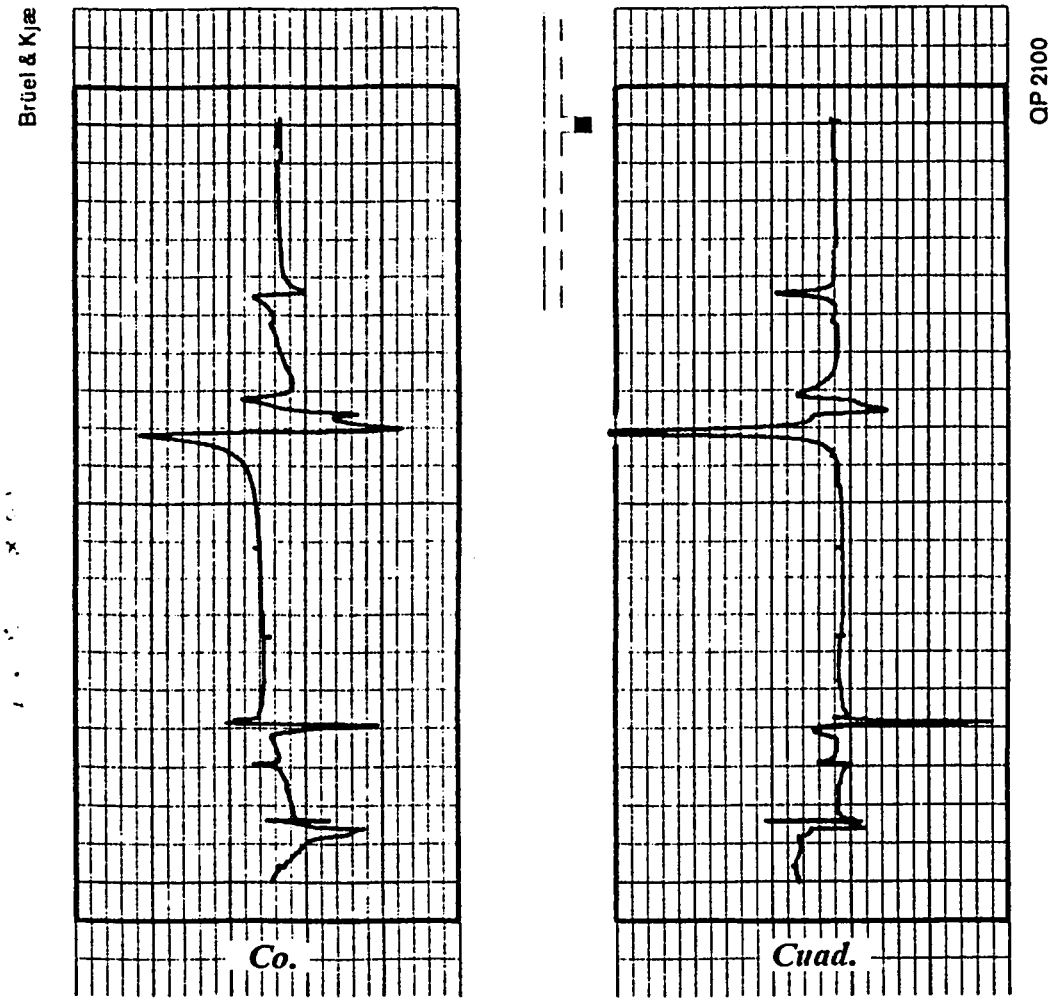

Figure A.4.4 Overall frequency response.
$\alpha = 0.1$, $\beta = 0.01$

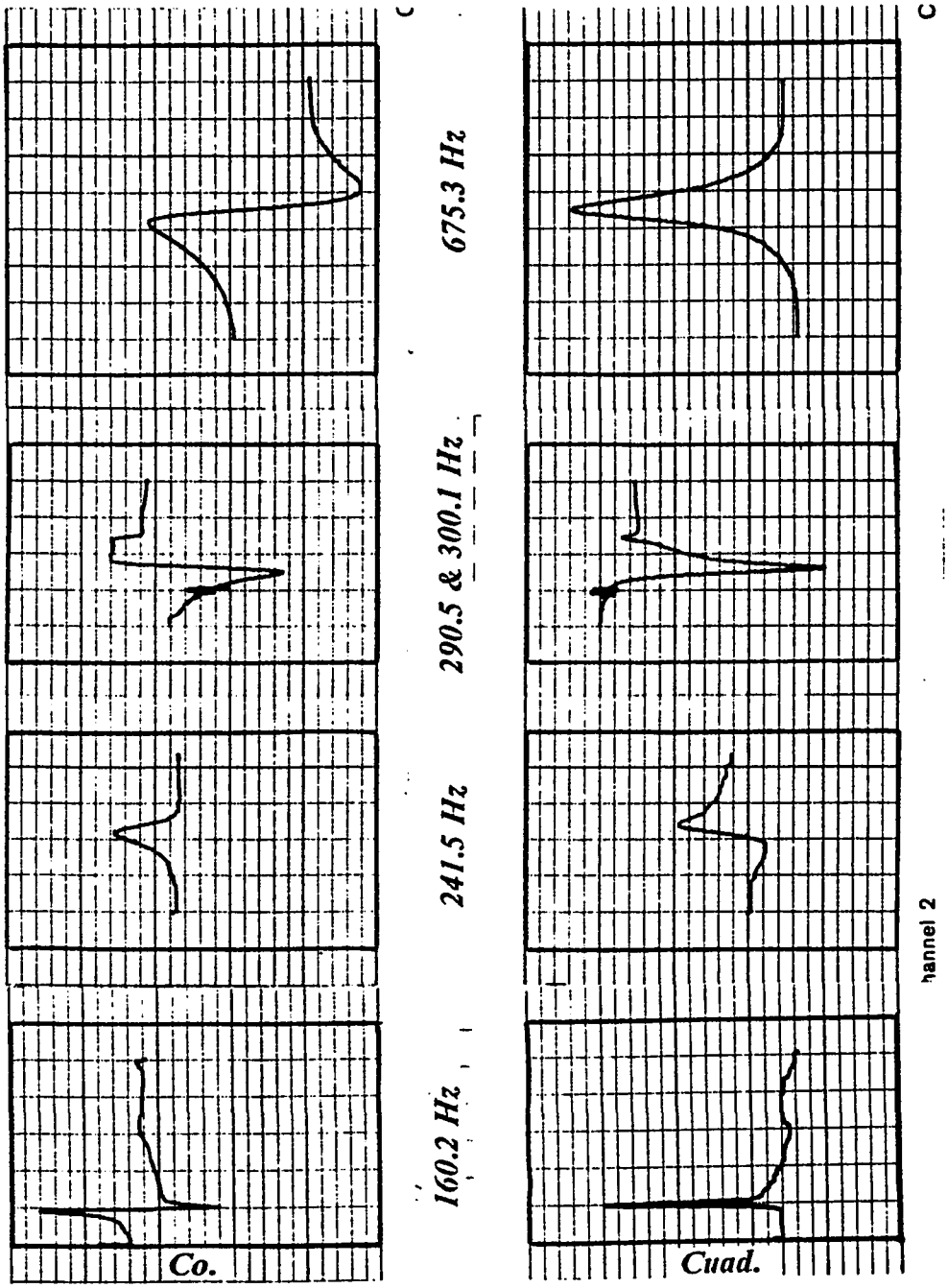

Figure A.4.5 Slow sweep of the 1st , 2nd , 3rd and 4th modes.
$\alpha = 0.1$, $\beta = 0.01$

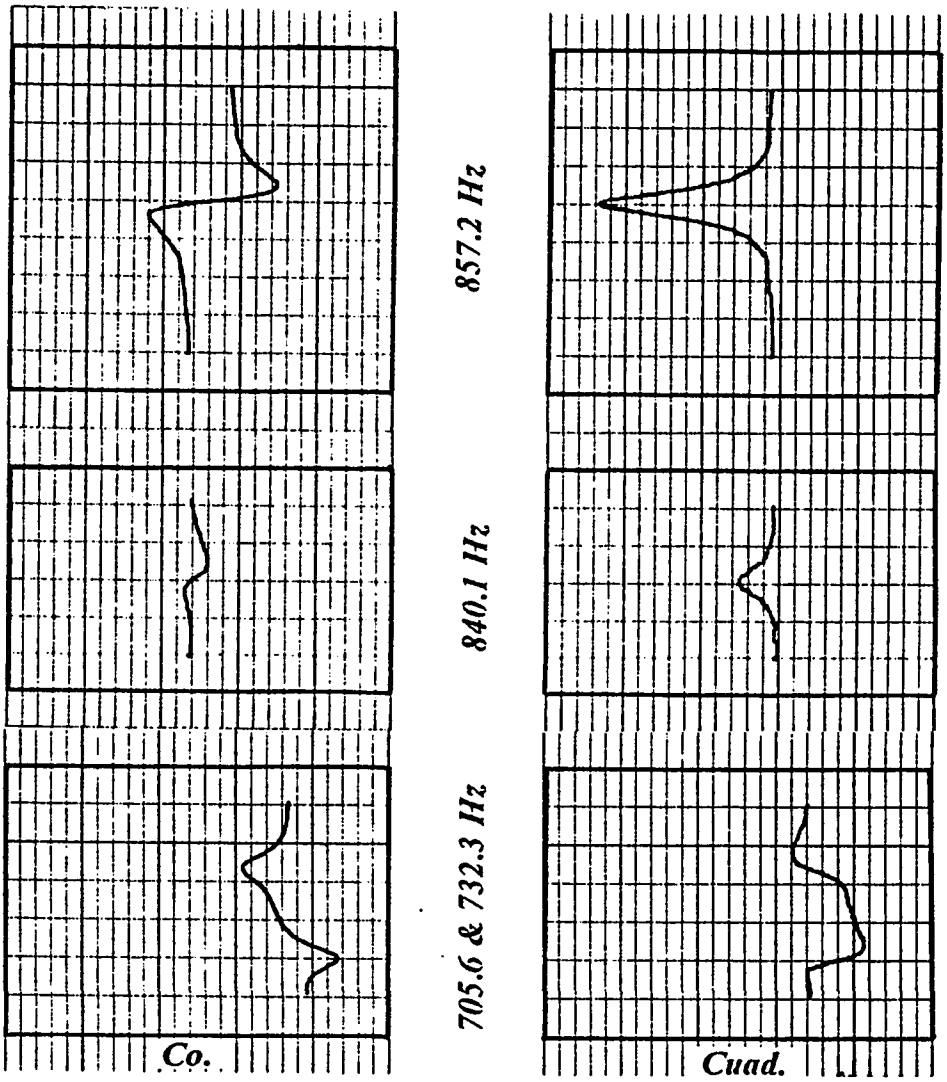

Figure A.4.6 Slow sweep of the 5th , 6th and 7th modes.
$\alpha = 0.1$, $\beta = 0.01$

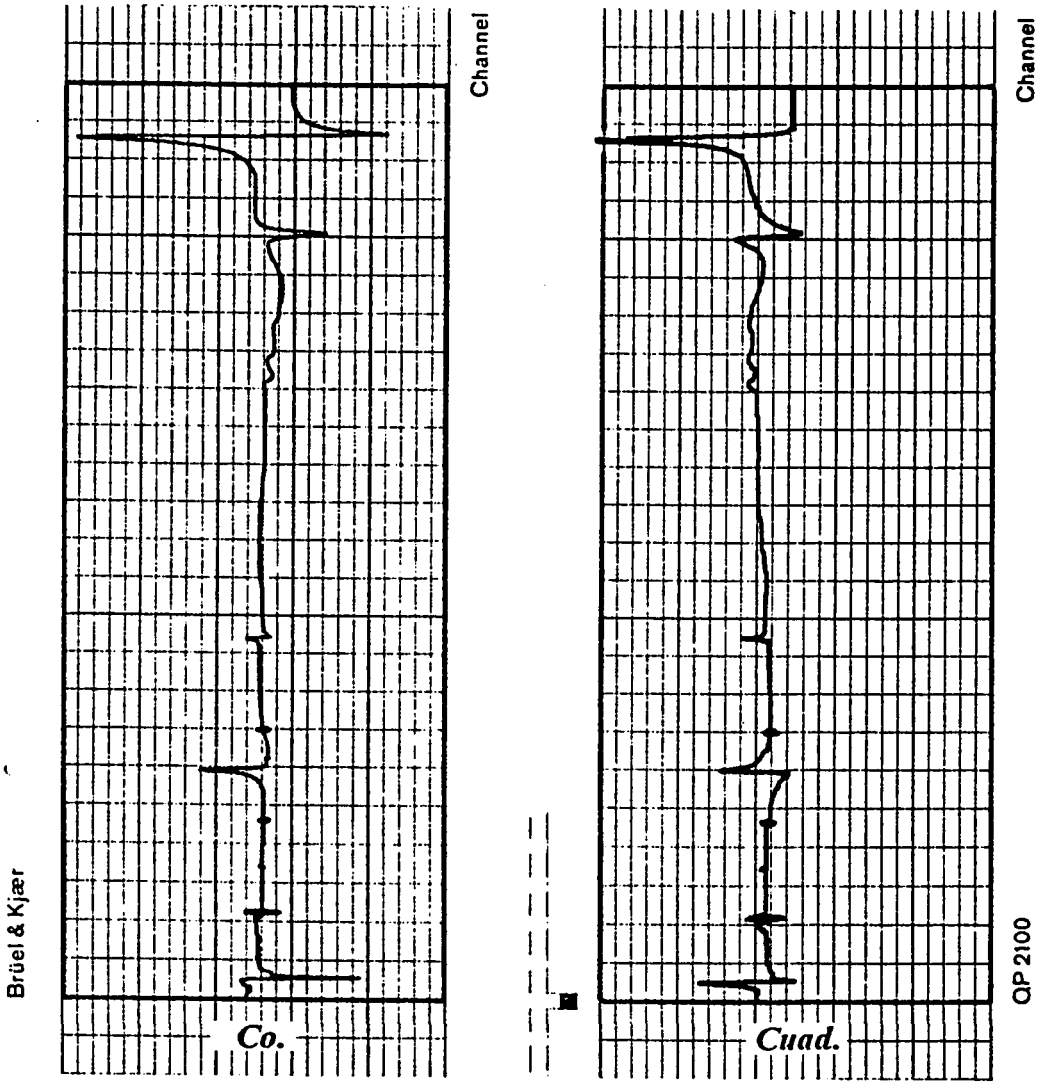

Figure A.4.7 Overall frequency response.
$\alpha = 0.0$, $\beta = 0.025$

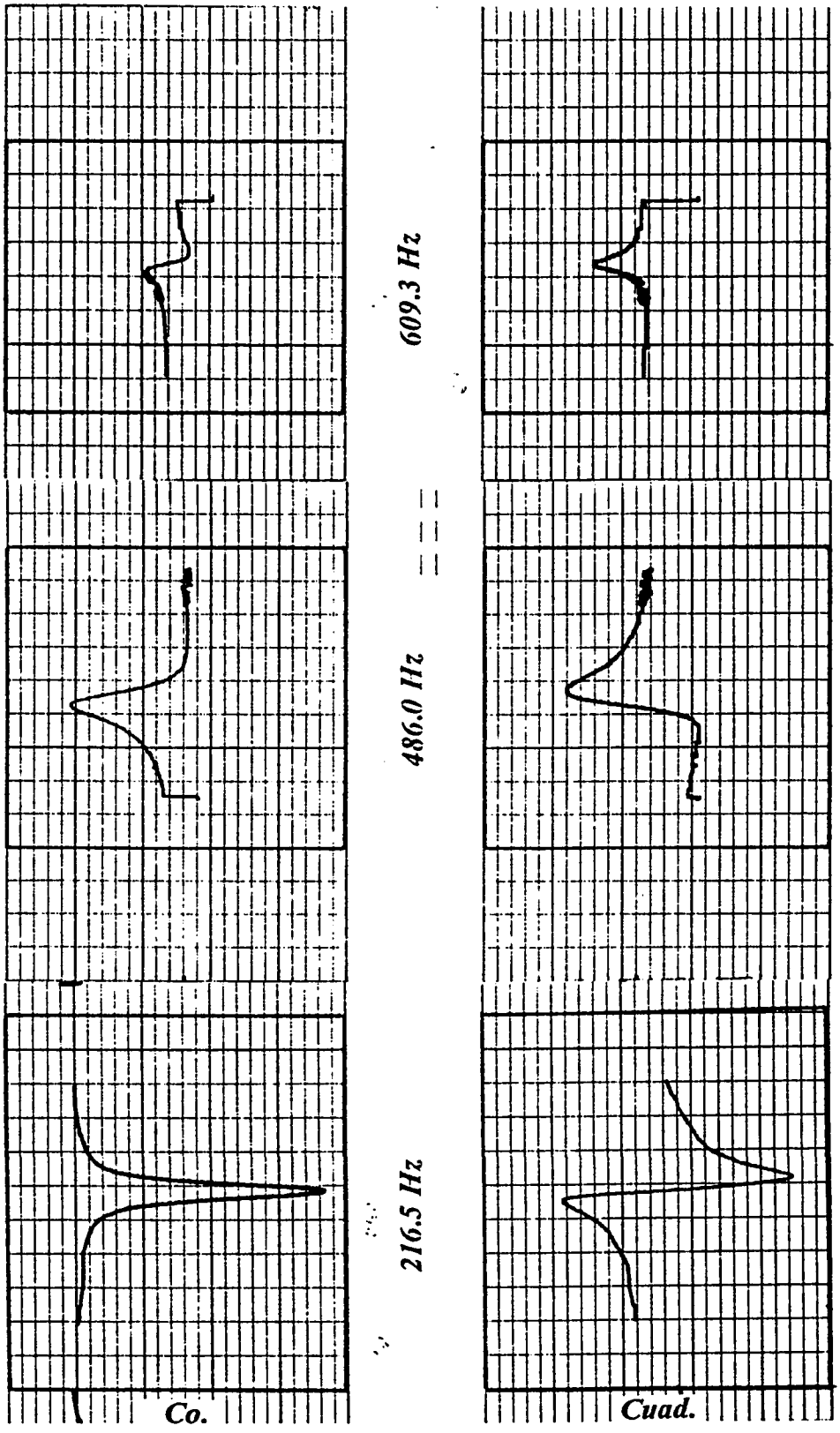

Figure A.4.8 Slow sweep of the 1st , 2nd and 3rd modes.
$\alpha = 0.0$, $\beta = 0.025$

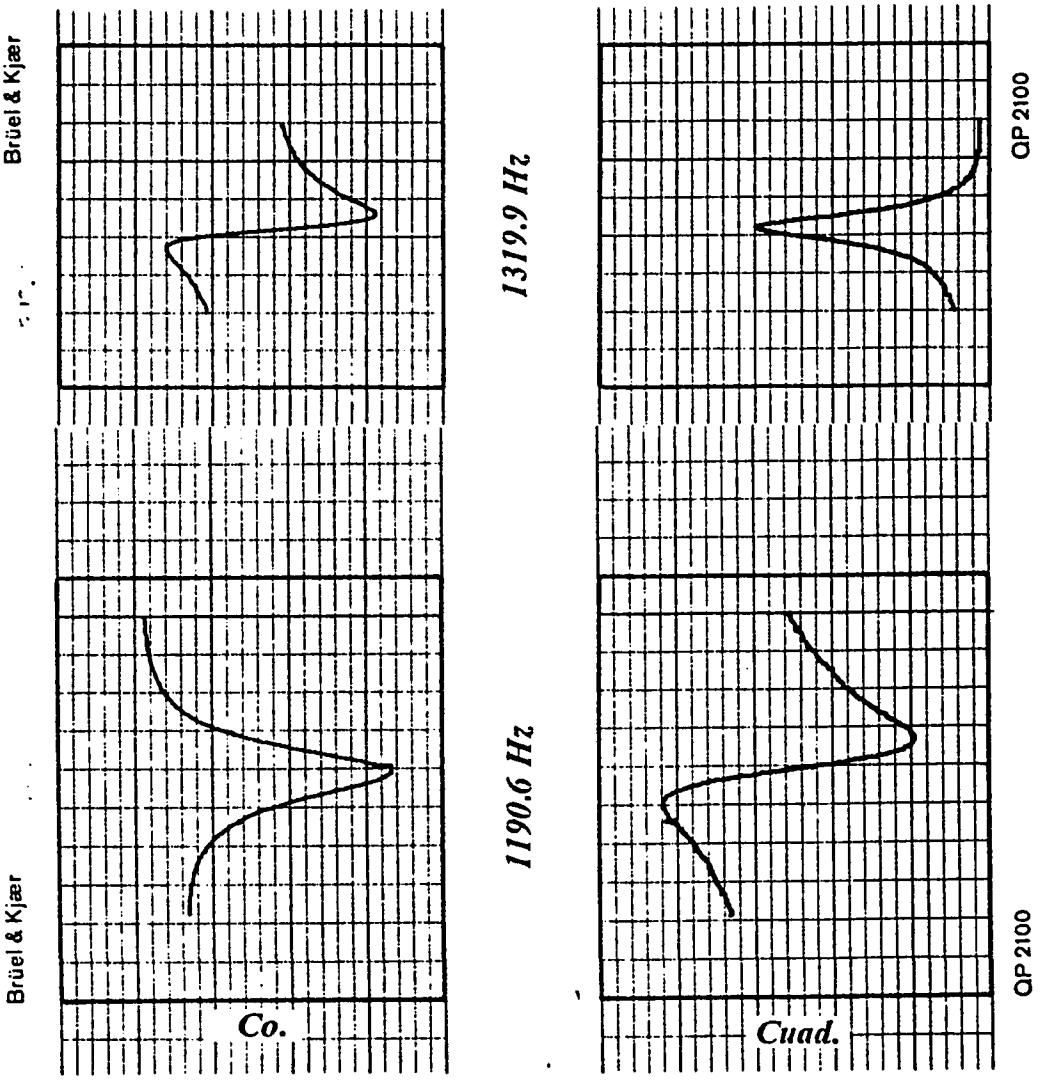

Figure A.4.9 Slow sweep of the 4th and 5th modes.
$\alpha = 0.0$, $\beta = 0.025$

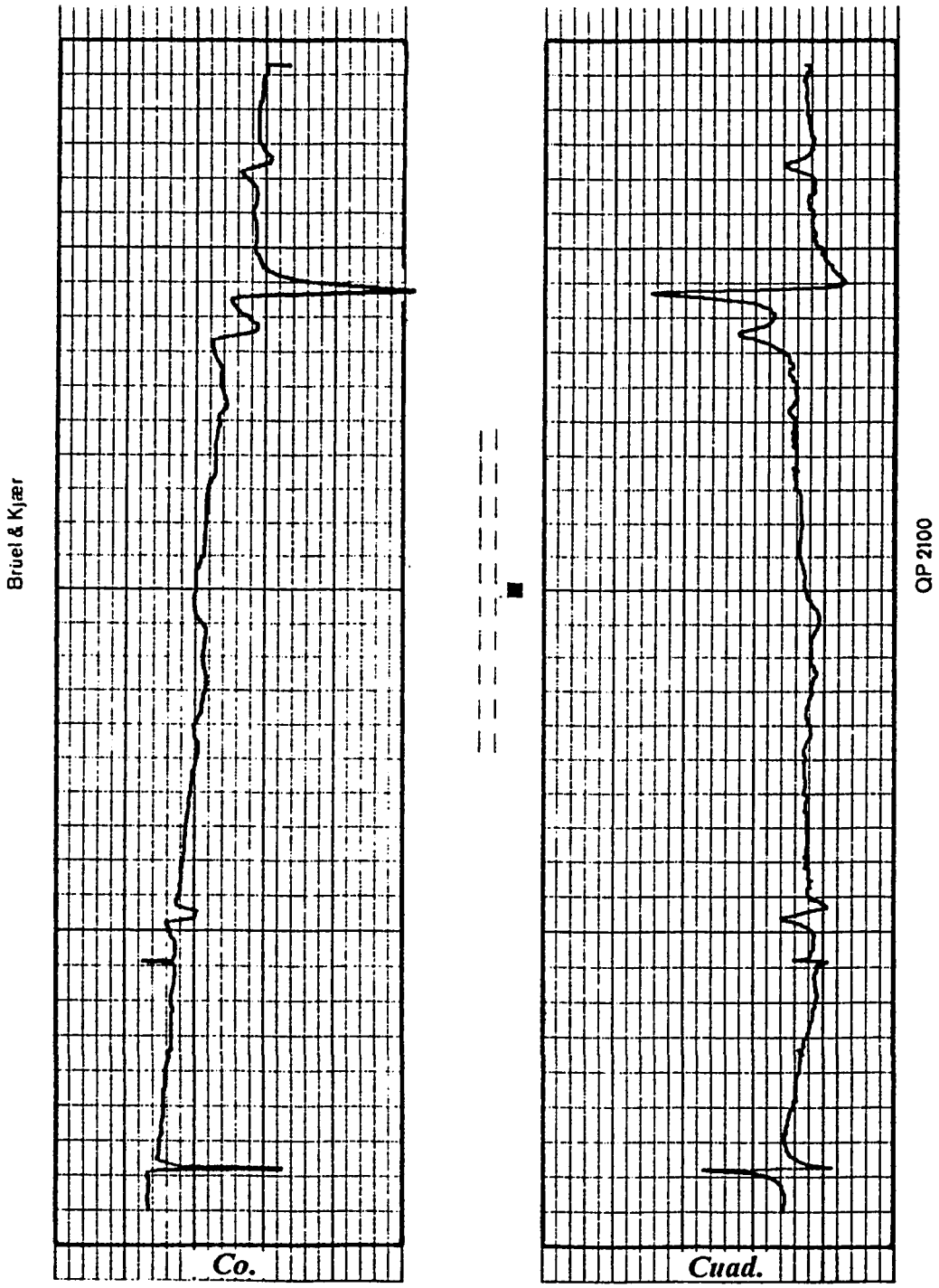

Figure A.4.10 Overall frequency response.
$\alpha = 0.1$, $\beta = 0.025$

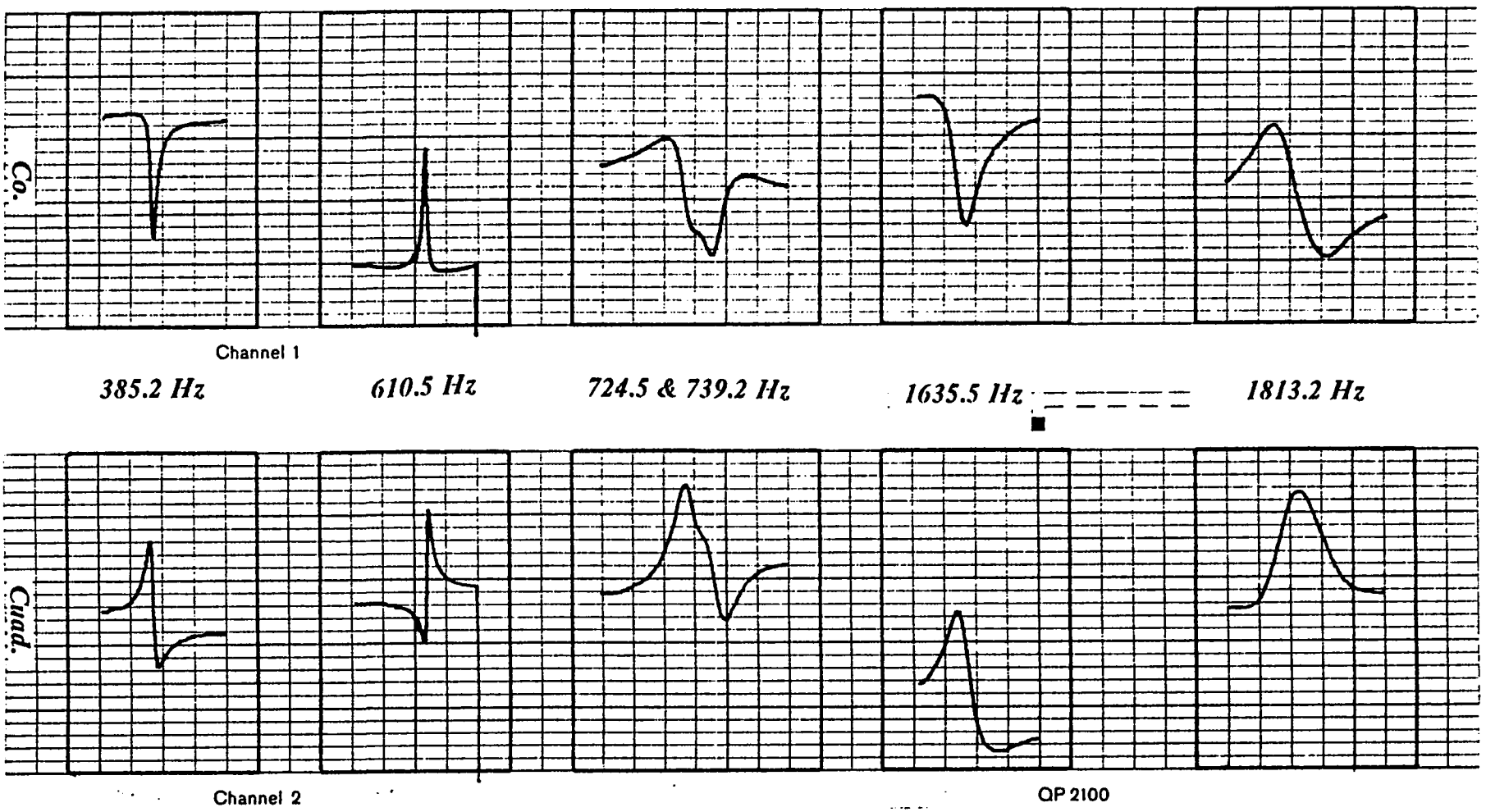

Figure A.4.11 Slow sweep of the frequency responce.
$\alpha = 0.1$, $\beta = 0.025$

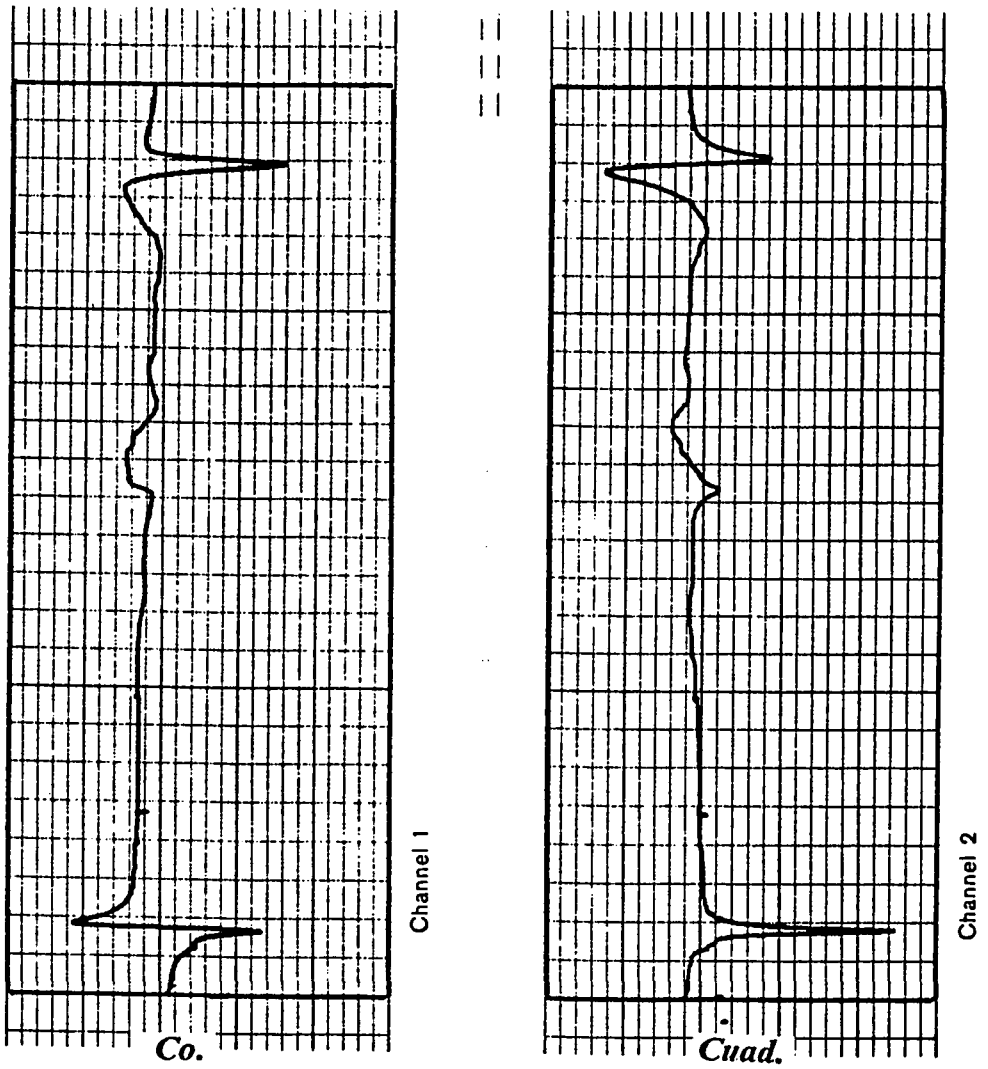

Figure A.4.12 Overall frequency response.
$\alpha = 0.0$, $\beta = 0.05$

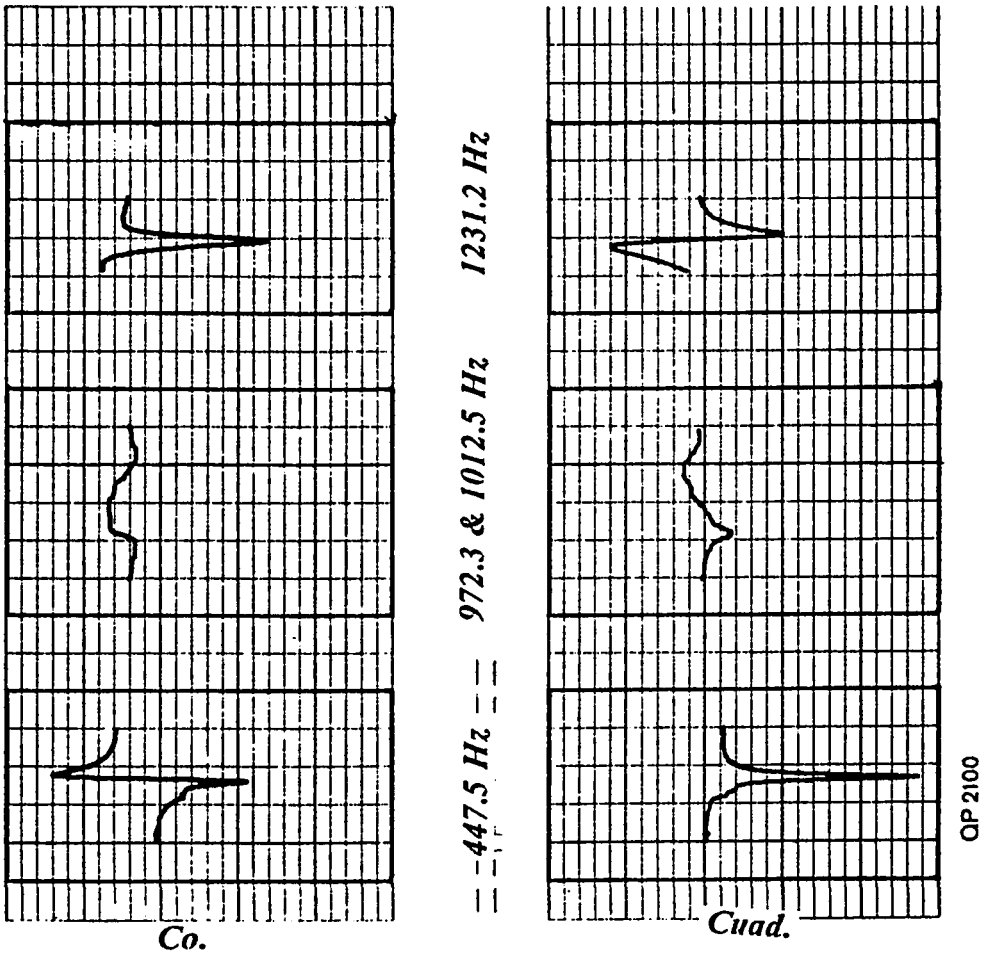

Figure A.4.13 Slow sweep of the frequency responce.
$\alpha = 0.0$, $\beta = 0.05$

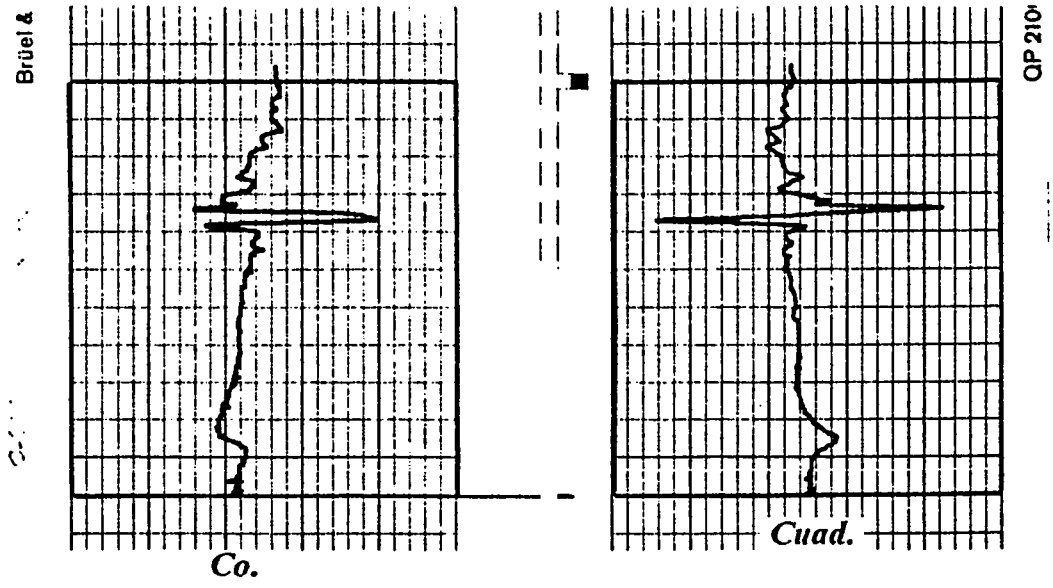

Figure A.4.14 Overall frequency response.
$\alpha = 0.1$, $\beta = 0.05$

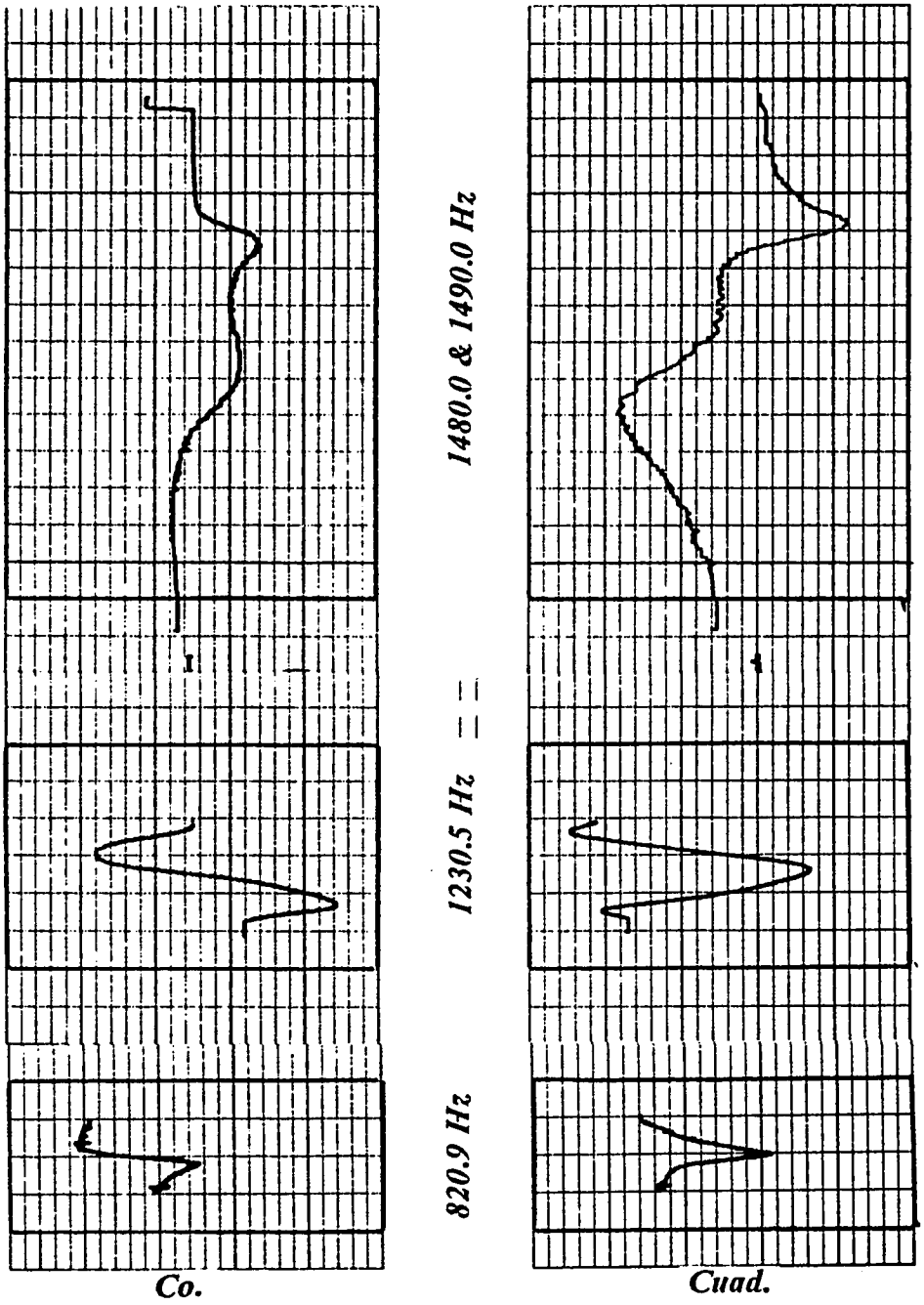

Figure A.4.15 Slow sweep of the frequency responce.
$\alpha = 0.1$, $\beta = 0.05$

APPENDIX A.5

NYQUIST PLOTS

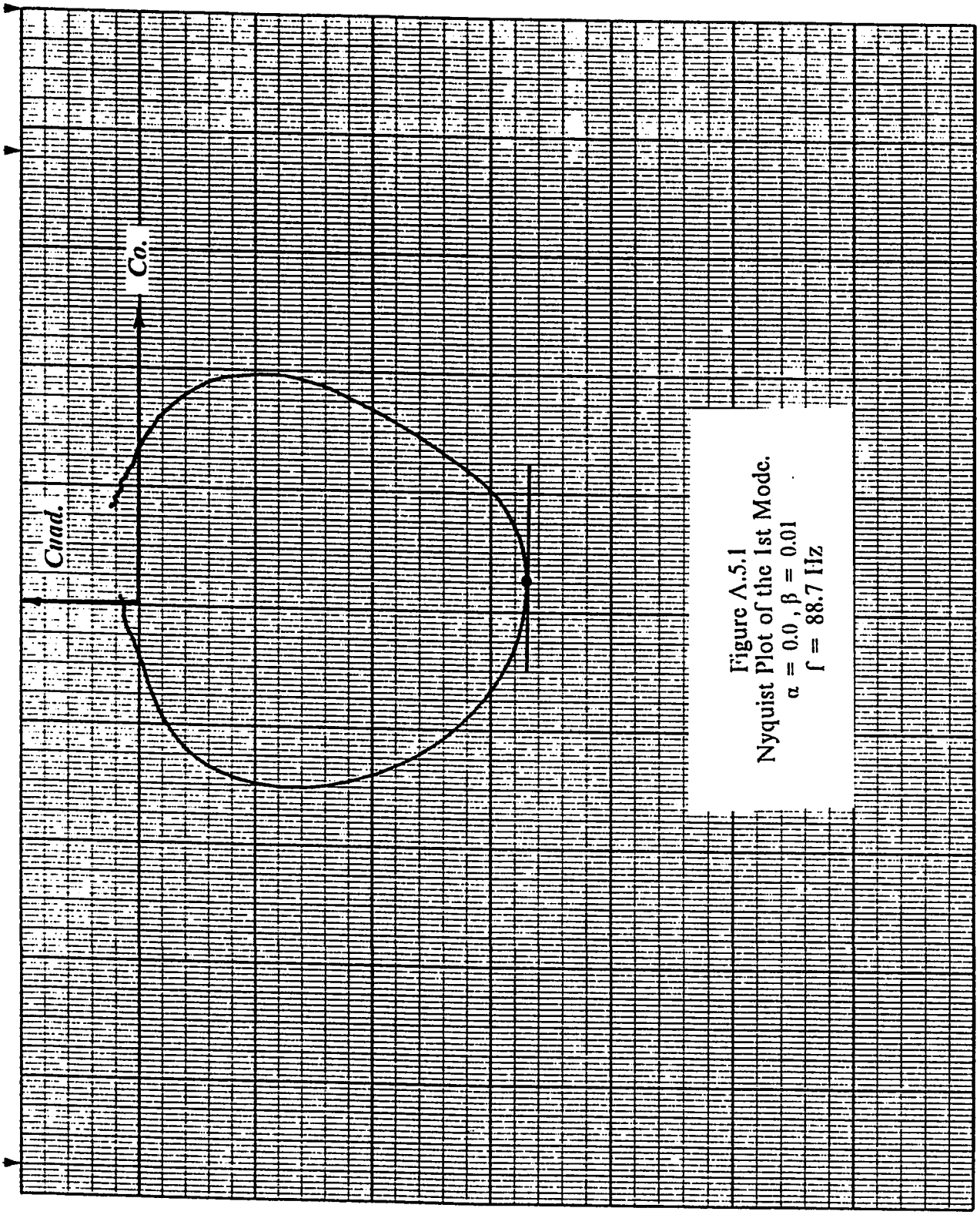

Figure A.5.1
Nyquist Plot of the 1st Mode.
$\alpha = 0.0$, $\beta = 0.01$
$\Gamma = 88.7$ Hz

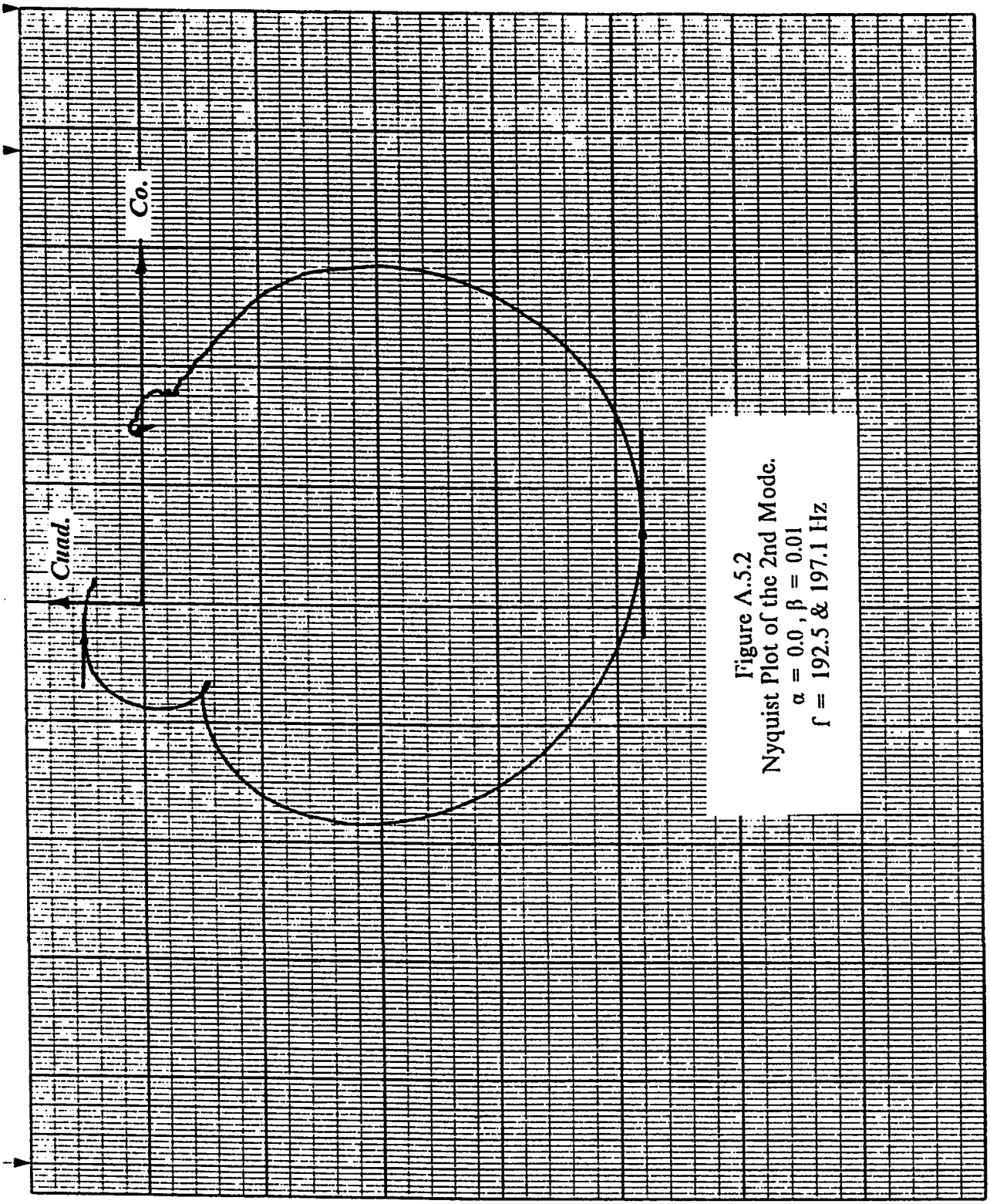

Figure A.5.2
Nyquist Plot of the 2nd Mode.
$\alpha = 0.0$, $\beta = 0.01$
$f = 192.5$ & 197.1 Hz

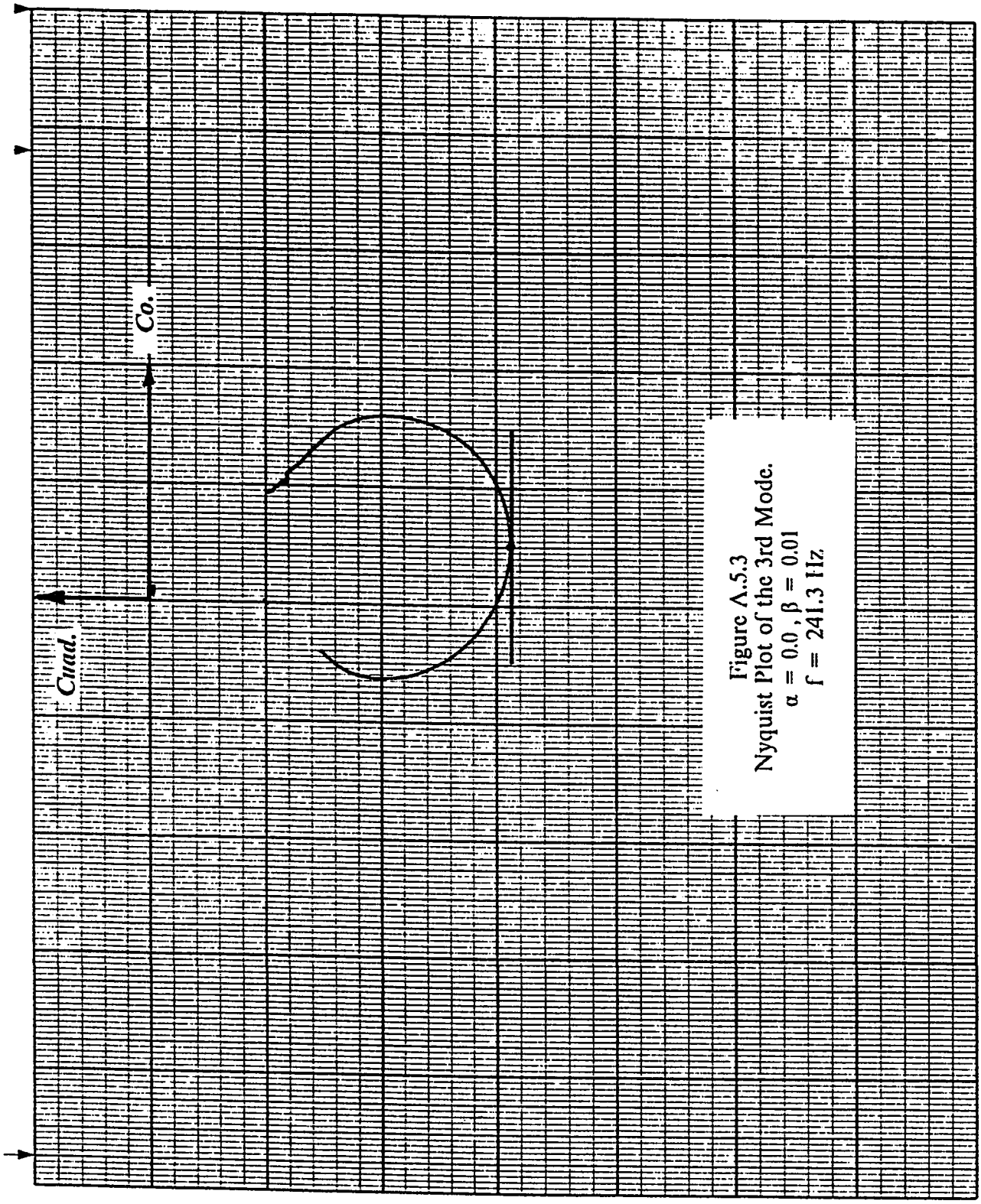

Figure A.5.3
Nyquist Plot of the 3rd Mode.
$\alpha = 0.0$, $\beta = 0.01$
$f = 241.3$ Hz

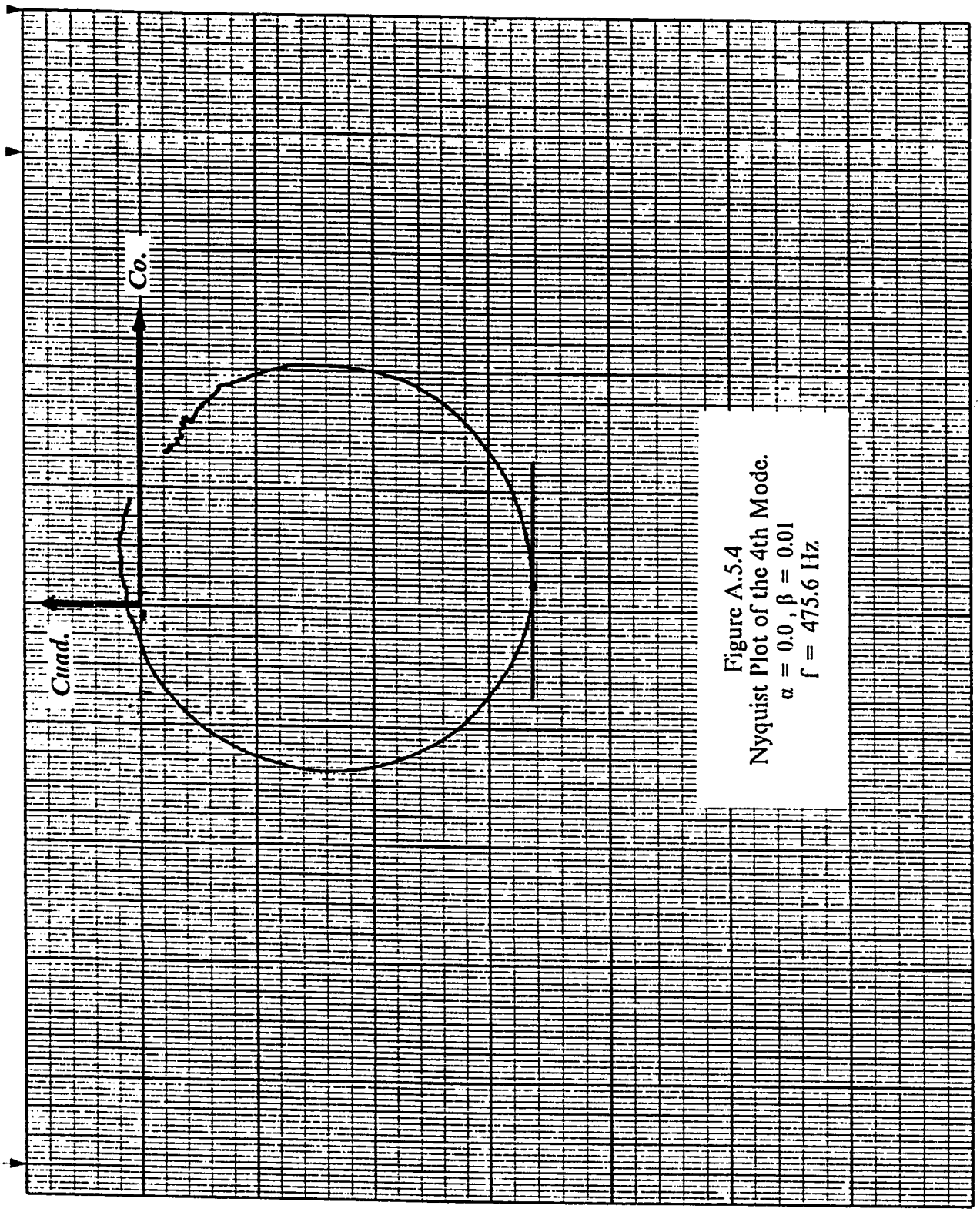

Figure A.5.4
Nyquist Plot of the 4th Mode.
$\alpha = 0.0$, $\beta = 0.01$
$f = 475.6$ Hz

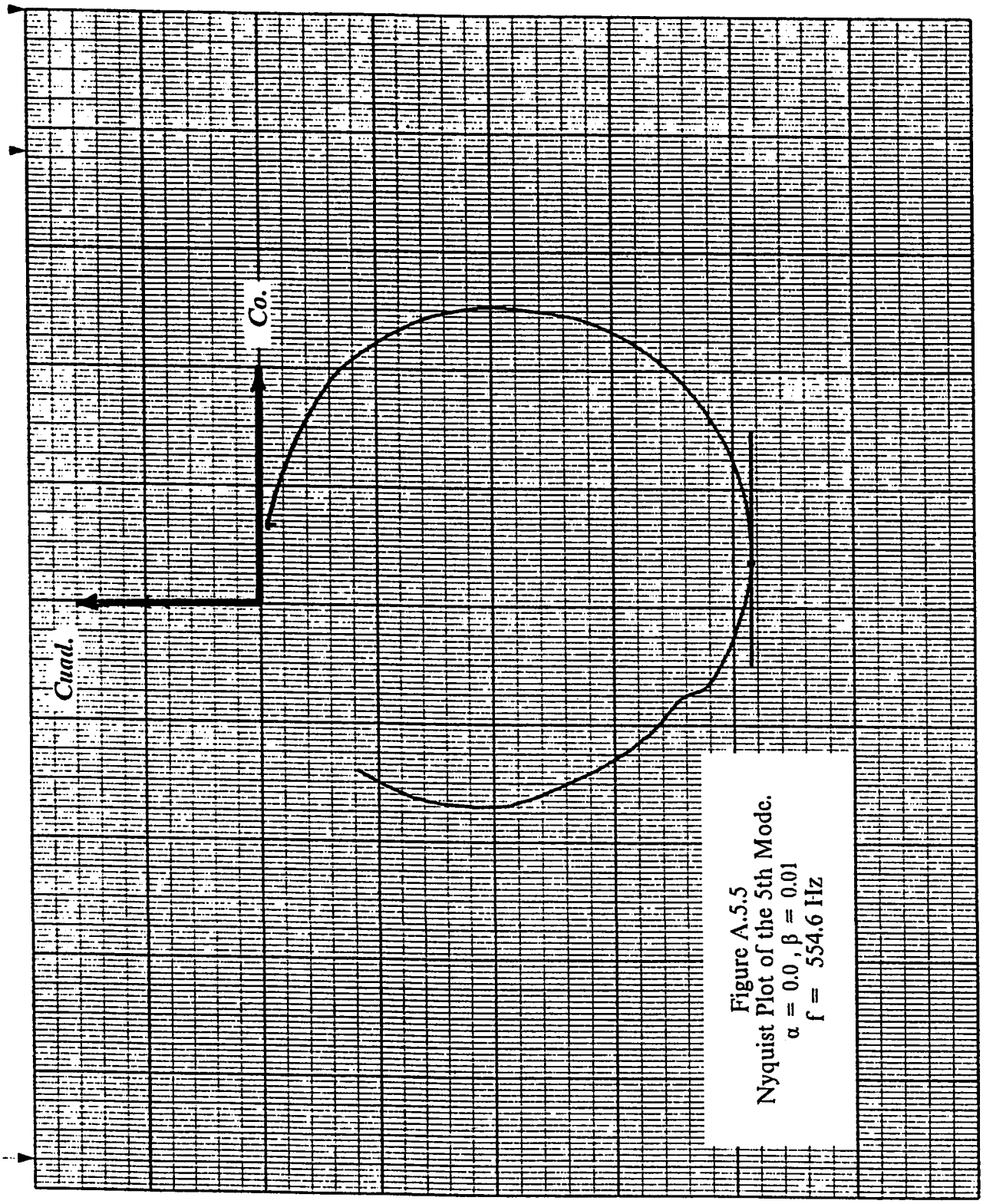

Figure A.5.5
Nyquist Plot of the 5th Mode.
$\alpha = 0.0$, $\beta = 0.01$
$f = 554.6$ Hz

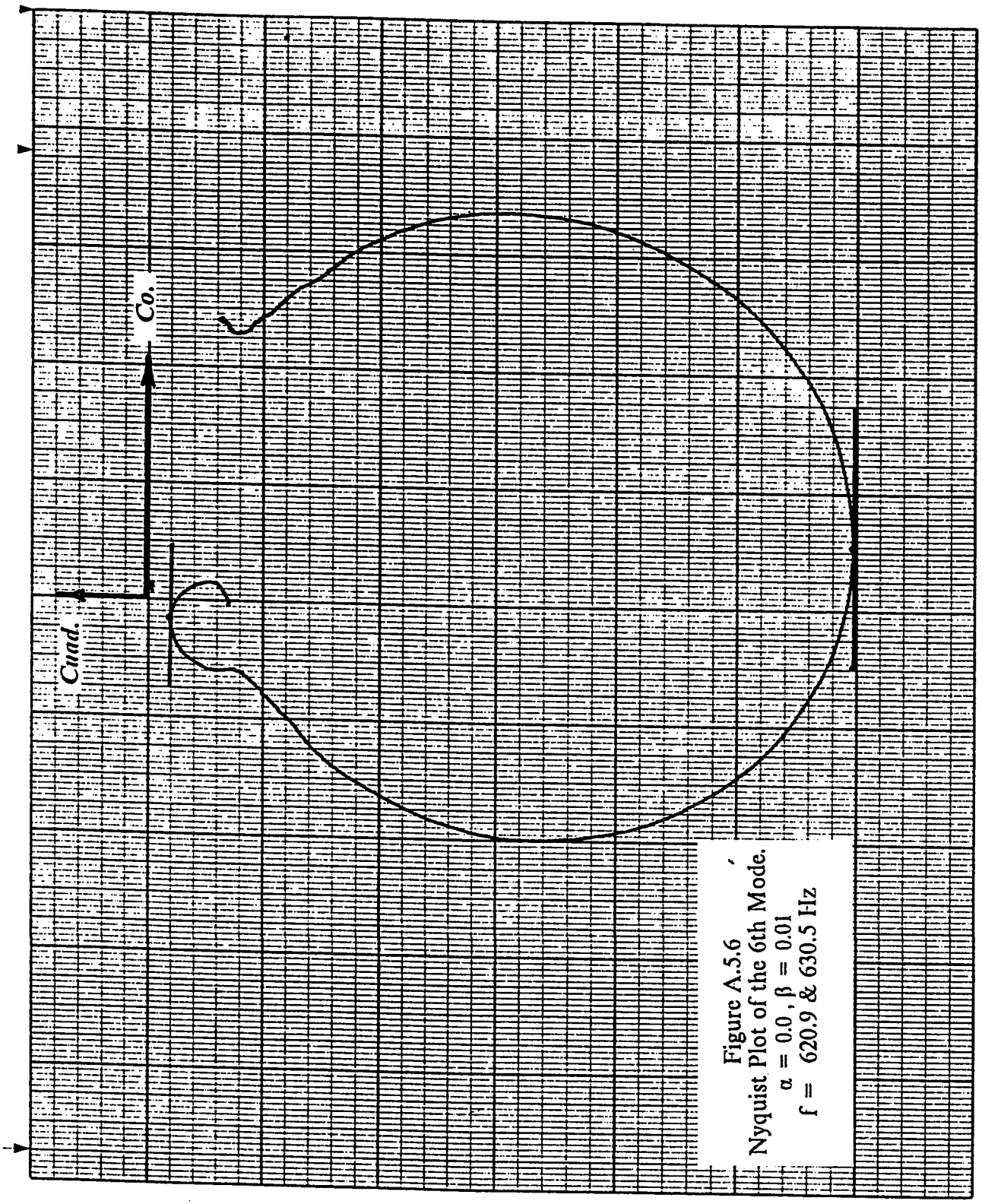

Figure A.5.6
Nyquist Plot of the 6th Mode.
$\alpha = 0.0$, $\beta = 0.01$
$f = 620.9$ & 630.5 Hz

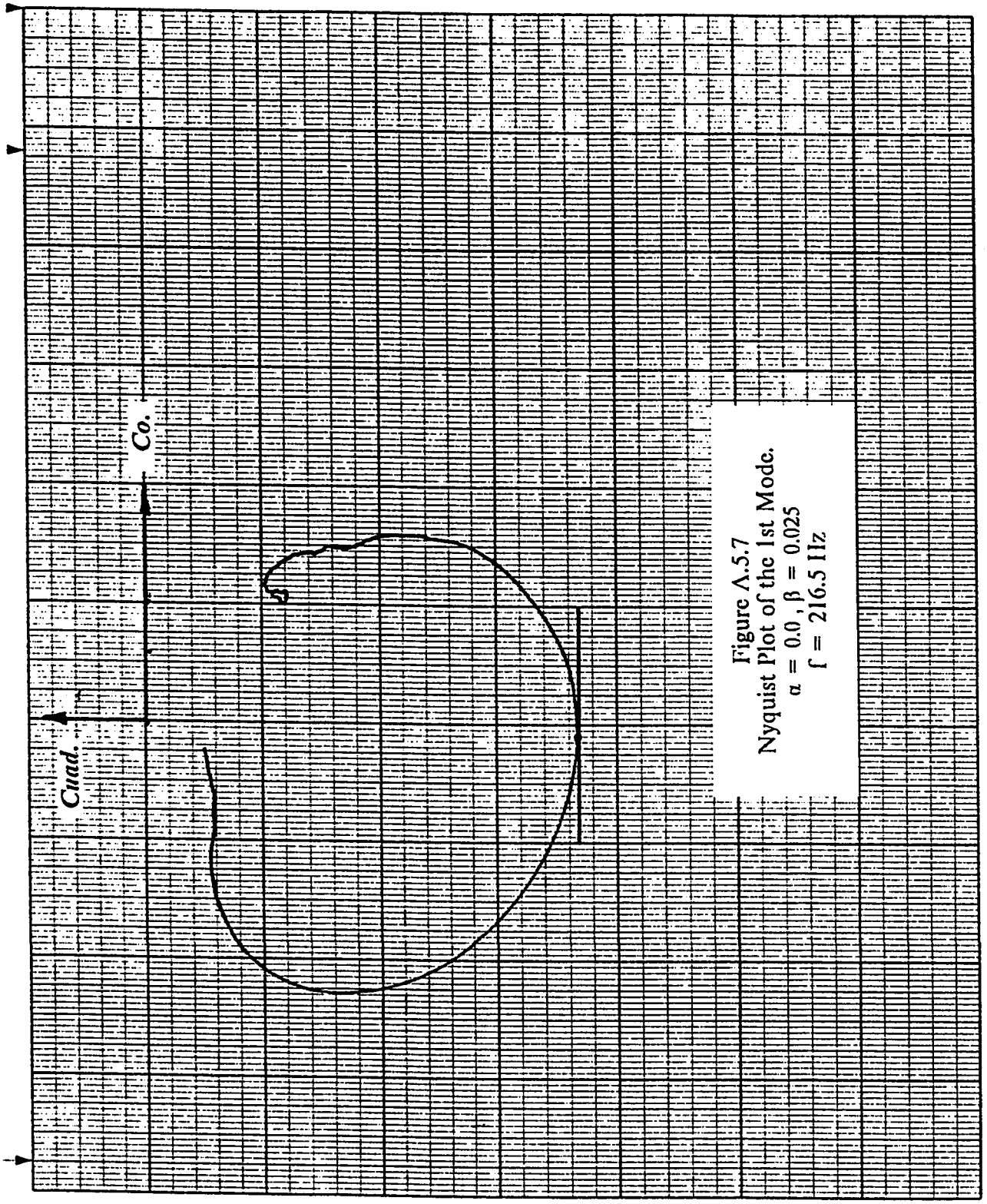

Figure A.5.7
Nyquist Plot of the 1st Mode.
$\alpha = 0.0$, $\beta = 0.025$
$f = 216.5$ Hz

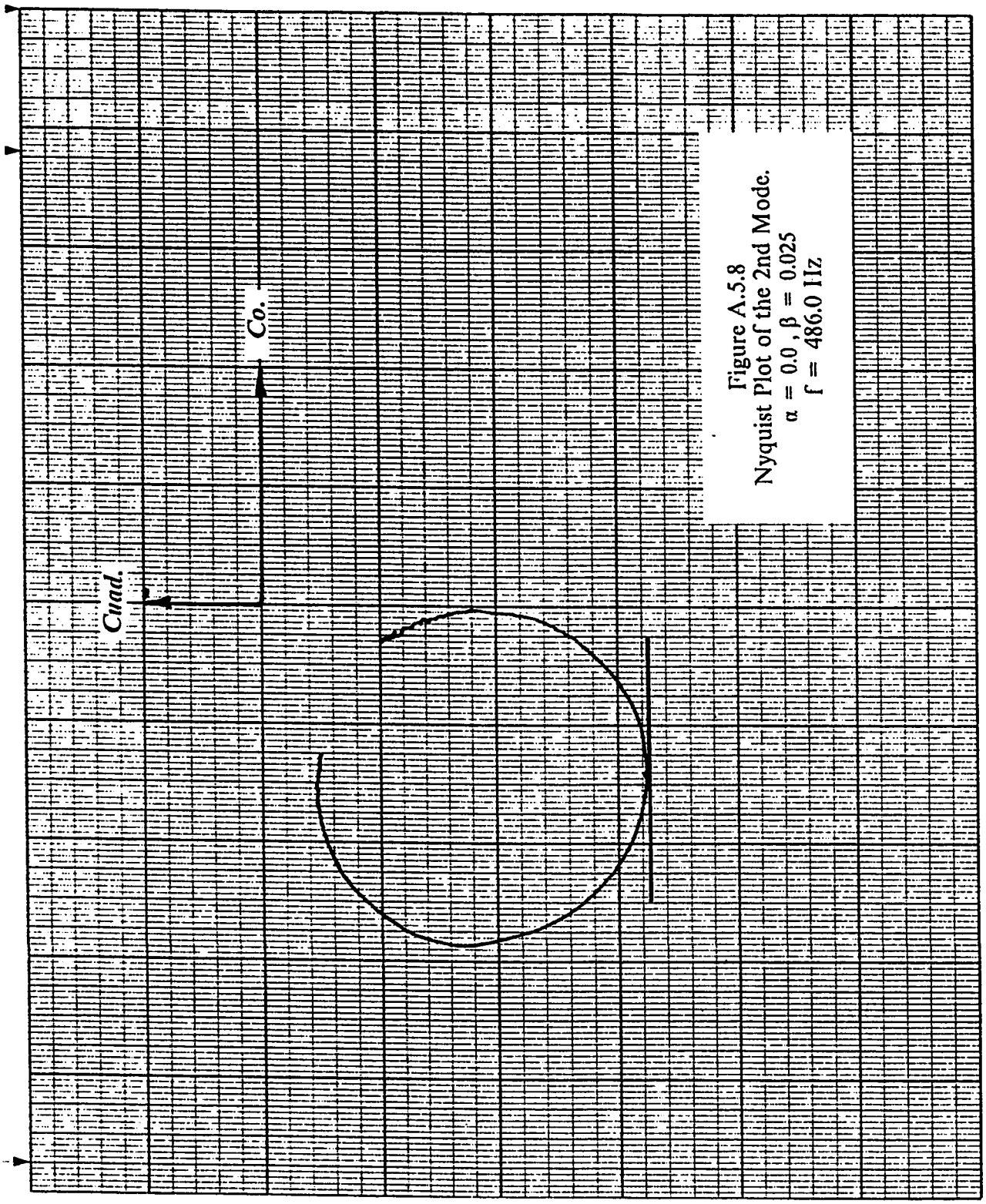

Figure A.5.8
Nyquist Plot of the 2nd Mode.
$\alpha = 0.0$, $\beta = 0.025$
$f = 486.0$ Hz

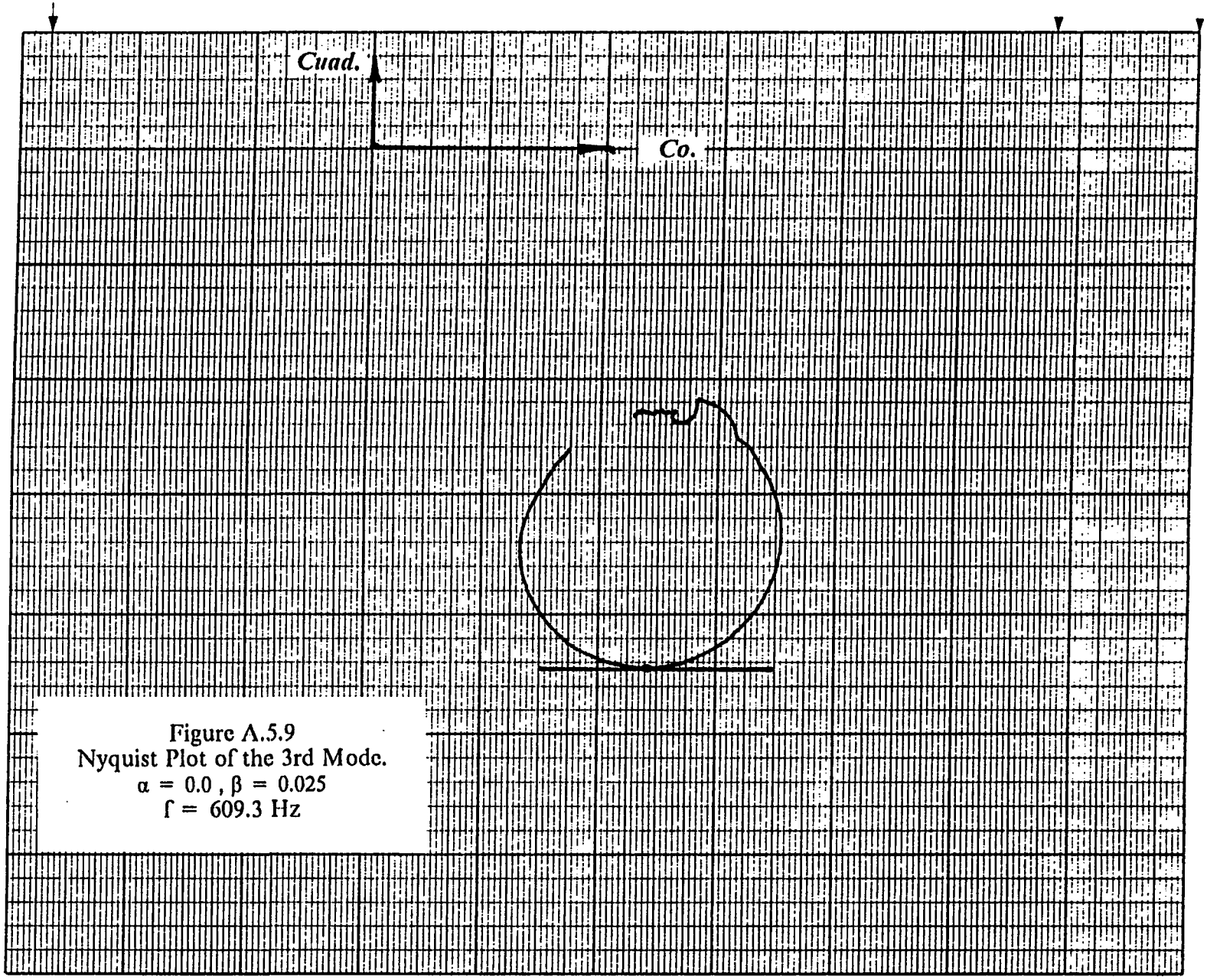

Figure A.5.9
Nyquist Plot of the 3rd Mode.
$\alpha = 0.0$, $\beta = 0.025$
$f = 609.3$ Hz

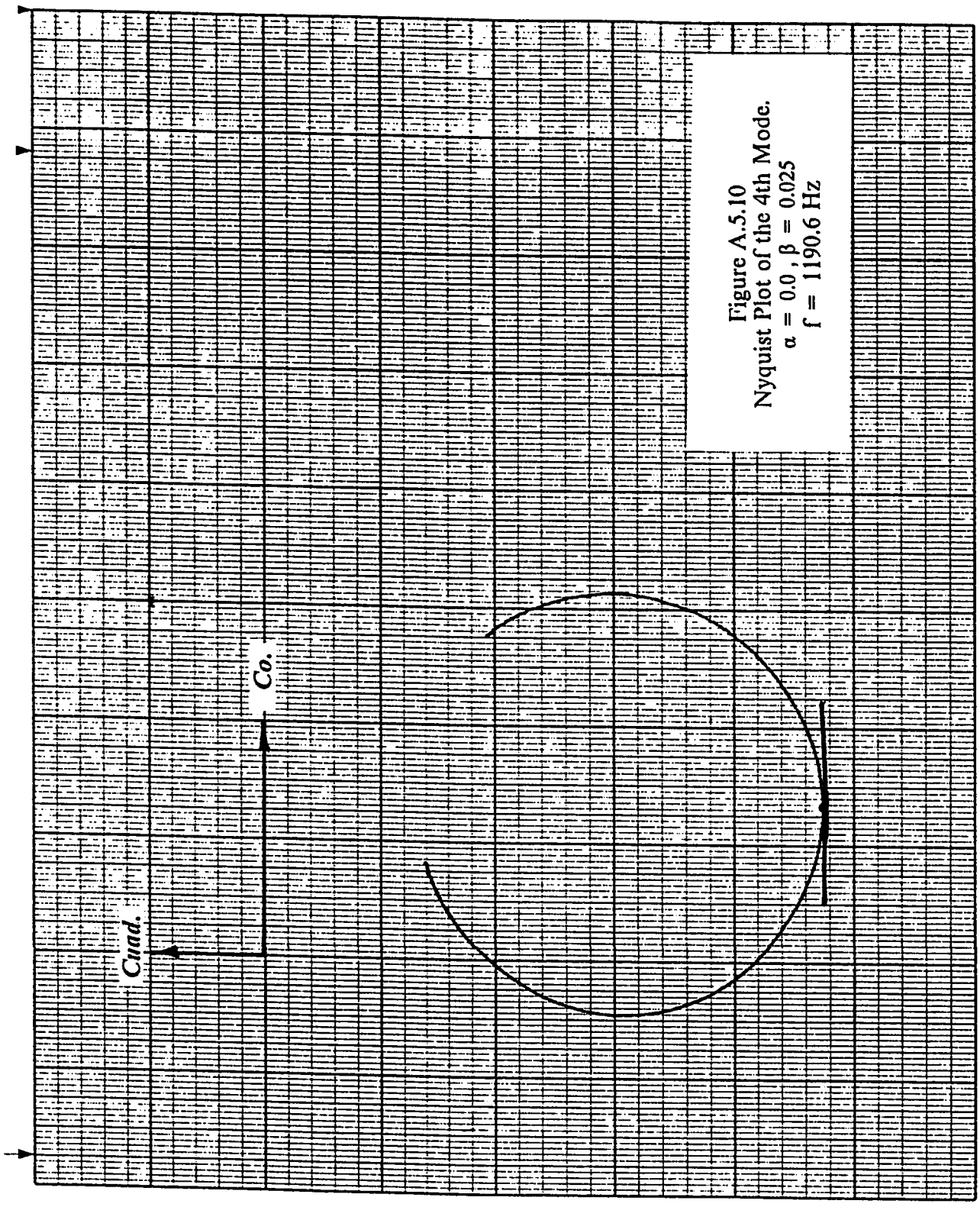

Figure A.5.10
Nyquist Plot of the 4th Mode.
$\alpha = 0.0$, $\beta = 0.025$
$f = 1190.6$ Hz

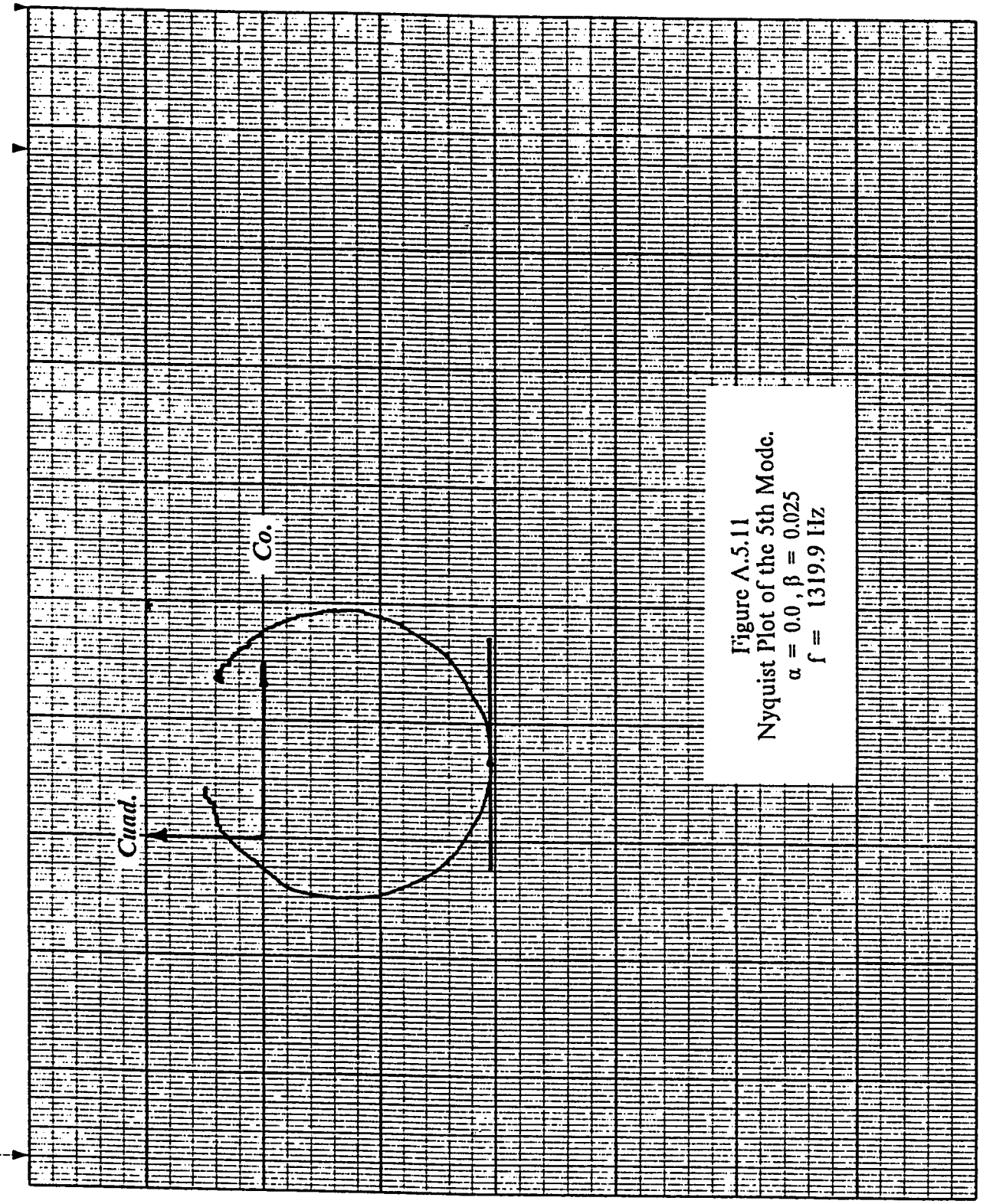

Figure A.5.11
Nyquist Plot of the 5th Mode.
$\alpha = 0.0$, $\beta = 0.025$
$f = 1319.9$ Hz

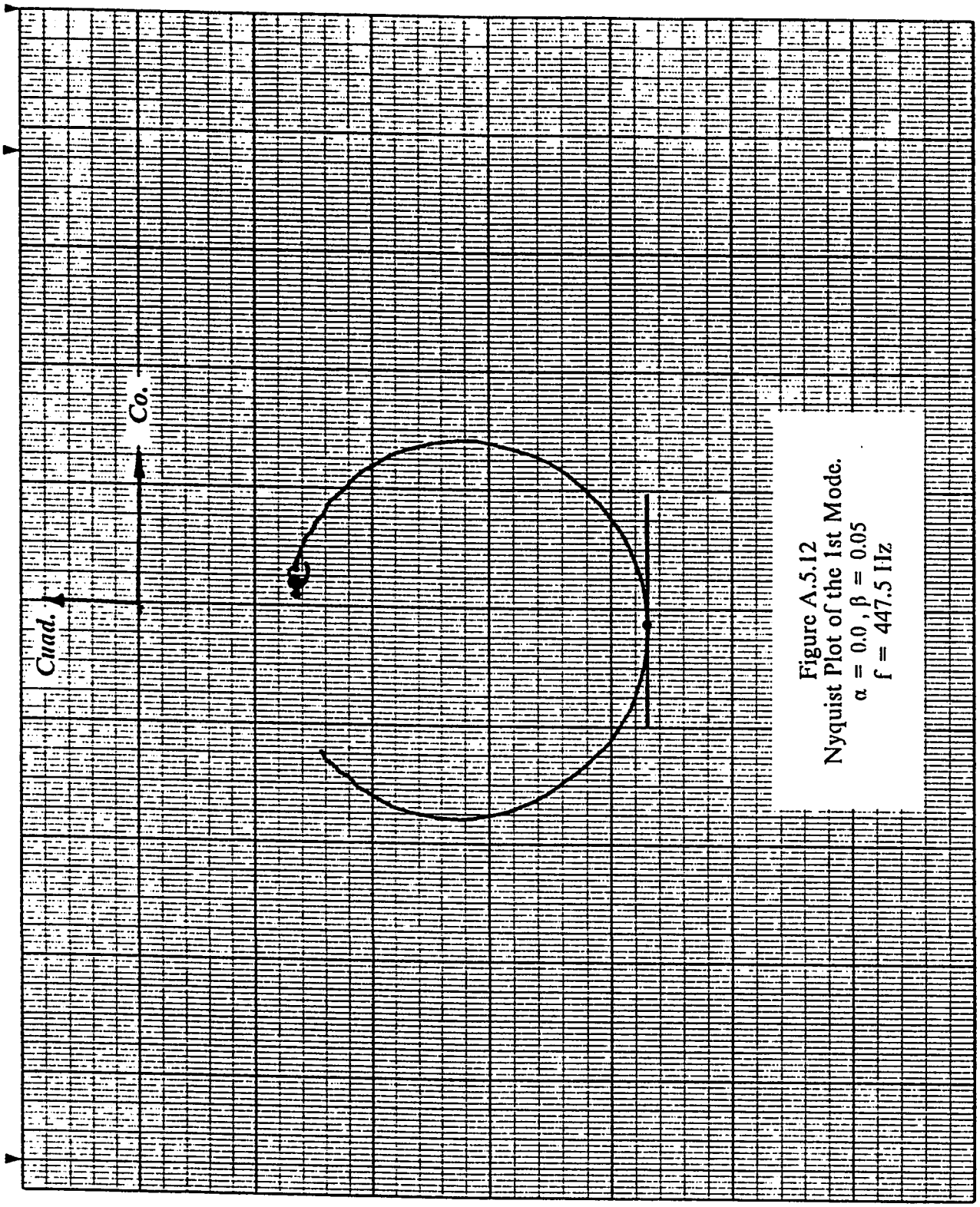

Figure A.5.12
Nyquist Plot of the 1st Mode.
$\alpha = 0.0$, $\beta = 0.05$
$f = 447.5$ Hz

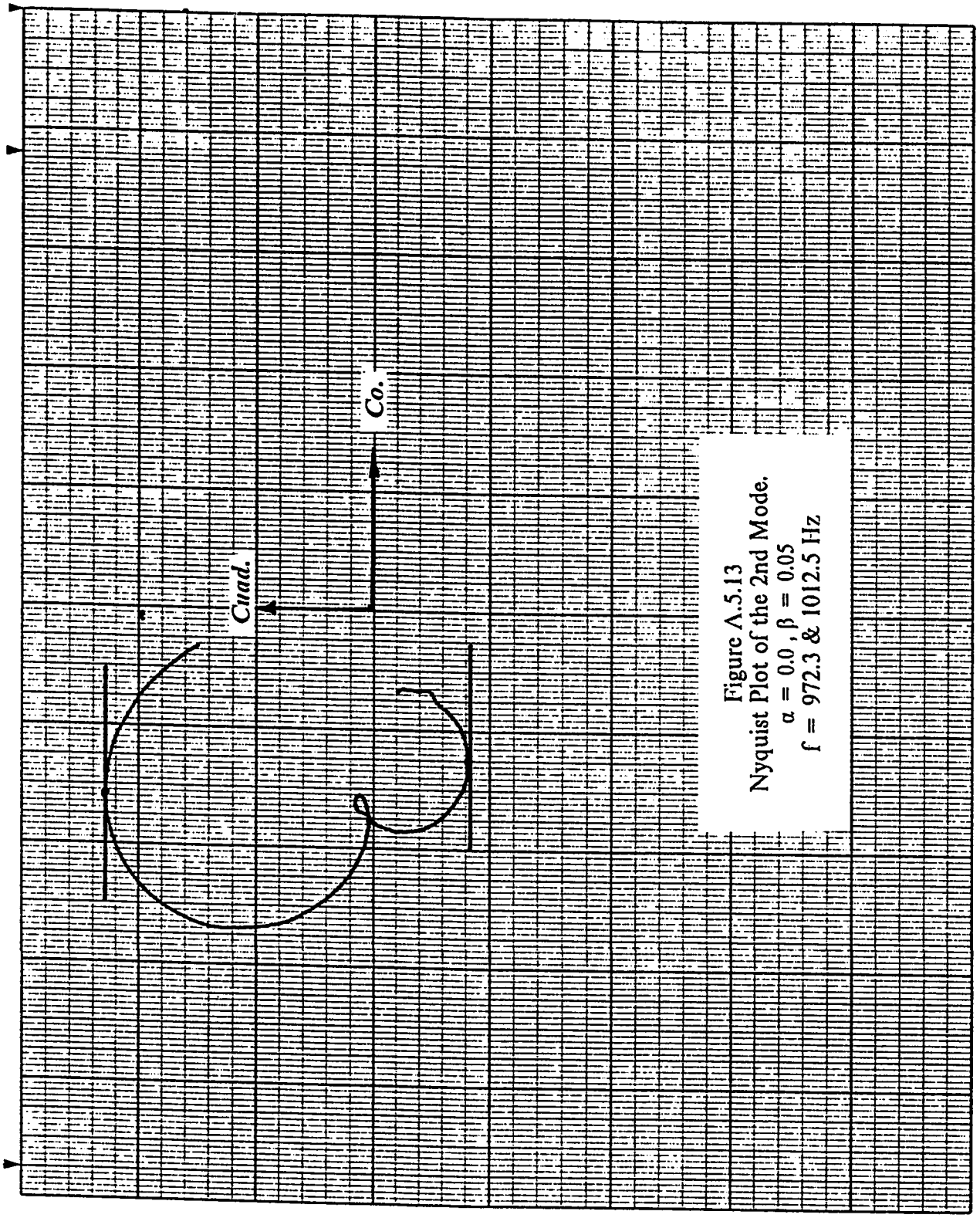

Figure A.5.13
Nyquist Plot of the 2nd Mode.
$\alpha = 0.0$, $\beta = 0.05$
$f = 972.3$ & 1012.5 Hz

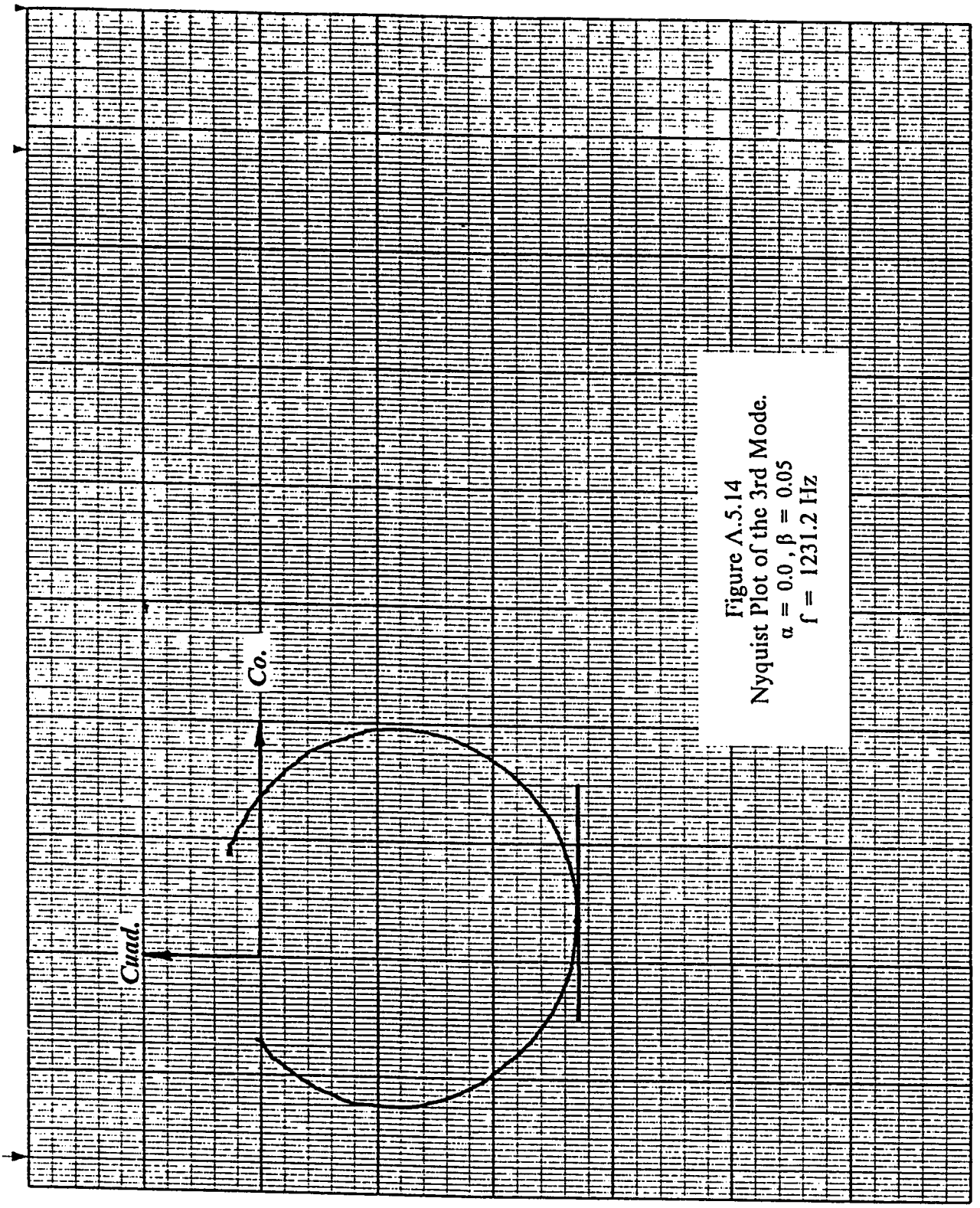

Figure A.5.14
Nyquist Plot of the 3rd Mode.
$\alpha = 0.0, \beta = 0.05$
$f = 1231.2$ Hz

APPENDIX A.6

COLUMN SUPPORTED PLATES

Legend used in the Variation & Correction and Effect of rigidity Plots :

Mode 1 : ——————

Mode 2 : – – – – – – – – –

Mode 3 : ·–·–·–·–·–·–·

Mode 4 : ----------

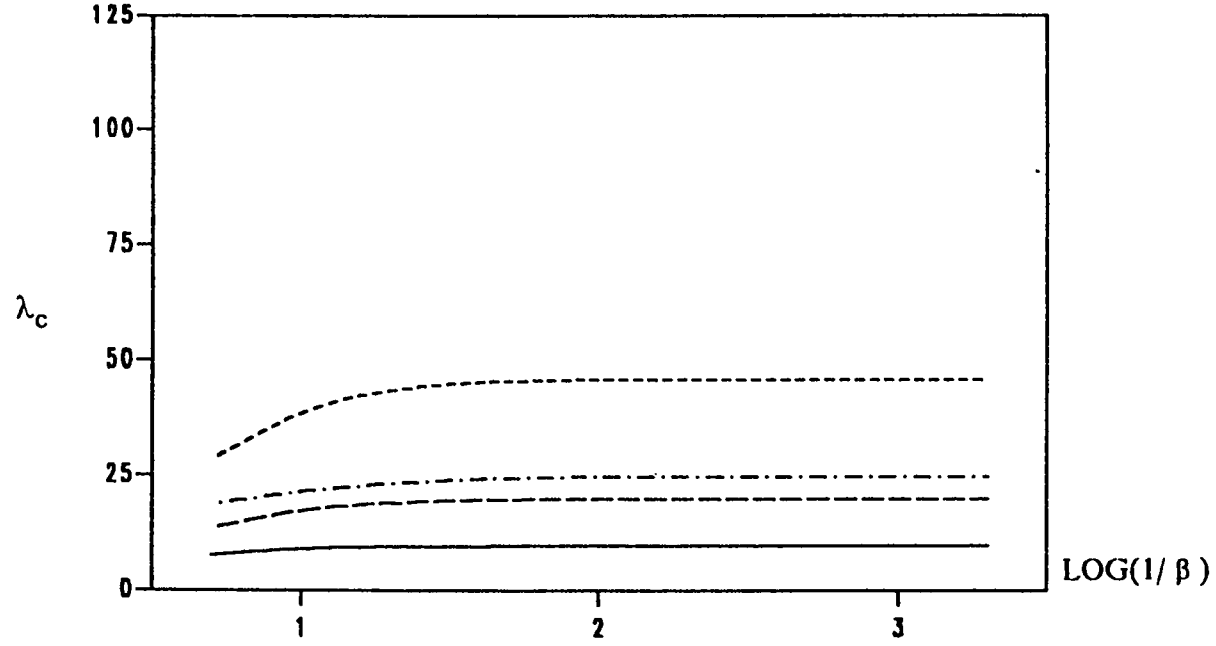

Figure A.6.1 : Variation of λ_c with β , ξ = 0.00

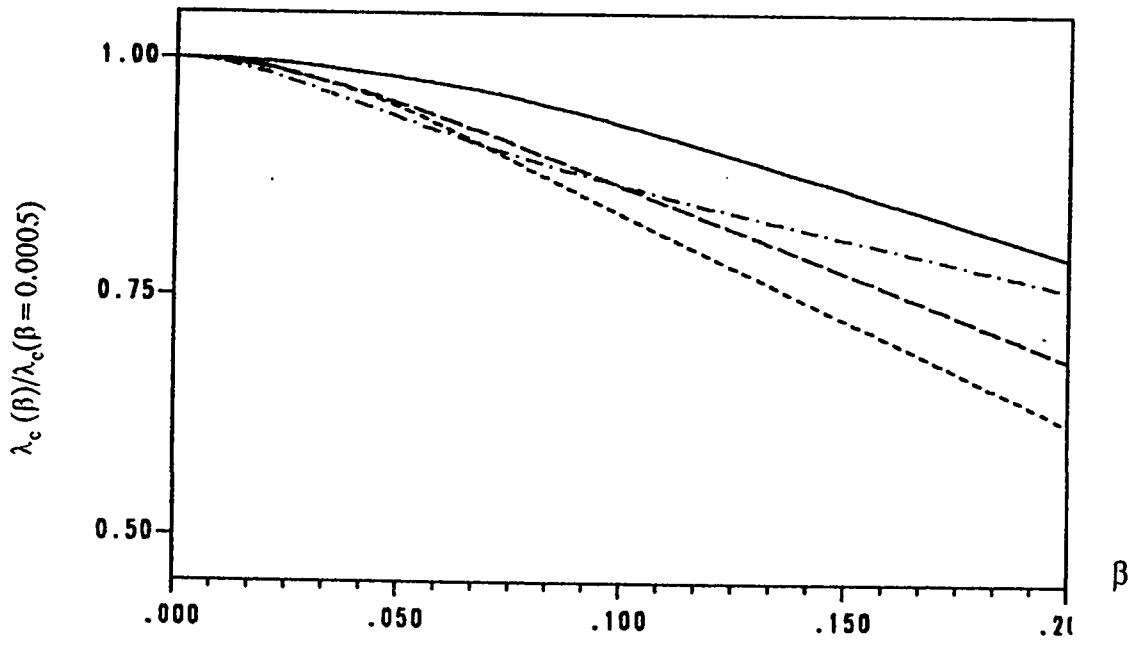

Figure A.6.2 : Correction in λ_c , ξ = 0.00

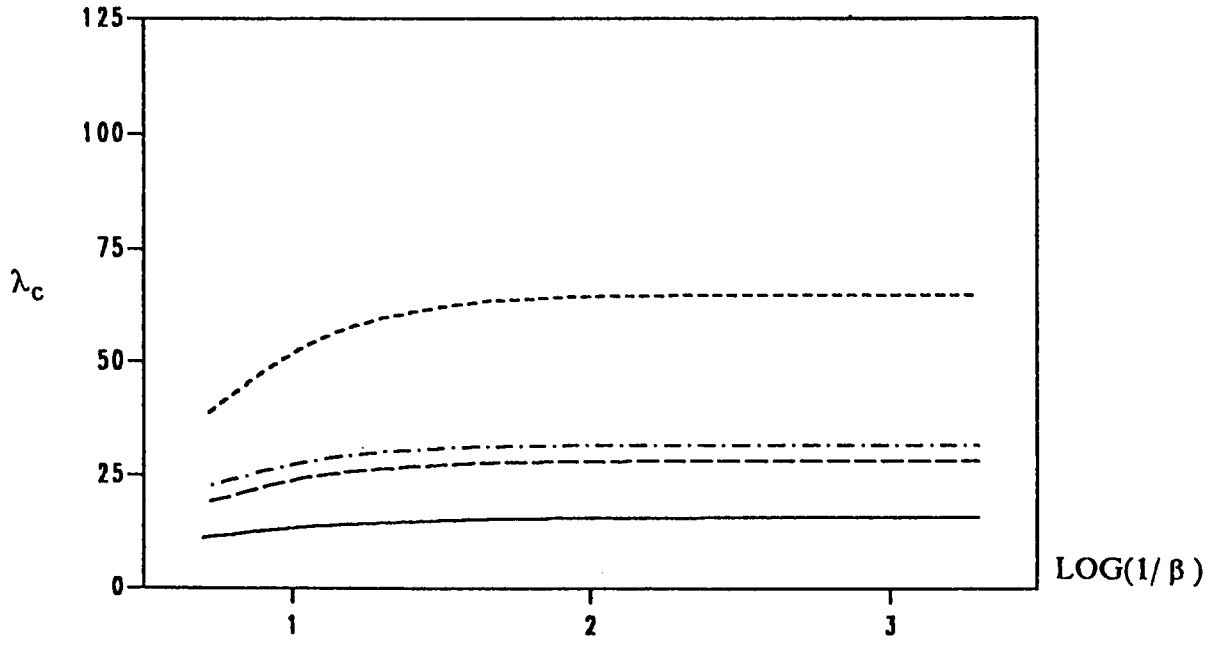

Figure A.6.3 : Variation of λ_c with β , ξ = 0.05

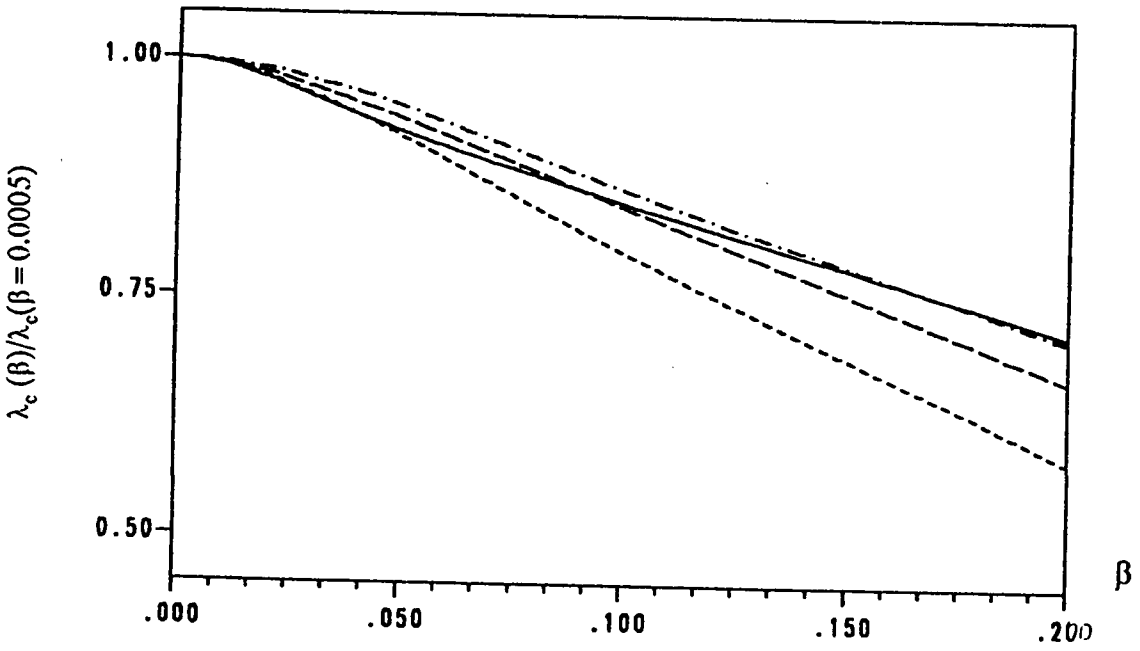

Figure A.6.4 : Correction in λ_c , ξ = 0.05

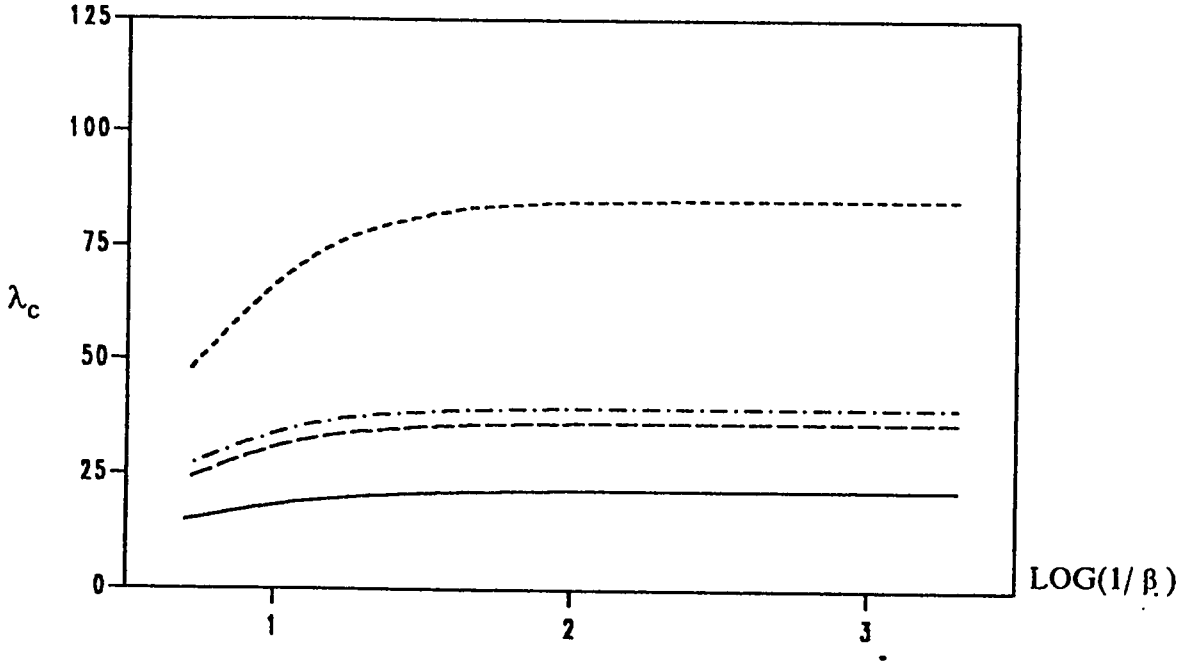

Figure A.6.5 : Variation of λ_c with β , ξ = 0.10

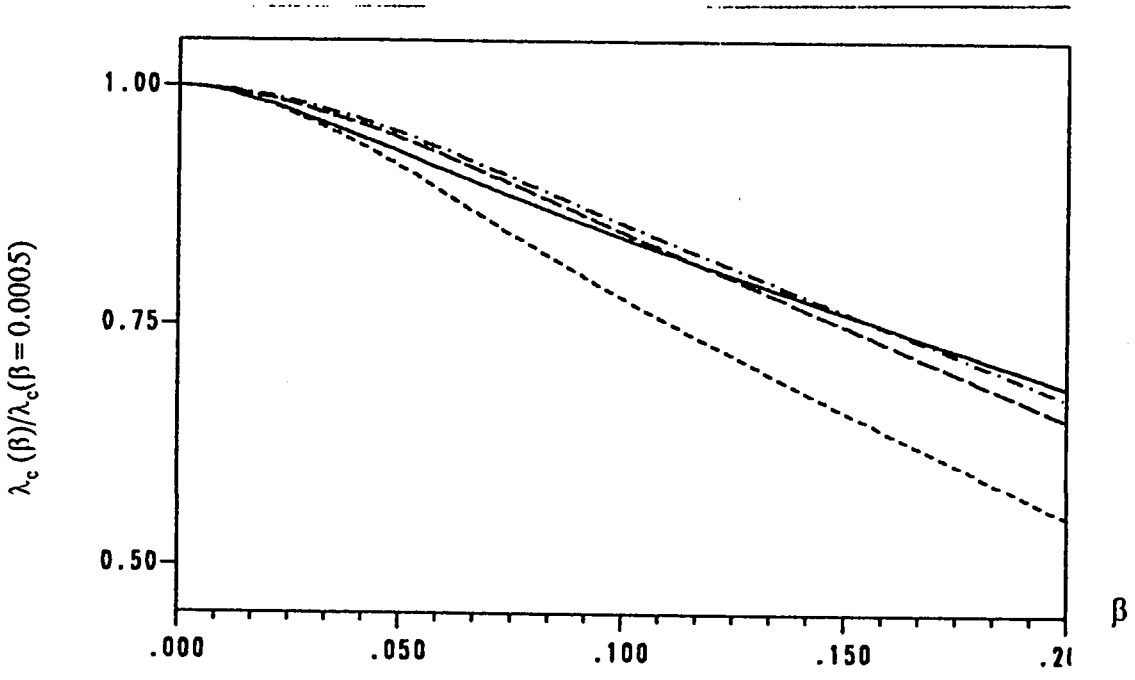

Figure A.6.6 : Correction in λ_c , ξ = 0.10

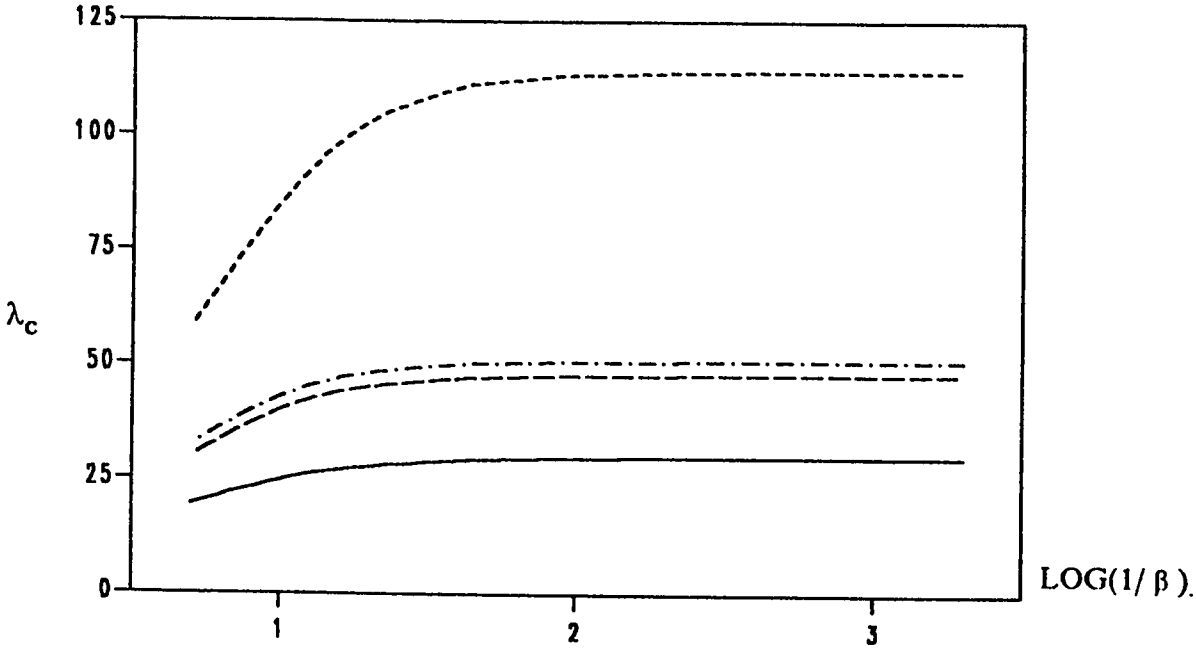

Figure A.6.7 : Variation of λ_c with β , ξ = 0.15

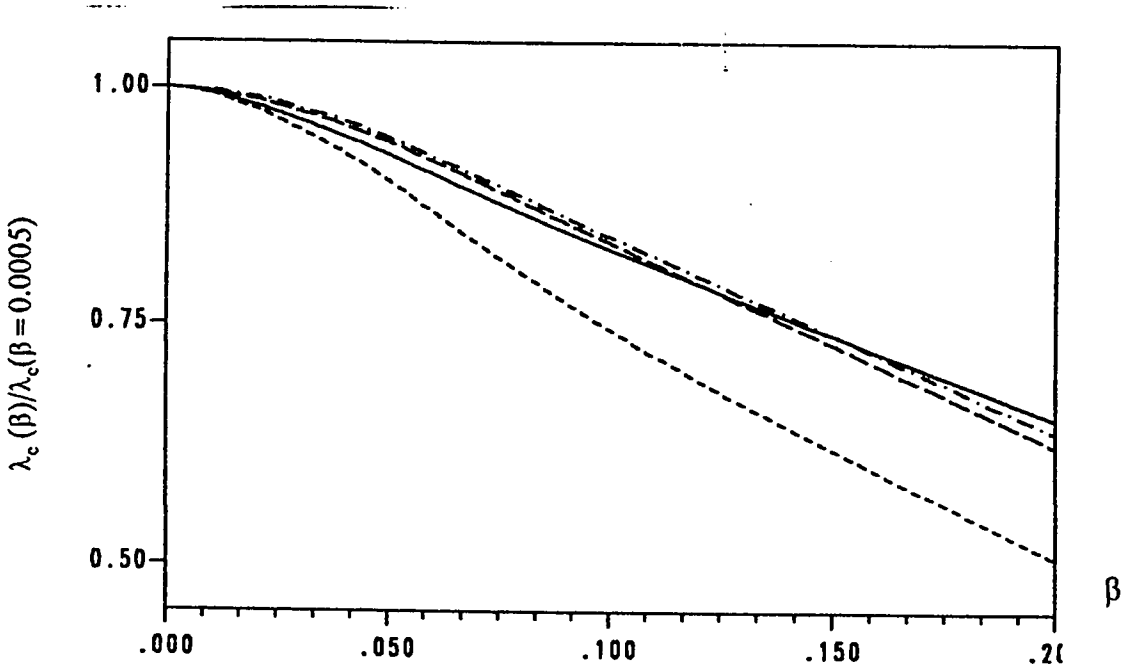

Figure A.6.8 : Correction in λ_c , ξ = 0.15

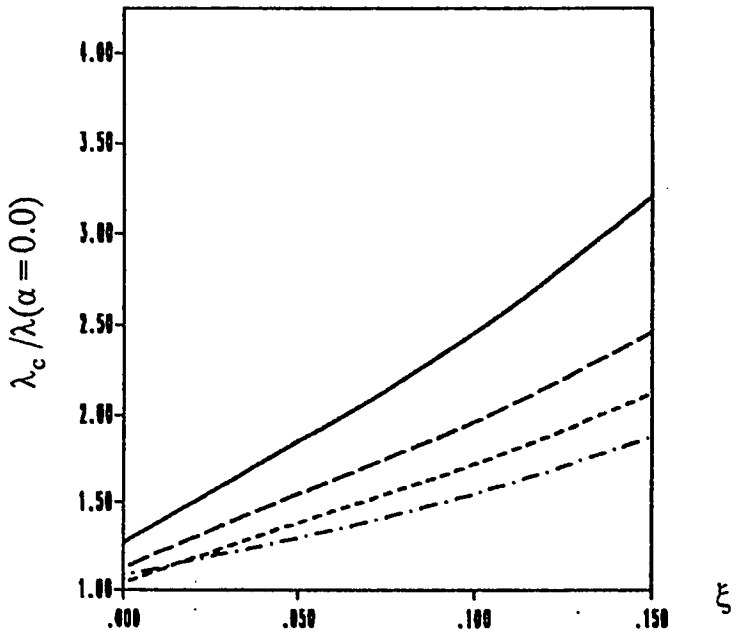

Figure A.6.9 : Effec of Rigid Column Support . β = 0.2000

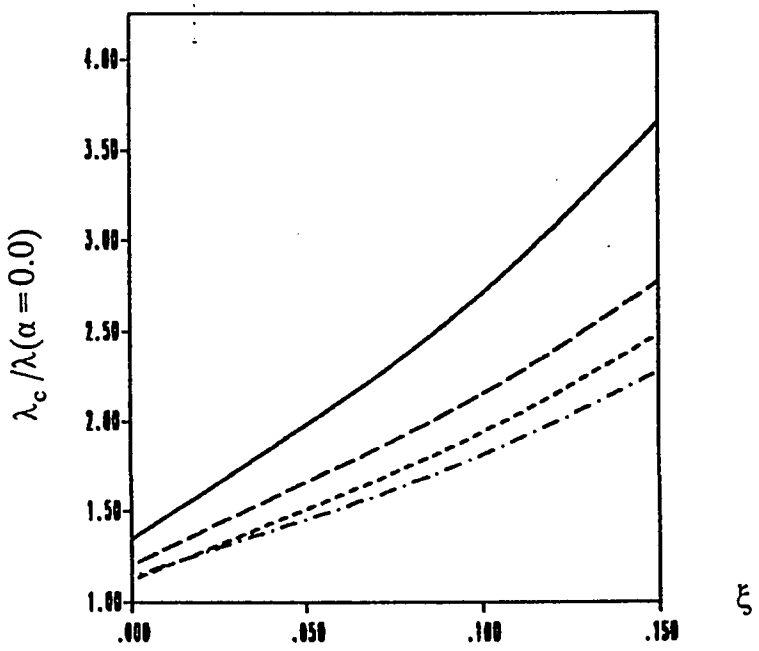

Figure A.6.10 : Effec of Rigid Column Support . β = 0.1000

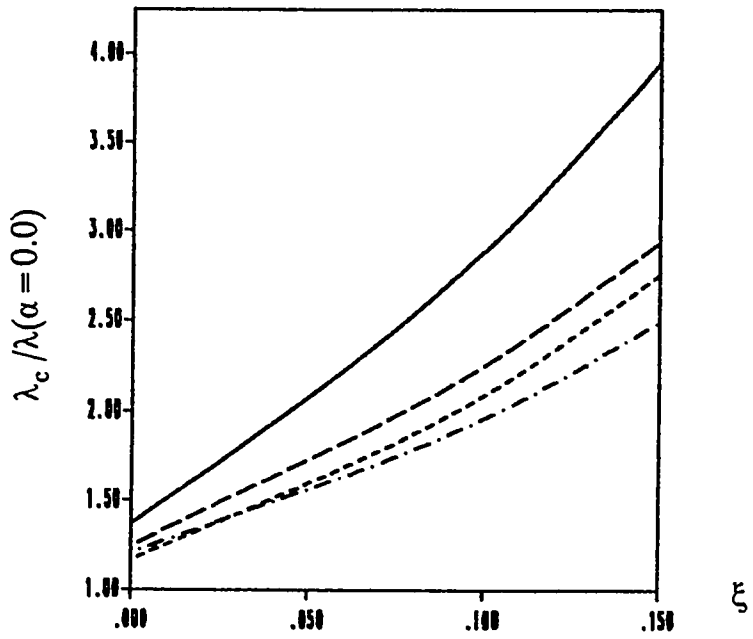

Figure A.6.11 : Effec of Rigid Column Support . β = 0.0500

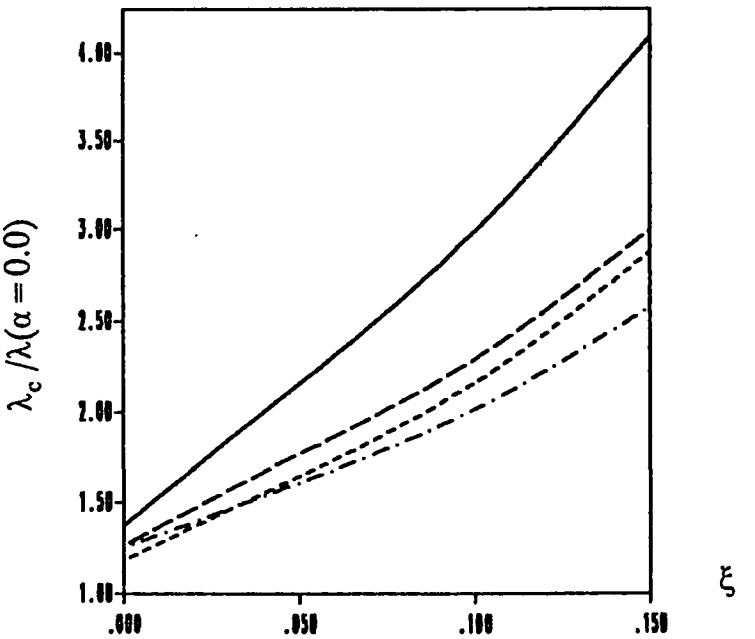

Figure A.6.12 : Effec of Rigid Column Support . β = 0.0250

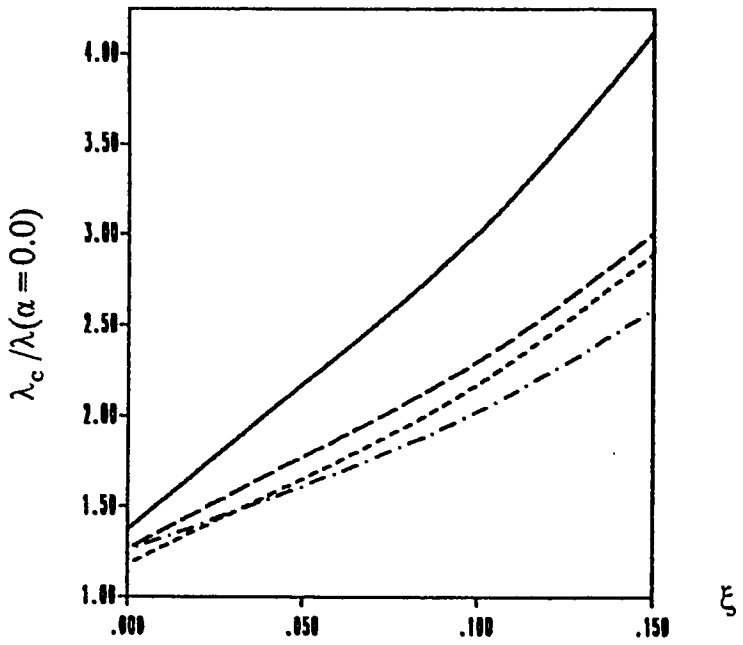

Figure A.6.13 : Effec of Rigid Column Support . β = 0.0200

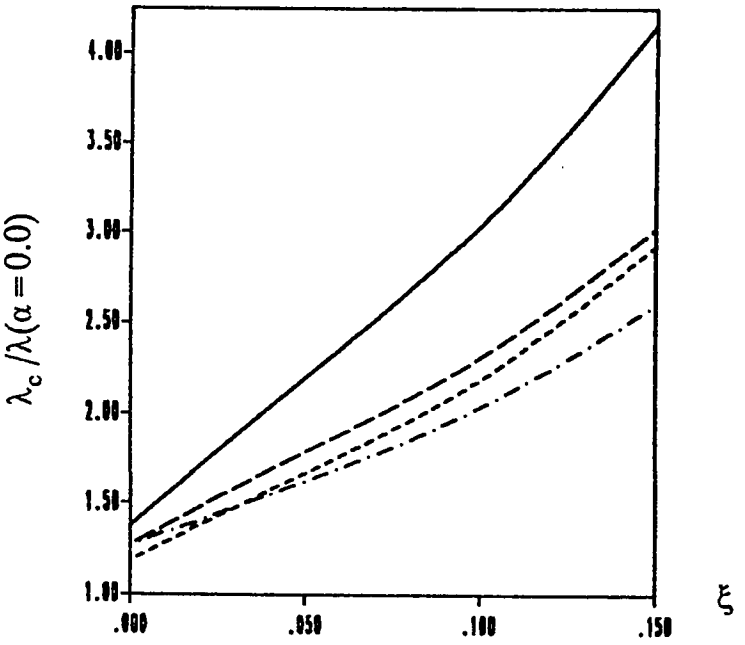

Figure A.6.14 : Effec of Rigid Column Support . β = 0.0125

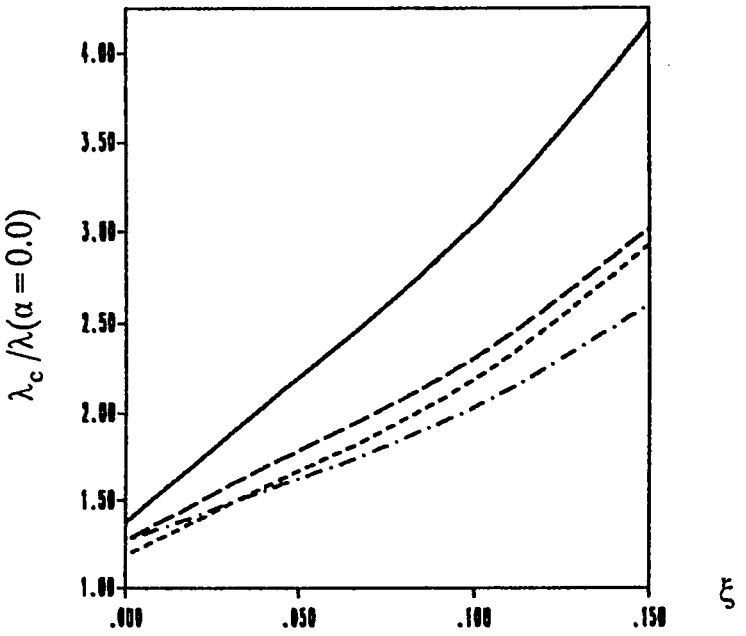

Figure A.6.15 : Effec of Rigid Column Support . β = 0.0100

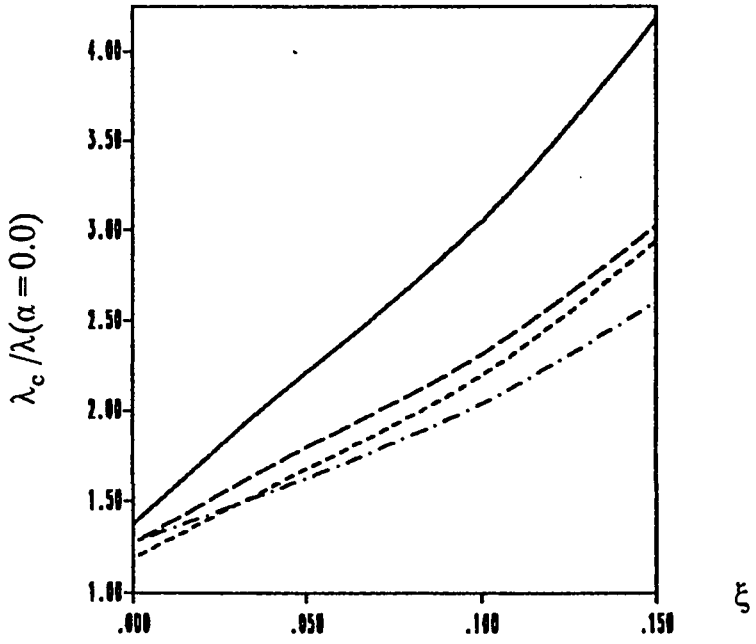

Figure A.6.16 : Effec of Rigid Column Support . β = 0.0050

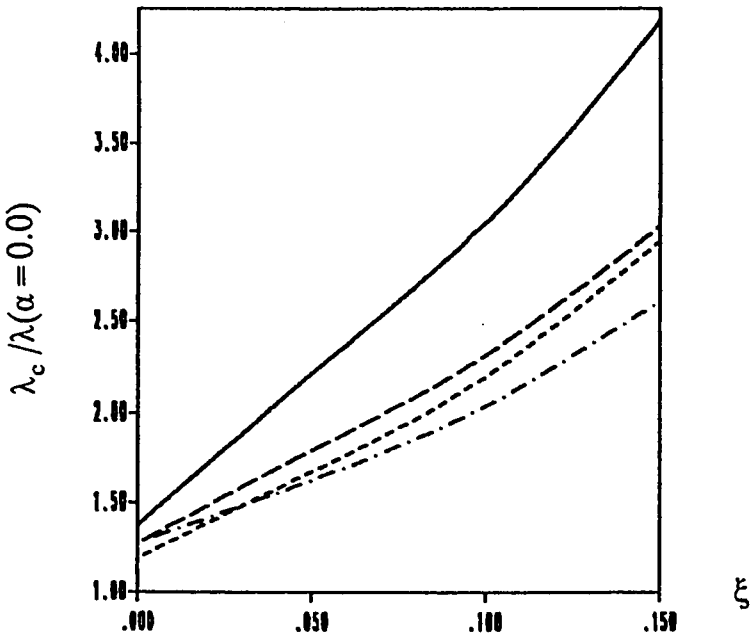

Figure A.6.17 : Effec of Rigid Column Support . β = 0.0025

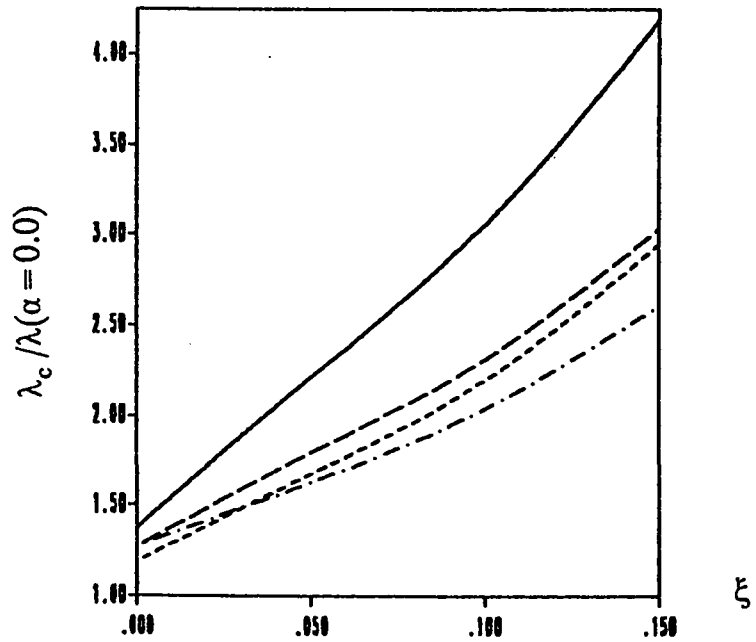

Figure A.6.18 : Effec of Rigid Column Support . β = 0.0010

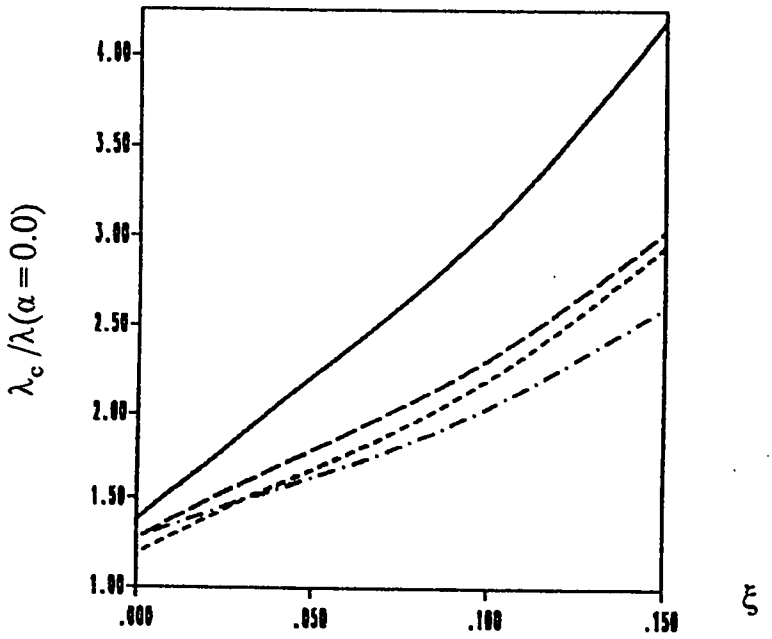

Figure A.6.19 : Effec of Rigid Column Support . β = 0.0005

APPENDIX A.a

MODE SHAPES

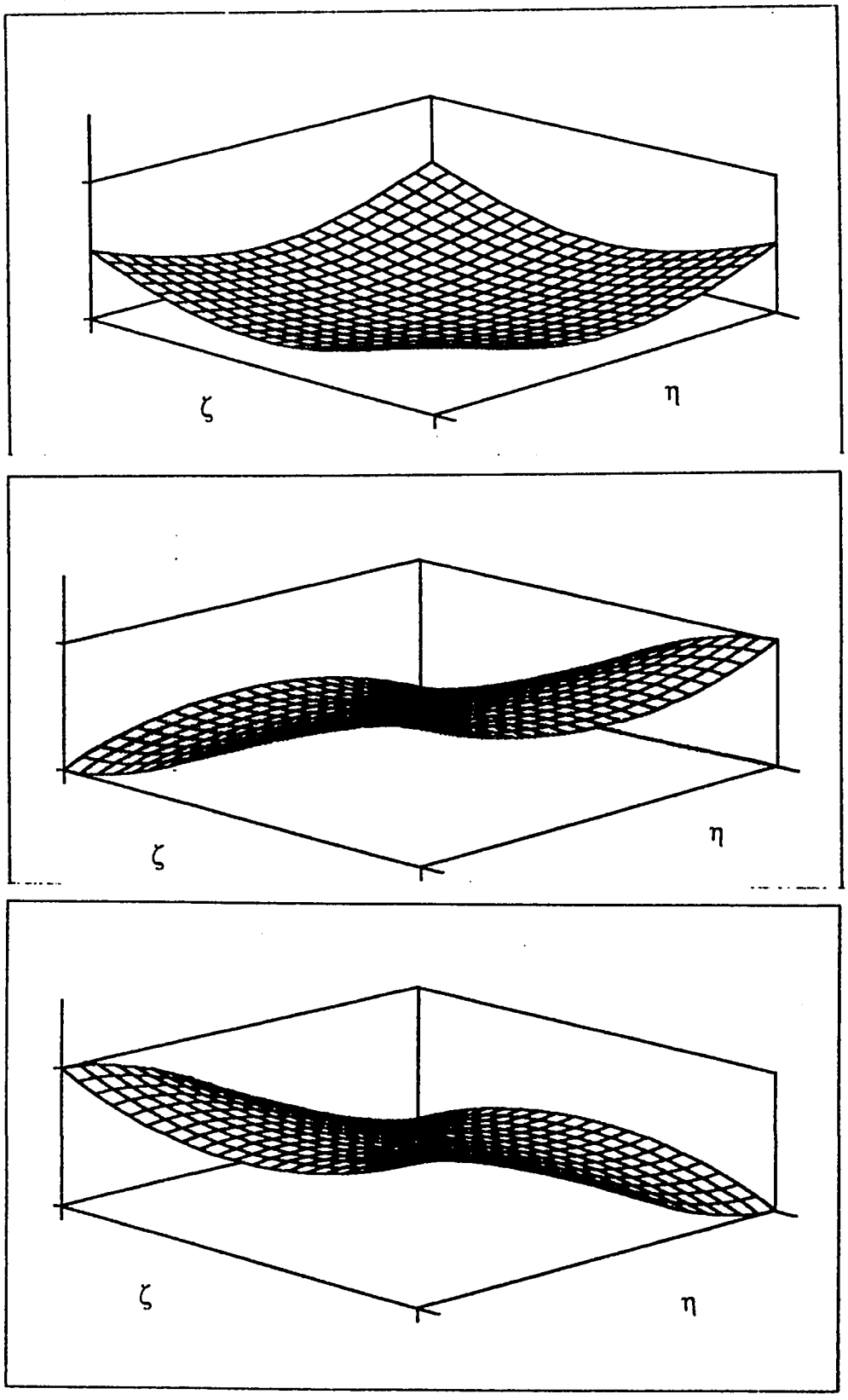

Figure A.a.1 : Mode Shapes for the First Frequency
Corner Supported : $\alpha = 0.0$

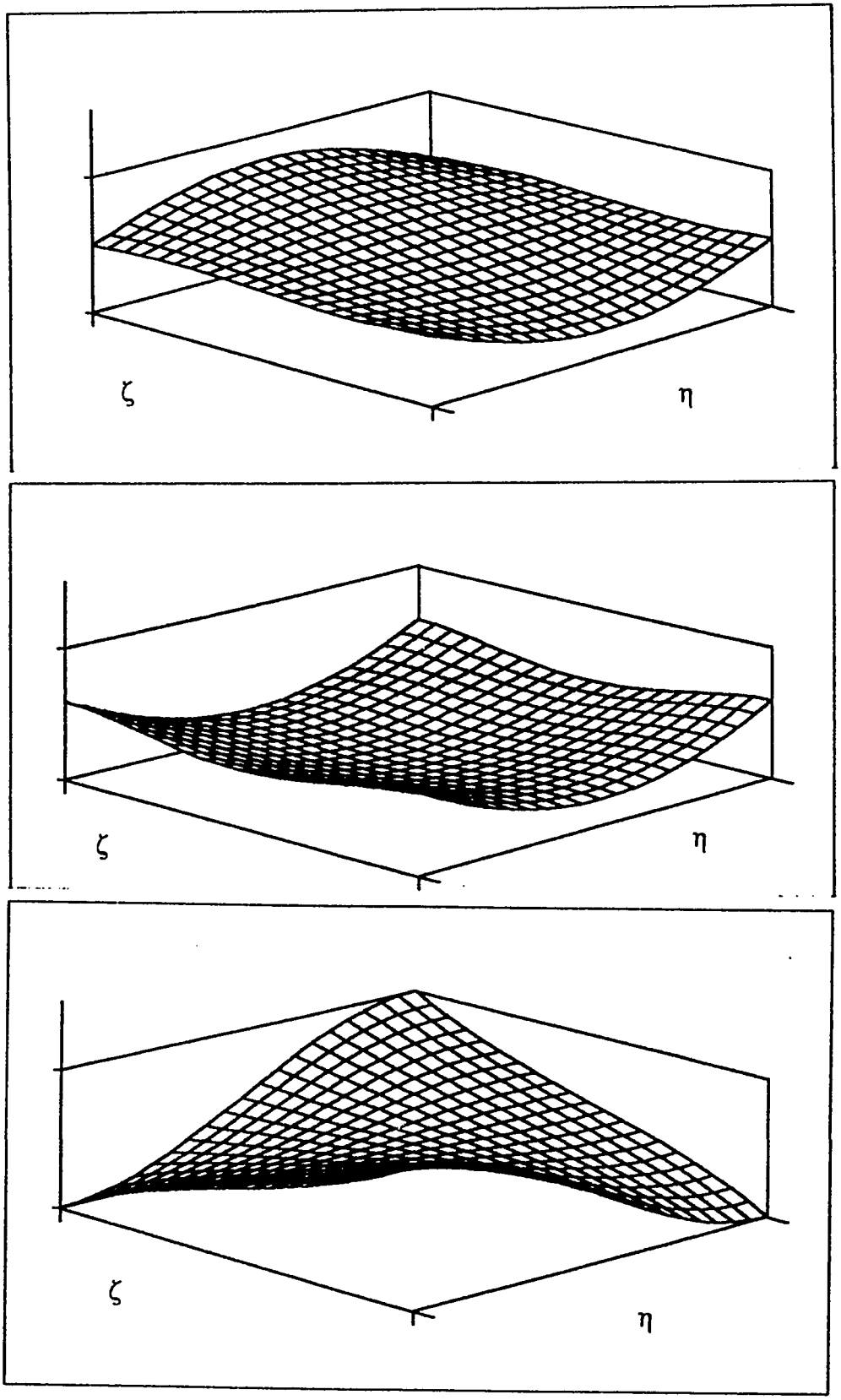

Figure A.a.2 : Mode Shapes for the Second Frequency
Corner Supported : $\alpha = 0.0$

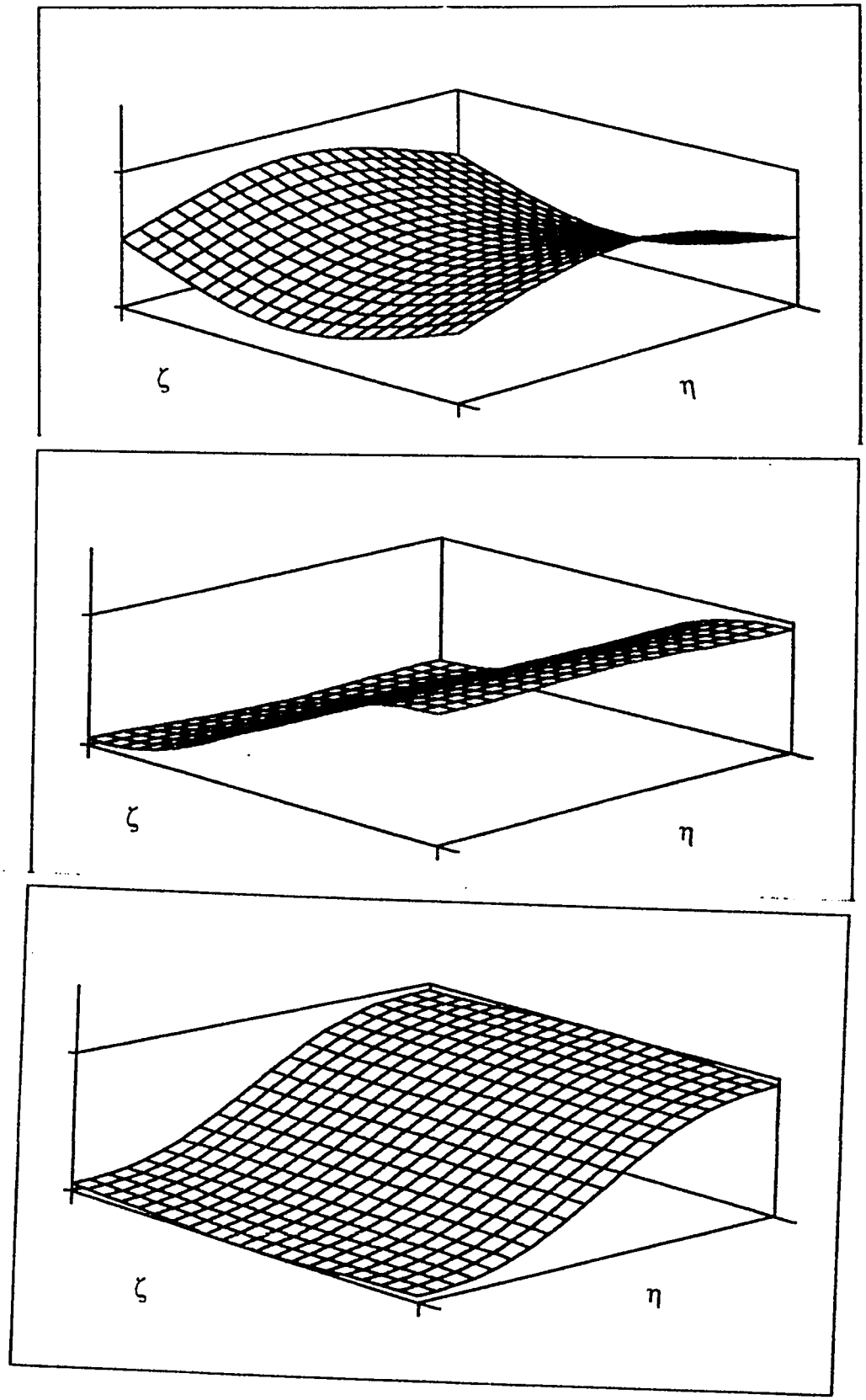

Figure A.a.3 : Mode Shapes for the Third Frequency
Corner Supported : $\alpha = 0.0$

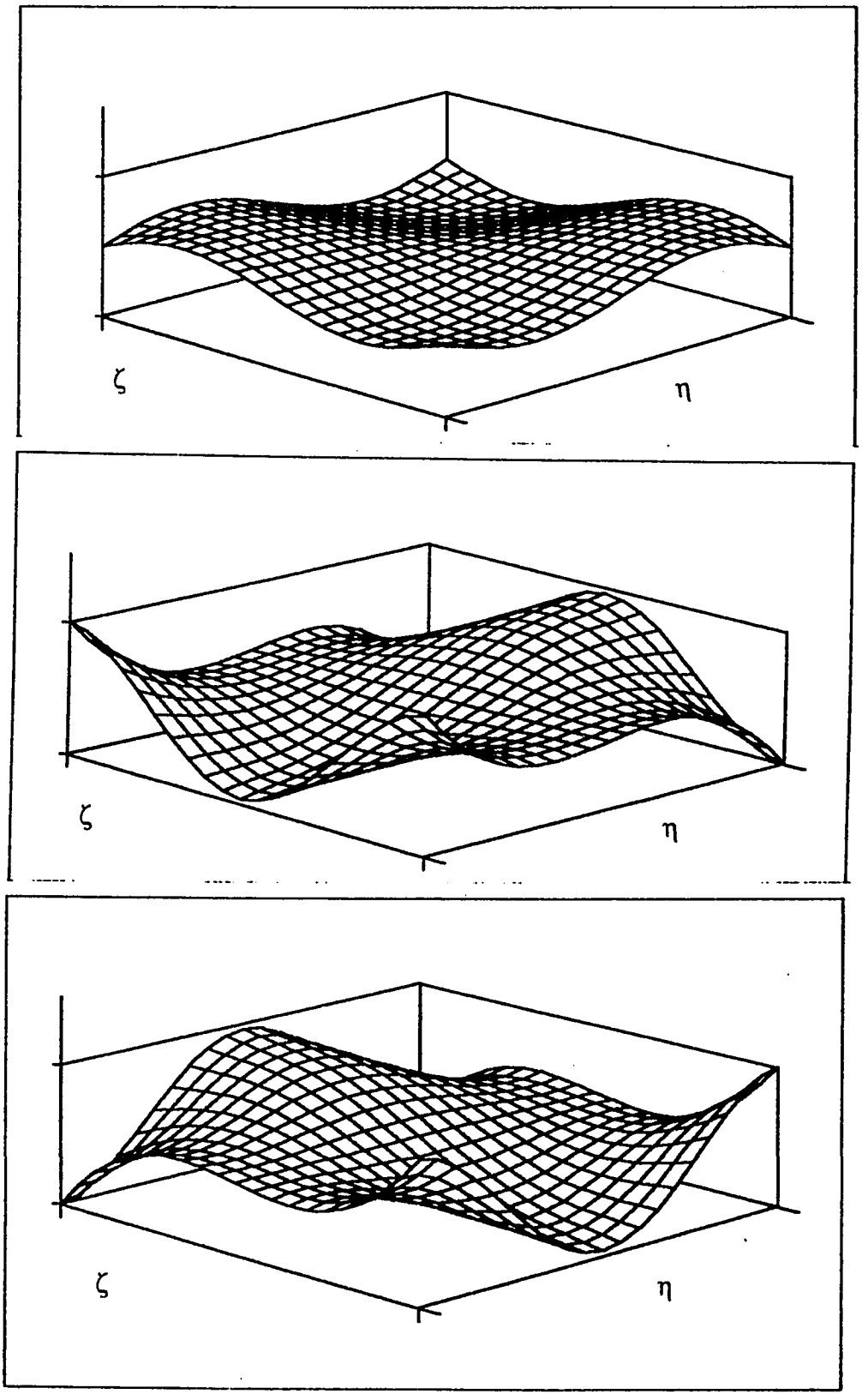

Figure A.a.4 : Mode Shapes for the Fourth Frequency
Corner Supported : $\alpha = 0.0$

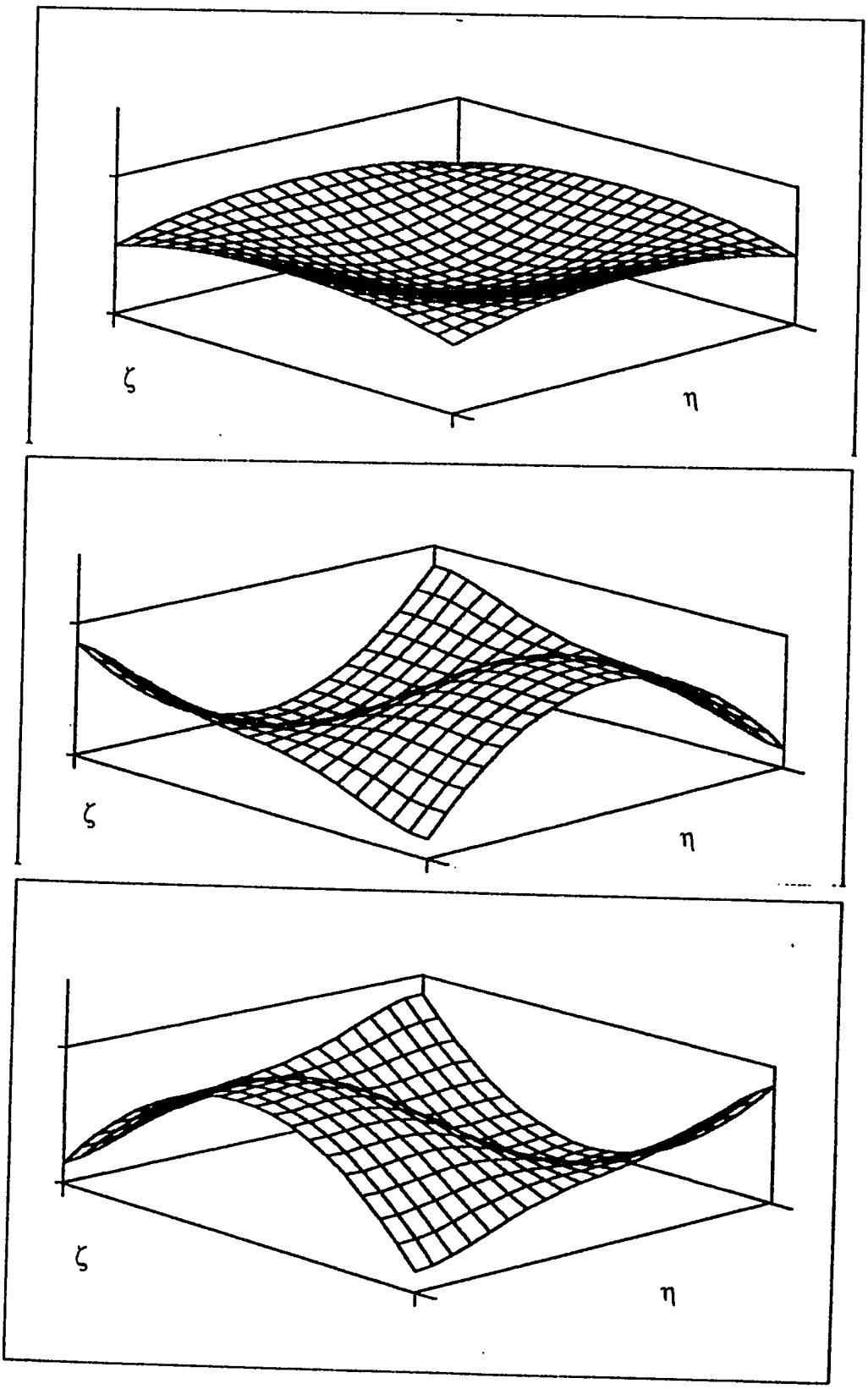

Figure A.a.5 : Mode Shapes for the Fifth Frequency
Corner Supported : $\alpha = 0.0$

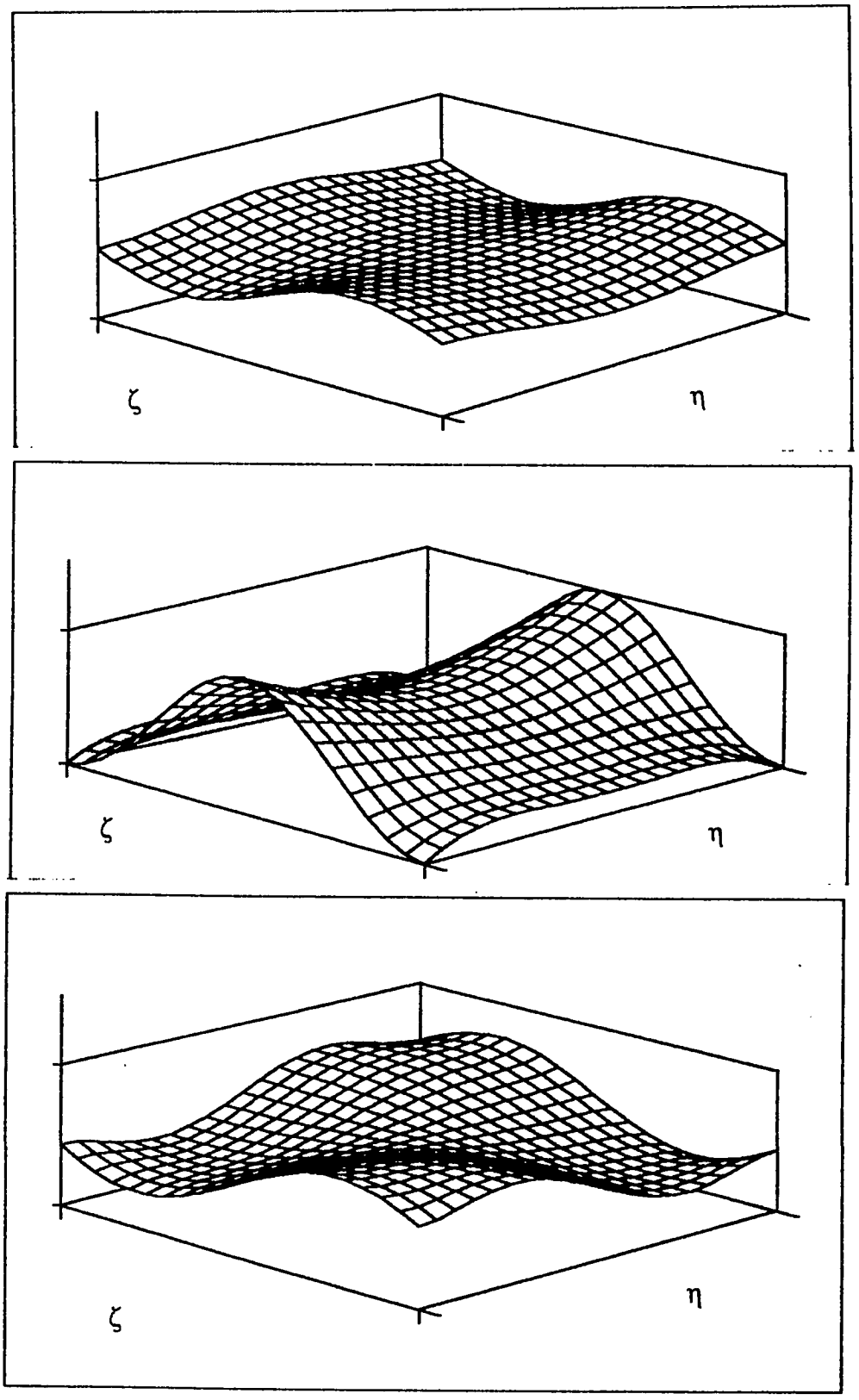

Figure A.a.6 : Mode Shapes for the Sixth Frequency
Corner Supported : $\alpha = 0.0$

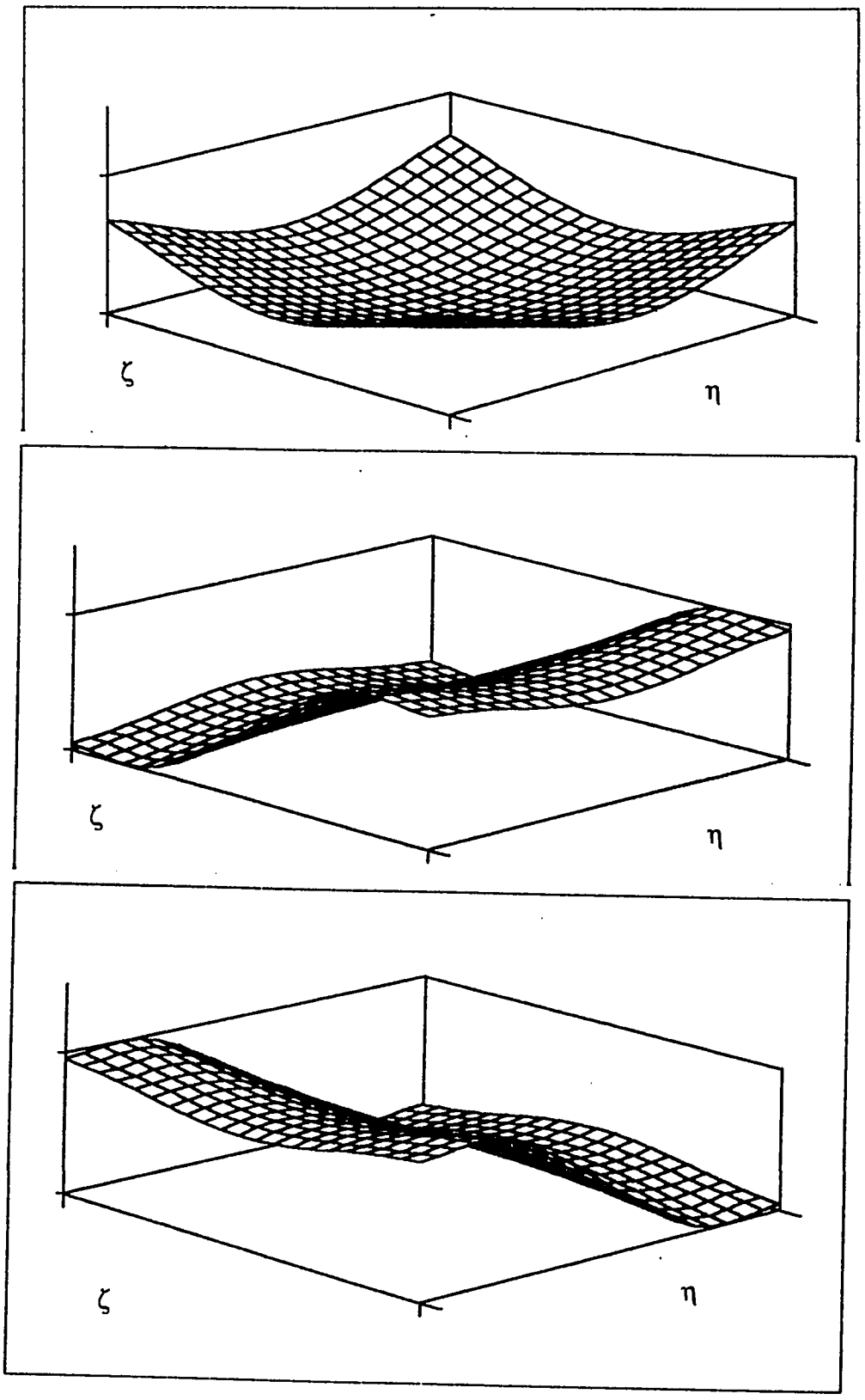

Figure A.a.7 : Mode Shapes for the First Frequency
Point Supported : $\alpha = 0.1$

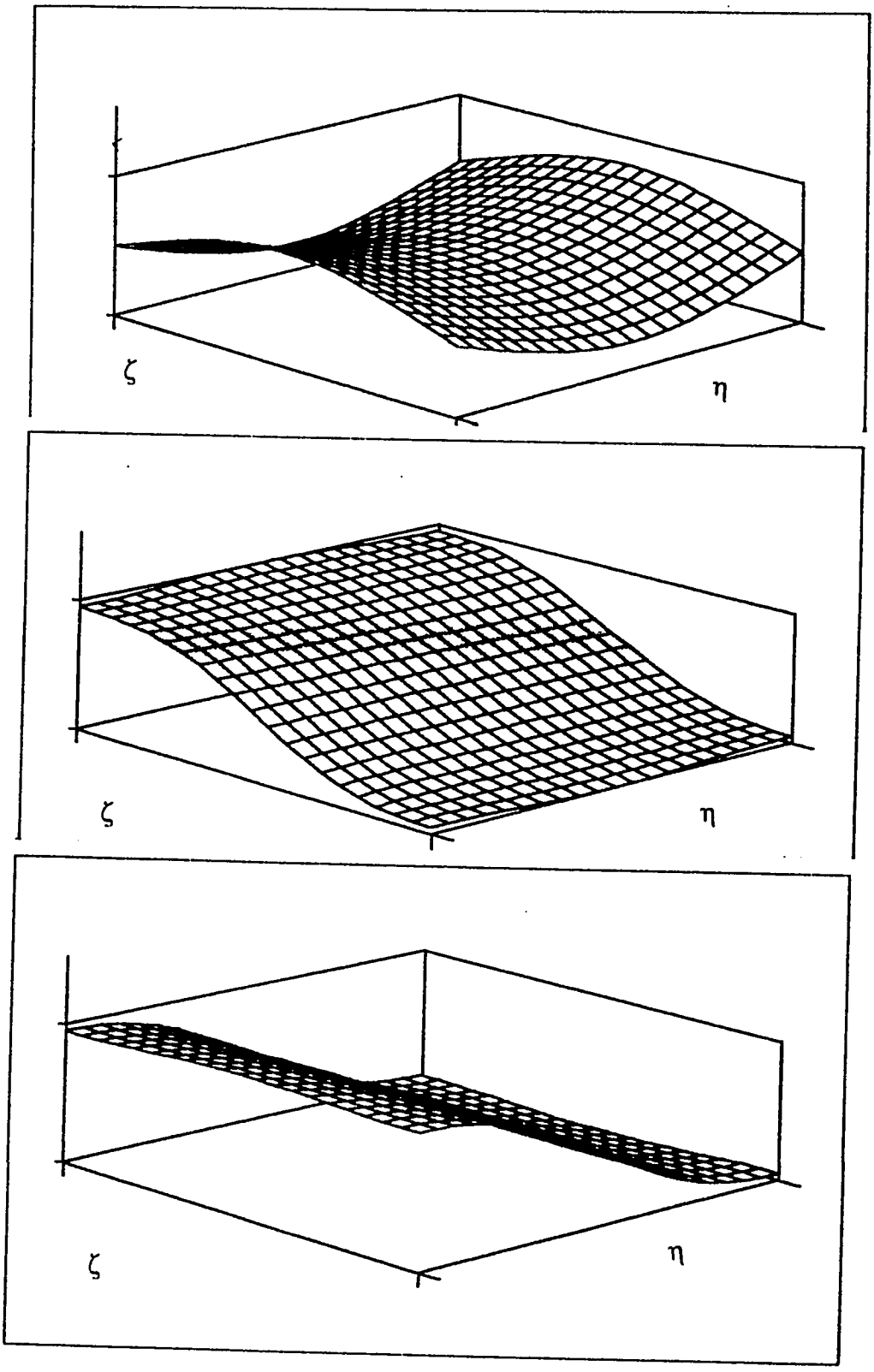

Figure A.a.8 : Mode Shapes for the Second Frequency
Point Supported : $\alpha = 0.1$

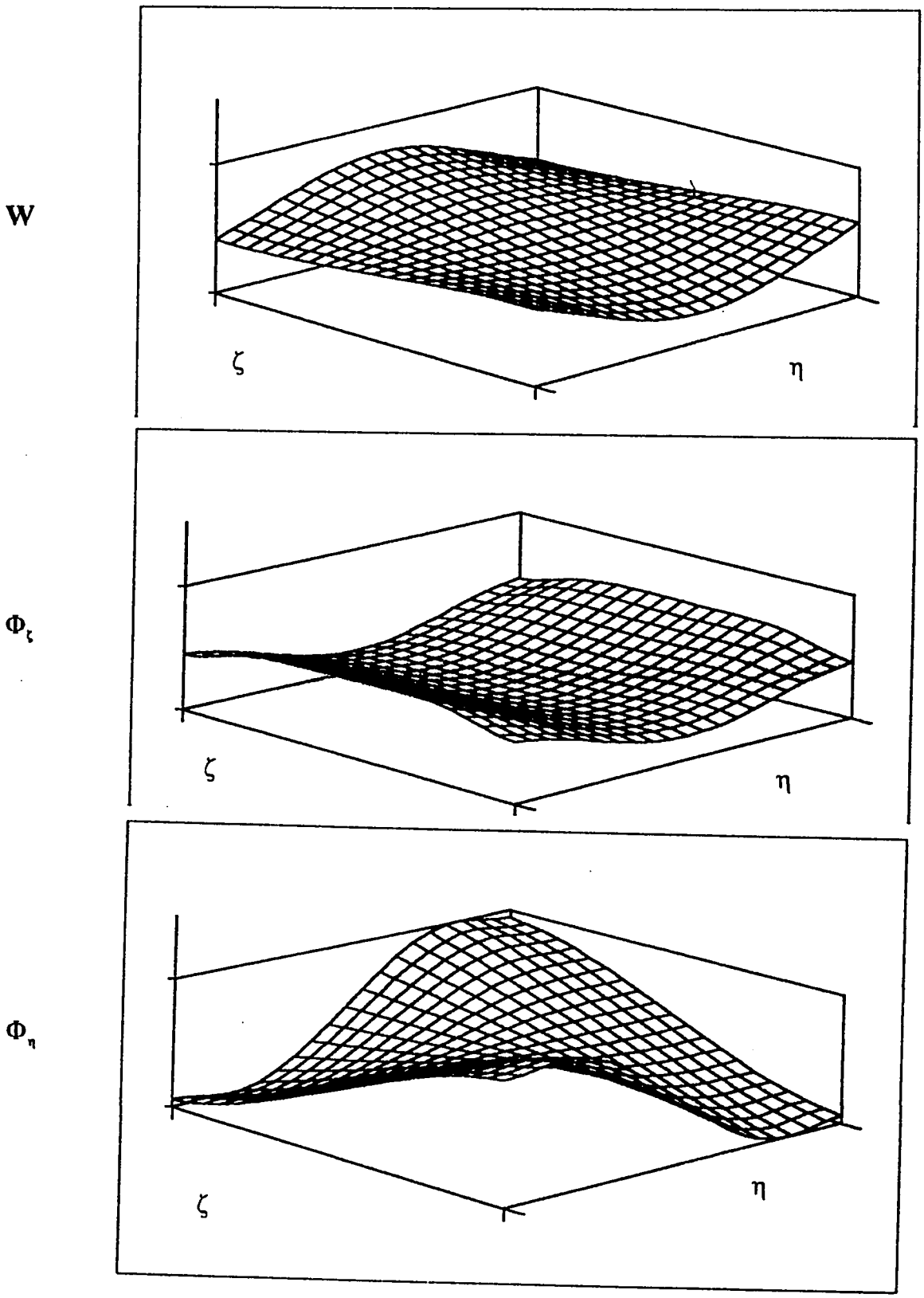

Figure A.a.9 : Mode Shapes for the Third Frequency
Point Supported : $\alpha = 0.1$

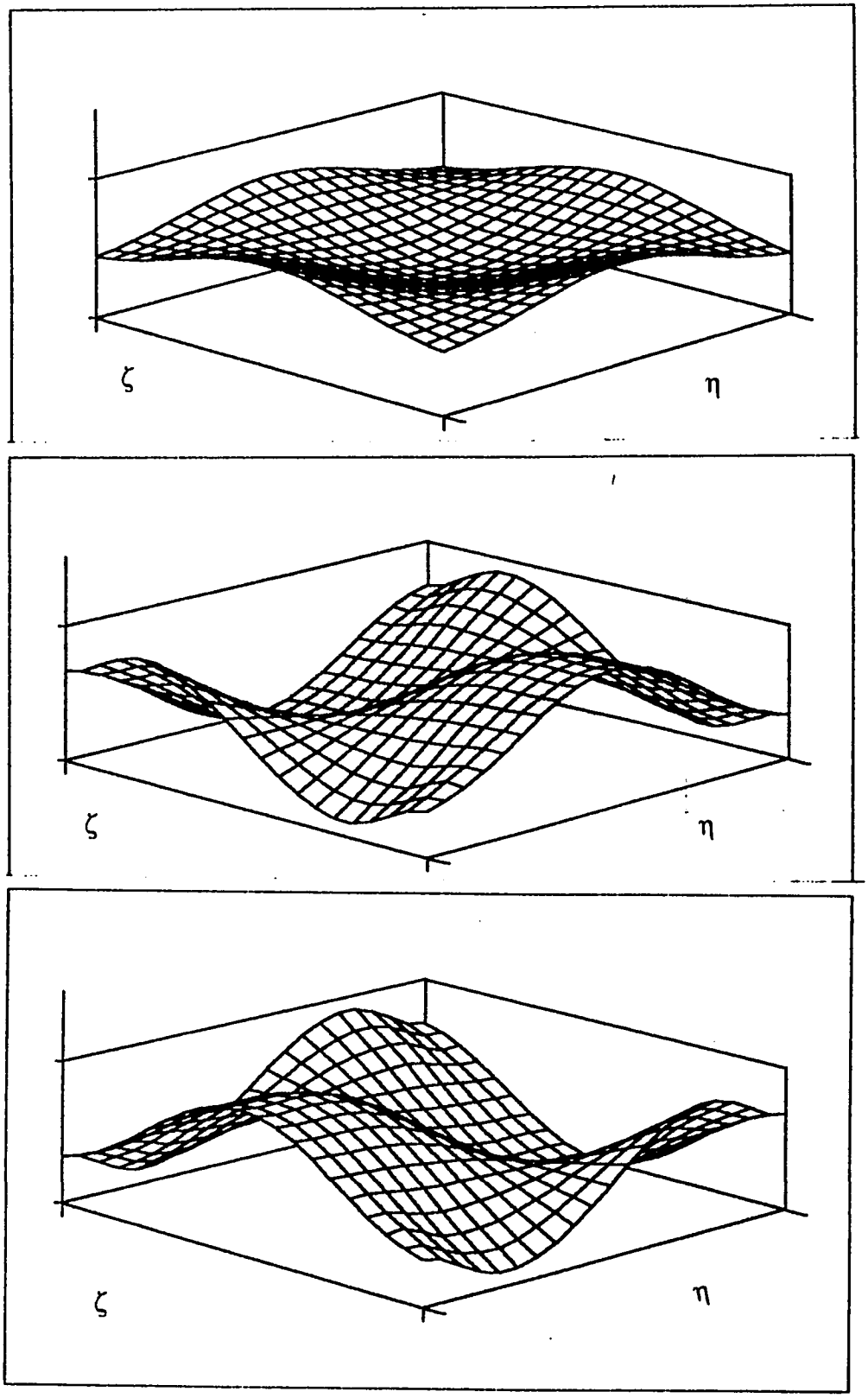

Figure A.a.10 : Mode Shapes for the Fourth Frequency
Point Supported : $\alpha = 0.1$

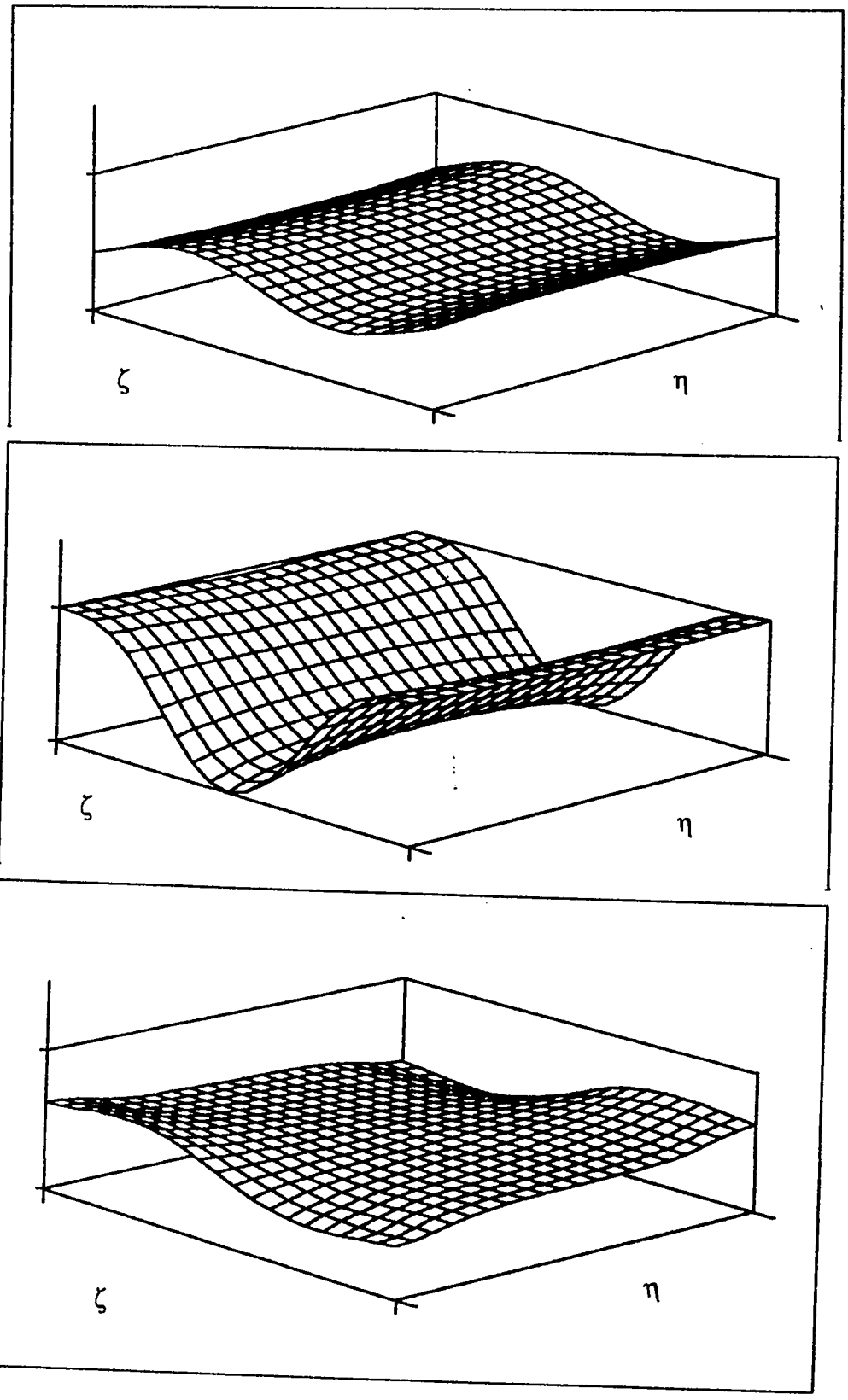

Figure A.a.11 : Mode Shapes for the Fifth Frequency
Point Supported : $\alpha = 0.1$

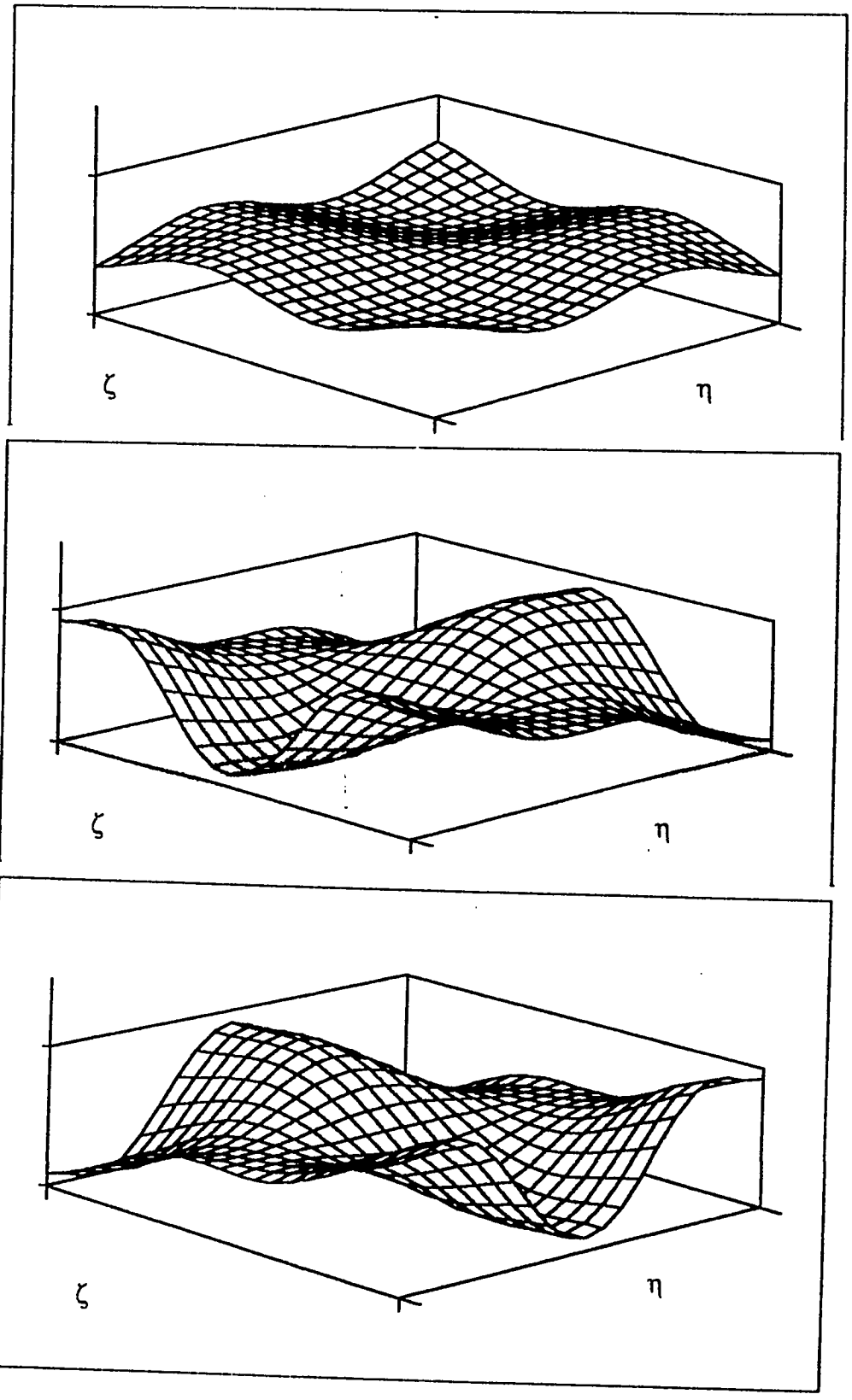

Figure A.a.12 : Mode Shapes for the Sixth Frequency
Point Supported : $\alpha = 0.1$

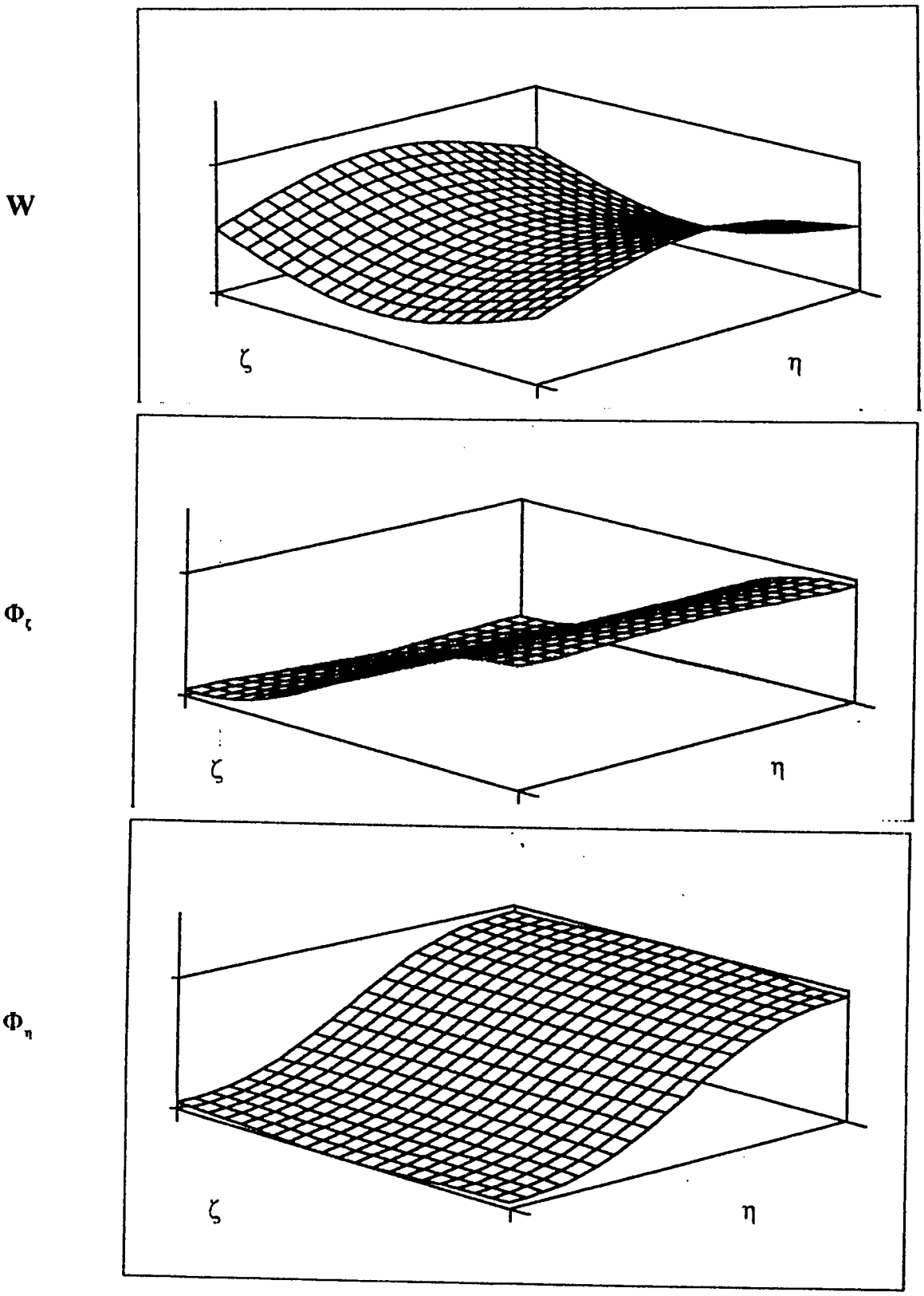

Figure A.a.13 : Mode Shapes for the First Frequency
Point Supported : $\alpha = 0.2$

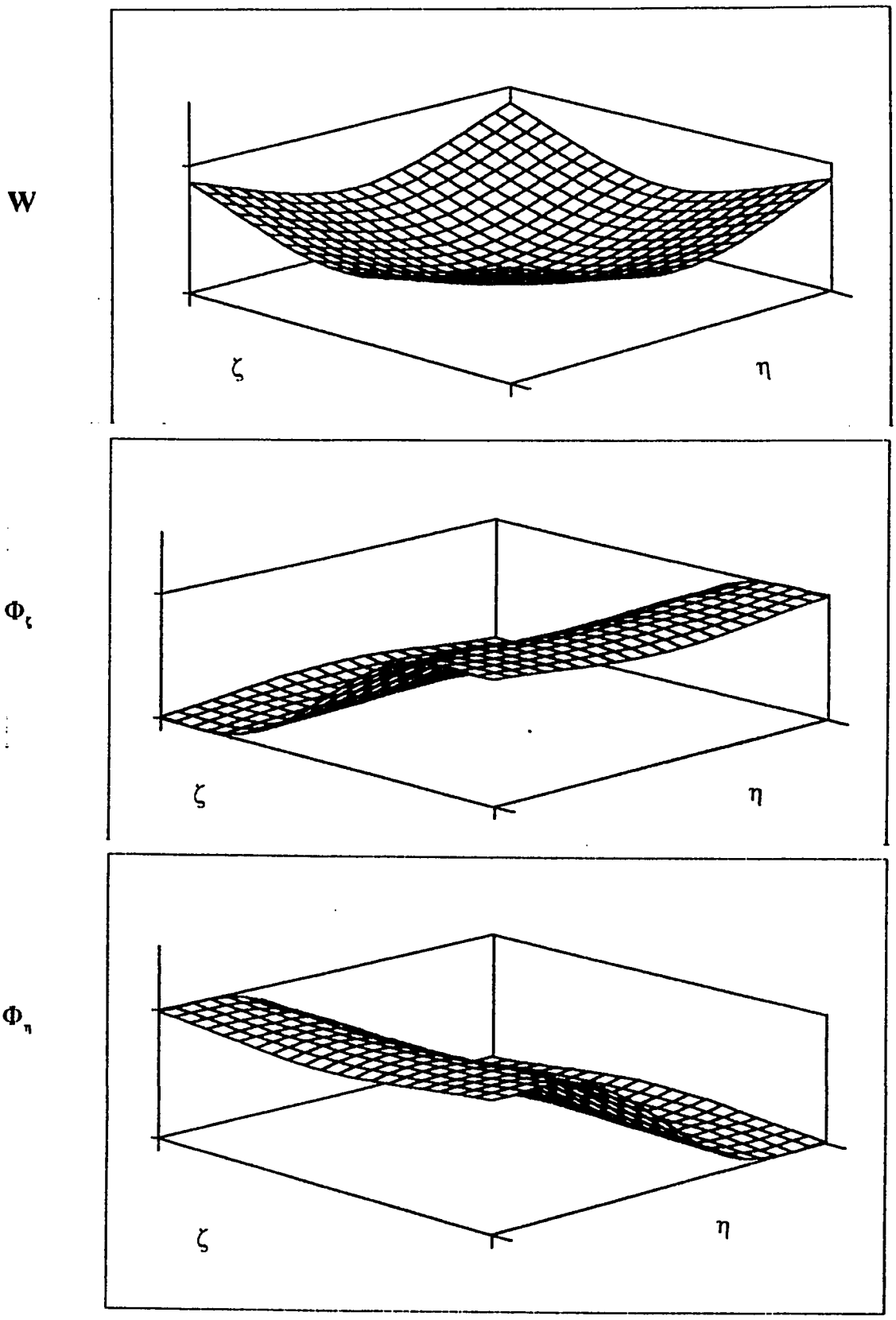

Figure A.a.14 : Mode Shapes for the Second Frequency
Point Supported : $\alpha = 0.2$

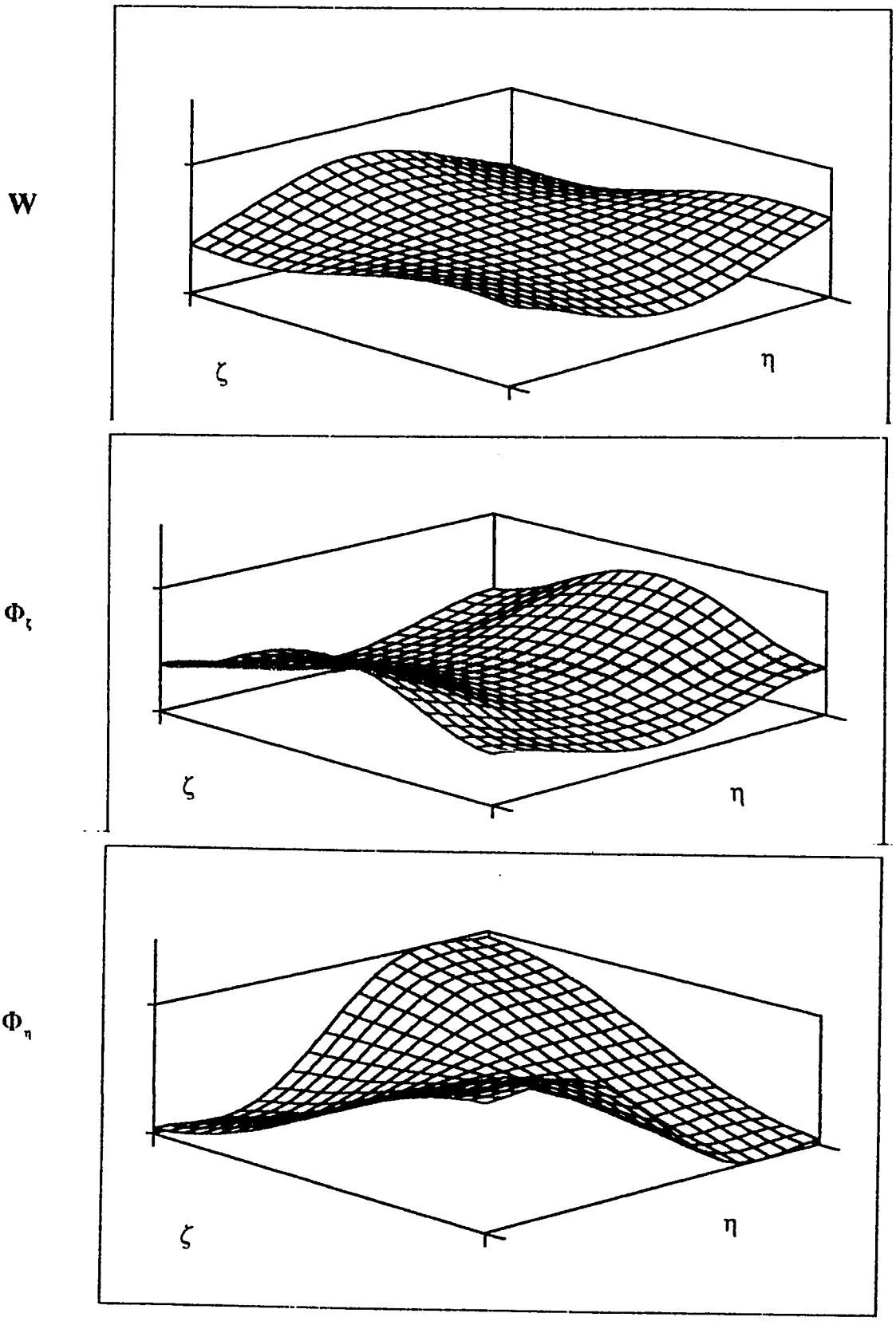

Figure A.a.15 : Mode Shapes for the Third Frequency
Point Supported : $\alpha = 0.2$

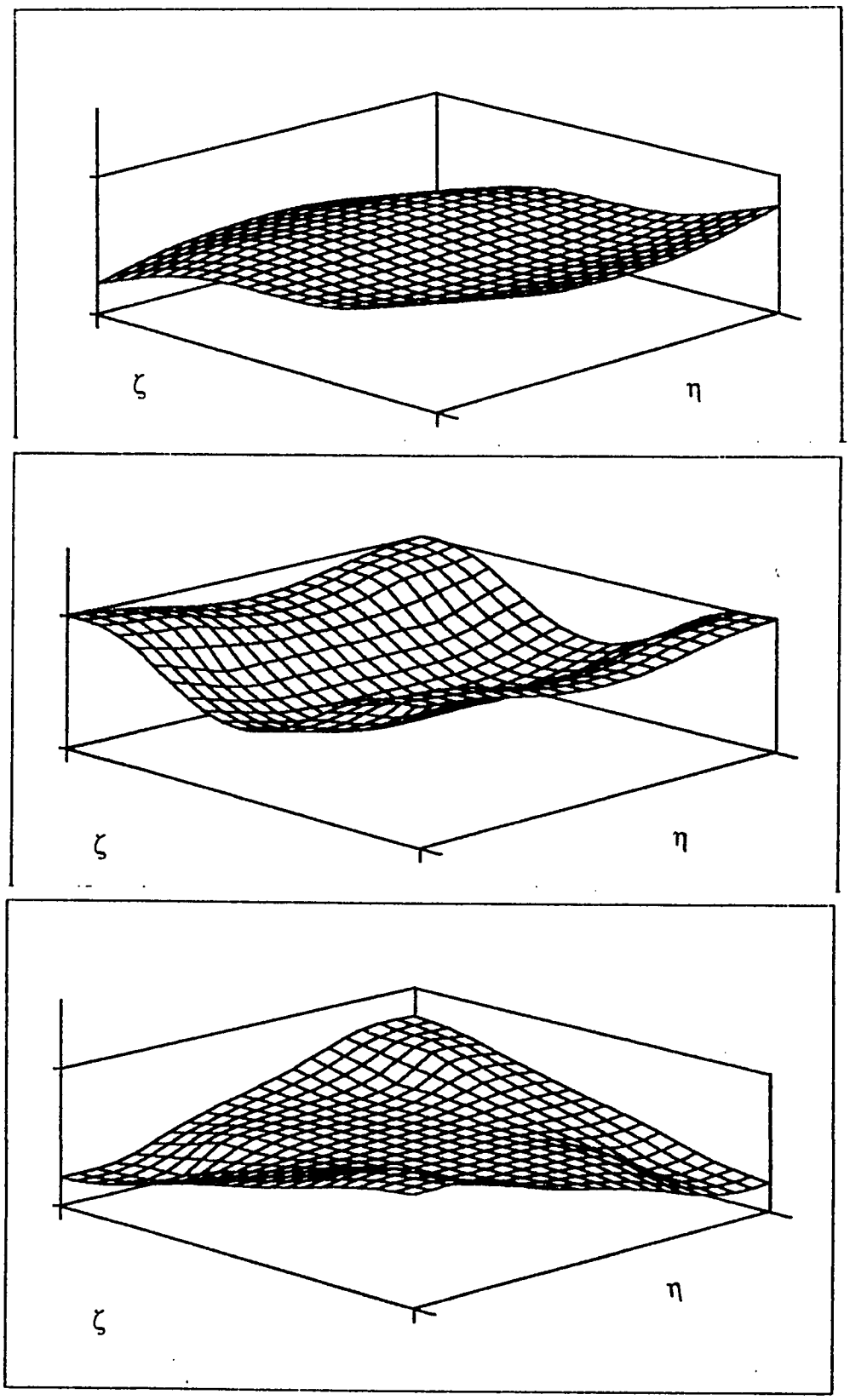

Figure A.a.16 : Mode Shapes for the Fourth Frequency
Point Supported : $\alpha = 0.2$

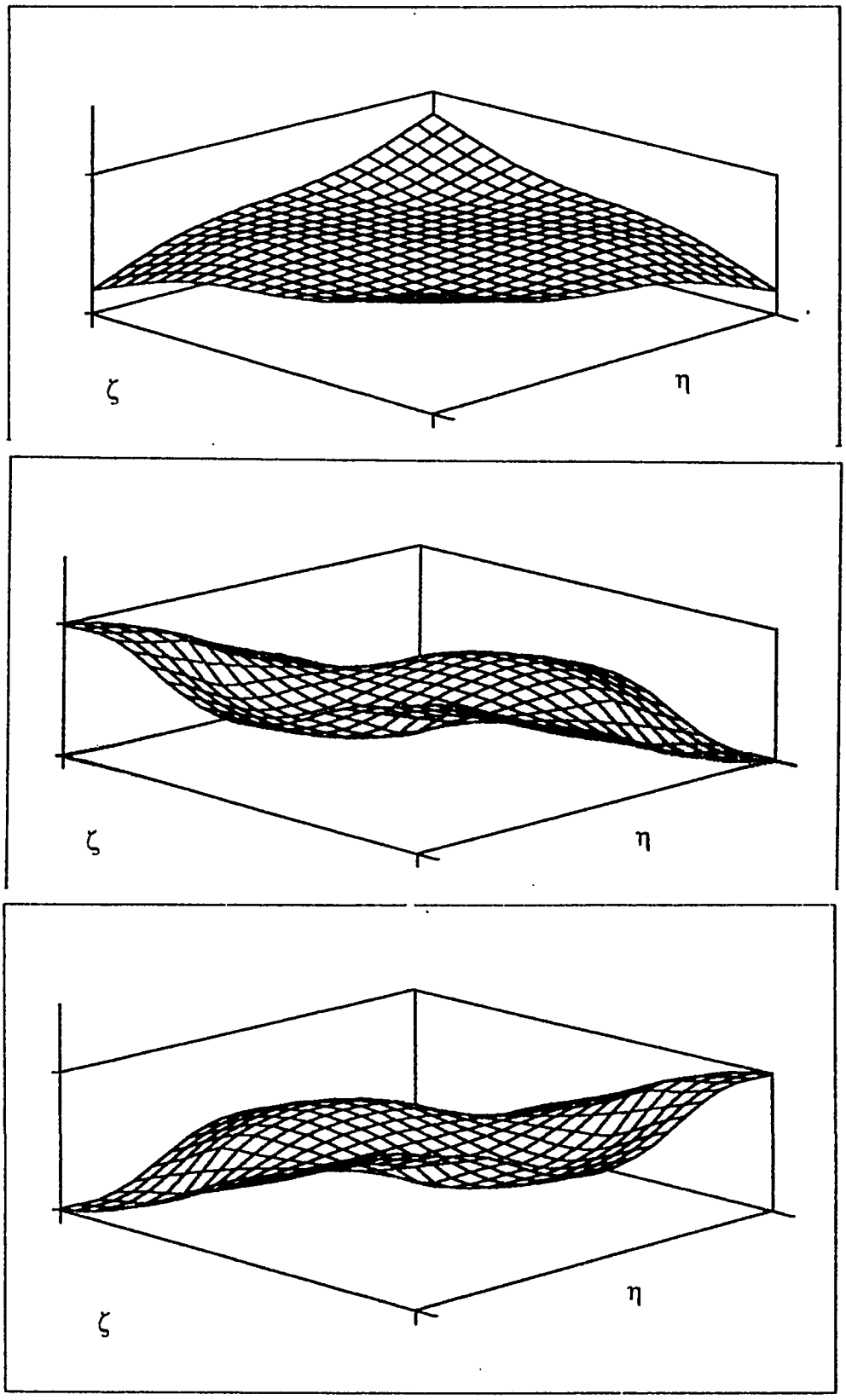

Figure A.a.17 : Mode Shapes for the Fifth Frequency
Point Supported : α = 0.2

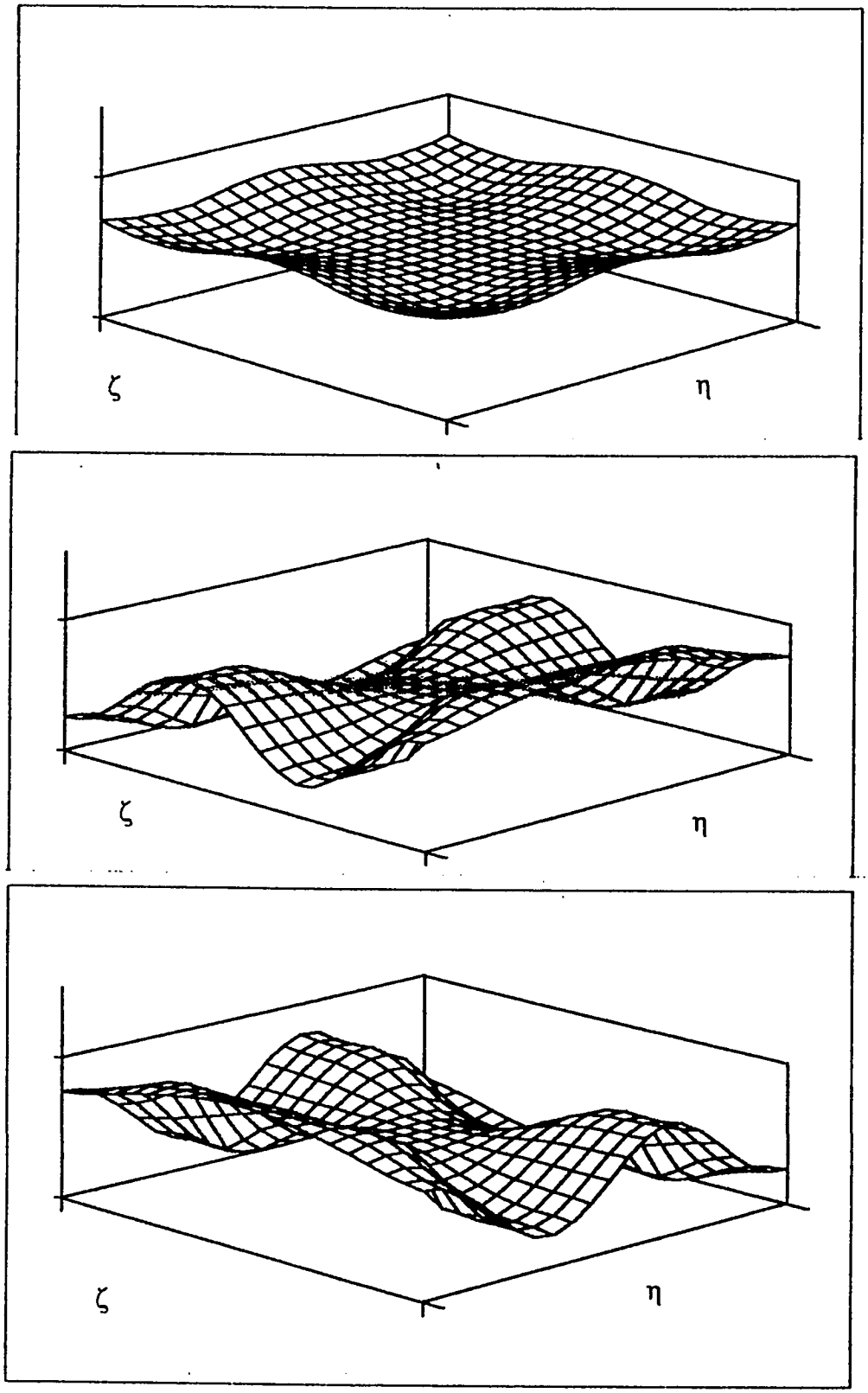

Figure A.a.18 : Mode Shapes for the Sixth Frequency
Point Supported : $\alpha = 0.2$

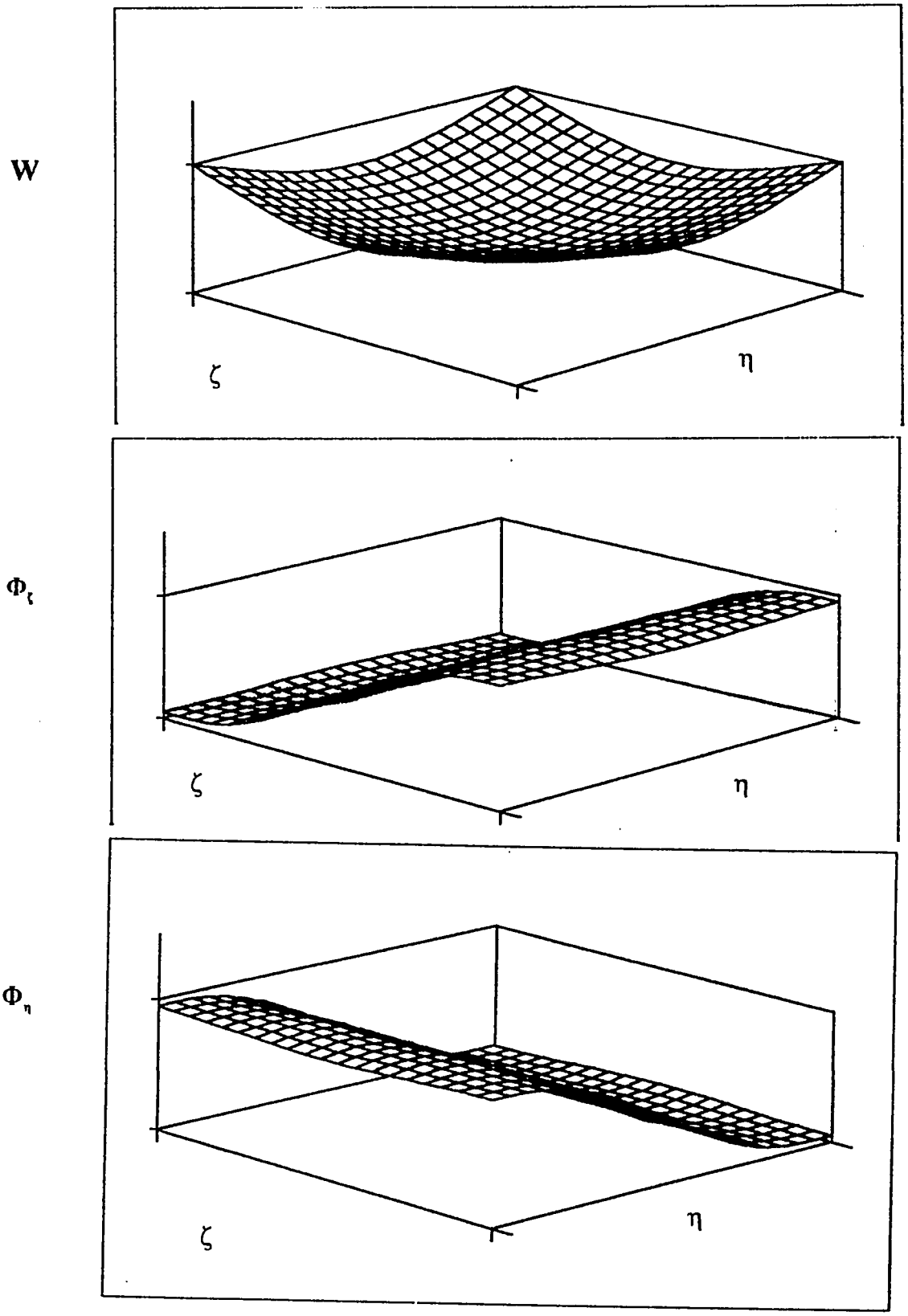

Figure A.a.19 : Mode Shapes for the First Frequency
Point Supported : $\alpha = 0.3$

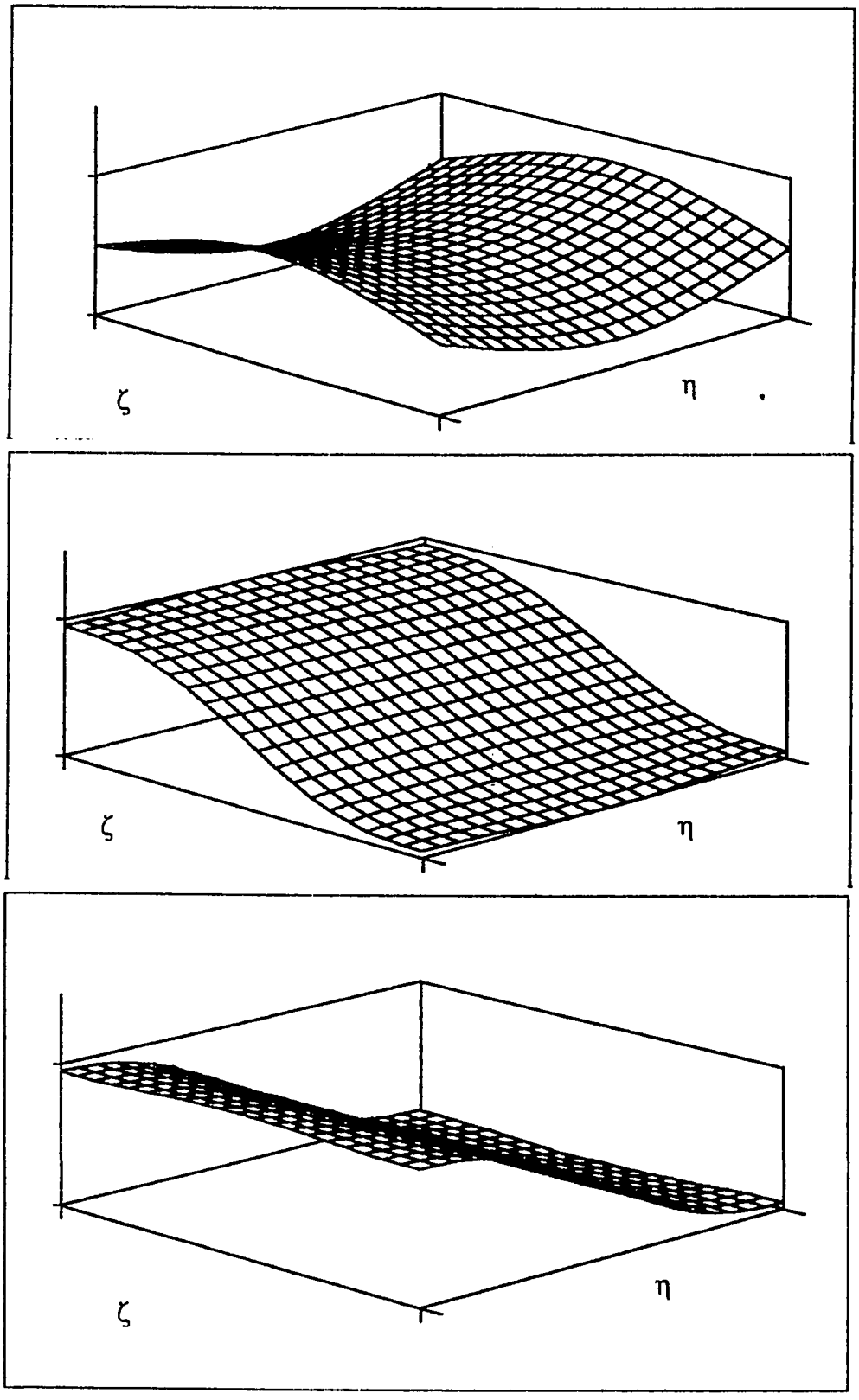

Figure A.a.20 : Mode Shapes for the Second Frequency
Point Supported : $\alpha = 0.3$

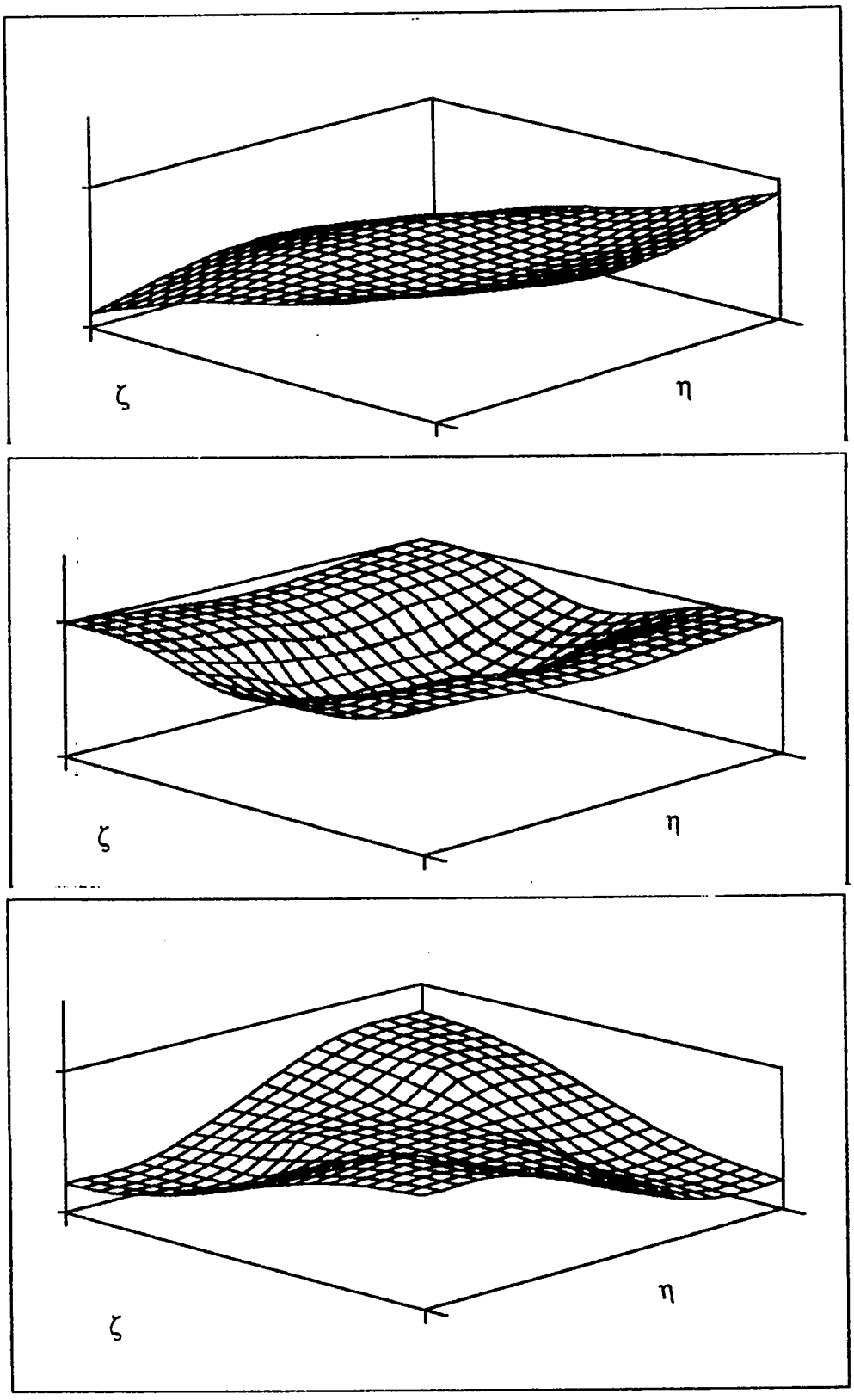

Figure A.a.21 : Mode Shapes for the Third Frequency
Point Supported : α = 0.3

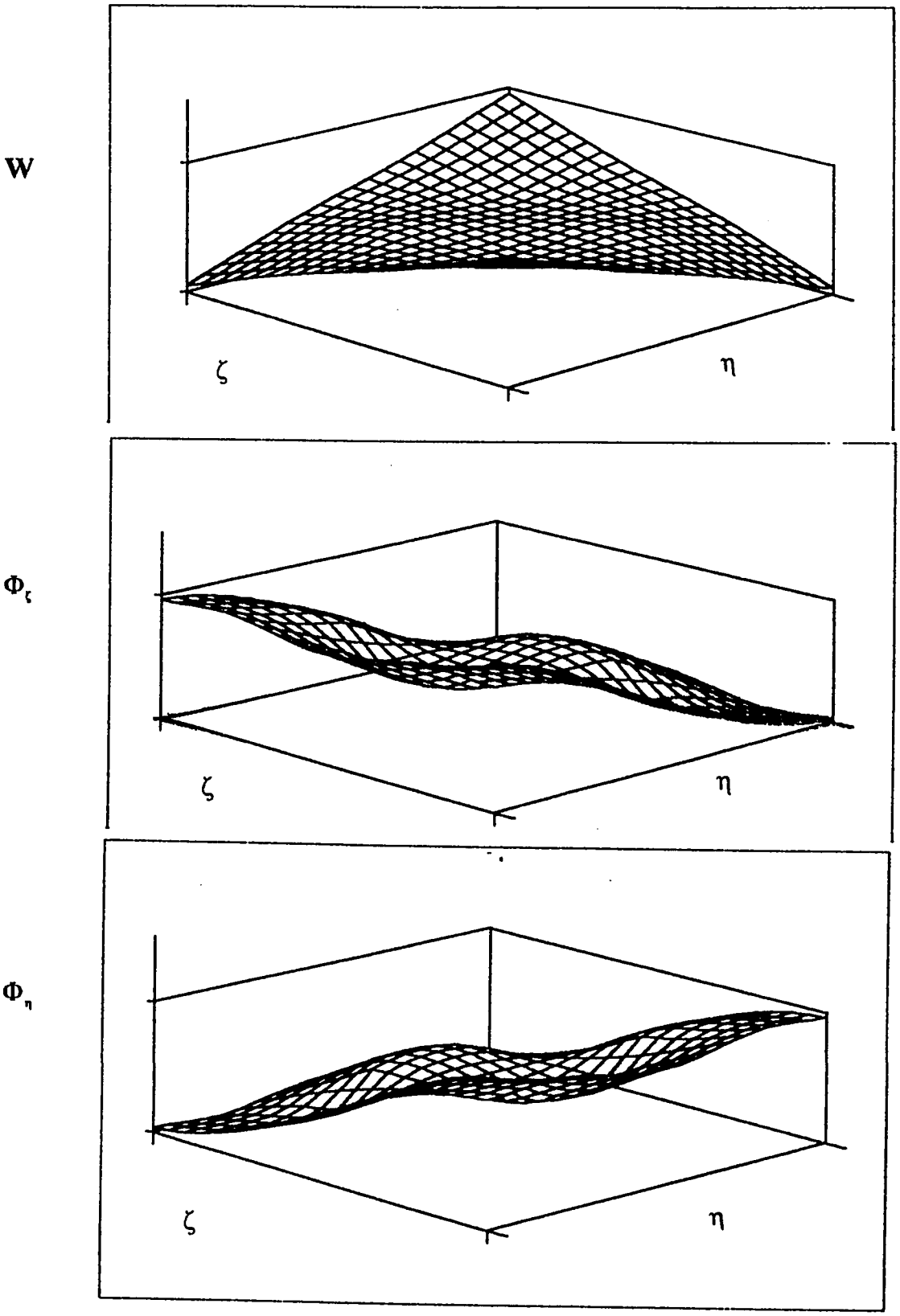

Figure A.a.22 : Mode Shapes for the Fourth Frequency
Point Supported : $\alpha = 0.3$

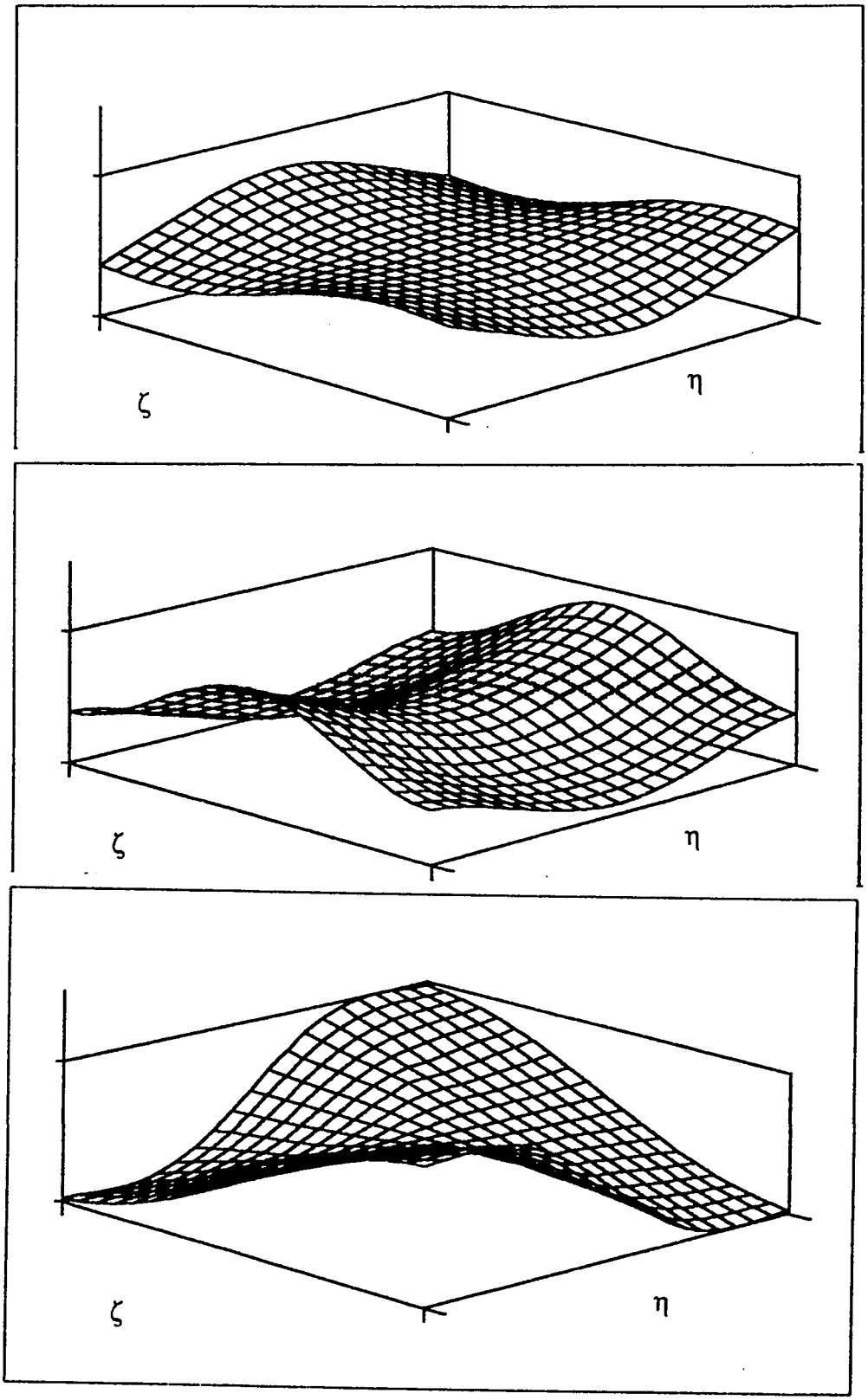

Figure A.a.23 : Mode Shapes for the Fifth Frequency
Point Supported : $\alpha = 0.3$

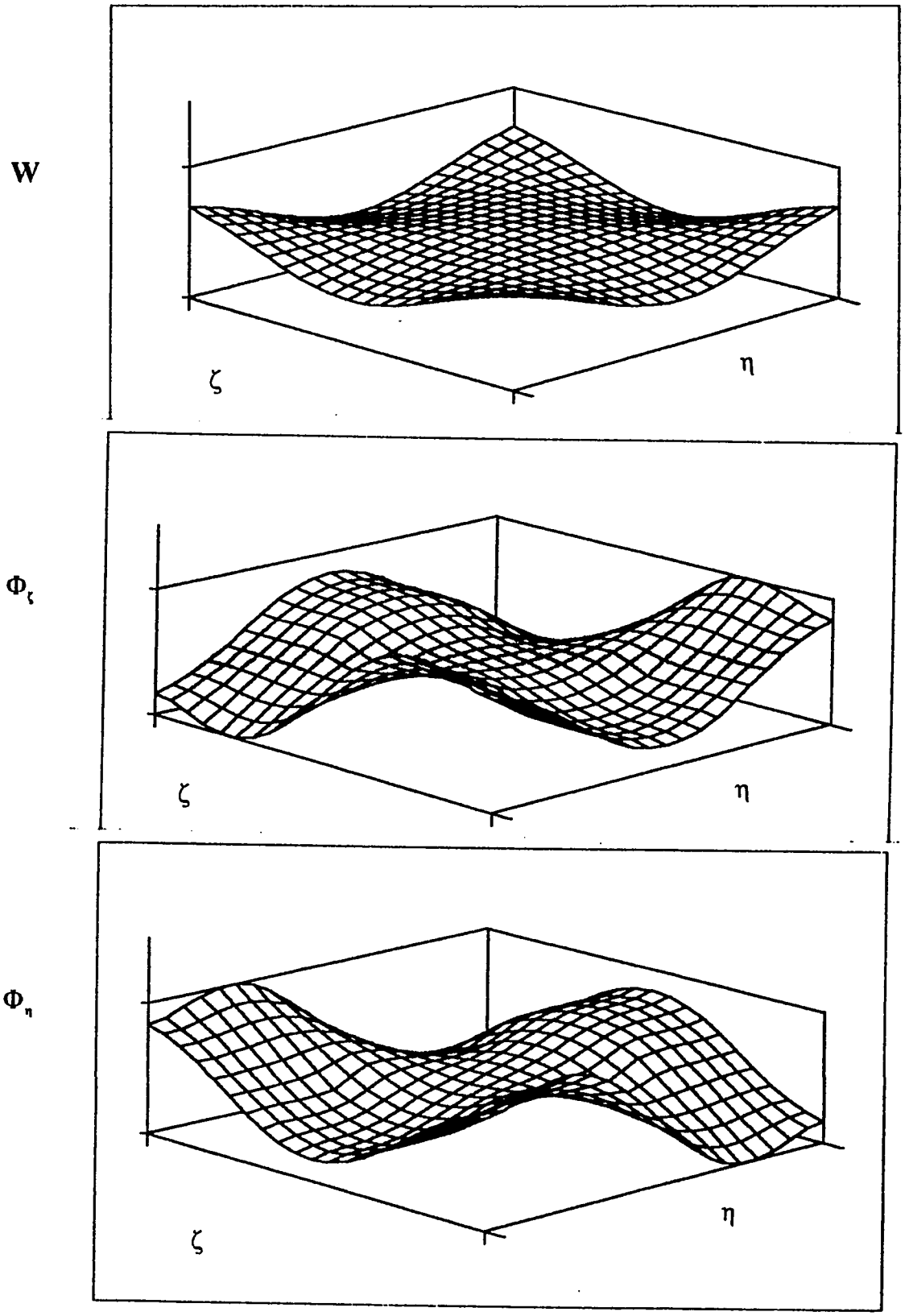

Figure A.a.24 : Mode Shapes for the Sixth Frequency
Point Supported : $\alpha = 0.3$

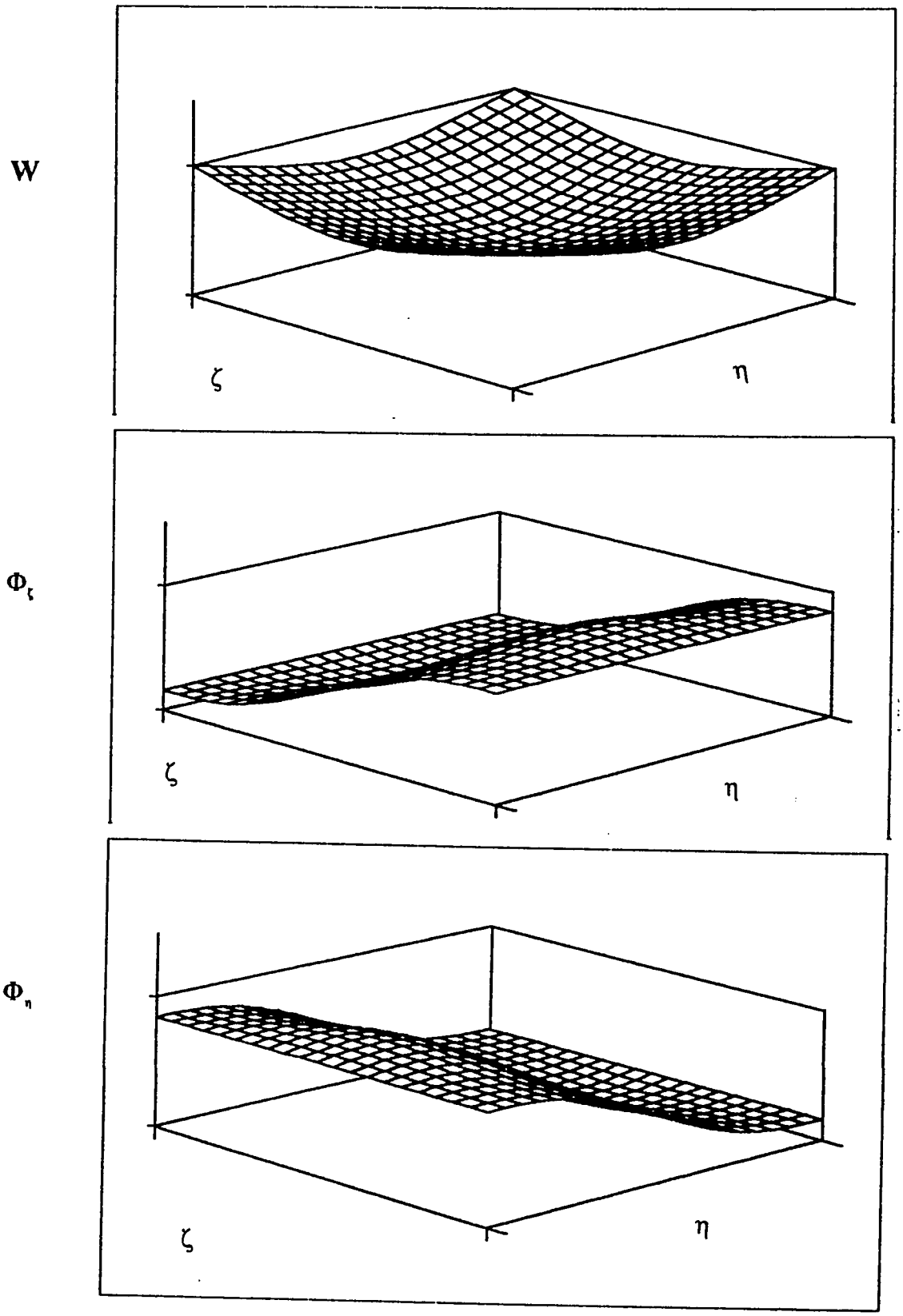

Figure A.a.25 : Mode Shapes for the First Frequency
Point Supported : $\alpha = 0.4$

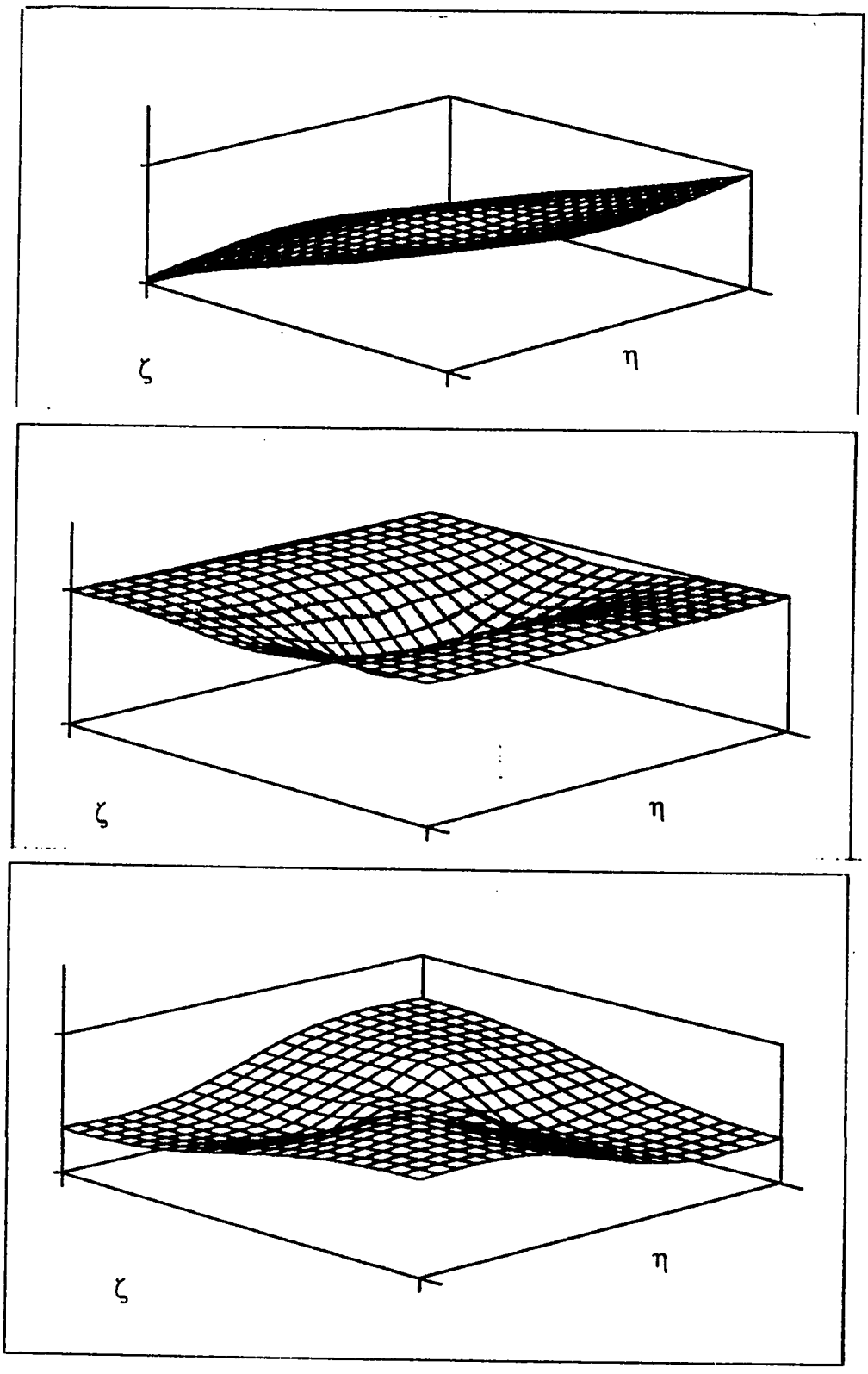

Figure A.a.26 : Mode Shapes for the Second Frequency
Point Supported : $\alpha = 0.4$

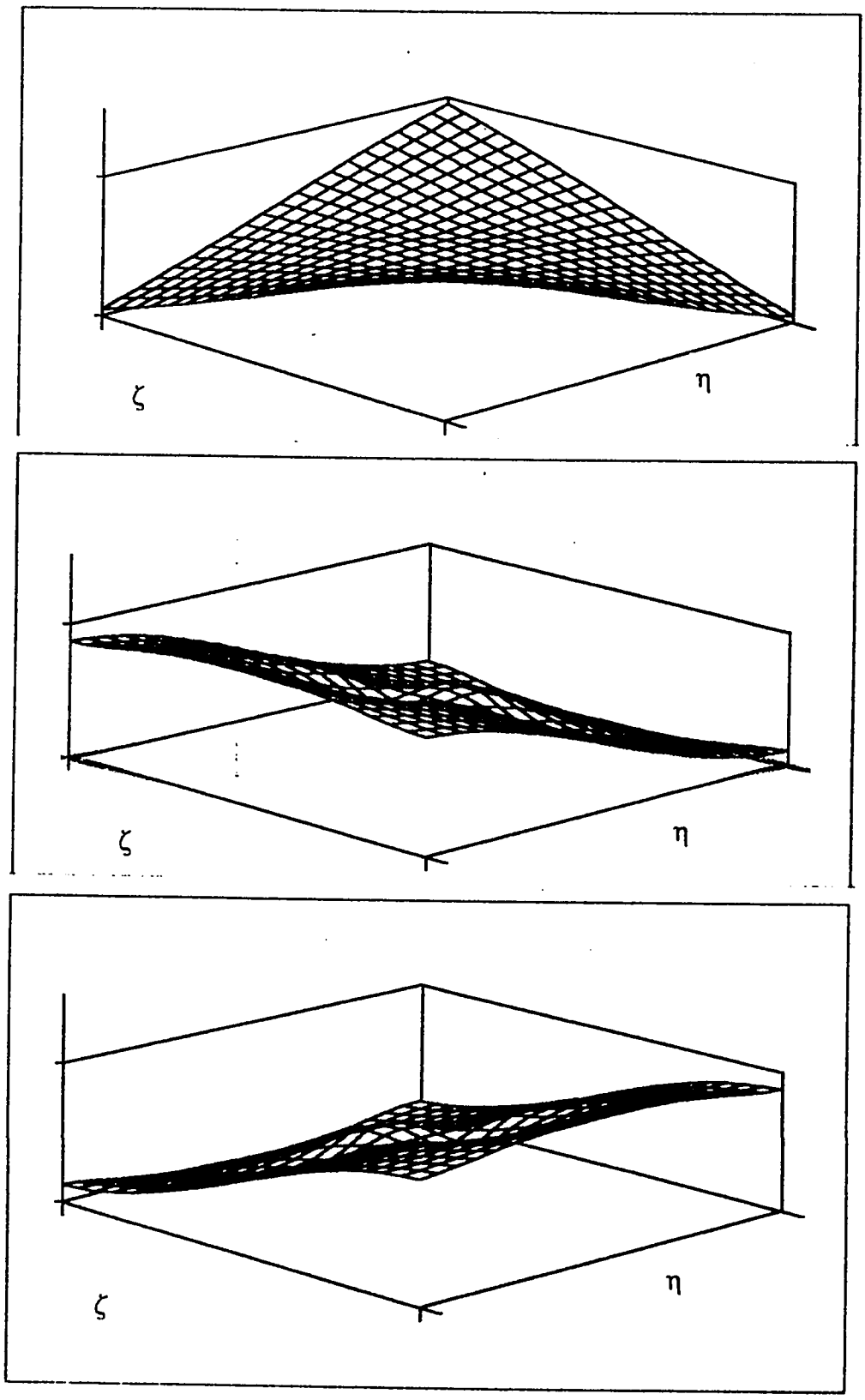

Figure A.a.27 : Mode Shapes for the Third Frequency
Point Supported : $\alpha = 0.4$

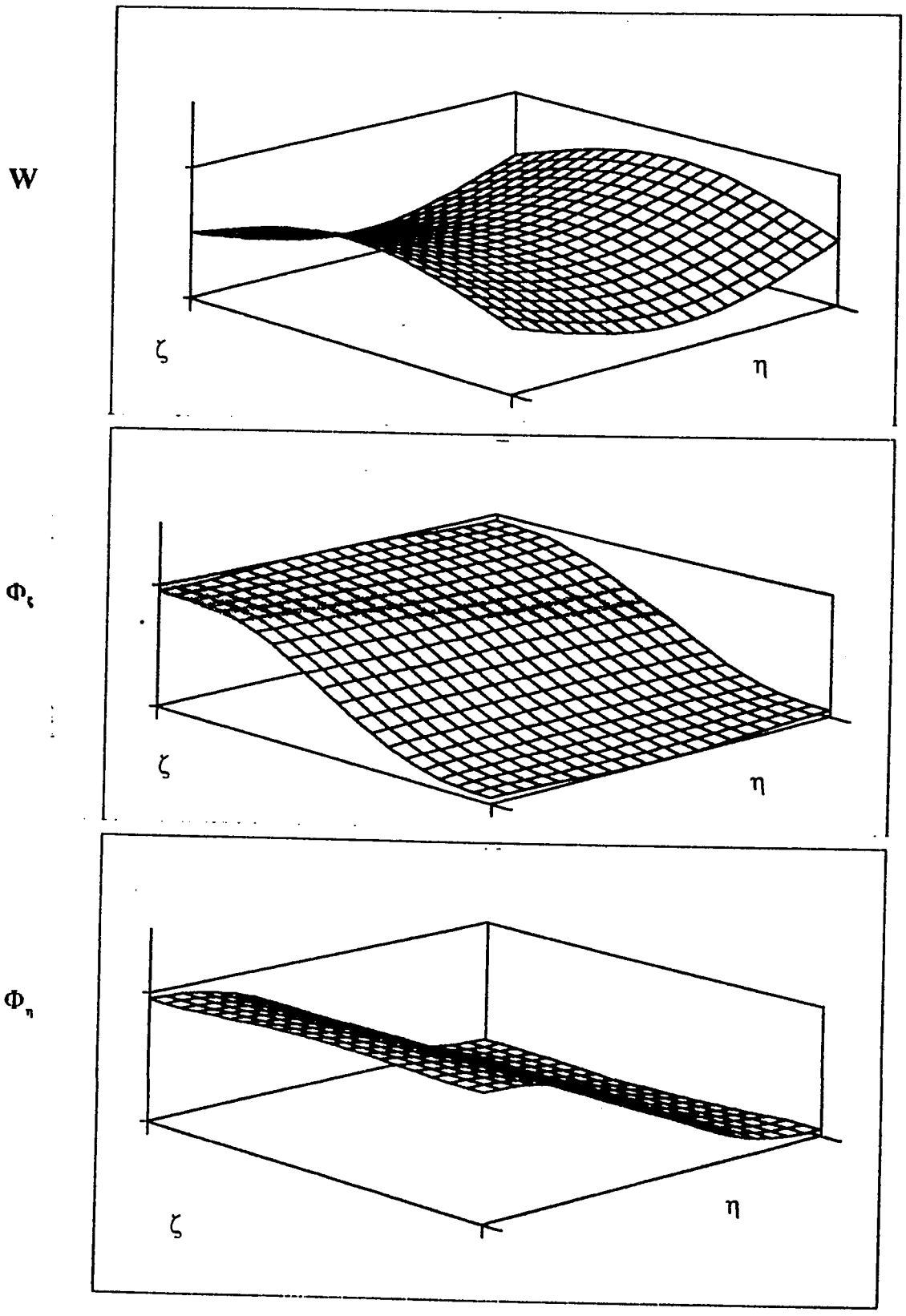

Figure A.a.28 : Mode Shapes for the Fourth Frequency
Point Supported : $\alpha = 0.4$

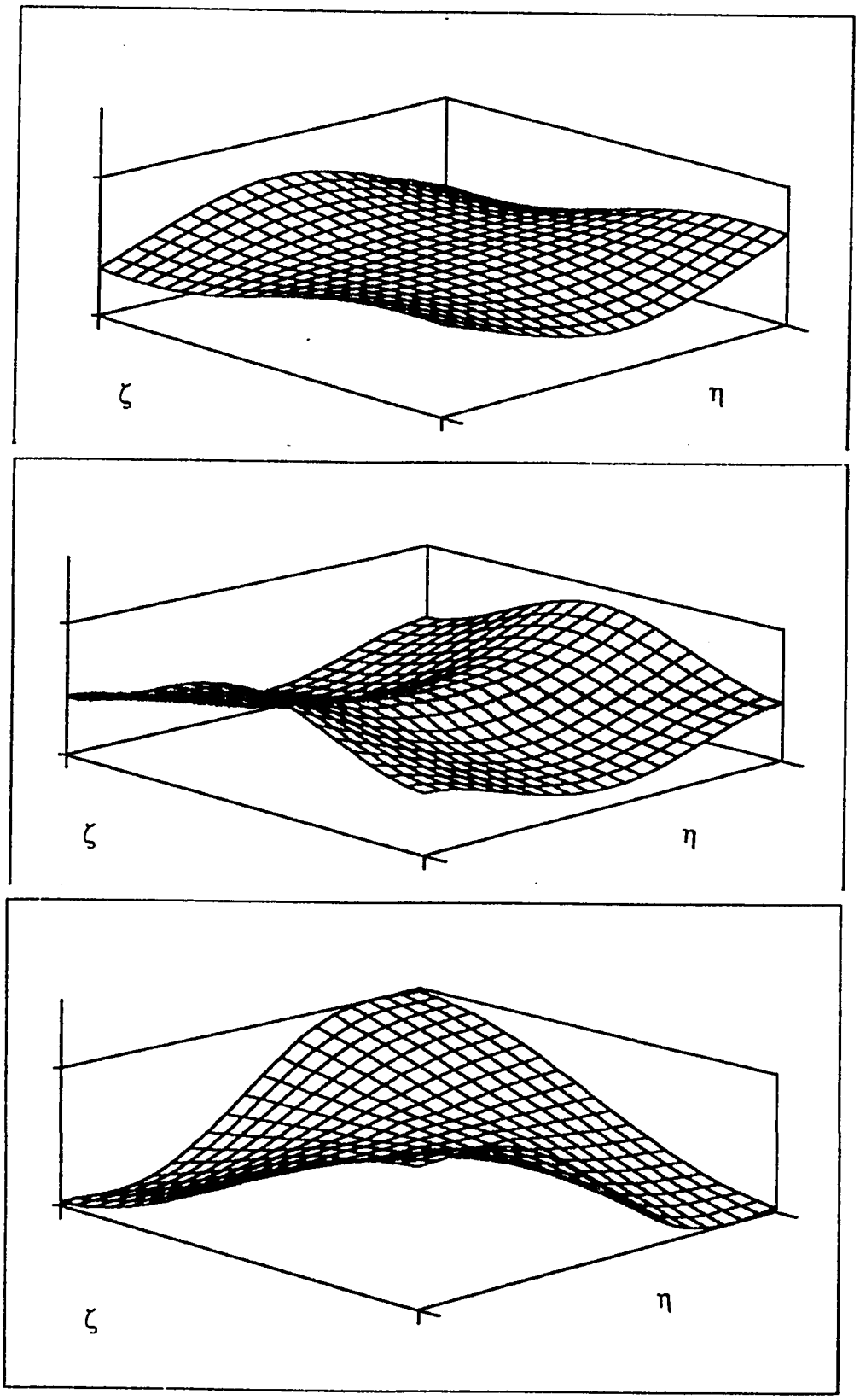

Figure A.a.29 : Mode Shapes for the Fifth Frequency
Point Supported : $\alpha = 0.4$

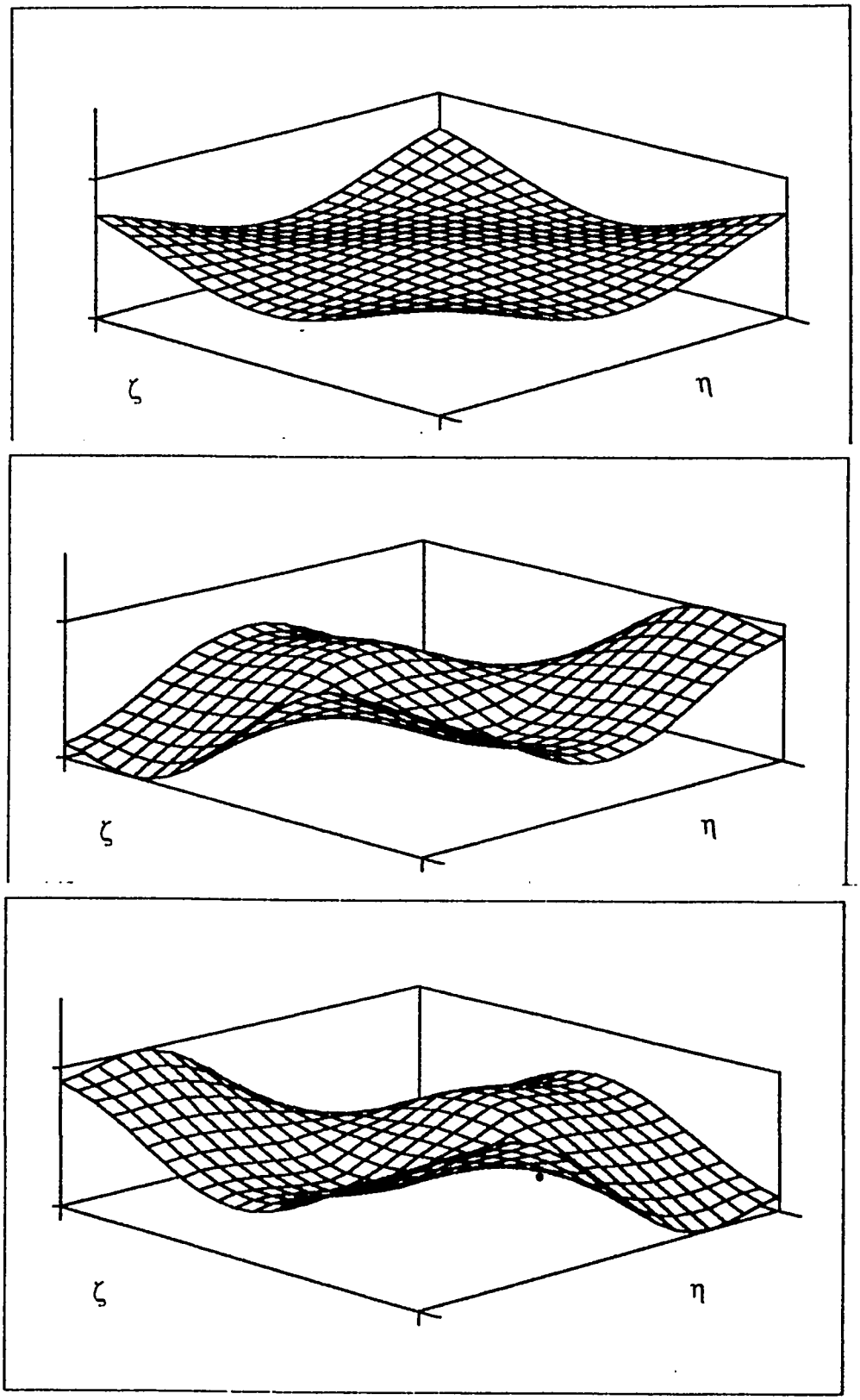

Figure A.a.30 : Mode Shapes for the Sixth Frequency
Point Supported : $\alpha = 0.4$

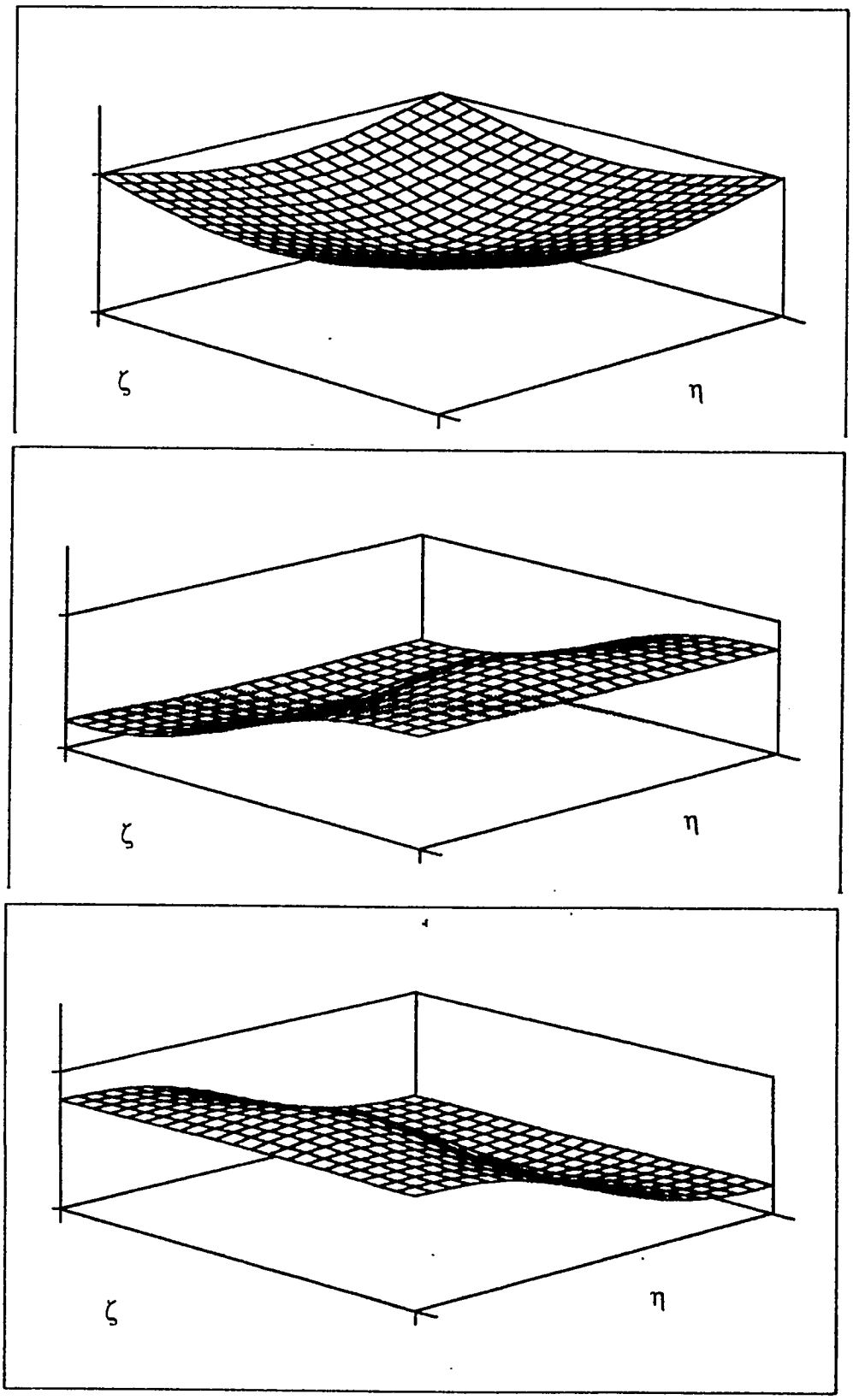

Figure A.a.31 : Mode Shapes for the First Frequency
Point Supported : $\alpha = 0.5$

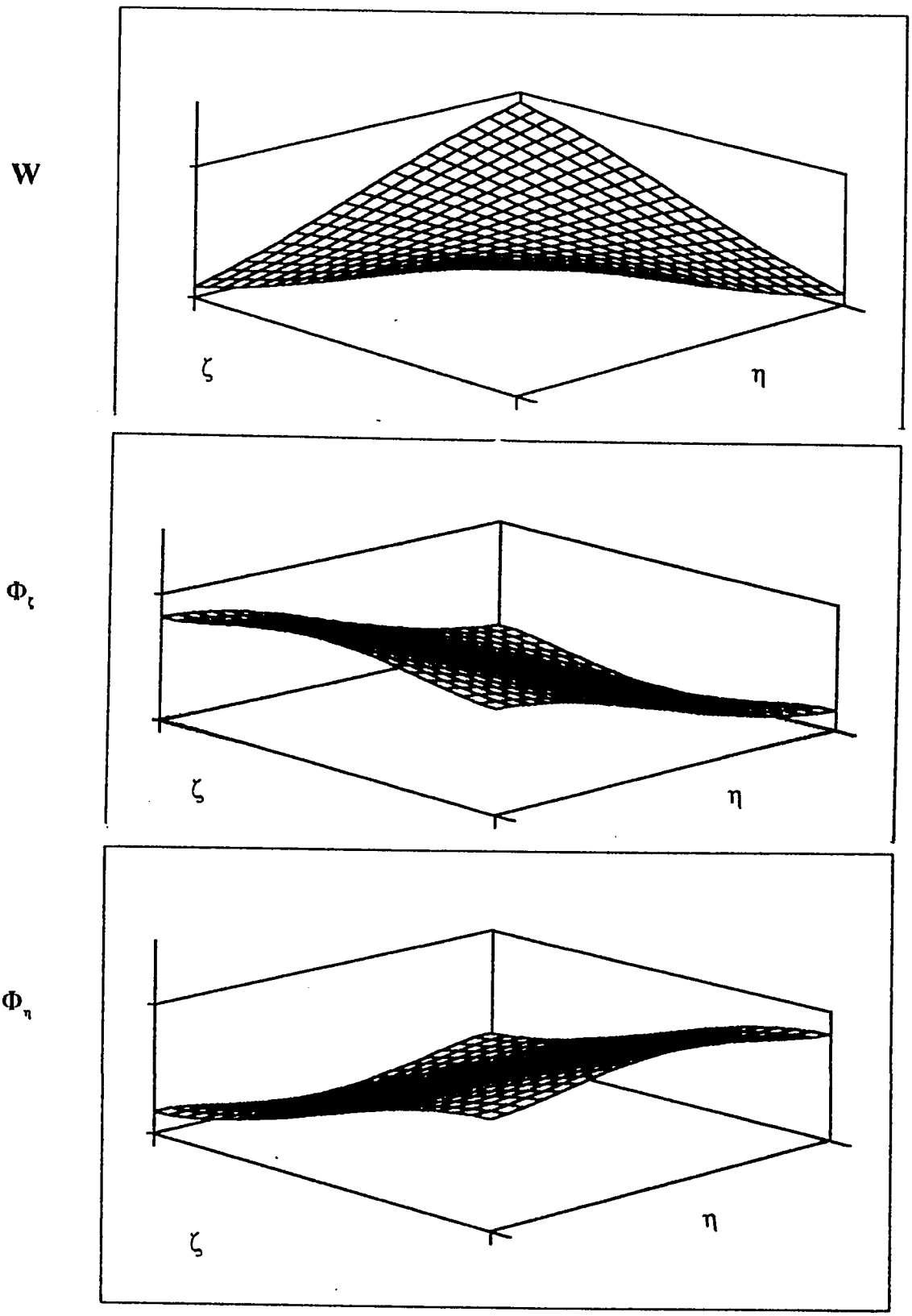

Figure A.a.32 : Mode Shapes for the Second Frequency
Point Supported : $\alpha = 0.5$

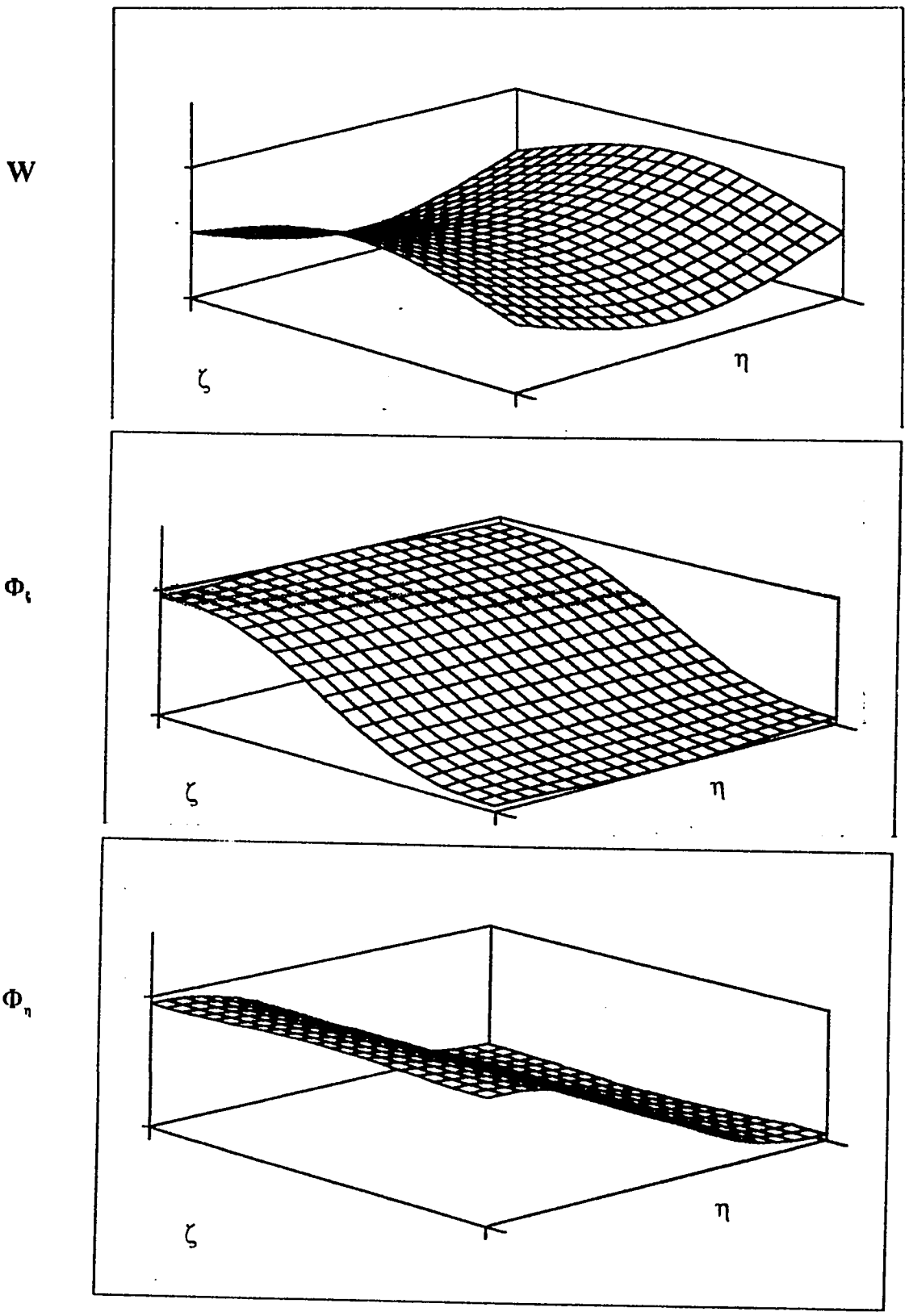

Figure A.a.33 : Mode Shapes for the Third Frequency
Point Supported : $\alpha = 0.5$

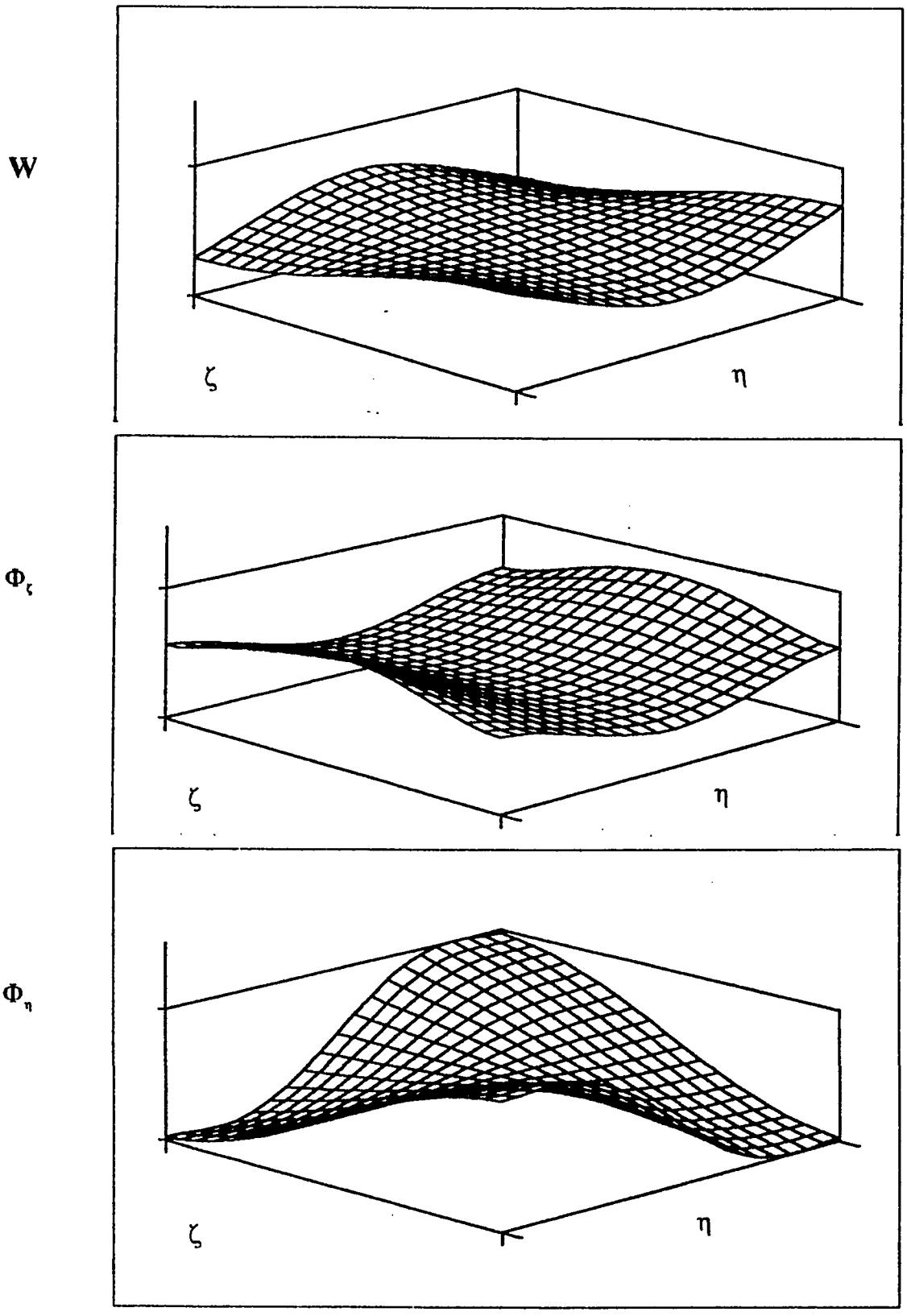

Figure A.a.34 : Mode Shapes for the Fourth Frequency
Point Supported : $\alpha = 0.5$

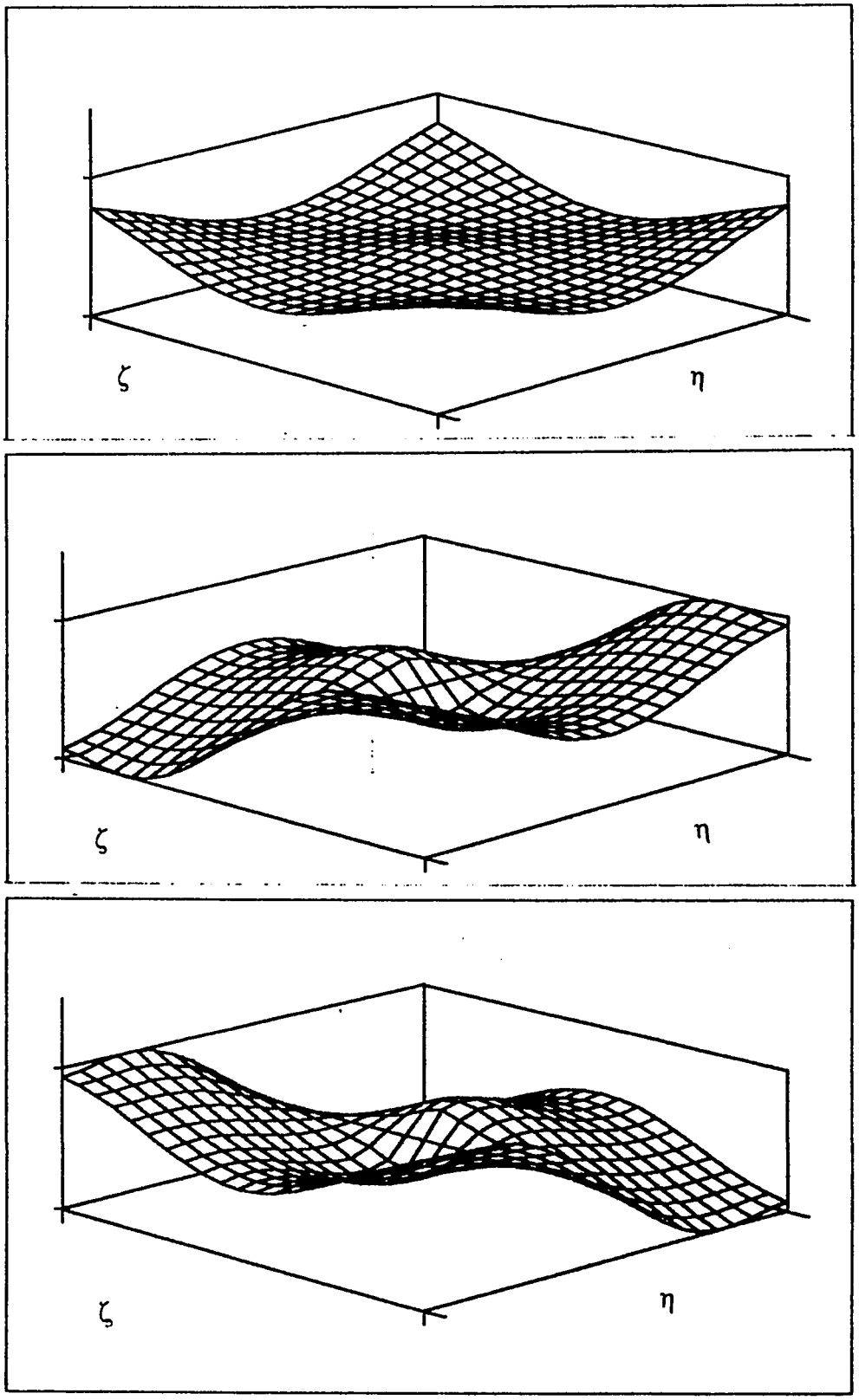

Figure A.a.35 : Mode Shapes for the Fifth Frequency
Point Supported : α = 0.5

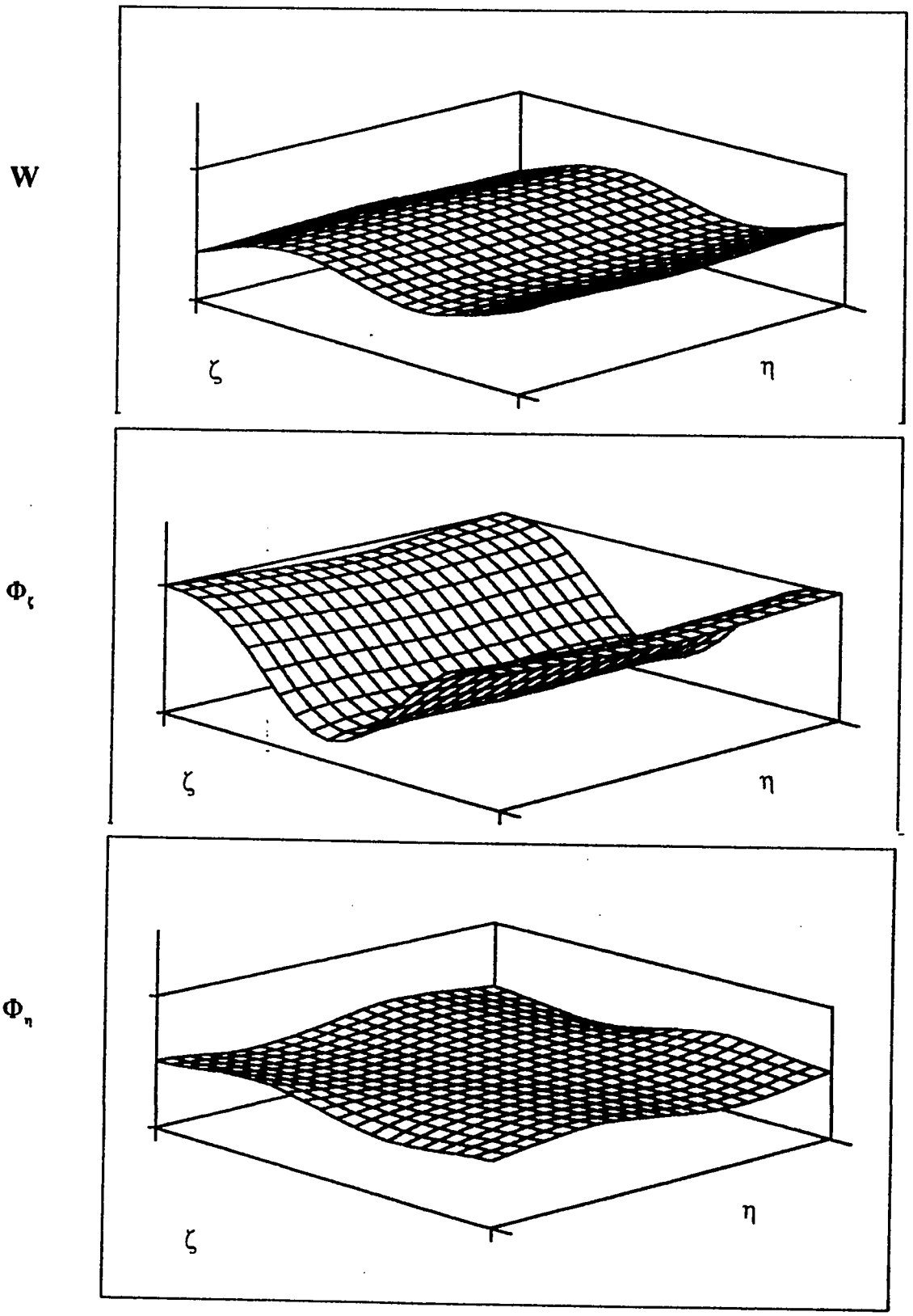

Figure A.a.36 : Mode Shapes for the Sixth Frequency
Point Supported : $\alpha = 0.5$

APPENDIX A.b

NODAL PATTERNS

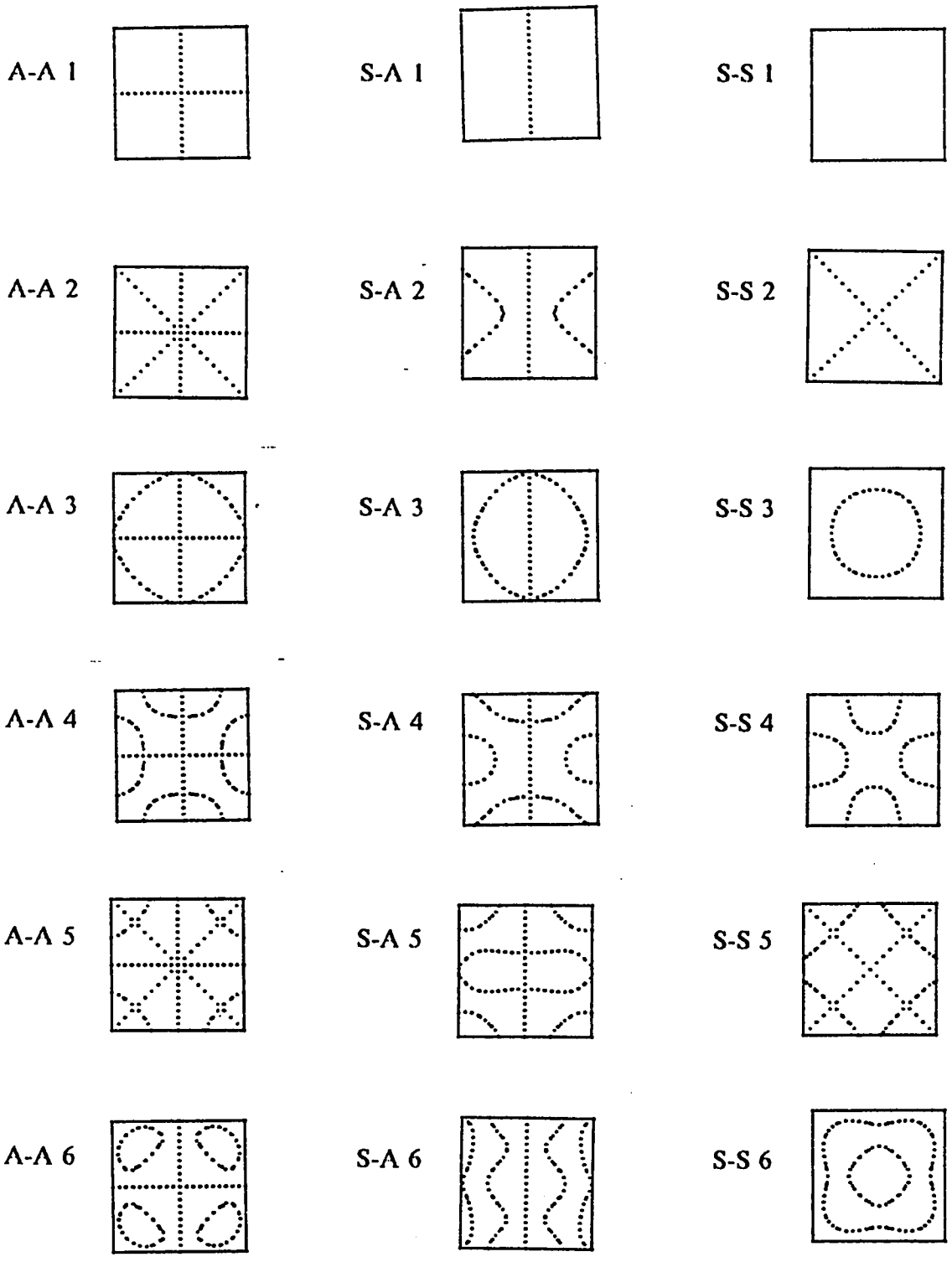

Figure A.b.1 : Nodal pattern
$\alpha = 0.0$, $\beta = 0.2000$.

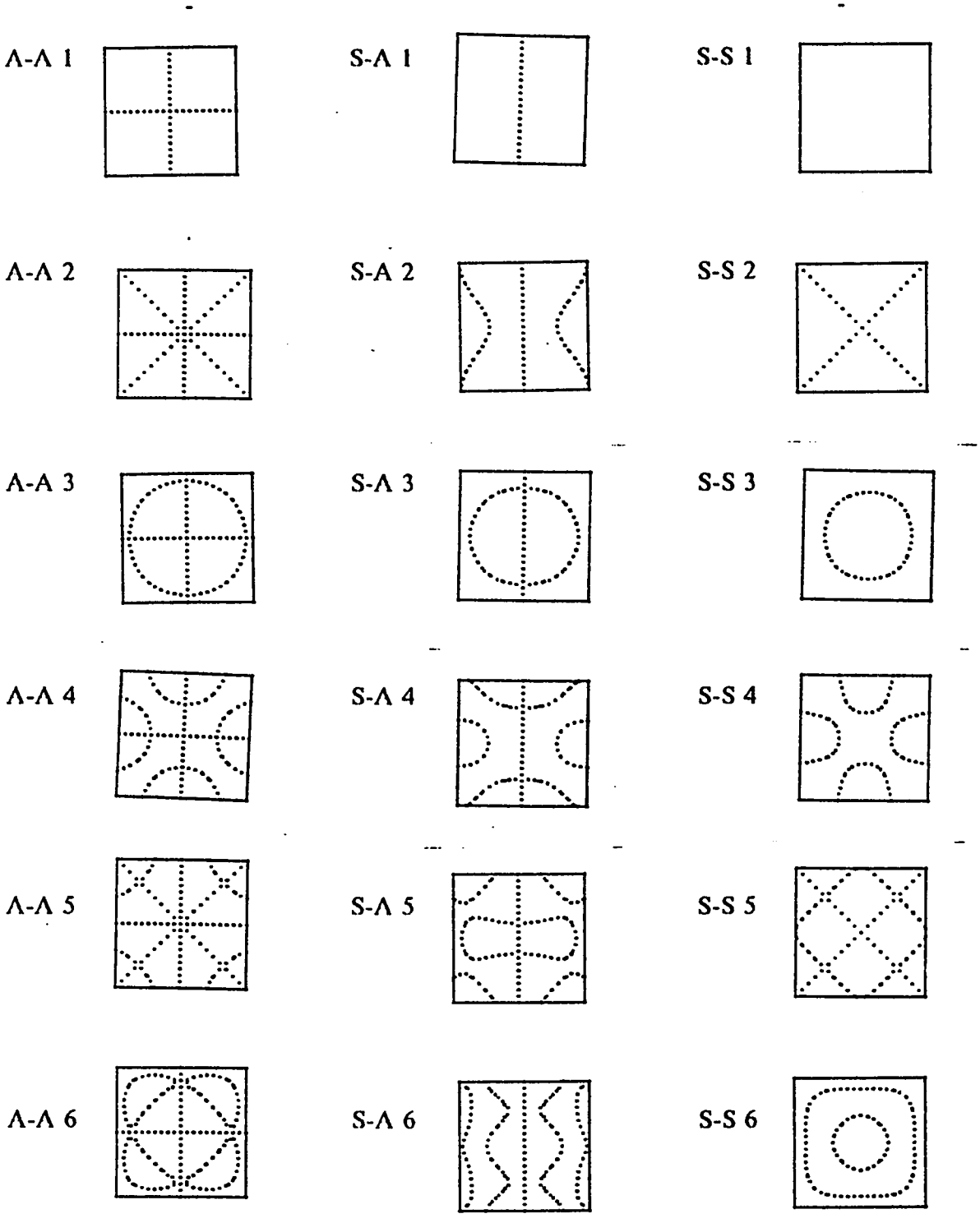

Figure A.b.2 : Nodal pattern
$\alpha = 0.0$, $\beta = 0.0005$.

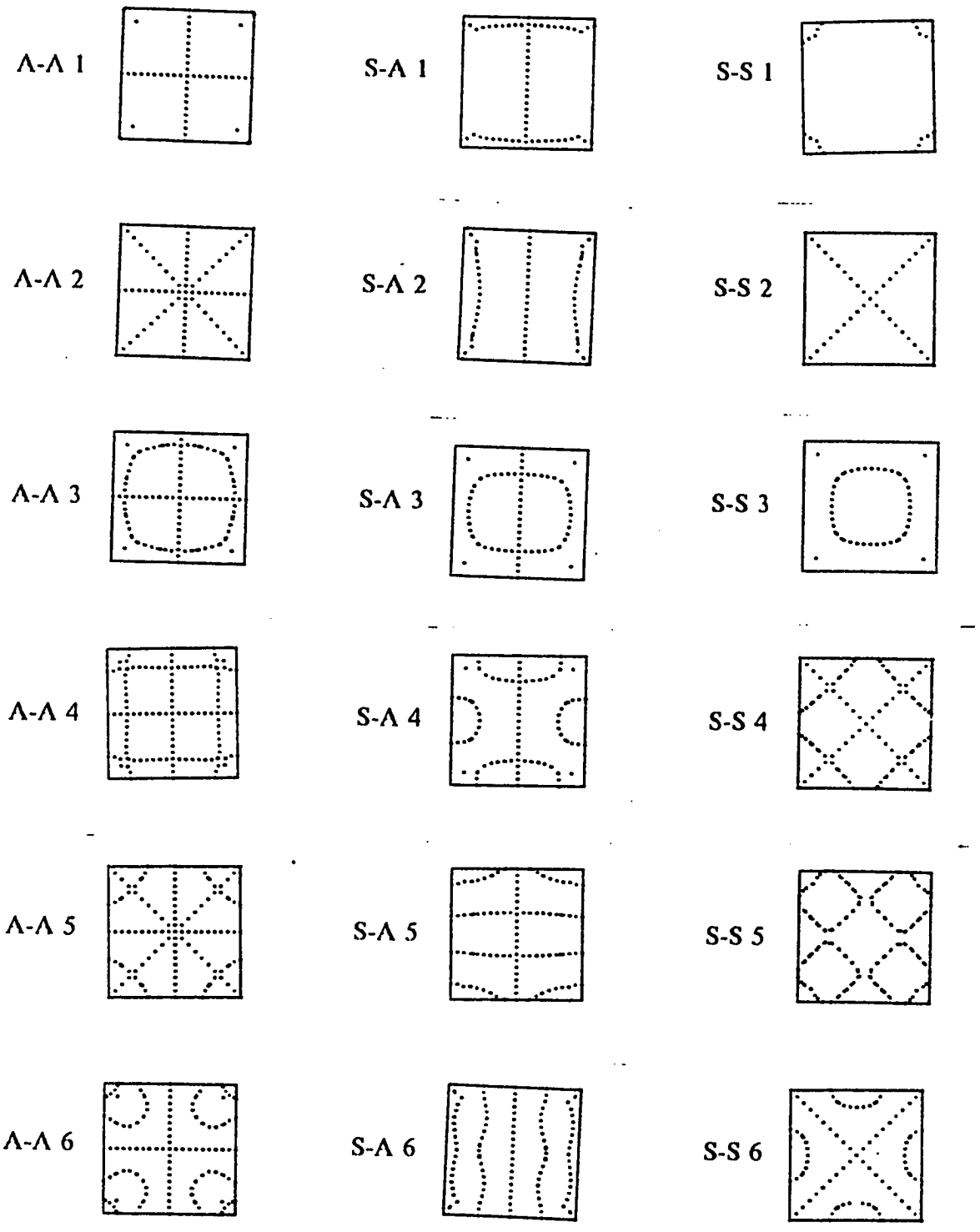

Figure A.b.3 : Nodal pattern
$\alpha = 0.1$, $\beta = 0.2000$.

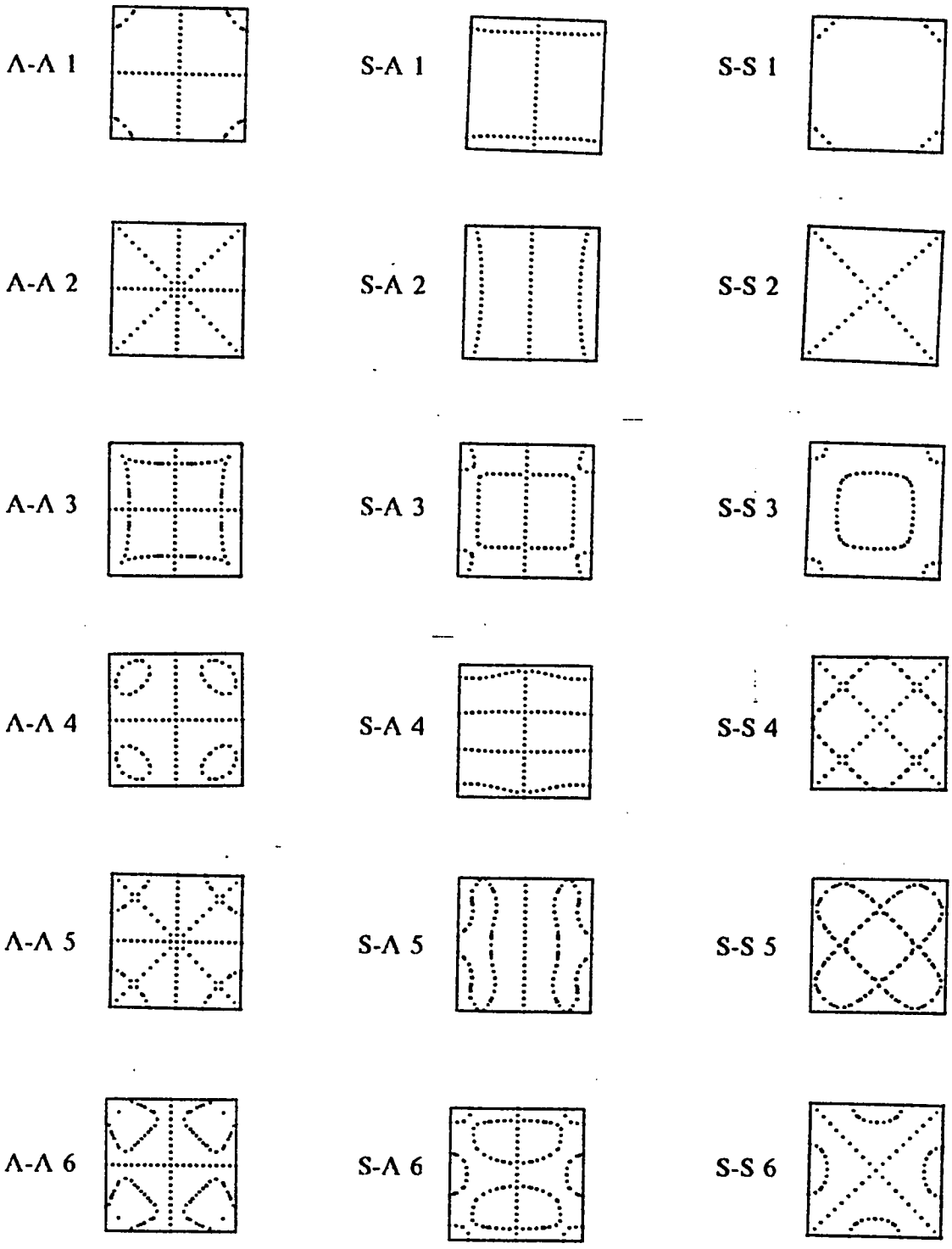

Figure A.b.4 : Nodal pattern
$\alpha = 0.1$, $\beta = 0.0005$.

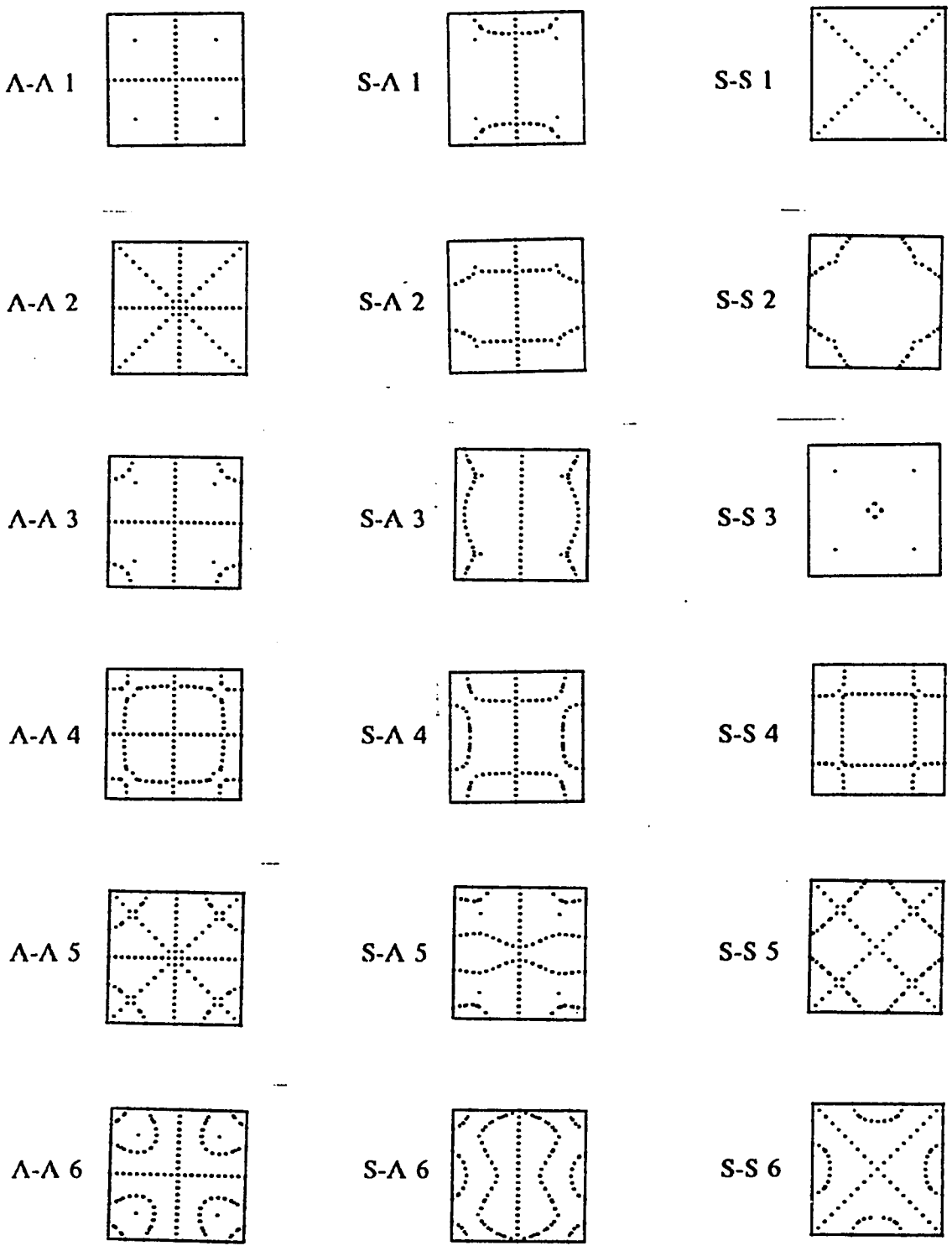

Figure A.b.5 : Nodal pattern
$\alpha = 0.2$, $\beta = 0.2000$.

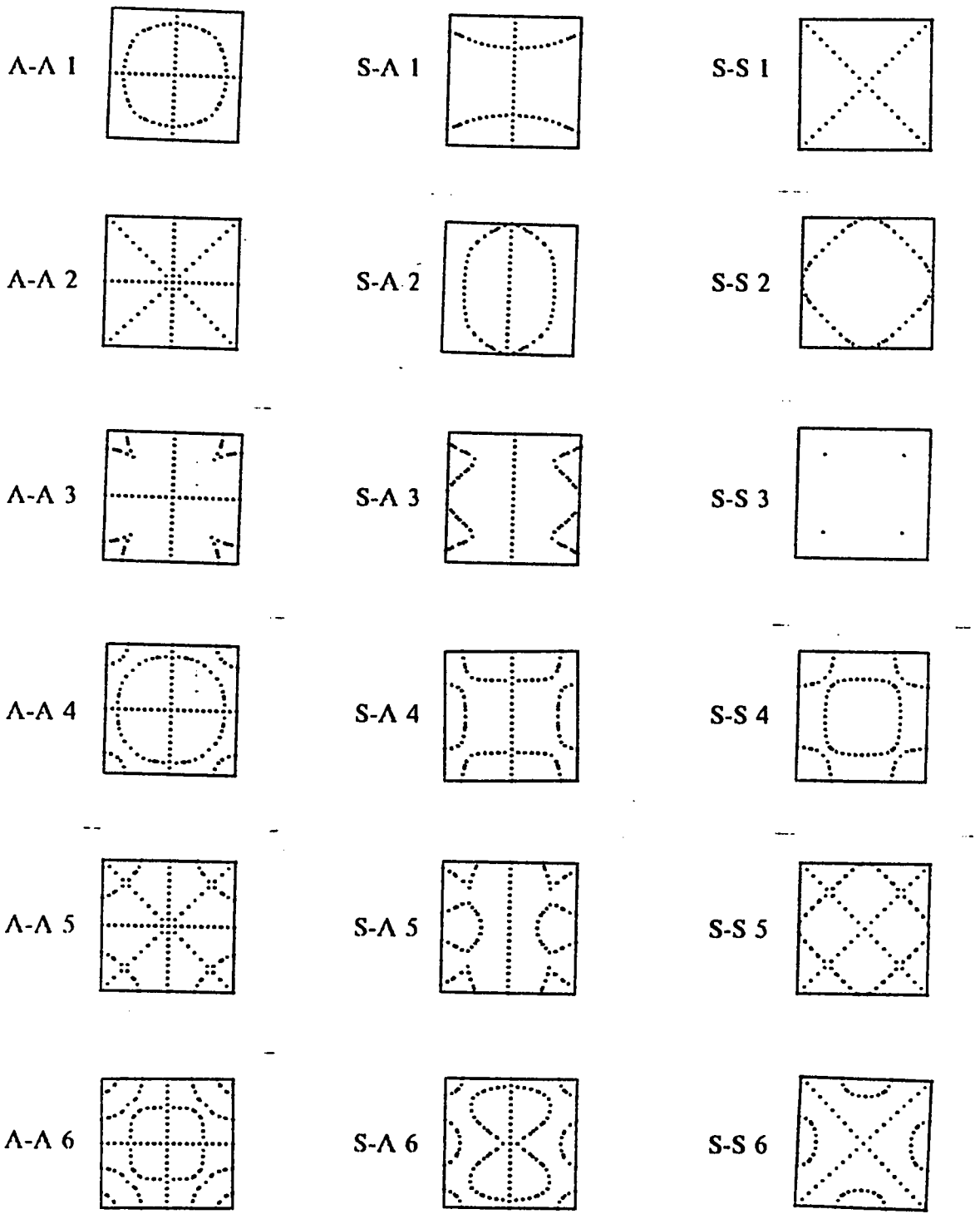

Figure A.b.6 : Nodal pattern
$\alpha = 0.2$, $\beta = 0.0005$.

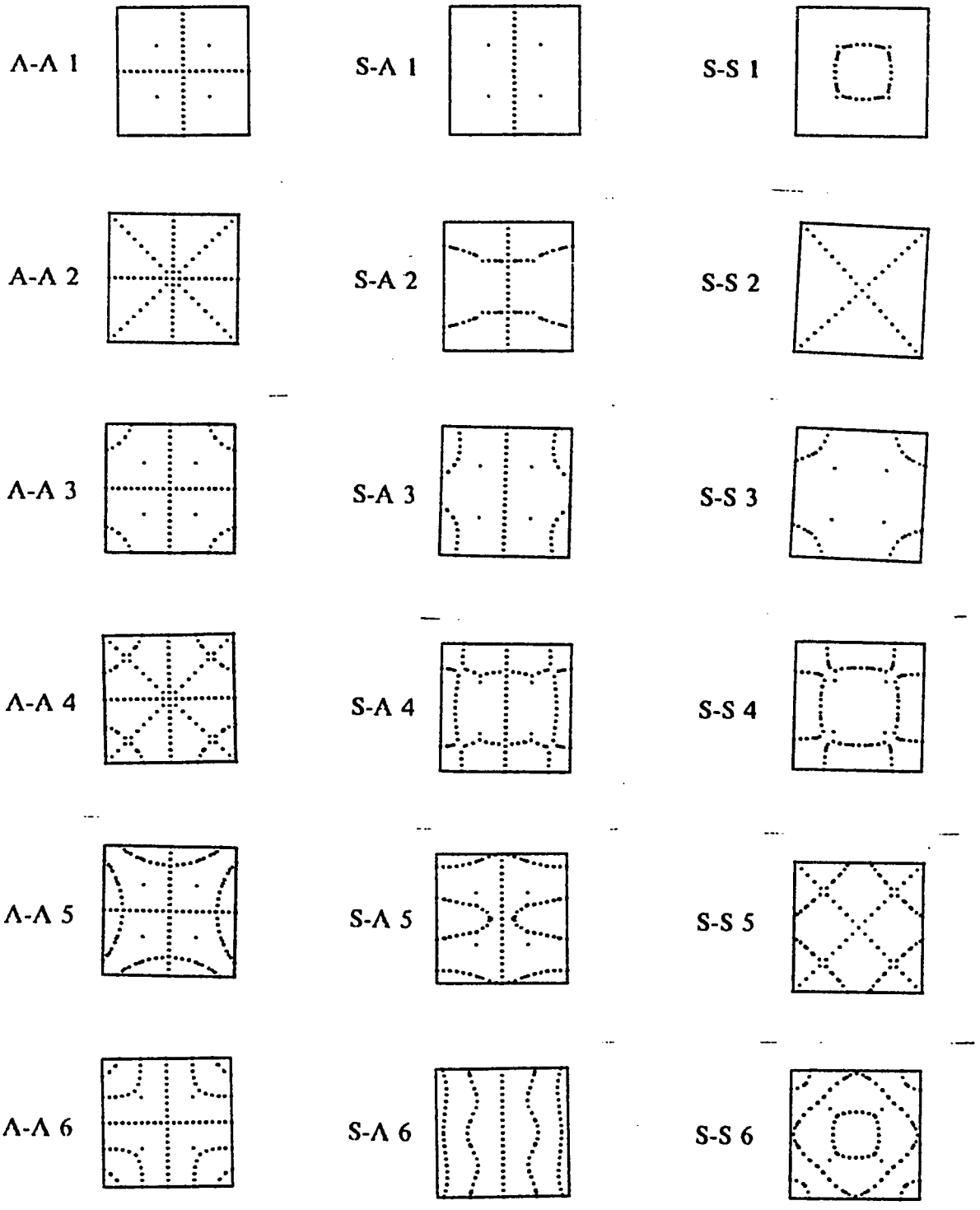

Figure A.b.7 : Nodal pattern
$\alpha = 0.3$, $\beta = 0.2000$.

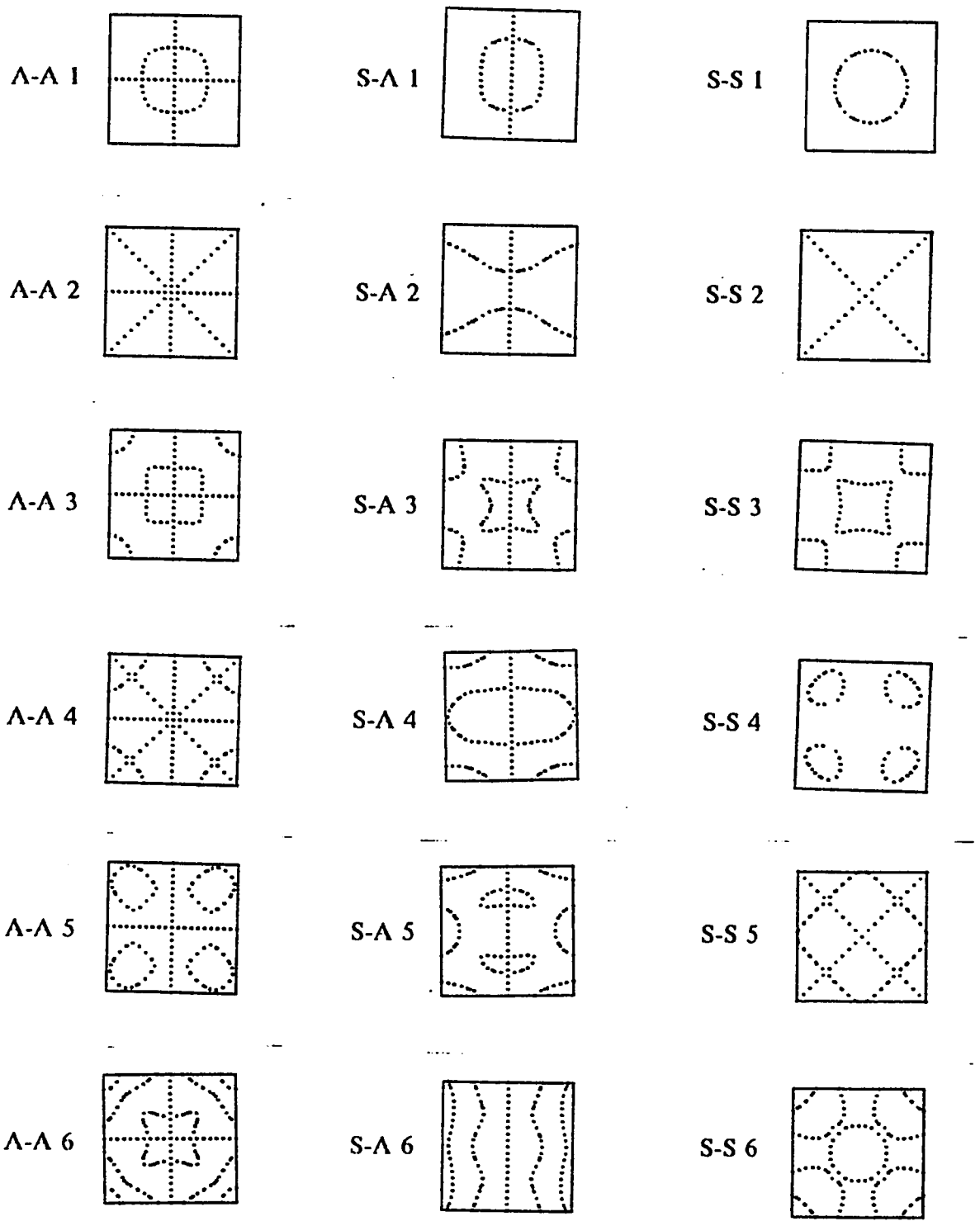

Figure A.b.8 : Nodal pattern
$\alpha = 0.3$, $\beta = 0.0005$.

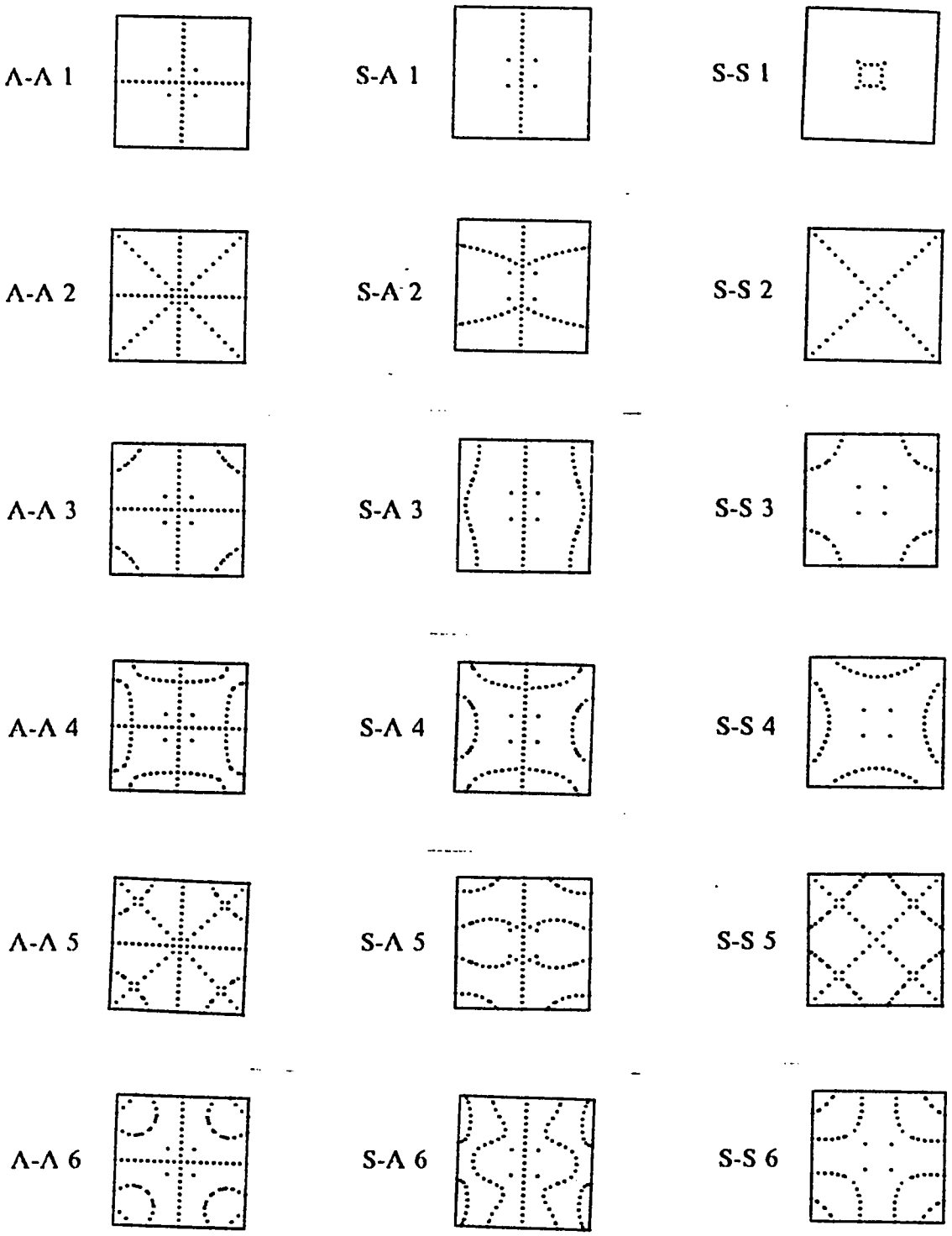

Figure A.b.9 : Nodal pattern
$\alpha = 0.4$, $\beta = 0.2000$.

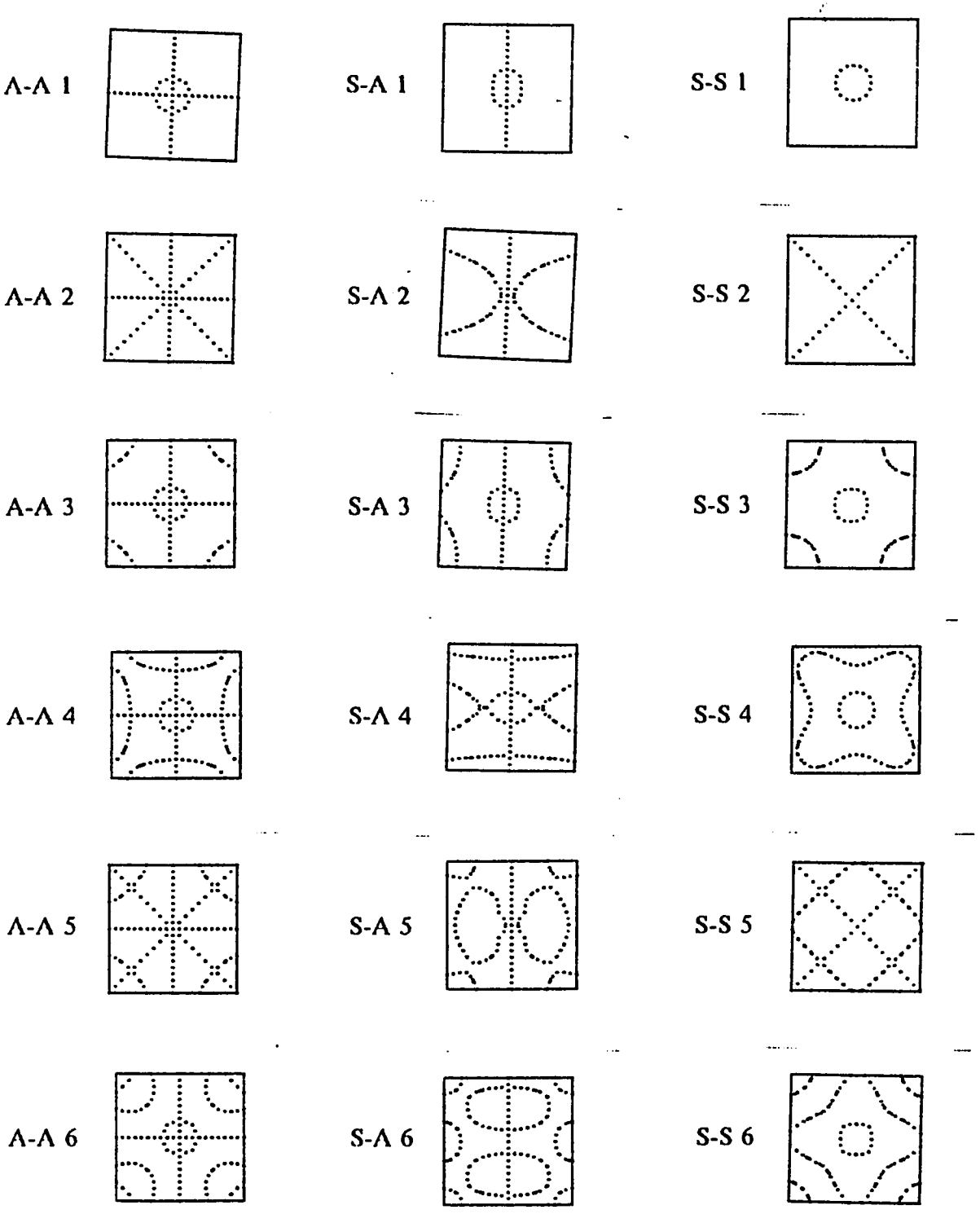

Figure A.b.10 : Nodal pattern
$\alpha = 0.4$, $\beta = 0.0005$.

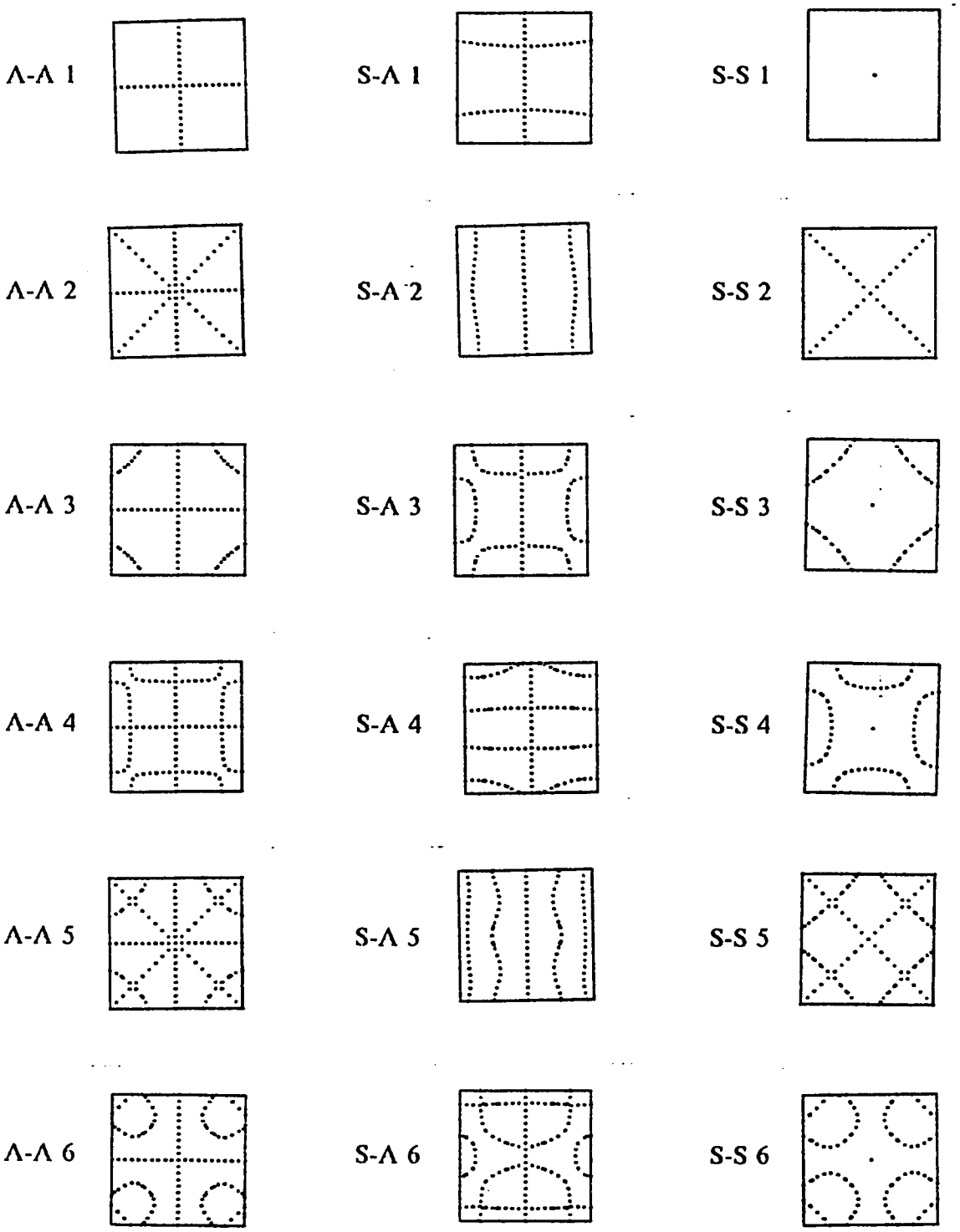

Figure A.b.11 : Nodal pattern
$\alpha = 0.5$, $\beta = 0.2000$.

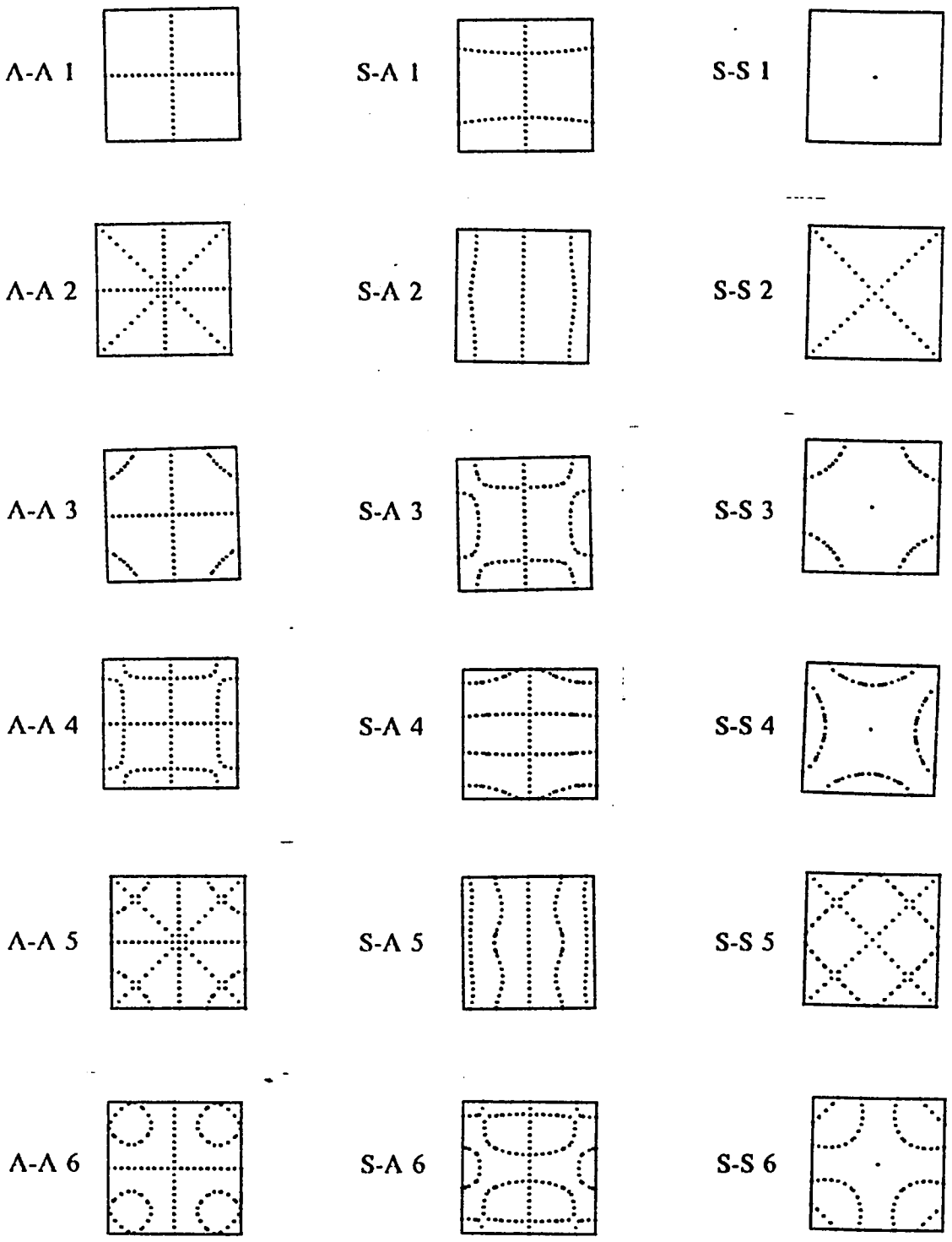

Figure A.b.12 : Nodal pattern
$\alpha = 0.5$, $\beta = 0.0005$.

APPENDIX A.c

COMPUTER PROGRAM

```
C##############################################################################
C
C    VIBRATION ANALYSIS OF POINT AND COLUMN SUPPORTED
C              MINDLIN PLATES
C
C##############################################################################
      IMPLICIT REAL *8 (A-H,O-Z)
      INTEGER R,C
      REAL *8 LAMBDA,MACHEP
      DIMENSION V(319),U(319),F(319,35),ZL(319,6)
      DIMENSION INT(319),L(319),C(319)
      DIMENSION LAMBDA(10)
      DIMENSION A2(319,71)
      COMMON / ARYS / WF(11,11),FZ(11,11),FN(11,11)
      COMMON / IWZN / IWF(121),IFN(121),IFZ(121)
      COMMON / POSN / HX,HY,MM,NN,MMF,NNF,LINE
      COMMON / STOR / IX,M1,M2,ITS(400)
      COMMON / HOLE / NH1,NH2,MH1,MH2
      COMMON / ATAR / A(319),TR(319)
      COMMON / ICQF / ICQ(6),ICF(6)
      COMMON / MESH / XX(15),YY(15)
      COMMON / COAR / A1(319,71)
      COMMON / ZRQF / ZR(319,6)
      COMMON / NODAL / D(10),AA(2),BB(2),CC(2,2),DD(2,2)
      COMMON / PONTQ / XPONTQ(121,6),YPONTQ(121,6)
      COMMON / PONTF / XPONTF(441,6),YPONTF(441,6)
      COMMON / CORDQ / XCORDQ(121),YCORDQ(121)
      COMMON / CORDF / XCORDF(441),YCORDF(441)
      COMMON / NETAQ / ANQ(121,6),FNQ(11,11,6)
      COMMON / ZETAQ / AZQ(121,6),FZQ(11,11,6)
      COMMON / WETAQ / AWQ(121,6),WFQ(11,11,6)
      COMMON / NETAF / ANF(441,6),FNF(21,21,6)
      COMMON / ZETAF / AZF(441,6),FZF(21,21,6)
      COMMON / WETAF / AWF(441,6),WFF(21,21,6)
      COMMON / CODEQ / XNODEQ(11),YNODEQ(11)
      COMMON / CODEF / XNODEF(21),YNODEF(21)
      COMMON / INTER / P,Q,S,T
C
      PI=DACOS(-1.D0)
      RK=(PI*PI)/12.D0
      BETA=0.2000D0
      RMU=0.3D0
      FACTOR=5.00D4
      LINE=9
      ALPHA = (LINE-1.)/20.
      BETA=BETA*2.0D0
      BP=BETA*BETA/12.D0
      D(1)=BP
      D(2)=(RK*(1.D0-RMU))/2.D0
      D(3)=BP
      D(4)=(RK*(1.D0-RMU))/2.D0
      D(5)=2.D0*RMU*BP
      D(6)=(BP*(1.D0-RMU))/2.D0
      D(7)=1.D0/12.D0
      D(8)=1.D0/(BETA*BETA)
```

```
      DO 31 I=1,6
   31 D(I)=D(I)/(12.D0*BP*BP)
      M1=35
      M2=35
      M=M1+M2+1
      GAMA=1.D0
      N=319
      NS=319
      NN=11
      MM=11
      IM=NN-IMM
      NE=6
      NM=NN*MM
      DO 42 I=1,NE
   42 LAMBDA(I)=(LAMBDA(I)**2)/(FACTOR*16.D0)
   15 HX=1.D0/(MM-1)
      HY=GAMA/(NN-1)
      RH=HY/HX
      DO 16 I=1,15
      XX(I)=1.D0
   16 YY(I)=1.D0
      MM1=MM-1
      DO 17 JJ=2,MM1
      WF(1,JJ)=1.D0
      WF(NN,JJ)=0.D0
      FZ(1,JJ)=1.D0
      FZ(NN,JJ)=0.D0
      FN(1,JJ)=1.D0
   17 FN(NN,JJ)=1.D0
      NN1=NN-1
      DO 18 II=2,NN1
      WF(II,1)=1.D0
      WF(II,MM)=0.D0
      FZ(II,1)=1.D0
      FZ(II,MM)=1.D0
      FN(II,1)=1.D0
   18 FN(II,MM)=0.D0
      WF(1,1)=1.D0
      FZ(1,1)=1.D0
      FN(1,1)=1.D0
      WF(1,MM)=0.D0
      FZ(1,MM)=1.D0
      FN(1,MM)=0.D0
      WF(NN,1)=0.D0
      FZ(NN,1)=0.D0
      FN(NN,1)=1.D0
      WF(NN,MM)=0.D0
      FZ(NN,MM)=0.D0
      FN(NN,MM)=0.D0
      NN1=NN-1
      MM1=MM-1
      DO 19 II=2,NN1
      DO 19 JJ=2,MM1
      WF(II,JJ)=1.D0
      FZ(II,JJ)=1.D0
```

```
   19 FN(II,JJ)=1.D0
      WF(LINE,LINE)=0.D0
      MM1=MM-1
      DO 40 II=1,NN
      DO 40 JJ=1,MM1
   40 CALL INTEG1(II,JJ,HX,RII,N,M,NS,NN,MM)
      NN1=NN-1
      DO 21 II=1,NN1
      DO 21 JJ=1,MM
   21 CALL INTEG2(II,JJ,HX,RII,N,M,NS,NN,MM)
      MM1=MM-1
      NN1=NN-1
      DO 22 II=1,NN1
      DO 22 JJ=1,MM1
   22 CALL INTEG3(II,JJ,HX,RII,N,M,NS,NN,MM)
      DO 23 II=1,NN
      DO 23 JJ=1,MM
   23 CALL INTEG4(II,JJ,HX,RII,NN,MM)
   25 DO 30 I=1,N
      DO 30 J=1,M
   30 A1(I,J)=A1(I,J)/(TR(I)*FACTOR)
      LA=10
      MACHEP=1.0D-18
      CALL UNSRAY(N,M1,M2,M,NE,MACHEP,A1,LA,LAMBDA,L,C,ZR,ZI,
     &          A2,V,F,U,INT)
      DO 34 I=1,NE
      RTLAMD=4.D0*DSQRT(LAMBDA(I)*FACTOR)
   34 WRITE(6,35) RTLAMD
   35 FORMAT(/10X,' RLAMD  =',E24.15)
      DO 43 I=1,NE
      EIGN=4.D0*((BETA*BETA)/DSQRT(12.D0))*(DSQRT(LAMBDA(I)*FACTOR))
   43 WRITE(6,44) EIGN
   44 FORMAT(/10X,' EIGEN  =',E24.15)
      CALL MODE(NM,N,NE)
      STOP
      END
C ***********************************************************************
      FUNCTION F(II,JJ)
      IMPLICIT REAL *8 (A-H,O-Z)
      COMMON / POSN / HX,HY,MM,NN,MMF,NNF,LINE
      KH =0
      KV =0
      KP =0
      IF(II.EQ.NN) KH=2
      IF(JJ.EQ.MM) KV=1
      IF(II.EQ.LINE.AND.JJ.GE.LINE) KP=1
      IF(II.GT.LINE) KP=1
   10 F=((3*MM)-2)*(II-1)-KP+JJ*(3-KH)-KV
      RETURN
      END
C ***********************************************************************
      SUBROUTINE MODE(NM,N,NE)
      IMPLICIT REAL *8 (A-H,O-Z)
      COMMON / ZRQF / ZR(319,6)
      COMMON / ICQF / ICQ(6),ICF(6)
```

```
      COMMON / POSN / HX,HY,MM,NN,MMF,NNF,LINE
      COMMON / IWZN / IWF(121),IFN(121),IFZ(121)
      COMMON / ARYS / WF(11,11),FZ(11,11),FN(11,11)
      COMMON / PONTQ / XPONTQ(121,6),YPONTQ(121,6)
      COMMON / PONTF / XPONTF(441,6),YPONTF(441,6)
      COMMON / CORDQ / XCORDQ(121),YCORDQ(121)
      COMMON / CORDF / XCORDF(441),YCORDF(441)
      COMMON / NETAQ / ANQ(121,6),FNQ(11,11,6)
      COMMON / ZETAQ / AZQ(121,6),FZQ(11,11,6)
      COMMON / WETAQ / AWQ(121,6),WFQ(11,11,6)
      COMMON / NETAF / ANF(441,6),FNF(21,21,6)
      COMMON / ZETAF / AZF(441,6),FZF(21,21,6)
      COMMON / WETAF / AWF(441,6),WFF(21,21,6)
      COMMON / CODEQ / XNODEQ(11),YNODEQ(11)
      COMMON / CODEF / XNODEF(21),YNODEF(21)
C-----------------------------------------------------------------------
      NNF = (2*NN)-1
      MMF = (2*MM)-1
      DO 10 J=1,MM
      XNODEQ(J)=(J-1)*HX
   10 YNODEQ(J)=(J-1)*HY
      K=1
      DO 11 I=1,NN
      DO 11 J=1,MM
      XCORDQ(K)=XNODEQ(J)
      YCORDQ(K)=YNODEQ(I)
   11 K=K+1
      DO 12 J=1,MMF
      XNODEF(J)=(J-1)*HX/2.D0
   12 YNODEF(J)=(J-1)*HY/2.D0
      K=1
      DO 13 I=1,NNF
      DO 13 J=1,MMF
      XCORDF(K)=XNODEF(J)
      YCORDF(K)=YNODEF(I)
   13 K=K+1
      DO 14 J1=1,NE
   14 CALL MODEQ(J1,NE)
      DO 15 J1=1,NE
   15 CALL MODEF(J1,NE)
      RETURN
      END
C ***********************************************************************
      SUBROUTINE MODEQ(J1,NE)
      IMPLICIT REAL *8 (A-H,O-Z)
      .
      .
        ALL COMMON UESD IN SUBROUTINE MODE
      .
      .
      IK=1
      DO 11 I=1,NN
      DO 11 J=1,MM
      IFN(IK)=F(I,J)
      IFZ(IK)=F(I,J)-1
```

```
      IWF(IK)=F(I,J)-2
      ANQ(IK,J1)=ZR(IFN(IK),J1)
      AZQ(IK,J1)=ZR(IFZ(IK),J1)
      IF(IWF(IK).EQ.0) GO TO 12
      AWQ(IK,J1)=ZR(IWF(IK),J1)/2.D0
   12 IF(FN(I,J).EQ.0.D0) ANQ(IK,J1) = 0.D0
      IF(FZ(I,J).EQ.0.D0) AZQ(IK,J1) = 0.D0
      IF(WF(I,J).EQ.0.D0) AWQ(IK,J1) = 0.D0
   11 IK=IK+1
      IK=1
      DO 13 I=1,NN
      DO 13 J=1,MM
      WFQ(I,J,J1)=AWQ(IK,J1)
      FZQ(I,J,J1)=AZQ(IK,J1)
      FNQ(I,J,J1)=ANQ(IK,J1)
   13 IK=IK+1
      CALL NODEQ(J1)
      RETURN
      END
C*********************************************************************
      SUBROUTINE NODEQ(J1)
      IMPLICIT REAL *8 (A-H,O-Z)
      .
      .
        ALL COMMON UESD IN SUBROUTINE MODE
      .
      .
      ICQ(J1)=0
      DO 41 I=1,NN
      DO 42 J=1,MM-1,1
      IF(WFQ(I,J+1,J1).EQ.0.D0) GO TO 44
      GO TO 45
   44 ICQ(J1)=ICQ(J1)+1
      XPONTQ(ICQ(J1),J1)=XNODEQ(J+1)
      YPONTQ(ICQ(J1),J1)=XNODEQ(I)
      GO TO 43
   45 IF((WFQ(I,J,J1)*WFQ(I,J+1,J1)).LE.0.D0)GO TO 46
      GO TO 43
   46 ICQ(J1)=ICQ(J1)+1
      AR=DABS(WFQ(I,J  ,J1))
      AL=DABS(WFQ(I,J+1,J1))
      RATIO=(AR/(AR+AL))*HX
      XPONTQ(ICQ(J1),J1)=XNODEQ(J)+RATIO
      YPONTQ(ICQ(J1),J1)=XNODEQ(I)
   43 CONTINUE
   42 CONTINUE
   41 CONTINUE
      DO 51 J=1,MM
      DO 52 I=1,NN-1,1
      IF(WFQ(I+1,J,J1).EQ.0.D0) GO TO 54
      GO TO 55
   54 ICQ(J1)=ICQ(J1)+1
      XPONTQ(ICQ(J1),J1)=XNODEQ(J)
      YPONTQ(ICQ(J1),J1)=XNODEQ(I+1)
      GO TO 53
```

```
   55 IF((WFQ(I,J,J1)*WFQ(I+1,J,J1)).LE.0.D0)GO TO 56
      GO TO 53
   56 ICQ(J1)=ICQ(J1)+1
      AR=ABS(WFQ(I,J,J1))
      AL=ABS(WFQ(I+1,J,J1))
      RATIO=(AR/(AR+AL))*HY
      XPONTQ(ICQ(J1),J1)=XNODEQ(J)
      YPONTQ(ICQ(J1),J1)=XNODEQ(I)+RATIO
   53 CONTINUE
   52 CONTINUE
   51 CONTINUE
      DO 61 I=1,ICQ(J1)
      DO 62 J=I+1,ICQ(J1)
   65 IF((DABS(XPONTQ(J,J1)-XPONTQ(I,J1)).LT.1.D-8).AND.
     &   (DABS(YPONTQ(J,J1)-YPONTQ(I,J1)).LT.1.D-8)) GO TO 63
      GO TO 62
   63 DO 64 IJ=J,ICQ(J1)-1,1
      XPONTQ(IJ,J1)=XPONTQ(IJ+1,J1)
      YPONTQ(IJ,J1)=YPONTQ(IJ+1,J1)
   64 CONTINUE
      ICQ(J1)=ICQ(J1)-1
      IF(J.LE.ICQ(J1))GO TO 65
   62 CONTINUE
   61 CONTINUE
      RETURN
      END
C ***********************************************************************
      SUBROUTINE MODEF(J1,NE)
      IMPLICIT REAL *8 (A-H,O-Z)
      .
      .
        ALL COMMON UESD IN SUBROUTINE MODE
      .
      .
      DO 11 I=1,NN
      DO 11 J=1,MM
      I3=NNF-I+1
      J3=MMF-J+1
      WFF(I ,J ,J1)=WFQ(I,J,J1)*(+1.D0)
      WFF(I ,J3,J1)=WFQ(I,J,J1)*(-1.D0)
      WFF(I3,J ,J1)=WFQ(I,J,J1)*(-1.D0)
      WFF(I3,J3,J1)=WFQ(I,J,J1)*(+1.D0)
      FZF(I ,J ,J1)=FZQ(I,J,J1)*(+1.D0)
      FZF(I ,J3,J1)=FZQ(I,J,J1)*(+1.D0)
      FZF(I3,J ,J1)=FZQ(I,J,J1)*(-1.D0)
      FZF(I3,J3,J1)=FZQ(I,J,J1)*(-1.D0)
      FNF(I ,J ,J1)=FNQ(I,J,J1)*(+1.D0)
      FNF(I ,J3,J1)=FNQ(I,J,J1)*(-1.D0)
      FNF(I3,J ,J1)=FNQ(I,J,J1)*(+1.D0)
      FNF(I3,J3,J1)=FNQ(I,J,J1)*(-1.D0)
   11 CONTINUE
      WRITE(6,10)
      IK=1
      DO 12 I=1,NNF
      DO 12 J=1,MMF
```

```
      AWF(IK,J1)=WFF(I,J,J1)
      AZF(IK,J1)=FZF(I,J,J1)
      ANF(IK,J1)=FNF(I,J,J1)
      WRITE(6,20)J1,IK,I,J,AWF(IK,J1),AZF(IK,J1),ANF(IK,J1)
     & ,XCORDF(IK),YCORDF(IK)
   12 IK=IK+1
      WRITE(6,31)J1
      DO 13 I=1,NNF
   13 WRITE(6,30)(WFF(I,J,J1),J=1,MMF)
      WRITE(6,32)J1
      DO 14 I=1,NNF
   14 WRITE(6,30)(FZF(I,J,J1),J=1,MMF)
      WRITE(6,33)J1
      DO 15 I=1,NNF
   15 WRITE(6,30)(FNF(I,J,J1),J=1,MMF)
   16 CALL NODEF(J1)
   10 FORMAT(//,2X,'NE',2X,'#',3X,'II',2X,'JJ',8X,'AW',11X,'AZ',
     & 11X,'AN',9X,'XCOR',3X,'YCOR'
     & ,/,72('-'))
   20 FORMAT(4(1X,I3),3(2X,F12.9),2(3X,F4.2))
   30 FORMAT(11(2X,F8.5))
   31 FORMAT(//,49('='),' AW BY NODE ',49('='),/,'NE =',I2)
   32 FORMAT(//,49('='),' AZ BY NODE ',49('='),/,'NE =',I2)
   33 FORMAT(//,49('='),' AN BY NODE ',49('='),/,'NE =',I2)
      RETURN
      END
C*********************************************************************
      SUBROUTINE NODEF(J1)
      IMPLICIT REAL *8 (A-H,O-Z)
      .
      .
        ALL COMMON UESD IN SUBROUTINE MODE
      .
      .
      ICF(J1)=0
      DO 11 IJ=1,ICQ(J1)
      XPONTF(ICF(J1)+1,J1) = XPONTQ(IJ,J1)/2.D0
      YPONTF(ICF(J1)+1,J1) = YPONTQ(IJ,J1)/2.D0
      XPONTF(ICF(J1)+2,J1) = XPONTQ(IJ,J1)/2.D0
      YPONTF(ICF(J1)+2,J1) = 1.D0-(YPONTQ(IJ,J1)/2.D0)
      XPONTF(ICF(J1)+3,J1) = 1.D0-(XPONTQ(IJ,J1)/2.D0)
      YPONTF(ICF(J1)+3,J1) = YPONTQ(IJ,J1)/2.D0
      XPONTF(ICF(J1)+4,J1) = 1.D0-(XPONTQ(IJ,J1)/2.D0)
      YPONTF(ICF(J1)+4,J1) = 1.D0-(YPONTQ(IJ,J1)/2.D0)
      ICF(J1)=ICF(J1)+4
   11 CONTINUE
      DO 21 I=1,ICF(J1)
      DO 22 J=I+1,ICF(J1)
   25 IF((DABS(XPONTF(J,J1)-XPONTF(I,J1)).LT.1.D-8).AND.
     &   (DABS(YPONTF(J,J1)-YPONTF(I,J1)).LT.1.D-8))GO TO 23
      GO TO 22
   23 DO 24 IJ=J,ICF(J1)-1,1
      XPONTF(IJ,J1)=XPONTF(IJ+1,J1)
      YPONTF(IJ,J1)=YPONTF(IJ+1,J1)
   24 CONTINUE
```

```
      ICF(J1)=ICF(J1)-1
      IF(J.LE.ICF(J1))GO TO 25
   22 CONTINUE
   21 CONTINUE
      WRITE(6,30)ICF(J1)
      WRITE(6,10)J1
      WRITE(6,20)(XPONTF(KL,J1),YPONTF(KL,J1),KL=1,ICF(J1))
   10 FORMAT(34('='),/,'NODAL LINE NE = ',I2,/,34('=')
     & ,/,'  XPOINT        YPOINT  ')
   20 FORMAT(2(F16.14,2X))
   30 FORMAT(/,'ICF(J1) = ',I4)
      RETURN
      END
C ***********************************************************************
      SUBROUTINE DATA(II,JJ)
      IMPLICIT REAL *8 (A-H,O-Z)
      COMMON / MESH / XX(15),YY(15)
      COMMON / INTER / P,Q,S,T
      I=II+1
      J=JJ+1
      J1=J-1
      P=XX(J1)
      Q=XX(J)
      I1=I-1
      S=YY(I1)
      T=YY(I)
      RETURN
      END
C ***********************************************************************
      SUBROUTINE INTEG1(II,JJ,HX,RH,N,M,NS,NN,MM)
      IMPLICIT REAL *8 (A-H,O-Z)
      COMMON / NODAL / D(10),AA(2),BB(2),CC(2,2),DD(2,2)
      COMMON / ARYS  / WF(11,11),FZ(11,11),FN(11,11)
      COMMON / HOLE  / NH1,NH2,MH1,MH2
      COMMON / ATAR  / A(319),TR(319)
      COMMON / COAR  / A1(319,71)
      COMMON / INTER / P,Q,S,T
      CALL DATA(II,JJ)
      IF(II.GT.1) GO TO 10
      TINTEG=(Q*T*RH*HX*HX)/2.D0
      GO TO 20
   10 IF(II.LT.NN) GO TO 15
      TINTEG=(Q*S*RH*HX*HX)/2.D0
      GO TO 20
   15 IF(II.EQ.1) GO TO 25
   25 TINTEG=(Q*(S+T)*RH*HX*HX)/2.D0
   20 IZ=1
      L=1
      J1=JJ+1
      AA(1)=(-1.D0/(Q*HX))*FZ(II,JJ)
      AA(2)=( 1.D0/(Q*HX))*FZ(II,J1)
      CALL DERIV(II,JJ,L,IZ,TINTEG,N,M,NS)
      IZ=2
      L=2
      J1=JJ+1
```

```
      AA(1)=0.5D0*FZ(II,JJ)
      AA(2)=0.5D0*FZ(II,J1)
      BB(1)=(-1.D0/(Q*HX))*WF(II,JJ)
      BB(2)=( 1.D0/(Q*HX))*WF(II,J1)
      CALL DERIV(II,JJ,L,IZ,TINTEG,N,M,NS)
   30 RETURN
      END
C ***********************************************************************
      SUBROUTINE INTEG2(II,JJ,HX,RH,N,M,NS,NN,MM)
      IMPLICIT REAL *8 (A-H,O-Z)
      COMMON / NODAL / D(10),AA(2),BB(2),CC(2,2),DD(2,2)
      COMMON / ARYS  / WF(11,11),FZ(11,11),FN(11,11)
      COMMON / HOLE  / NH1,NH2,MH1,MH2
      COMMON / ATAR  / A(319),TR(319)
      COMMON / COAR  / A1(319,71)
      COMMON / INTER / P,Q,S,T
      CALL DATA(II,JJ)
      IF(JJ.GT.1) GO TO 10
      TINTEG=(T*Q*RH*HX*HX)/2.D0
      GO TO 20
   10 IF(JJ.LT.MM) GO TO 15
      TINTEG=(T*P*RH*HX*HX)/2.D0
      GO TO 20
   15 IF(II.EQ.1) GO TO 25
   25 TINTEG=(T*(P+Q)*RH*HX*HX)/2.D0
   20 IZ=3
      L=3
      II=II+1
      AA(1)=(-1.D0/(T*RH*HX))*FN(II,JJ)
      AA(2)=( 1.D0/(T*RH*HX))*FN(II,JJ)
      CALL DERIV(II,JJ,L,IZ,TINTEG,N,M,NS)
      IZ=4
      L=4
      II=II+1
      AA(1)=0.5D0*FN(II,JJ)
      AA(2)=0.5D0*FN(II,JJ)
      BB(1)=(-1.D0/(T*RH*HX))*WF(II,JJ)
      BB(2)=( 1.D0/(T*RH*HX))*WF(II,JJ)
      CALL DERIV(II,JJ,L,IZ,TINTEG,N,M,NS)
   30 RETURN
      END
C ***********************************************************************
      SUBROUTINE INTEG3(II,JJ,HX,RH,N,M,NS,NN,MM)
      IMPLICIT REAL *8 (A-H,O-Z)
      COMMON / NODAL / D(10),AA(2),BB(2),CC(2,2),DD(2,2)
      COMMON / ARYS  / WF(11,11),FZ(11,11),FN(11,11)
      COMMON / HOLE  / NH1,NH2,MH1,MH2
      COMMON / ATAR  / A(319),TR(319)
      COMMON / COAR  / A1(319,71)
      COMMON / INTER / P,Q,S,T
      CALL DATA(II,JJ)
      IF(II.EQ.1) GO TO 10
   10 TINTEG=Q*T*RH*HX*HX
      IZ=5
      L=5
```

```
      II = II + 1
      JJ = JJ + 1
      CC(1,1) = (-0.5D0/(Q*HX))*FZ(II,JJ)
      CC(1,2) = ( 0.5D0/(Q*HX))*FZ(II,JJ)
      CC(2,1) = (-0.5D0/(Q*HX))*FZ(II,JJ)
      CC(2,2) = ( 0.5D0/(Q*HX))*FZ(II,JJ)
      DD(1,1) = (-0.5D0/(T*RH*HX))*FN(II,JJ)
      DD(1,2) = (-0.5D0/(T*RH*HX))*FN(II,JJ)
      DD(2,1) = ( 0.5D0/(T*RH*HX))*FN(II,JJ)
      DD(2,2) = ( 0.5D0/(T*RH*HX))*FN(II,JJ)
      CALL DERIV(II,JJ,L,IZ,TINTEG,N,M,NS)
      IZ = 6
      L = 6
      II = II + 1
      JJ = JJ + 1
      CC(1,1) = (-0.5D0/(T*RH*HX))*FZ(II,JJ)
      CC(1,2) = (-0.5D0/(T*RH*HX))*FZ(II,JJ)
      CC(2,1) = ( 0.5D0/(T*RH*HX))*FZ(II,JJ)
      CC(2,2) = ( 0.5D0/(T*RH*HX))*FZ(II,JJ)
      DD(1,1) = (-0.5D0/(Q*HX))*FN(II,JJ)
      DD(1,2) = ( 0.5D0/(Q*HX))*FN(II,JJ)
      DD(2,1) = (-0.5D0/(Q*HX))*FN(II,JJ)
      DD(2,2) = ( 0.5D0/(Q*HX))*FN(II,JJ)
      CALL DERIV(II,JJ,L,IZ,TINTEG,N,M,NS)
   15 RETURN
      END
C*********************************************************************
      SUBROUTINE INTEG4(II,JJ,HX,RH,NN,MM)
      IMPLICIT REAL *8 (A-H,O-Z)
      COMMON / NODAL / D(10),AA(2),BB(2),CC(2,2),DD(2,2)
      COMMON / ARYS  / WF(11,11),FZ(11,11),FN(11,11)
      COMMON / HOLE  / NH1,NH2,MH1,MH2
      COMMON / ATAR  / A(319),TR(319)
      COMMON / COAR  / A1(319,71)
      COMMON / INTER / P,Q,S,T
C
      CALL DATA(II,JJ)
      I = F(II,JJ)
      I1 = I-1
      I2 = I-2
      IF(II.EQ.1.OR.II.EQ.NN) GO TO 3
      IF(JJ.GT.1.AND.JJ.LT.MM) GO TO 4
    3 IF(II.GT.1) GO TO 5
      TINTEG = (T*(P + Q)*RH*HX*HX)/4.D0
      IF(JJ.EQ.1)TINTEG = (T*Q*RH*HX*HX)/4.D0
      IF(JJ.EQ.MM) TINTEG = (P*T*RH*HX*HX)/4.D0
      GO TO 10
    5 IF(II.EQ.NN) GO TO 6
      IF(JJ.EQ.1) TINTEG = (Q*(S + T)*RH*HX*HX)/4.D0
      IF(JJ.EQ.MM) TINTEG = (P*(S + T)*RH*HX*HX)/4.D0
      GO TO 10
    6 TINTEG = (S*(P + Q)*RH*HX*HX)/4.D0
      IF(JJ.EQ.1) TINTEG = (S*Q*RH*HX*HX)/4.D0
      IF(JJ.EQ.MM) TINTEG = (P*S*RH*HX*HX)/4.D0
      GO TO 10
```

```
    4 IF(III.EQ.1) GO TO 7
    7 TINTEG=((P+Q)*(S+T)*RII*HX*HX)/4.D0
   10 IF(FN(II,JJ).EQ.1.D0) TR(I)=D(7)*TINTEG
      IF(FZ(II,JJ).EQ.1.D0) TR(I1)=D(7)*TINTEG
      IF(WF(II,JJ).EQ.1.D0) TR(I2)=D(8)*TINTEG
    9 RETURN
      END
C ***********************************************************************
      SUBROUTINE DERIV(II,JJ,L,IZ,TINTEG,N,M,NS)
      IMPLICIT REAL *8 (A-H,O-Z)
      COMMON / NODAL / D(10),AA(2),BB(2),CC(2,2),DD(2,2)
      COMMON / ARYS  / WF(11,11),FZ(11,11),FN(11,11)
      COMMON / ATAR  / A(319),TR(319)
      COMMON / COAR  / A1(319,71)
      GO TO (7,8,9,10,11,12),IZ
    7 II=II
      DO 15 JI=1,2
      IF(AA(JI).EQ.0.D0) GO TO 15
      J1=JJ+JI-1
      I=F(II,J1)-1
      J=F(II,JJ)-1
      IF(AA(1).EQ.0.D0) GO TO 16
      A(J)=TINTEG*D(L)*AA(JI)*AA(1)
   16 J2=JJ+1
      J=F(II,J2)-1
      IF(AA(2).EQ.0.D0) GO TO 17
      A(J)=TINTEG*D(L)*AA(JI)*AA(2)
   17 CALL STORAG(I,N,M,NS)
   15 CONTINUE
      DO 18 LL=1,2
   18 AA(LL)=0.D0
      GO TO 20
    8 KX=1
      KY=2
   26 II=II
      DO 21 JI=1,2
      IF(AA(JI).EQ.0.D0) GO TO 21
      J1=JJ+JI-1
      I=F(II,J1)-KX
      DO 22 IK=1,2
      J2=JJ+IK-1
      J=F(II,J2)-KX
      IF(AA(IK).EQ.0.D0) GO TO 23
      A(J)=TINTEG*D(L)*AA(JI)*AA(IK)
   23 J=F(II,J2)-KY
      IF(BB(IK).EQ.0.D0) GO TO 22
      A(J)=TINTEG*D(L)*AA(JI)*BB(IK)
   22 CONTINUE
      CALL STORAG(I,N,M,NS)
   21 CONTINUE
      IF(KX.EQ.2) GO TO 24
      KX=2
      KY=1
      DO 25 LL=1,2
      VR=AA(LL)
```

```
      AA(LL)=BB(LL)
25    BB(LL)=VR
      GO TO 26
24    DO 27 LL=1,2
      AA(LL)=0.D0
27    BB(LL)=0.D0
      GO TO 20
 9    J1=JJ
      DO 31 IJ=1,2
      IF(AA(IJ).EQ.0.D0) GO TO 31
      I1=II+IJ-1
      I=F(I1,J1)
      J=F(II,JJ)
      IF(AA(1).EQ.0.D0) GO TO 33
      A(J)=TINTEG*D(I)*AA(IJ)*AA(1)
33    I2=II+1
      J=F(I2,JJ)
      IF(AA(2).EQ.0.D0) GO TO 34
      A(J)=TINTEG*D(I)*AA(IJ)*AA(2)
34    CALL STORAG(I,N,M,NS)
31    CONTINUE
      DO 28 LL=1,2
28    AA(LL)=0.D0
      GO TO 20
10    KX=0
      KY=2
40    J1=JJ
      DO 35 IJ=1,2
      IF(AA(IJ).EQ.0.D0) GO TO 35
      I1=II+IJ-1
      I=F(I1,J1)-KX
      DO 36 IK=1,2
      I2=II+IK-1
      J=F(I2,JJ)-KX
      IF(AA(IK).EQ.0.D0) GO TO 37
      A(J)=TINTEG*D(I)*AA(IJ)*AA(IK)
37    J=F(I2,JJ)-KY
      IF(BB(IK).EQ.0.D0) GO TO 36
      A(J)=TINTEG*D(I)*AA(IJ)*BB(IK)
36    CONTINUE
      CALL STORAG(I,N,M,NS)
35    CONTINUE
      IF(KX.EQ.2) GO TO 38
      KX=2
      KY=0
      DO 39 LL=1,2
      VR=AA(LL)
      AA(LL)=BB(LL)
39    BB(LL)=VR
      GO TO 40
38    DO 41 LL=1,2
      AA(LL)=0.D0
41    BB(LL)=0.D0
      GO TO 20
11    KX=1
```

```
      KY=0
51    DO 47 IJ=1,2
      DO 47 JI=1,2
      IF(CC(IJ,JI).EQ.0.D0) GO TO 47
      II=II+IJ-1
      J1=JJ+JI-1
      I=F(I1,J1)-KX
      DO 48 IK=1,2
      DO 48 JK=1,2
      I2=II+IK-1
      J2=JJ+JK-1
      J=F(I2,J2)-KY
      IF(DD(IK,JK).EQ.0.D0) GO TO 48
      A(J)=TINTEG*D(L)*CC(IJ,JI)*DD(IK,JK)/2.D0
48    CONTINUE
      CALL STORAG(I,N,M,NS)
47    CONTINUE
      IF(KX.EQ.0) GO TO 49
      KX=0
      KY=1
      DO 50 LL=1,2
      DO 50 KK=1,2
      VR=CC(LL,KK)
      CC(LL,KK)=DD(LL,KK)
50    DD(LL,KK)=VR
      GO TO 51
49    DO 52 LL=1,2
      DO 52 KK=1,2
      CC(LL,KK)=0.D0
52    DD(LL,KK)=0.D0
      GO TO 20
12    KX=1
      KY=0
63    DO 58 IJ=1,2
      DO 58 JI=1,2
      IF(CC(IJ,JI).EQ.0.D0) GO TO 58
      II=II+IJ-1
      J1=JJ+JI-1
      I=F(I1,J1)-KX
      DO 59 IK=1,2
      DO 59 JK=1,2
      I2=II+IK-1
      J2=JJ+JK-1
      J=F(I2,J2)-KX
      IF(CC(IK,JK).EQ.0.D0) GO TO 60
      A(J)=TINTEG*D(L)*CC(IJ,JI)*CC(IK,JK)
60    J=F(I2,J2)-KY
      IF(DD(IK,JK).EQ.0.D0) GO TO 59
      A(J)=TINTEG*D(L)*CC(IJ,JI)*DD(IK,JK)
59    CONTINUE
      CALL STORAG(I,N,M,NS)
58    CONTINUE
      IF(KX.EQ.0) GO TO 61
      KX=0
      KY=1
```

```
      DO 62 LL=1,2
      DO 62 KK=1,2
      VR=CC(LL,KK)
      CC(LL,KK)=DD(LL,KK)
   62 DD(LL,KK)=VR
      GO TO 63
   61 DO 64 LL=1,2
      DO 64 KK=1,2
      CC(LL,KK)=0.D0
   64 DD(LL,KK)=0.D0
   20 RETURN
      END
C *********************************************************************
      SUBROUTINE STORAG(I,N,M,NS)
      IMPLICIT REAL *8 (A-H,O-Z)
      COMMON / ARYS / WF(11,11),FZ(11,11),FN(11,11)
      COMMON / STOR / IX,M1,M2,ITS(400)
      COMMON / ATAR / A(319),TR(319)
      COMMON / COAR / A1(319,71)
      J=I
   10 JJ=M1+1
   12 IF(J.EQ.1) GO TO 11
      JJ=JJ-1
      J=J-1
      A1(I,JJ)=A1(I,JJ)+A(J)
      IF(JJ.EQ.1) GO TO 11
      GO TO 12
   11 J=I
      JJ=M1+1
      A1(I,JJ)=A1(I,JJ)+A(J)
   13 IF(J.EQ.N) GO TO 7
      J=J+1
      JJ=JJ+1
      A1(I,JJ)=A1(I,JJ)+A(J)
      IF(JJ.EQ.M) GO TO 7
      GO TO 13
    7 DO 15 J=1,N
   15 A(J)=0.D0
      RETURN
      END
C *********************************************************************
C *********************************************************************
      SUBROUTINE UNSRAY(N,M1,M2,MM,R,MACHEP,A,LA,LAMBDA,
     &          L,C,ZR,ZL,AA,V,F,U,INT)
      IMPLICIT REAL*8 (A-H,O-Z)
      DOUBLE PRECISION Z,S,Z1,Z2,S1,S2
      INTEGER R,C,D2,P,Q
      REAL*8 MACHEP ,LAMBDA
      DIMENSION LAMBDA(R),A(N,MM),L(N),C(N),ZR(N,R),ZL(N,R),
     &      AA(N,MM),V(N),U(N),F(N,M1),INT(N)
      EPS=0.D0
      DO 101 I=1,N
      X=0.D0
      DO 100 J=1,MM
  100 X=X+DABS(A(I,J))
```

```
      IF(EPS.LT.X) EPS=X
  101 CONTINUE
      EPS=EPS*MACHEP
      DO 127 K=1,R
      DO 102 I=1,N
      V(I)=1.D0
      DO 102 J=1,MM
  102 AA(I,J)=A(I,J)
      LB=0
      CALL BANDET(N,M1,M2,MM,1,LAMBDA(K),MACHEP,AA,D1,D2,F,INT)
      CALL BANSOL(N,M1,M2,MM,1,1,AA,F,INT,V)
      X=0.D0
      DO 103 I=1,N
      IF(DABS(V(I)).LE.DABS(X)) GO TO 103
      X=V(I)
      P=I
  103 CONTINUE
      X=1.D0/X
      DO 104 I=1,N
      V(I)=X*V(I)
  104 U(I)=V(I)
    1 D1=0.D0
      LB=LB+1
      CALL BANSOL (N,M1,M2,MM,0,1,AA,F,INT,V)
      Y=1.D0/V(P)
      X=0.D0
      DO 105 I=1,N
      IF(DABS(V(I)).LE.DABS(X)) GO TO 105
      X=V(I)
      P=I
  105 CONTINUE
      X=1.D0/X
      DO 106 I=1,N
      R1=DABS((U(I)-Y*V(I))*X)
      IF(R1.GT.D1) D1=R1
      V(I)=X*V(I)
  106 U(I)=V(I)
      IF(D1.LE.EPS) GO TO 108
      IF(LB.LT.LA) GO TO 1
      LB=LB+1
  108 CONTINUE
      DO 109 I=1,N
      U(I)=V(I)
  109 ZR(I,K)=V(I)
      L(K)=LB
      LAMBDA(K)=LAMBDA(K)+Y
      LB=0
    2 D1=0.D0
      D2=1
      LB=LB+1
      V(I)=V(I)/AA(1,1)
      DO 111 J=2,N
      X=V(J)
      Q=J-1
      DO 110 I=D2,Q
```

```
      IN1=J-I+1
110   X=X-AA(I,IN1)*V(I)
      V(J)=X/AA(J,I)
      IF(J.GE.MM) D2=D2+1
111   CONTINUE
      J=N
112   X=0.D0
114   Q=J+1
      D2=J+M1
      IF(D2.GT.N) D2=N
      IF(Q.GT.D2) GO TO 113
      DO 115 I=Q,D2
      IN2=I-J
115   X=X-F(J,IN2)*V(I)
113   V(J)=V(J)+X
      I=INT(J)
      IF(I.EQ.J) GO TO 116
      X=V(J)
      V(J)=V(I)
      V(I)=X
116   J=J-1
      IF(J.GE.1) GO TO 112
      Y=1.D0/V(P)
      X=0.D0
      DO 117 I=1,N
      IF(DABS(V(I)).LE.DABS(X)) GO TO 117
      X=V(I)
      P=I
117   CONTINUE
      X=1.D0/X
      DO 118 I=1,N
      R1=DABS((U(I)-Y*V(I))*X)
      IF(R1.GT.D1) D1=R1
      V(I)=X*V(I)
118   U(I)=V(I)
      IF(D1.LE.EPS) GO TO 119
      IF(LB.LT.LA) GO TO 2
      LB=LB+1
119   C(K)=LB
      D1=LAMBDA(K)
      X=0.D0
      D2=M1
      DO 121 I=1,M1
      S1=D1
      S2=ZR(I,K)
      S=S1*S2
      Z=0.D0
      Q=2-I+M1
      DO 120 J=Q,MM
      Z1=A(I,J)
      IN3=J-D2
      Z2=ZR(IN3,K)
120   Z=Z+Z1*Z2
      D2=D2-1
      Y=SNGL(Z-S)
```

```
  121  X=X+Y*V(I)
       Q=M1+1
       LB=N-M2
       DO 123 I=Q,LB
       S1=D1
       S2=ZR(I,K)
       S=S1*S2
       Z=0.D0
       DO 122 J=1,MM
       Z1=A(I,J)
       IN9=J+D2
       Z2=ZR(IN9,K)
  122  Z=Z+Z1*Z2
       Y=SNGL(Z-S)
       X=X+Y*V(I)
  123  D2=D2+1
       LB=LB+1
       Q=MM-1
       DO 125 I=LB,N
       S1=D1
       S2=ZR(I,K)
       S=S1*S2
       Z=0.D0
       DO 124 J=1,Q
       Z1=A(I,J)
       IN4=J+D2
       Z2=ZR(IN4,K)
  124  Z=Z+Z1*Z2
       Y=SNGL(Z-S)
       X=X+Y*V(I)
       D2=D2+1
  125  Q=Q-1
       Y=0.D0
       DO 126 I=1,N
       Y=Y+ZR(I,K)*V(I)
  126  ZL(I,K)=V(I)
       LAMBDA(K)=LAMBDA(K)+X/Y
  127  CONTINUE
       RETURN
       END
C ***********************************************************************
       SUBROUTINE BANSOL (N,M1,M2,MM,E,R,A,M,INT,B)
       IMPLICIT REAL *8 (A-H,O-Z)
       REAL*8 M
       INTEGER E,R,W
       DIMENSION A(N,MM),INT(N),M(N,M1),B(N)
C
       L=M1
       IF(E.NE.0) GO TO 204
       DO 200 K=1,N
       I=INT(K)
       IF(I.EQ.K) GO TO 202
       X=B(K)
       B(K)=B(I)
       B(I)=X
```

```
  202 IF(L.LT.N) L=L+1
      II=K+1
      IF(II.GT.N) GO TO 200
      DO 203 I=II,L
      IN7=I-K
      X=M(K,IN7)
  203 B(I)=B(I)-X*B(K)
  200 CONTINUE
  204 L=-M1
      I=N
  205 X=B(I)
      W=M1+I
      K=I-M1
  206 IF(K.GT.L) GO TO 207
      KK=K+M1+1
      IN8=K+W
      X=X-A(I,KK)*B(IN8)
      K=K+1
      GO TO 206
  207 B(I)=X/A(I,1)
      IF(L.LT.M2) L=L+1
      I=I-1
      IF(I.GE.1) GO TO 205
      RETURN
      END
C *********************************************************************
      SUBROUTINE BANDET(N,M1,M2,MM,E,LAMBDA,MACHEP,A,D1,D2,M,INT)
      IMPLICIT REAL*8 (A-H,O-Z)
      REAL*8 LAMBDA,MACHEP,M,NORM
      INTEGER D2,E
      DIMENSION A(N,MM),M(N,M1),INT(N)
C
      NORM=0.D0
      IF(E.NE.1) GO TO 102
      DO 101 I=1,N
      X=0.D0
      DO 100 J=1,MM
  100 X=X+DABS(A(I,J))
      IF(NORM.LT.X) NORM=X
  101 CONTINUE
  102 J=M1+1
      DO 103 I=1,N
  103 A(I,J)=A(I,J)-LAMBDA
      L=M1
      DO 105 I=1,M1
      JJ=M1+2-I
      DO 104 J=JJ,MM
      IN5=J-L
  104 A(I,IN5)=A(I,J)
      L=L-1
      JJ=MM-L
      DO 105 J=JJ,MM
      A(I,J)=0.D0
  105 CONTINUE
      D2=0
```

```
      D1=1.D0
      L=M1
      DO 115 K=1,N
      X=A(K,1)
      I=K
      IF(L.LT.N) L=L+1
      JJ=K+1
      IF(JJ.GT.N) GO TO 1006
      DO 106 J=JJ,L
      IF(DABS(A(J,1)).LE.DABS(X)) GO TO 106
      X=A(J,1)
      I=J
  106 CONTINUE
 1006 CONTINUE
      INT(K)=I
      D1=D1*X
   46 IF(X.NE.0.D0) GO TO 107
      D2=0
      IF(E.EQ.1) A(K,1)=NORM*MACHEP
      IF(E.NE.1) RETURN
  107 CONTINUE
      IF(D1.EQ.0.D0)GO TO 110
      IF(DABS(D1).GE.1.D0) GO TO 108
      IF(DABS(D1).LT.0.0625D0) GO TO 109
      GO TO 110
  108 D2=D2+4
      D1=D1*0.0625D0
      GO TO 110
  109 D2=D2-4
      D1=D1*16.D0
  110 CONTINUE
      IF(I.EQ.K) GO TO 112
      D1=-D1
      DO 111 J=1,MM
      X=A(K,J)
      A(K,J)=A(I,J)
  111 A(I,J)=X
  112 JJ=K+1
      IF(JJ.GT.N) GO TO 115
      I=JJ
  177 X=A(I,1)/A(K,1)
      IN6=I-K
      M(K,IN6)=X
      DO 113 J=2,MM
  113 A(I,J-1)=A(I,J)-X*A(K,J)
  114 A(I,MM)=0.D0
      I=I+1
      IF(I.LE.L) GO TO 177
  115 CONTINUE
      RETURN
      END
C*********************************************************************
```

MAMDOUH B. AL-AIDAROUS

Born in Tiaf (Western Province) / Saudi Arabia in 1963. Finished high school study (Science Branch) from ***Al-Saih High School*** at ***Al-Kharj/Saudi Arabia*** in 1980. Graduate with a B.Sc degree in Mechanical Engineering from ***U.P.M.*** (University Of Petroleum and Minerals) / Dhahran / Saudi Arabia in 1985. Then joined the Department of Mechanical Engineering of the same university as a Graduate Assistant while persuing his M.S. degree in Mechanical Engineering which obtained in May 1989.